



**INSTYTUT GENETYKI
I BIOTECHNOLOGII ZWIERZĄT
Polskiej Akademii Nauk**

mgr Katarzyna Michniak

**THE ROLE OF THE HIPPO PATHWAY IN
THE TROPHECTODERM LINEAGE SPECIFICATION
IN THE RABBIT EMBRYO**

**PhD manuscript prepared in
Department of Experimental Embryology
under supervision of
dr hab. Anna Piliszek (supervisor)
dr Katarzyna Filimonow (auxiliary supervisor)**

JASTRZĘBIEC, 2023

Table of contents

1	Summary	6
2	Streszczenie	7
3	Abbreviation list	9
4	Introduction	11
4.1	Preimplantation development of the mammalian embryo	11
4.2	Embryo compaction	14
4.3	The cell polarity	15
4.4	Trophectoderm versus Inner Cell Mass – the first cell-fate decision	17
4.5	Trophectoderm - specific markers	18
4.6	The Hippo pathway signalling	21
4.6.1	Major components of the Hippo pathway in mammals	22
4.6.2	The Hippo pathway upstream signals - regulating factors.....	23
4.6.3	The Hippo pathway downstream signal - regulating factors	27
4.7	The role of the RHO-ROCK signalling in trophectoderm differentiation in mammals 29	
4.8	The rabbit as a valuable animal model in biological and medical research	33
5	Research hypotheses	36
6	Aims of the research	36
7	Materials and methods	37
7.1	Animals	37
7.2	Manipulation and culture media	37
7.3	Embryo collection	38
7.3.1	Embryo culture.....	39
7.3.2	Embryo culture with a time-lapse system	39
7.3.3	Treatment with ROCK kinase inhibitor	40
7.4	Embryo fixation	40
7.5	Removal of embryonic coats	40

7.6	Immunofluorescent detection of proteins	41
7.7	Phalloidin staining	43
7.8	Nuclear staining.....	43
7.9	Embryo imaging by confocal microscope	43
7.10	Confocal image analysis	43
7.11	Molecular biology methods.....	45
7.11.1	Sample collection for gene expression analysis	45
7.11.2	RNA extraction	46
7.11.3	RNA precipitation	46
7.11.4	Reverse transcription PCR	47
7.11.5	Primer design	48
7.11.6	Quantitative PCR	49
7.11.7	Agarose gel electrophoresis	51
7.12	Reagents and kits used in the study.....	51
7.13	Statistical analysis.....	54
8	Results	55
8.1	Timeline of in vitro rabbit embryo development from zygote to blastocyst stage	55
8.2	Analysis of relative expression levels of genes involved in the Hippo pathway cascade in rabbit embryos at consecutive stages: 1.5, 2.5, 3.25, 4.0 dpc.	57
8.3	Localisation of the early TE marker GATA3 in the preimplantation rabbit embryo	59
8.4	Localisation of cell polarity-related factors in the preimplantation rabbit embryo	61
8.4.1	P-Ezrin (P-ERM)	62
8.4.2	Atypical protein kinase C (aPKC)	64
8.4.3	F-actin	67
8.4.4	β -catenin	69
8.5	YAP localisation in the rabbit embryo from 8-cell stage to the blastocyst stage ..	72
8.5.1	Nuclear localisation of YAP at stages II-IX	75
8.5.2	Analysis of subcellular YAP localisation at stages III-VII	80
8.6	Colocalisation of YAP and GATA3	85
8.6.1	YAP and GATA3 colocalisation in morula stage embryos (stages III-IV).....	86
8.6.2	YAP and GATA3 colocalisation in the inside cells at stages V, VI and VII	87

8.6.3	YAP and GATA3 colocalisation in the outside cells at stages V, VI and VII.....	90
8.7	Analysis of the role of the Hippo pathway and polarity in the rabbit embryo via inhibition of the ROCK kinase function	93
8.7.1	Inhibition of ROCK kinase.....	93
8.7.2	Embryo growth after ROCK inhibition	96
8.8	Influence of ROCK inhibition on the Hippo pathway and the distribution of polarity markers.....	100
8.8.1	Colocalisation of YAP and GATA3 after ROCK inhibition treatment	103
8.8.2	Subcellular YAP localisation in embryos cultured for 48h with ROCK kinase inhibitor....	107
8.8.3	Localisation of aPKC in the outside cells after 48h of culture with ROCK kinase inhibition	110
8.8.4	Signal intensity profiles of aPKC in the apical domain of outside cells after ROCK inhibition	112
9	Discussion	116
9.1	Expression of genes involved in the Hippo pathway.....	117
9.1.1	TEAD1-4	117
9.1.2	LATS1/2	119
9.1.3	YAP	120
9.2	TE-specific transcription factors in the rabbit embryo	122
9.3	Polarity-associated factors	124
9.3.1	P-Ezrin	126
9.3.2	aPKC	126
9.3.3	F-actin	127
9.3.4	β -catenin	128
9.4	Dynamic patterns of YAP localisation during early rabbit development	130
9.5	Colocalisation of GATA3 and YAP in preimplantation embryo	132
9.6	The influence of the RHO-ROCK signalling on the Hippo pathway and TE differentiation	134
9.7	Differences in the regulation of the Hippo signalling between rabbits and other mammalian species	137
9.8	Conclusions	140
9.9	The limitation of the study and further directions.....	140

10	References	142
12	Supplementary data	165
12.1	Quantification of the contribution of YAP+ and GATA3+ cells in individual embryos at stages III-IV	165
12.2	Quantification of the contribution of YAP+ and GATA3+ cells in inside and outside cells at stage V	165
12.3	Quantification of the contribution of YAP+ and GATA3+ cells in ICM and TE cells at stage VI	166
12.4	Quantification of the contribution of YAP+ and GATA3+ cells in ICM and TE cells at stage VII	166
12.5	Colocalisation of nuclear YAP and GATA3 in the inside cells of control and ROCK-inhibited embryos.....	167
12.6	Colocalisation of nuclear YAP and GATA3 in the outside cells of control and ROCK-inhibited embryos.....	168

1 Summary

Preimplantation development in mammals leads to the formation of a blastocyst composed of trophoblast (TE) and inner cell mass (ICM). TE comprises the polarised outer cells of the embryo, involved in implantation and formation of the embryonic part of the placenta, while ICM gives rise to epiblast (Epi) and primitive endoderm (PrE). Epi will further develop into the embryo proper, whereas primitive endoderm (PrE) contributes to the future endoderm of the yolk sac. Correct differentiation of TE lineage is essential for successful implantation and pregnancy.

The Hippo pathway is a crucial signalling cascade, found in various mammalian cell types, involved in stem cell potency, regulation of cell proliferation and differentiation. Additionally, research on the mouse model uncovered the Hippo pathway involvement in TE differentiation in the preimplantation embryo. A distinct Hippo pathway activity between outside and inside cells during preimplantation mouse embryo development regulates proper TE and ICM differentiation.

Several studies proposed the rabbit as a convenient and valuable model for studying trophoblast development in mammalian species. This work presents evidence for the involvement of the Hippo pathway in TE/ICM specification in the rabbit embryo by the detailed analysis of localisation of selected proteins from the early morula to the blastocyst stage. Moreover, the relative levels of expression of specific genes involved in Hippo pathway regulation were compared between various preimplantation rabbit embryo stages. A link between Rho kinase (ROCK) and TE lineage specification has been demonstrated recently. Rho-ROCK cascade is considered to be a key factor in apicobasal polarisation, cell adhesion and correct trophoblast differentiation. Additionally, ROCK has been confirmed to regulate the activity of the Hippo pathway during mammalian preimplantation development. Following the initial discovery, I examined the influence of the chemical ROCK inhibition on rabbit embryonic development. Immunofluorescence did not indicate differences in YAP and GATA3 protein levels between control and ROCK-treated embryos, however, ROCK inhibition by Y27632 disturbs rabbit embryo cavitation and drives an abnormal distribution of aPKC and F-actin. My research sheds new light on TE differentiation in rabbit embryos.

Obtained results let me compare the rabbit model with available knowledge about other mammalian models, indicating differences and similarities in cell polarisation and the Hippo pathway regulation during the first cell-fate decision.

2 Streszczenie

W trakcie rozwoju przedimplantacyjnego, u ssaków dochodzi do powstania blastocysty składającej się z trofektodermy (TE) oraz wężła zarodkowego (ICM). TE to pozazarodkowa linia komórkowa powstające ze spolaryzowanych komórek zewnętrznych, otaczająca ICM, powstały z komórek wewnętrznych. TE jest zaangażowana w późniejszy proces implantacji oraz w powstawanie zarodkowej części łożyska, natomiast ICM różnicuje dalej w kierunku epiblastu (Epi) oraz endodermy pierwotnej (PrE). W trakcie dalszego rozwoju, Epi daje początek wszystkim komórkom ciała zarodka oraz części błon płodowych, z kolei komórki PrE tworzą pęcherzyk żółtkowy. Prawidłowe różnicowanie TE jest kluczowe dla właściwego przebiegu procesu implantacji oraz utrzymania ciąży.

Zaangażowanie szlaku sygnałowego Hippo w regulację potencji komórek macierzystych, proliferacji czy różnicowania komórek, zostało potwierdzone w badaniach na wielu typach komórek. Co więcej, w przedimplantacyjnych zarodkach myszy, gdzie szlak Hippo został obszernie zbadany, stwierdzono jego kluczową rolę w trakcie różnicowania TE. Odmienna aktywność szlaku Hippo pomiędzy zewnętrznymi i wewnętrznymi komórkami zarodka inicjuje proces różnicowania w kierunku TE lub ICM.

Do tej pory rola szlaku Hippo nie została zbadana w trakcie przedimplantacyjnego rozwoju królika, choć gatunek ten wydaje się być obiecującym oraz wartościowym modelem do badań związanych z rozwojem trofektodermy u ssaków.

W tej pracy przedstawiłam dowody na obecność szlaku Hippo w różnicowaniu TE/ICM w zarodku królika poprzez szczegółową analizę immunolokalizacji wybranych białek od stadium wczesnej moruli do stadium blastocysty. Także względny poziom ekspresji

genów zaangażowanych w regulację szlaku Hippo został porównany między poszczególnymi stadiami rozwojowymi królika.

W zarodku myszy kaskada Rho-ROCK uważana jest za kluczowy czynnik regulacji polaryzacji szczytowo-bocznej, adhezji komórek, a także prawidłowego różnicowania TE. W moich badaniach sprawdziłam wpływ inhibicji kinazy ROCK na przedimplantacyjny rozwój królika. Sygnał immunofluorescencyjny białek YAP oraz GATA3 nie różnił się między zarodkami kontrolnymi oraz traktowanymi inhibitorem ROCK (Y-27632), chociaż inhibicja ROCK zaburzyła proces kawitacji oraz przyczyniła się do nietypowej dystrybucji białek aPKC oraz F-aktyny.

Moje badania rzucają nowe światło na zagadnienie różnicowania TE w zarodkach królika. Uzyskane wyniki pozwoliły porównać model królika z dostępną wiedzą na temat innych modeli ssaków, wskazując na różnice i podobieństwa w polaryzacji komórek i regulacji szlaku Hippo podczas pierwszej decyzji o losach komórek.

3 Abbreviation list

Ajs – Adherent junctions

AMOT – Angiomotin

AMOTL1 – Angiomotin-like 1

AMOTL2 – Angiomotin-like 2

ART – Artificial Reproduction Techniques

BSA – Bovine Serum Albumin

CDX2 – transcription factor, caudal – related homeobox 2

dpc – days post coitum

dpi – days post insemination

DS – Donkey Serum

E – Embryonic day

EGA – Embryonic Genome Activation

EPI – epiblast

FBS – Foetal Bovine Serum

GATA3 – GATA binding protein 3

hpc – Hours post coitum

ICM – Inner Cell Mass

ivc – in vitro culture

LATS1/2 – large tumour suppressor kinase 1 and 2

MTS1/2 – mammalian sterile 20-like 1 and 2

NF2 – Neurofibromin type 2

OCT4 - Octamer-binding transcription factor 4, the transcriptional factor associated with ICM lineage

PBS – Phosphate-Buffered Saline

PBX – Phosphate-Buffered Saline with TRITON-X

PFA – Paraformaldehyde

p-ERM – phosphorylated Ezrin-Radixin-Moesin complex, apical polarity markers

p-Ezrin – phosphorylated Ezrin

PrE – Primitive Endoderm

RDH – culture medium composed of media: RPMI 1640, DMEM, Ham’s F10, in ratio 1:1:1 (culture medium)

ROCK – Rho-associated kinases

SOX2 – transcription factor, Sex determining region Y box containing gene 2

SOX17 – transcription factor, SRY - a box containing gene 17, primitive endoderm marker

TAZ (WWTR1) – WW domain containing transcription regulator 1

TCM199 – Tissue Culture medium 199 (manipulating medium)

TE – Trophectoderm

TEAD1-4 – TEA domain 1-4

Tjs – Tight junctions

TL – Transmitted light

YAP – Yes-associated protein, Hippo pathway coactivator

4 Introduction

4.1 Preimplantation development of the mammalian embryo

Mammalian preimplantation development begins in the oviduct, where a diploid zygote is formed following the fusion of the haploid gametes: an oocyte and a sperm. During the first series of embryo cleavages (mitotic cell divisions), the embryo cells, called blastomeres, become smaller with each cell division, however, the total mass and volume of the embryo do not change (Ducibella et al. 1975). This contributes to creating a multicellular structure called the morula. During the next rounds of cell divisions, the embryo forms a fluid-filled cavity in the process commonly known as cavitation (Ducibella et al. 1975). The timing of different events during the early development described above is species-specific. Size and embryo cell number also vary across mammalian species.

Embryo development depends on maternal proteins, RNA, and storage materials accumulated in the oocyte before fertilisation (Telford, Watson, and Schultz 1990). During initial embryo cleavages, maternal transcripts progressively degrade, and then specific events prepare blastomeres for embryonic genome activation (EGA). The EGA in mammals occurs during the first several cleavages, whereas its specific timing varies among species (Telford, Watson, and Schultz 1990; Schultz 1993). For instance, in rabbits, EGA occurs between 3-4 cell stage (Léandri et al. 2009), while in cattle and sheep it is observed not earlier than 8-16 cell stage (Crosby, Gandolfi, and Moor 1988; Meirelles et al. 2004). The preimplantation period ends with the blastocyst hatching and implanting into the endometrium of the uterine wall. The length of the preimplantation period in mammals greatly varies between species, from 4.5 days in mice (Yoshinaga 2013), 7-9 days in humans (Muyan and Boime 1997), 14 days in pigs (Papaioannou and Ebert 1988), and 20-21 days in cattle (Pedersen et al. 2017). During this period of embryogenesis, multiple crucial events and changes must take place in the embryo in order to ensure the proper developmental program through consecutive stages. For rabbit preimplantation development, which lasts around 6 days (Hoos and Hoffman 1980; Hoffman, Breinan, and Blaeuer 1999), a staging

classification system (stage I-XII) was adapted based on the total cell number, and corresponding to a number of cell division rounds that the embryo cells have undergone (Piliszek, Madeja, and Plusa 2017). Based on our observations, compaction of the morula takes place between 1.5-3.0 dpc, and then cavity formation begins around 3.0-3.25 dpc. During early blastocyst development at 3.25-3.75 dpc embryos are highly asynchronous, and blastocysts at all stages between VI-VIII can be found in rabbit uterus at each time point. Finally, implantation occurs at 6.0 dpc (Hoos and Hoffman 1980; Hoffman, Breinan, and Blaeuer 1999). Morphological changes of the rabbit embryo during preimplantation development, their timing and relation to other events are depicted in **Figure 1**.

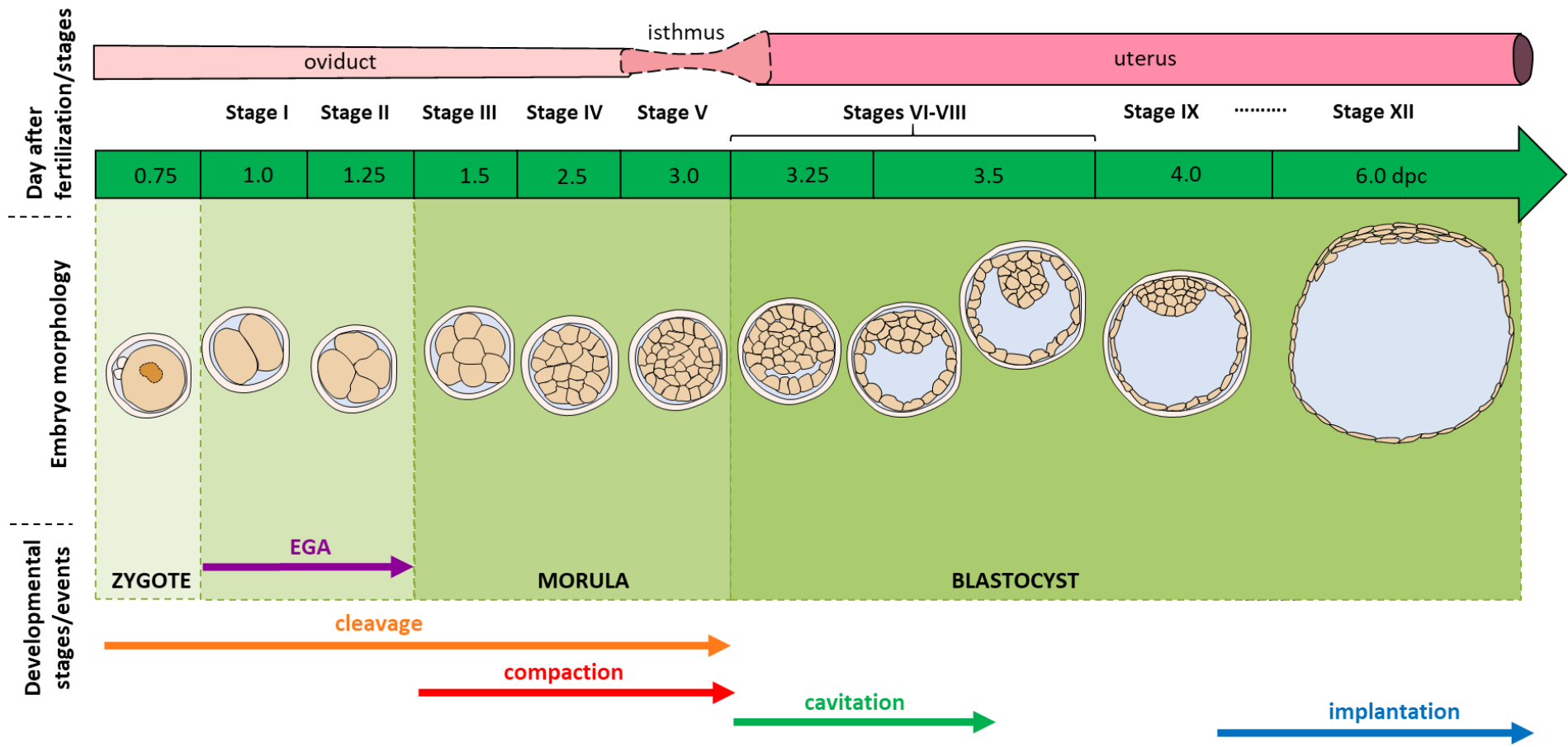


Figure 1. The timeframe of the rabbit embryo development showing morphology changes at subsequent stages

4.2 Embryo compaction

At initial stages of mammalian embryo development, several crucial morphogenetic events are required for proper blastocyst formation later on. During compaction, which is the first of these events, adjacent spherical blastomeres start to adhere more to each other, increasing the surface area in physical contact. This process changes the embryo from one with clearly identifiable cells into a tightly packed structure where blastomeres' outlines are not easily distinguishable (Tarkowski 1959; Tarkowski and Wróblewska 1967; Tarkowski et al. 2010).

It was proposed in previous studies that those changes occur due to the reorganisation of cytoskeleton proteins and the formation of intercellular connections between blastomeres. Proteins involved in the compaction process include E-cadherin and α - and β -catenins, actin and keratins (T. P. Fleming et al. 1994; Aberle, Schwartz, and Kemler 1996; C. L. Adams et al. 1998; Lim et al. 2020). The activity of E-cadherin, a calcium ion-dependent adhesion protein, is required for the compaction process to occur (Sefton et al. 1996; Vestweber et al. 1987). Culturing mouse embryos in a calcium-free medium or in a medium supplemented with antibodies blocking E-cadherin causes inhibition of the compaction process, and placing already compacted embryos in such a modified medium causes complete decompaction of embryos at the morula stage (Tarkowski 1959; Ducibella et al. 1975; Ducibella and Anderson 1979; Shirayoshi, Okada, and Takeichi 1983). Furthermore, similar observations were confirmed in humans (De Paepe et al. 2013; Zakharova, Zaletova, and Krivokharchenko 2014), swine (Matsunari et al. 2020) and hamsters (H. Suzuki et al. 1999). Additionally, mouse embryos with E-cadherin knockout (both maternal and zygotic) exhibited disruption of the apical and basolateral domains segregation and altered formation of the blastocyst. The ratio of TE and ICM cells was disturbed in those mutants (Stephenson, Yamanaka, and Rossant 2010). Furthermore, in E-cadherin deficient mutants *Cdx2* was expressed in a larger proportion of inside cells than in wild-type embryos, suggesting that E-cadherin is responsible for the restriction of *Cdx2* expression to TE cells (Stephenson, Yamanaka, and Rossant 2010).

The timing of compaction initiation and the duration of this process differ between mammalian species. For example, in mice and rats, compaction is initiated at the 8-cell stage (Pratt et al. 1982; Reeve 1981), in humans at the 8-16-cell stage (Nikas et al. 1996), in cattle at the 16-32-cell stage (Koyama et al. 1994), and in porcine embryos the process begins at the 16-32-cell stage, however, the full compaction occurs shortly before blastocyst cavity formation at the 32-64-cell stage (Reima et al. 1993). In rabbits, some researchers suggest the initiation of compaction at the 8-16 cell stage (Sultana et al. 2009), while other studies report it at the 32-64 cell stage (Koyama et al. 1994). It has been demonstrated in several mammalian species that blastomeres undergo brief decompaction and re-compaction during each successive cell division, including bovine (Betteridge and Fléchon 1988; Ducibella et al. 1977), porcine (Reima et al. 1993) and mouse embryos (Skrzecz and Karasiewicz 1987).

4.3 The cell polarity

Although compaction and acquisition of polarity are initiated at a similar time during preimplantation development and in the presence of similar protein complexes (Kidder and McLachlin 1985; Levy et al. 1986), they are regulated independently (Hirate et al. 2013; Pratt et al. 1982; Stephenson, Yamanaka, and Rossant 2010). As a result of the cell polarisation, two regions can be distinguished in the blastomere, namely the apical and basolateral domains. These surface areas differ in the distribution of cytoskeletal elements and plasma membrane proteins, as described below (Johnson and Ziomek 1981a; Maro et al. 1984; Johnson and Ziomek 1981b) (**Figure 2**).

Phosphorylation of the protein Ezrin, which belongs to the ERM (Ezrin/Radixin/Moesin) family and is localised in the microvilli of outer cells is one of the first signs of the initiation of polarisation (Reeve and Ziomek 1981). Ezrin was described as a linker between the actin cytoskeleton and cell membrane proteins (Bretscher 1983; Hanzel et al. 1991; Dard et al. 2004). The spherical blastomeres of pre-compacted embryos contain microvilli evenly distributed on their entire cell surface, however as soon as blastomeres start polarisation, the microvilli become restricted to the apical domain of the outer cells (Reeve and Ziomek 1981).

The initiation of polarisation is also evidenced by the localisation of cell polarity factors, including the apical polarity protein complex aPKC-PAR, which consists of aPKC (atypical protein kinase C), and the PAR group of proteins such as Pard3 (partitioning defective 3 homologue) and Pard6B (partitioning defective 6 homologue) (Plusa et al. 2005; Vinot et al. 2005; Eckert et al. 2004; Alarcon 2010). Complementary, restricted distribution of the factors Emk1 (ELKL motif kinase 1/mammalian homologue of PAR-1) and Scrib (Scribble) contribute to the definition of the basolateral compartment (Vinot et al. 2005; Yamanaka et al. 2006) (**Figure 2**). The activity of PARD3 and aPKC are suggested to be essential for correct TE differentiation. Plusa and co-authors have shown that the disruption of these proteins leads to the failure of the TE lineage differentiation (Plusa et al. 2005).

Differential distribution of proteins in cell membranes, associated with the formation of adherens junctions (AJs) on the basolateral surface and tight junctions (TJs) on the apical-lateral surface, is considered to be an indicator of cell polarisation. Proteins involved in this process are E-cadherin, α - and β -catenins, occludins, claudins, JAM-1 or ZO-1 proteins (C. Y. Leung, Zhu, and Zernicka-Goetz 2016; Mihajlović and Bruce 2017; Srinivas and Rodriguez 2017; Rodriguez-Boulan and Macara 2014). Tight junctions localised in the outer cells are required for cavity and blastocyst formation (Moriwaki, Tsukita, and Furuse 2007), by ensuring the integrity of the TE epithelium and restricting the flow of ions and solutions. Additionally, cell polarity is also reflected in the asymmetric distribution of microtubule populations (Houliston, Pickering, and Maro 1987; Yan et al. 2006).

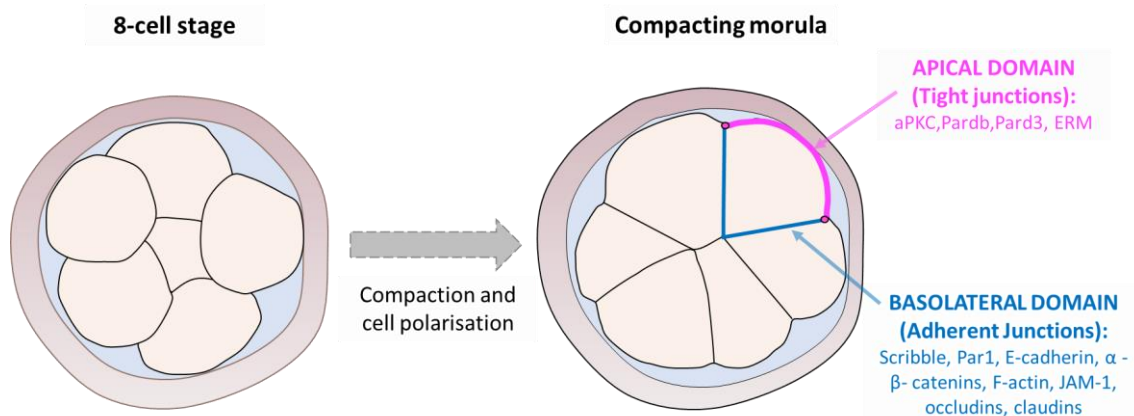


Figure 2. Mouse at 8-cell stage undergoes morphogenetic event – the compaction. Simultaneously with compaction, the apicobasal polarity is established in the outer cell as represented by the apical (magenta) and basolateral (blue) membrane domains of specific blastomeres.

4.4 Trophectoderm versus Inner Cell Mass – the first cell-fate decision

Prior to implantation, the embryo cells become specified as precursors of the future embryonic and extra-embryonic lineages. The first cell-fate decision leading to the generation of the TE and ICM depends on multiple factors. During decades of research on the first lineages specification, three different models were hypothesised and tested. The first model, named “inside-outside”, was proposed by Tarkowski and Wróblewska and postulated that the positional information of each cell in the embryo at the morula stage dictates cell fate. The outside cells then follow the TE fate, and the inside cells adopt ICM fate (Tarkowski and Wróblewska 1967).

The second model, known as “cell polarity” was proposed by Johnson and Ziomek. They postulated that at the 8-cell stage, embryo undergoes compaction and achieves apicobasal polarity. The apical domain is formed by microvilli, while the basolateral domains adhere to the other cells. According to the “cell polarity” model, the apicobasal polarity establishment between 8-cell to 16-cell stage is critical for the first cell-fate specification. Acquisition of polarity by the definition of an apical domain in the cell depends on the area of membrane exposed to the outside as a result of cell division (Anani et al. 2014; Korotkevich et al. 2017). This area of the cell membrane may contribute to daughter cells in different ways. Following symmetric cell division, when the division plane is parallel to the embryo axis, both daughter cells inherit apical domains. In case of asymmetric cell division, where the division plane is perpendicular to the embryo axis, only one daughter cell inherits the apical domain and becomes polar. In this model, two different cell fates are generated via asymmetric inheritance controlled by cell polarisation and following asymmetric cell division (Johnson and Ziomek 1981b).

The third model, named “self-organisation”, or “reaction-diffusion pattern mechanism”, postulated by Y. Yamanaka and colleagues, relies on more recent observations of the cell-fate decision phenomenon. The gene expression is controlled

by cells in a self-governing manner, the polarised cells adopt the TE fate, and the apolar cells become the ICM. Cell-fate differentiation depends on various factors such as cell division pattern, cell shape, cell adhesion and expression of lineage-specific factors (Yamanaka et al. 2006; Müller et al. 2012; Wennkamp et al. 2013).

To summarise, in mouse embryo development, the first cell fate decision occurs during the cleavage time at 8-16-cell stage. The outside cells are polarised, forming the TE, whereas the apolar inside cells follow the ICM fate (Johnson and Maro 1984; Pratt et al. 1982). As a result, the blastocyst is composed of the outside epithelial layer of TE, which surrounds a cavity, while ICM is attached to one side of the TE.

4.5 Trophectoderm - specific markers

During preimplantation development, the establishment of two distinct cell lineages, i.e., TE and ICM, is required to form a blastocyst. An essential role of trophoctoderm epithelium is to act as a barrier controlling small molecules and fluid exchange and accumulation during blastocyst maturation (Cockburn and Rossant 2010). Specific transcription factors control correct TE development. Expression of the ***Cdx2* gene (Caudal-type homeodomain 2)** in the mammalian TE is highly conserved. The presence of CDX2 has been found in TE in species such as mice (Strumpf et al. 2005; Ralston and Rossant 2008; Jedrusik et al. 2010), humans (Niakan and Eggan 2013), macaques (Nakamura et al. 2006), cattle (Madeja et al. 2013; Goissis and Cibelli 2014), pigs (Bou et al. 2017), rabbits (Piliszek, Madeja, and Plusa 2017) and marsupials (Morrison et al. 2013). In mouse embryos, CDX2 is detected in cell nuclei from the 8-cell stage onwards (Niwa et al. 2005; Yagi et al. 2007; Dietrich and Hiiragi 2007). Later, the CDX2 protein is found mainly in the outer cells and its signal progressively reduced in the inner cells (Strumpf et al. 2005; Ralston and Rossant 2008). CDX2 is required for normal trophoctoderm formation. It was evidenced in mouse embryos that depletion of CDX2 protein results in the inability of the embryo to hatch from the *zona pellucida*. Additionally, the loss of *Cdx2* in ICM cells may be understood as a decrease in their cell potency and the inability to differentiate into TE (Strumpf et al. 2005; Ralston and Rossant 2008). It has been shown that the ICM-associated factor *Oct4* (Octamer-

binding transcription factor 4) and *Cdx2* are co-expressed in the outer cells of the morula and also in TE of the early mouse blastocyst (Dietrich and Hiragi 2007; Ralston et al. 2010). Therefore, it was shown that in already formed TE cells, the expression level of *Oct4* subsequently decreases due to the increasing *Cdx2* expression (Strumpf et al. 2005).

Several studies suggest that other transcription factors are involved in TE differentiation and development, such as TEAD4, EOMES, TFAP2C and GATA3 (Russ et al. 2000; Niwa et al. 2005; Yagi et al. 2007; Nishioka et al. 2008; Home et al. 2009; Choi et al. 2012; Cao et al. 2015; Gerri et al. 2020). The protein TEAD4, which belongs to **TEAD family (TEAD1-4)**, was found in mouse embryos as an early transcription factor that controls trophoctoderm specification. Its crucial role in TE development is supported by the fact that *Tead4* deficient embryos fail to cavitate (Nishioka et al. 2008). TEAD4 protein is detected in the cell nuclei from the 4-cell stage onward in mice (Nishioka et al. 2008; Home et al. 2012), while in porcine embryos TEAD4 is detected from the morula stage (Emura et al. 2016) and in bovine embryos from the 8-cell stage onward (Fujii et al. 2010; Ozawa et al. 2012; Sakurai et al. 2017). In Sawada and colleagues work, mouse *Tead4*-deficient embryos exhibited weak *Cdx2* expression at the morula stage and disrupted TE development (Sawada et al. 2005). However, in bovine embryos, *TEAD4* downregulation does not affect *Oct4*, *Nanog*, *Cdx2* or *Gata3* expression, suggesting that TEAD4 is not a crucial factor in bovine TE differentiation (Sakurai et al. 2017). In rabbit embryos, it has not yet been determined when *Tead4* expression is initiated or whether it affects trophoctoderm differentiation and development. Other TEAD family members analysed in mouse embryos, *Tead1*, *Tead2* are also expressed during preimplantation development. However, lack of *Tead1* or *Tead2* expression does not affect TE specification (Sawada et al. 2008), while *Tead3* expression is not detected before implantation (Nishioka et al. 2008; Home et al. 2012).

Another TE fate-related protein, **EOMES (Eomesodermin)**, is detected in mouse embryos in every cell from the zygote stage up to the early blastocyst, but it becomes restricted to TE cells as soon as 3.5 dpc. However, *Eomes* expression is not required for the initial TE/ICM decision in mice (Strumpf et al. 2005; McConnell et al. 2005). It is worth to mention that studies in mouse show that although *Eomes*-deficient embryos

cannot form blastocyst cavity, *Cdx2* expression level remains unchanged in these mutants (Strumpf et al. 2005).

The transcription factor **AP-2 γ (TFAP2C)** was found to be an important regulator of blastocyst formation in mice. Prior to the morula stage, TFAP2C is widely detected across all cells. Then, it is restricted to the outer cells throughout the blastocyst development, while being downregulated in the inside cells (Choi et al. 2012). In a different study, the role of TFAP2C in mouse TE differentiation was analysed more widely. Namely, they reported that at the 2-8-cell stage, this regulatory factor plays a key role in initiating CDX2 activity and cell polarisation. From 8-cell stage up to the morula stage, TFAP2C is involved in the regulation of the critical player associated with the TE differentiation - the Hippo pathway, described in detail in subsequent chapters. TFAP2C, through transcriptional regulation of genes such as *Pard6b* and *Rock1/2*, is involved in Hippo pathway downregulation in TE cells. Additionally, mouse embryos with loss of TFAP2C function or after ROCK1/2 kinase inhibition exhibited altered signalling of the Hippo pathway and downregulation of *Cdx2* expression (Cao et al. 2015).

GATA3 (GATA binding protein 3) is another important player involved in TE differentiation in mammals. It is known as a downstream effector of TEAD4 and was found to be a lineage-specific transcription factor in TE cells in murine (Ralston et al. 2010; Home et al. 2009; Gerri et al. 2020), human (Gerri et al. 2020), bovine (Ozawa et al. 2012; Gerri et al. 2020; Smith et al. 2010) and horse embryos (Iqbal et al. 2014). Previous studies on a mouse model have shown that *Gata3* expression is detected as early as 4-cell stage and expressed continuously until blastocyst stage when it becomes restricted to the nuclei of TE cells. *Gata3* is selectively induced in TE cells of the mouse blastocyst and its downregulation at the morula stage affects blastocyst cavity formation (Home et al. 2009).

Unpublished data from our group revealed that GATA3 is localised in nuclei in the vast majority of outside cells in the rabbit embryo shortly after cavitation, suggesting that it is an earlier marker of TE than CDX2. The pictures below demonstrate the localisation by immunofluorescence of CDX2 and GATA3 in the rabbit embryo at 3.25 dpc (**Figure 3**).

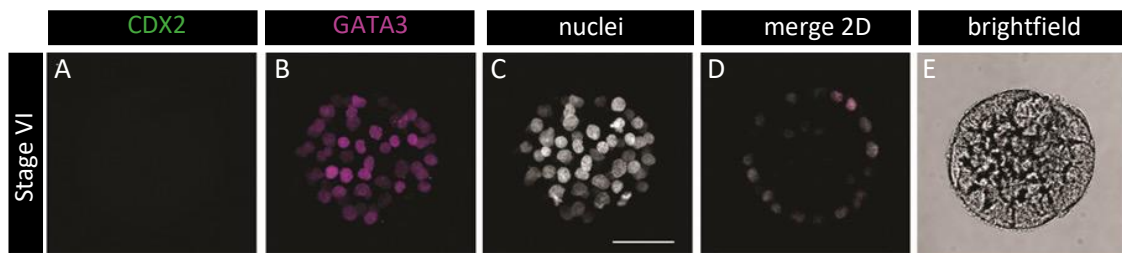


Figure 3. CDX2 and GATA3 colocalisation in rabbit embryos at stage VI (3.25 dpc).
 Panel of confocal images: 3D projections showing rabbit embryo stained for CDX2 (A), GATA3 (B), and chromatin (C). Merge 2D confocal image (D), brightfield 2D image (E). Scale bar = 50 μ m (K. Filimonow and co-authors, manuscript in preparation)

4.6 The Hippo pathway signalling

Multiple studies have revealed that the Hippo pathway plays a critical role in regulating a variety of important biological processes, from single cell-fate decisions to tissue structure. The Hippo pathway was first detected in *Drosophila melanogaster* as a crucial regulator of tissue growth, and it is evolutionarily highly conserved, with its homologs found in yeast, roundworms, mice or even humans (Neto-Silva, de Beco, and Johnston 2010; Rock et al. 2013; Harvey, Zhang, and Thomas 2013; Lee et al. 2019). The characteristic name of the cell pathway originally comes from the kinase Hippo (Hpo) in the fly, where mutations in the gene encoding the Hippo kinase induce a tissue overgrowth, also called a hippopotamus-like phenotype (Saucedo and Edgar 2007).

It has been shown in recent studies on mammals that the Hippo pathway is involved in stem cell potency and regulation of cell proliferation and differentiation. In addition, the Hippo pathway was also found as a regulator of cell fate decision during early mouse development, and moreover, abnormal regulation of the pathway was implicated in cancer development (Pan 2007; Saucedo and Edgar 2007; Reddy and Irvine 2008; Pan 2010; Genevet and Tapon 2011).

Multiple studies on different mammalian species confirmed that involvement of the Hippo pathway in TE differentiation is also evolutionarily highly conserved (Nishioka et al. 2009; Sasaki 2017a; Gerri et al. 2020; Sharma and Madan 2020; Emura et al. 2020). Recently, C. Gerri and colleagues confirmed similarities in the regulation of Hippo

pathway across mammalian species such as mice, cattle and humans, during the transition from the morula stage to the blastocyst (Gerri et al. 2020).

4.6.1 Major components of the Hippo pathway in mammals

The Hippo pathway cascade elements regulate cell proliferation, survival, mobility, cell potency and differentiation (reviewed in Ma et al. 2019). In the Hippo pathway cascade, the main core is composed of kinases MST1 and MST2 (mammalian sterile 20-like 1 and 2), kinases LATS1 and LATS2 (large tumour suppressor kinase 1 and 2) (Gumbiner and Kim 2014) and downstream regulators, coactivators YAP (Yes-associated protein), and TAZ (WWTR1 - WW domain-containing transcription regulator protein) (Nishioka et al. 2009; K. Zhang et al. 2015).

In mouse post-implanting embryos, MST kinases were confirmed as a crucial factors in cell proliferation inhibition and apoptosis (Oh et al. 2009; Du et al. 2014). In cattle preimplantation embryos, MST1/2 were detected in the cytoplasm of blastomeres, suggesting these proteins are evolutionarily conserved in mammals (Sharma and Madan 2020).

The coactivator YAP (Yes-associated protein) is a major downstream regulator of the Hippo pathway (Dong et al. 2007). TAZ (also called WWTR1, WW domain-containing transcription regulator protein) is known as a mammalian YAP paralog, which is in a similar way controlled by the Hippo pathway (Lei et al. 2008). When LATS kinases are activated, YAP/TAZ activity is blocked by phosphorylation, leading to cytoplasmic retention of these factors. When LATS kinases are phosphorylated (the Hippo pathway is switched off), YAP and TAZ translocate from the cytoplasm to the nucleus and activate the TEAD family transcription factor, thus resulting in the expression of target genes (Zhao et al. 2010). The control of nuclear-cytoplasmic localization of YAP/TAZ proteins by LATS kinases was described in blastomeres of early mouse embryos (Sawada et al. 2008; Lorthongpanich et al. 2013). Knocking out the *Lats1/2* genes in the mouse embryo leads to an increased amount of nuclear YAP in the inside cells during preimplantation development (Nishioka et al. 2009). The regulation of cellular signalling pathways mediated by LATS occurs by transduction of cell-cell contact during

lineage specification in the embryo (Sasaki 2015). To summarise, the Hippo pathway is a major player in cell-fate decision regulation in preimplantation embryos, and it can be controlled by multiple factors.

4.6.2 The Hippo pathway upstream signals - regulating factors

The Hippo pathway is strictly controlled by endogenous and exogenous factors, including hormones and stress signals, mechanical forces, cell adhesion, cell polarity and cell-cell contact. Most hormonal factors operate through G protein-coupled receptors (GPCRs) (reviewed in Ma et al. 2019).

4.6.2.1 Hormonal signals, enzymes and bioactive mediators

Multiple studies have shown that hormones and growth factors mediated by GPCRs are involved in YAP/TAZ activation. GPCRs are members of the large surface receptors group (approximately 1000 types), which are coupled to 15 different $G\alpha$ proteins (Wettschureck and Offermanns 2005). These receptors mediate various diffusive signals resulting in modulation of the Hippo pathway activity in a positive or negative way, depending on the type of signals, receptors or adaptor proteins. For example, lysophosphoric acid (LPA), sphingosine-1-phosphate (S1P), thrombin, angiotensin II, and estrogen via GPCRs coupled to $G\alpha_{12/13}$, $G\alpha_{i/o}$, or $G\alpha_q/11$ ligands contribute to YAP/TAZ activation, which is followed by inhibition of LATS1/2 activity (F.-X. Yu et al. 2012; Zhou et al. 2015). Ligands signalling by $G\alpha_s$ -coupled GPCRs, such as glucagon or epinephrine, attenuate YAP/TAZ activity and stimulate LATS1/2 activity (F.-X. Yu et al. 2012; Zhou et al. 2015).

In addition, it was found that the GPCRs action on YAP/TAZ can be mediated by the Rho family GTPases (RHOA). The negative regulation of the Hippo pathway occurs by the $G\alpha_{12/13}$ - and $G\alpha_q/11$ -coupled GPCRs, which activate RHOA. This leads to LATS1/2 inactivation by RHOA, mediated by F-actin-dependent mechanism, which is still poorly understood (F.-X. Yu et al. 2012).

4.6.2.2 Stress signals

The Hippo pathway downstream regulators YAP and TAZ are involved in multiple biological processes, one of which is the cellular stress response. Biological events such as stress signals, including mechanical stress, hypoxia or osmotic stress, regulate the Hippo pathway in cells (DeRan et al. 2014; Gailite, Aerne, and Tapon 2015; W. Wang et al. 2015).

During organogenesis, tissue homeostasis maintenance requires correctly organised cells. It was proposed that the mechanical forces generated via cell-cell contact, cell-extracellular matrix interactions and microenvironment can control cell growth, morphogenesis, proliferation, migration and death through specific transcription factors (Bissell and Aggeler 1987). It was discovered that YAP and TAZ are mechanically regulated, transmitting physical cues to modulate gene expression and eventually the cell fate (Kim et al. 2011; Aragona et al. 2013).

It has been confirmed that RHOA is involved in regulating YAP/TAZ activity by promoting actin polymerisation (Seo and Kim 2018). In other studies, it was revealed that actin depolymerisation contributes to LATS1/2 activation leading to YAP/TAZ cytoplasmic retention (Sawada et al. 2005; Dupont et al. 2011). It has been confirmed in various cell types that the Hippo pathway core cascade, including LATS1/2, responds to physical cues by modulating the activity of YAP/TAZ (Wada et al. 2011; Codelia, Sun, and Irvine 2014; L. Wang et al. 2016; K.-C. Wang et al. 2016; Fletcher et al. 2018). It is most likely that the RHOA is indirectly responsible for LATS1/2 inhibition (Zhong et al. 2013; F.-X. Yu et al. 2012). Therefore, different mechanical signals and matrix stiffness may modulate the Hippo pathway through the RHOA pathway. Additionally, it was revealed that hypoxic conditions also activate YAP/TAZ by LATS1/2 inhibition, which leads to attenuation of the Hippo pathway (Ma et al. 2019). It was revealed that hyperosmotic stress prevents the nuclear localisation of YAP/TAZ by promoting the activation of LATS1/2 (K. Zhang et al. 2015; Moon et al. 2017; Hong et al. 2017). Altogether, studies that employ cell models indicate that mechanical factors are essential elements regulating the Hippo pathway.

4.6.2.3 Cell adhesion and cell polarity

Cell-cell junctions in epithelial cells are composed of AJs, TJs and desmosomes. The cell adhesion-related proteins such as zonula occludens (ZO), occludins and claudins are transmembrane proteins (Tsukita et al. 2008). The establishment of apicobasal polarity is strongly dependent on the cell position in the embryo. A key feature of all epithelial cells is apicobasal polarity, where the apical domain defines one side of the cell in contact with the outer environment. Meanwhile, the opposite side - the basolateral domain - remains in contact with other neighbouring cells. Furthermore, the apical and basolateral membranes are associated with conserved sets of proteins, including aPKC, PARD3, and PARD6, for the apical side and PAR1 (also known as EMK1), SCRIB and LGL for the basolateral side (Rodriguez-Boulan and Macara 2014).

E-cadherin is a critical component of adherens junctions (AJs), forming protein complexes at the cell-cell interface in many mammalian epithelia (Niessen and Gottardi 2008). It has been shown in mice that the lack of E-cadherin contributes to defective adherens junctions, which further disrupt TJs (Larue et al. 1994; Ohsugi et al. 1997). Since Hippo pathway signalling depends on cell-cell contact, it is understandable that the Hippo pathway regulation is impaired in E-cadherin-deficient embryos (Stephenson, Yamanaka, and Rossant 2010). Inhibition of E-cadherin-mediated cell-to-cell contact leads to the downregulation of the Hippo pathway, which blocks trophoblast development, resulting in abnormal further development (Nishioka et al. 2009; Stephenson, Yamanaka, and Rossant 2010).

The essential role of cell polarity during trophoblast specification was confirmed. The PAR-aPKC complex was found to be a central player in controlling the regulation of the apicobasal polarity of blastomeres (A. Suzuki and Ohno 2006; Assémat et al. 2008; Johnston and Ahringer 2010). Cell polarity factors are required for YAP/TAZ nuclear distribution in the outer cells to promote TE differentiation. It was previously discovered that loss or dysfunction of the apical domain proteins, including aPKC, PARD3, PARD6, is responsible for impaired blastocyst formation and for the hampering of YAP/TAZ nuclear distribution (Alarcon 2010; Hirate et al. 2013; 2015; Cao et al. 2015; Plusa et al. 2005; Korotkevich et al. 2017). Similar effects were also reported after loss of function of the component of the basolateral domain EMK1 (Hirate et al.

2013; 2015). Additionally, knocking down of *Prkci* and *Prkcz* (isoforms of the aPKC gene) causes ectopic localization of SOX2 in the outer cells of the mouse embryo (*mcPrkci*^{-/-}, *Prkcz*^{-/-}) (Korotkevich et al. 2017). All of the above suggests an essential role for apicobasal polarity in interpreting the inside-outside position.

AMOT family members, which includes angiomin (AMOT), angiomin-like 1 (AMOTL1), angiomin-like 2 (AMOTL2), is another component of the Hippo pathway signalling cascade. Members of this family were recently suggested to act as mediators between apicobasal polarity and the Hippo pathway regulation, subsequently being involved in cell fate specification (W. Wang, Huang, and Chen 2011; Hirate et al. 2013). These proteins are necessary to activate the Hippo signalling in the inside cells and promote YAP/TAZ nuclear localisation in outer cells (Zhao et al. 2011; Hirate et al. 2013; Chuen Yan Leung and Zernicka-Goetz 2013). Hashimoto and Sasaki reported that AMOT and AMOTL1 localisations are widely detected in ICM of early mouse blastocyst until EPI formation. However, it was found to be gradually decreased toward later blastocyst stages (Hashimoto and Sasaki 2019).

In outer cells, the Hippo pathway is inactivated due to the exclusion of AMOT from the basolateral membrane (where adherens junctions are located) and restriction to apical domains. However, AMOTs are not sequestered to the apical domains of TE cells; they are associated with AJs in the basolateral domains when apical-basal polarity is disrupted (Hirate and Sasaki 2014).

NF2 (Merlin) is another player within the Hippo pathway signalling, required for LATS1/2-dependent YAP/TAZ phosphorylation in the early embryo (Cockburn et al. 2013). It was discovered in the mouse embryo that the inhibition of NF2 results in ectopic YAP/TAZ localisation in inside cells, as well as atypical *Cdx2* expression in ICM cells. Therefore, it is a powerful evidence that the NF2 protein is an essential regulator of the Hippo pathway involved in preimplantation development of mouse embryos (Cockburn et al. 2013; Hirate et al. 2013).

Due to the formation of outer and inner cell compartments, the Hippo pathway is modulated differently accordingly, being position-dependent (Alarcon 2010). Additional studies have proposed that differential activity of the Hippo pathway is the consequence of variations in the cell-cell interactions. The proper establishment of the position-dependent Hippo pathway is thought to be a critical event during TE lineage

differentiation, which supports the inside-outside model (Nishioka et al. 2009; Hirate and Sasaki 2014).

4.6.2.4 Cell-cell contact

Cells growing in a colony stop their proliferation when they reach the appropriate confluence level, a phenomenon known as a contact inhibition. High cell density regulates the Hippo pathway by activating LAT1/2 kinases, causing YAP/TAZ to remain in the cytoplasm (Zhao et al. 2007). This effect contributes to the cytoplasmic localisation of YAP in inner cells of the morula and nuclear localisation in outer cells (Nishioka et al. 2009). As a result of the high confluence, the cells change shape, and there is a reduction in the adhesive surface area. The shape changes occurring in the cells cause inhibition of RHOA activity, which leads to a decrease in the generation of stress fibres, resulting in the inactivation of YAP/TAZ (Dupont et al. 2011; Wada et al. 2011; Aragona et al. 2013). The cell-cell interaction is the important regulatory factor which induces the proper position-dependent cell response in the Hippo pathway modulation. It can be assumed that similar interactions and regulations, as observed in the cell model, are also present in the embryo, however, it has not been confirmed yet.

4.6.3 The Hippo pathway downstream signal - regulating factors

The evolutionarily conserved Hippo pathway is regulated by the transcriptional coactivators YAP and TAZ and transcription factor TEAD4. YAP/TAZ localisation is crucial for the Hippo pathway, which activation/inactivation depends on the position of the cell in the mammalian embryo (**Figure 4**). When the Hippo pathway is active, YAP and TAZ are phosphorylated (p-YAP, p-TAZ) and arrested in the cytoplasm. Conversely, when the Hippo pathway is inactive, non-phosphorylated YAP/TAZ enters the nucleus (reviewed in Pan 2007, Lei et al. 2008; Nishioka et al. 2009).

Studies on mice have reported that at 8-16-cell stage, the Hippo pathway is activated in the inside cells, which leads to YAP/TAZ phosphorylation by AMOT-NF2-LATS signalling. In consequence, YAP/TAZ is excluded from the nuclei. Consequently, the

transcription factor TEAD4 remains inactive in the nucleus, and the TE-specific genes are not expressed. Thus, in the inside cells, the expression of *Oct3/4* is not suppressed, and these cells follow the ICM fate (Nishioka et al. 2009; Hirate et al. 2013). However, due to the inactivation of the Hippo pathway cascade in the outside cells, active forms of YAP/TAZ are translocated to nuclei and bind to TEAD4. The functional TEAD4-YAP/TAZ complex promotes the expression of TE-fate-associated genes, including *Cdx2*, *Gata3* and *Eomes* (**Figure 4**) (Nishioka et al. 2009; Pan 2010; Lorthongpanich et al. 2013; Meng, Moroishi, and Guan 2016; Sun and Irvine 2016; Negrón-Pérez, Zhang, and Hansen 2017).

Originally, Hippo pathway signalling involvement in the first cell-fate decision has been implicated by the analysis of *Tea4* knockout embryos, where TE cells exhibited decreased *Cdx2* levels and adopted ICM fate (Yagi et al. 2007; Nishioka et al. 2009). Therefore, it clearly demonstrates that TEAD4 is necessary for the activation of the TE-associated genes and for the suppression of ICM-specific factors in TE cells (Yagi et al. 2007; Nishioka et al. 2009). Unlike in mice, in preimplantation bovine embryos, p-YAP is localised in both the cytoplasm and nucleus and TAZ is distributed in the cytoplasm of most blastomeres during early embryo development (Sharma and Madan 2020). Although the current understanding of the Hippo pathway regulation is based on the mouse model, recent studies show that the Hippo pathway may be regulated differently in other species.

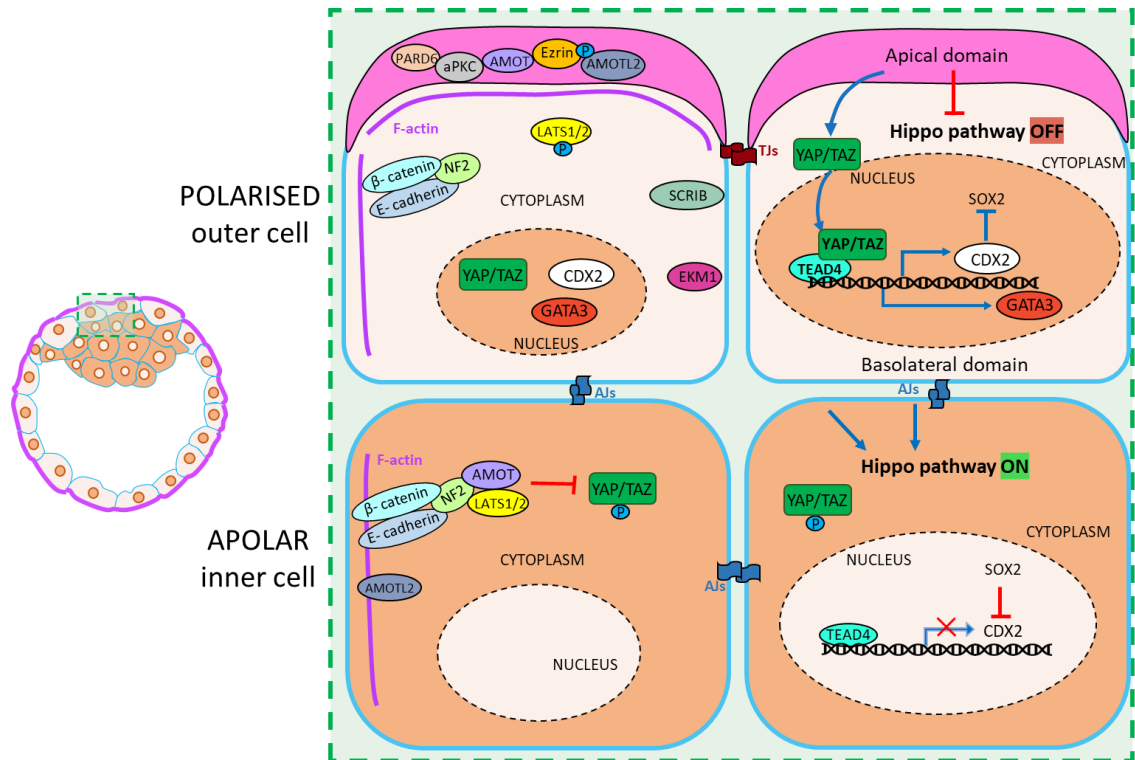


Figure 4. Regulation of trophoblast (TE) and inner cell mass (ICM) differentiation by the Hippo pathway in the mouse embryo. Apical-basal polarity in the inside and outside cells has been already established at the blastocyst stage in the mouse embryo. Polarity proteins including PARD3, PARD6, aPKC and the membrane-cytoskeleton linker p-Ezrin are localised in the apical membrane, whereas E-cadherin, b-catenin and SCRIB are restricted to the basolateral membrane, based on studies on the mouse model. In polarised TE cells, due to LATS1/2 suppression, the Hippo pathway is inactivated: YAP/TAZ translocates to the cell nucleus, activating the transcription of the TE-specific gene Cdx2. However, in non-polarised inner cells, the Hippo pathway is activated: due to LATS1/2-NF2-AMOT signalling, phosphorylated YAP and TAZ remain in the cytoplasm leading to the initiation of ICM-specific gene activation.

4.7 The role of the RHO-ROCK signalling in trophoblast differentiation in mammals

RHOA (RHOA, RHOB, RHOC) subfamily and RHO-associated, coiled-coil containing protein kinases (ROCK1, ROCK2) are important players during trophoblast specification. RHOAs belong to RHO small GTPases, whereas ROCK kinases are the main downstream regulators of RHO small GTPases. The function of RHO GTPases relies on switching between inactive (GDP-bound) and active (GT-bound) state, and this process is regulated by multiple upstream factors (Hodge and Ridley 2016). The active forms of RHOAs drive the activity of serine/threonine ROCK kinases. Both the

RHOA subfamily and ROCK1/2 play essential functions in multiple cellular events such as cell division, morphology, polarity, mobility and gene expression (Hodge and Ridley 2016). In addition, it has been suggested that modulations of the cytoskeletal actomyosin system (actin assembly/depolymerisation) contribute to many of RHO-ROCK actions (Hodge and Ridley 2016).

Previous studies have reported the expression of all RHOA subfamily and ROCK members in mouse embryos during preimplantation development (Hamatani et al. 2004; Zeng, Baldwin, and Schultz 2004; D. Xie et al. 2010; Kono, Tamashiro, and Alarcon 2014). The function of kinases of the RHOA family can be pharmacologically inhibited by the commonly used inhibitor C3 exoenzyme derived from *Clostridium botulinum* (Wilde et al. 2000; Vogelsgesang, Pautsch, and Aktories 2007).

ROCK inhibition has been achieved using multiple pharmacological agents, however, most studies use the specific small molecule Y-27632 (Davies et al. 2000). The RHO kinase inhibitors modify the conformation of the target protein, and prevent ATP-dependent phosphorylation, which blocks RHOA and ROCK binding. Y-27632, the highly potent and selective inhibitor of ROCK1/2, acts through competition with ATP for binding to the ROCK1/2 catalytic site. (Davies et al. 2000; Yamaguchi et al. 2006).

The first evidence regarding the involvement of RHO-ROCK in cell fate specification was provided in mouse embryos. Embryos cultured with the ROCK inhibitor Y -27632 from the 2-cell stage developed to the compact morula stage, but most of them failed to form a cavity. These embryos also exhibited disrupted tight junctions and cell polarity (Kawagishi et al. 2004). Moreover, ROCK inhibition at the blastocyst stage resulted in altered ICM morphology and a decreased cavity size and even caused fetal lethality during post-implantation development (Laeno, Tamashiro, and Alarcon 2013). RHOA pharmacological inhibition by C3 exoenzyme also results in impaired cavity formation (Kono, Tamashiro, and Alarcon 2014). Additionally, C3-mediated reduced expression of the TE-specific transcription factors *Cdx2* and *Gata3*, along with increased expression of the ICM-specific transcription factors *Nanog* and *Sox2*, was reported in the outer cells. Therefore, mouse embryos with impaired RHO-ROCK signalling exhibit molecular and morphological changes associated with impaired TE differentiation (Kono, Tamashiro, and Alarcon 2014). Since RHO-ROCK activity is essential for TE specification, it is also likely to be related to the regulation of the

Hippo pathway. Thus, it is not surprising that several studies have reported a decrease in the proportion of TE cells with nuclear YAP localisation after Y-27632 or C3 treatment (Kono, Tamashiro, and Alarcon 2014; Cao et al. 2015; Mihajlović and Bruce 2016). In bovine embryos after ROCK inhibition, an increased number of cells with nuclear YAP signal in TE cells was observed (Negrón-Pérez and Hansen 2018). However, similarly to what has been observed in mice, RHOA inhibition using C3 in bovine embryos leads to a significantly decreased nuclear YAP signal in outer cells (Kohri et al. 2020).

The role of Rho-associated kinases 1/2 was also investigated during the preimplantation development of porcine embryos. The vast majority of porcine embryos cultured with the ROCK inhibitor Y-27632 for 72h from 4-cell stage onwards exhibited developmental arrest before compaction. Additionally, embryos at the morula stage treated with the ROCK inhibitor exhibited blastocyst formation failure. Moreover, Kwon and co-authors discovered visible disruption in AJs and TJs distribution in embryos after ROCK inhibition treatment (Kwon, Kim, and Choi 2016).

Human embryos at E3 cultured for 5 days with the ROCK inhibitor (Y-27632) exhibited a failure in cavity formation. Instead, embryos developed from single blastomeres (E3) cultured for 5 days with the ROCK inhibitor exhibited improved blastocyst formation, including higher expression of E-cadherin than in the control group (Huang et al. 2016). So far, only one group has analysed the role of ROCK kinases in the rabbit embryo. In embryos at 6.2 dpc, the ROCK inhibition treatment affected pre-gastrulation cell movements and modified primitive streak shape (Stankova, Tsikolia, and Viebahn 2015). However, the role of ROCK kinase in preimplantation rabbit embryos has not yet been analysed. Supporting evidence for the link between RHO-ROCK signaling and TE differentiation is well documented in the mouse model, specifically regarding the nuclear localization of YAP/TAZ (Alarcon 2010; Hirate and Sasaki 2014; Kono, Tamashiro, and Alarcon 2014; Cao et al. 2015; Mihajlović and Bruce 2016) (**Figure 5**). Namely, the RHO-ROCK signalling is required for apicobasal polarity establishment, where the components of the apical domain in TE cells initiate the Hippo pathway regulation, which allows for YAP/TAZ localisation in the nuclei. This model is further supported by the fact that after RHO-ROCK inhibition, the proper localisation of crucial members of the apical domain, including PARD6 and aPKC, was disrupted (Kono,

Tamashiro, and Alarcon 2014; Mihajlović and Bruce 2016). Due to the lack and loss of function of these apical factors, nuclear localisation of YAP/TAZ is impaired, and consequently, TE specification is affected (Alarcon 2010; Hirate et al. 2013; 2015; Mihajlović and Bruce 2016). Recent work has uncovered that the prevention of nuclear localisation of YAP/TAZ resulting from the interference of RHO and ROCK functions depends on the LATS1/2 phosphorylation activity. Additionally, AMOT-deficient embryos after ROCK inhibition treatment, exhibited nuclear localisation of YAP/TAZ (Mihajlović and Bruce 2016)(**Figure 5**).

RHO and ROCK had also been confirmed to be cytoskeleton regulators in various cell types (Amano, Nakayama, and Kaibuchi 2010; Amin et al. 2013; Thumkeo, Watanabe, and Narumiya 2013). In studies on different cell types, it was discovered that the Hippo pathway is in turn regulated by signalling pathways involved in actomyosin activity. Actomyosin-modulated Hippo pathway activity has been confirmed in response to various physical conditions, including substrate stiffness and mechanical stress (Dupont et al. 2011; Sun and Irvine 2016). Nevertheless, the exact interaction pattern between actomyosin and Hippo signalling is still not well understood.

It has been hypothesized that the pharmacological inhibition of RHO-ROCK activity may contribute to actomyosin disruption, leading in turn to the Hippo signalling modulation. This hypothesis was addressed in the study with various cell types, where it was demonstrated that nuclear YAP/TAZ distribution is prevented by interruption of actomyosin activity with small molecules, including latrunculin and cytochalasin (Sansores-Garcia et al. 2011; Wada et al. 2011; reviewed in Alarcon and Marikawa 2018) (**Figure 5**).

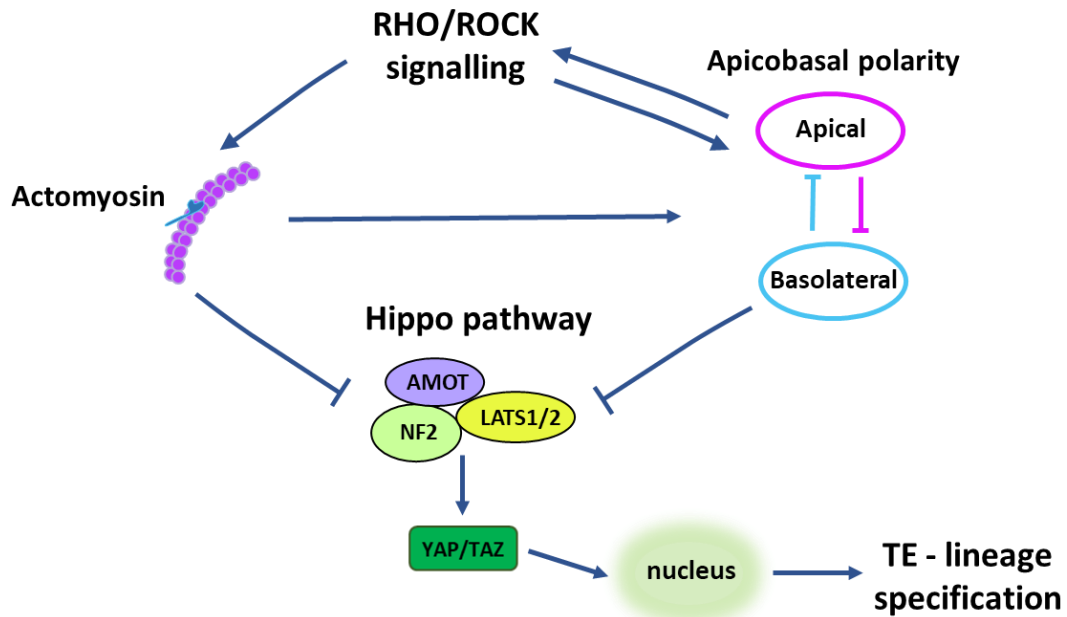


Figure 5. The mechanism of RHO-ROCK-dependent regulation of trophoderm differentiation in mammals through the Hippo pathway. For trophoderm lineage specification, YAP/TAZ nuclear localisation is required. RHO-ROCK is involved in apicobasal polarity establishment and actomyosin activity regulation, both upstream regulators of the Hippo pathway. Cell polarity factors and actomyosin inhibit Hippo signalling in TE cells by LATS1/2 suppression, allowing for active YAP and TAZ translocation from the cytoplasm to the nucleus to promote TE-fate. RHO-ROCK and polarisation regulate each other mutually. Additionally, RHO-ROCK influences apical-basal polarity through actomyosin modulation (Modified scheme from Alarcon et al., 2018).

4.8 The rabbit as a valuable animal model in biological and medical research

The European rabbit belongs to the order *Lagomorpha* and the family *Leporidae*. The rabbit is a domestic animal mainly bred for meat and fur production, and it is also a common companion and a laboratory animal. Rabbits, due to their high protein content in milk (about 14%) (Duby et al. 1993) are used in the pharmaceutical industry as bioreactors for the production of therapeutic proteins (Fan and Watanabe 2003). In addition, rabbits are used for antibody production (Weber, Peng, and Rader 2017). The ability of rabbits to gain weight rapidly in response to a high-calorie, low-fibre diet has made these animals an excellent model for studying fat metabolism (Watanabe 1980; Ardern et al. 1999) and obesity-related diseases in humans, such as hyperlipidemia (La

Ville et al. 1987; K.-C. Wang et al. 2016), atherosclerosis (Taylor and Fan 1997) and thrombosis (Yamashita et al. 2004). Rabbits share many similarities with humans, a proportionally larger heart when compared to body size, slower heart rate than rodents or a similar protein structure responsible for contraction and ion channels responsible for repolarization. Therefore, transgenic rabbit strains have been used as a model for heart diseases, including hypertrophic cardiomyopathy (Wigle et al. 1995) and a heart conduction disorder (Long QT syndrome) (Brunner et al. 2008; Odening et al. 2012). The pathogenesis of bacterial and viral diseases in rabbits is often very similar to that in humans, thus, the rabbit also found a place as a model for infectious diseases (Hu et al. 2007; Mendez et al. 2008). The rabbit model was found to be helpful for the study of viral diseases induced by Herpes simplex (HSV1) (A. B. Nesburn, Cook, and Stevens 1972; Haruta et al. 1987; Naito et al. 2005; Anthony B. Nesburn et al. 2007; Webre et al. 2012), Human papillomavirus (HPV) (Hu et al. 2007; McBride 2017) and Human T-cell Leukaemia HTLV (Miyoshi et al. 1984; Yamade, Ishiguro, and Seto 1991; Duc Dodon et al. 2012; Peng, Knouse, and Hernon 2015). Rabbit transgenic lines are a model for AIDS disease in research to understand the mechanisms of the onset and development of the disease, as well as the effectiveness of potential drugs and vaccines (Dunn et al. 1995; Snyder et al. 1995; Speck et al. 1998). Rabbits, like cats, ferrets and camels, belong to a group of animals distinguished by the unique feature of induced ovulation (Heape and Sedgwick 1997; Bakker and Baum 2000). The secretion of GnRH (gonadotropin-releasing hormone), a hypothalamic neuropeptide that controls reproductive function and the pre-ovulatory surge of LH (luteinising hormone), is induced by the reception of genital somatosensory stimuli during copulation. In rabbits, ovulation occurs after 10-13 hpc (Harper 1961). The length of the preimplantation period in a rabbit is 6 days, and the gestation period averages 31 days. Thanks to these features, it is possible to obtain and study rabbit embryos or fetuses at consecutive developmental stages within a short period of time after mating, insemination or embryo transfer (Gumbiner and Kim 2014).

Moreover, the rabbit exhibits convenient features for handling and manipulation for research, including the size of the female and its reproductive system - compounds such as the infundibulum of the fallopian tube or the oviductal-uterine isthmus are visible without magnification (Chavatte-Palmer et al. 2008; Polisca et al. 2010).

Additionally, the large-sized blastocysts make the rabbit a convenient research model for performing embryo micromanipulation or conducting cell lineage-specific analyses. Rabbit placenta development, function and morphology are more similar to humans than rodents (Enders and Blankenship 1999; Foote and Carney 2000; Soares, Varberg, and Iqbal 2018), which initially made this species an important model for research on mammalian embryo development. All the above-described features of the rabbit make it an attractive model for studying in the field of biological sciences and developmental biology.

5 Research hypotheses

- I. Trophectoderm differentiation in the rabbit embryo depends on polarity establishment at the morula stage.
- II. Trophectoderm differentiation in rabbit embryo is controlled by the Hippo pathway activity.
- III. Regulation of TE specification differs between mouse and rabbit.

6 Aims of the research

- I. To investigate whether there are differences in the expression of genes involved in the Hippo pathway cascade between specific preimplantation stages in the rabbit embryo.
- II. To investigate the distribution of the Hippo pathway and polarity factors from 4-cell stage to the blastocyst stage in the rabbit embryo.
- III. To verify the involvement of the Hippo pathway and ROCK kinase in trophectoderm differentiation by ROCK inhibition treatment in rabbit embryos.

7 Materials and methods

7.1 Animals

Experiments were conducted using rabbits (*Oryctolagus cuniculus*, white Popielno breed) derived from a colony at the Institute of Genetics and Animal Biotechnology of the Polish Academy of Sciences (IGAB PAS Jastrzębiec, breeder registration number – 068, user registration number - 0030). For these experiments, 6- to 15-month-old females and males of the same age were used for mating. In the animal facility, the temperature was maintained between 15-21°C. Additional conditions, including relative humidity, air circulation, or lighting (day/night) were maintained according to institutional guidelines. Animals had unlimited access to feed and water. All procedures conducted on animals were approved by the Third Local Ethics Committee (Warsaw, Poland, WAW2/167/2018).

7.2 Manipulation and culture media

Two types of media were employed for rabbit embryo assays. For embryo collection and manipulation, freshly prepared manipulation medium - Tissue Culture Medium (TCM199) containing 10% Fetal Bovine Serum (Sigma Aldrich) was used, warmed up to 38.5°C. Embryo culture, in turn, required the use of a particular standard culture medium commonly employed at the Department of Experimental Embryology IGAB PAS - RDH medium (RPMI1640: DMEM: Ham's F10, ThermoFisher, USA, 1:1:1) supplemented with 0.3% BSA (Bovine Serum Albumin Fraction V, Sigma Aldrich, USA) (Jin et al. 2000). Embryos subjected to *in vitro* development were kept in a HeraCell incubator (Thermo Scientific, USA) in a humidified atmosphere at 38.5°C and 5% CO₂. The culture medium (RDH + 0.3% BSA) was also freshly prepared prior to embryo culture and incubated for at least 1 hour for pH equilibration before embryos were transferred to it.

7.3 Embryo collection

For the purposes of this study, embryos at the following stages of development were used: 1.0, 1.25, 1.5, 2.0, 2.5, 3.25, 3.5, 3.75, 4.0 dpc. Embryos were harvested following natural matings by flushing either oviducts or the uterus of donor females under general anaesthesia. A combination of anaesthetic and analgesic agents were administered intramuscularly for anaesthesia: xylazine (Xylapan, Vetoquinol, France) in the amount of 3 – 5 mg (1.6 ml) per 1 kg of body weight, and ketamine (VetaKetam, Vet-Agro, Poland) in the amount of 30 – 40mg (0.3 ml) per 1 kg of body weight. Embryos were also recovered by flushing oviducts and the uterus, obtained from a slaughterhouse.

Embryos at stages 1.0 – 3.0 dpc were obtained from the oviducts. To collect embryos at 3.25 dpc, both oviducts and the uterus were flushed, since embryos are normally passing from the oviducts to the uterus through the isthmus at this stage. Embryos at later stages 3.5 – 4.0 dpc were obtained from the uterus (**Figure 1**). The procedure of the oviduct and uterus flushing was performed by two operators. Glass dishes containing freshly flushed embryos in manipulating medium were immediately transferred to a laminar flow chamber (MSC class I, ESCO). On a warm plate maintained at 38.5°C, the embryos were recovered using an automatic pipette (Eppendorf) with a 200 µl tip, and transferred to a 4-well dish containing 0.5 ml of culture medium. Embryos were then sequentially washed twice in fresh culture medium and the 4-well dish with embryos was returned to the incubator until all remaining embryos were recovered. Embryos collected at stages 1.0 – 4.0 dpc were either fixed and immunostained or processed for qPCR (1.5, 2.5, 3.25 and 4.0 dpc). Embryos at stages 1.0 dpc were subjected to *in vitro* culture.

Oviduct flushing:

First, one operator placed a plastic, sterile tube into the oviduct lumen via infundibulum, with the other end of the tube placed in a sterile glass dish warmed up to 38.5°C. Next, 5 ml of pre-warmed manipulation medium (TCM199 + 10% FBS) was injected into oviduct via isthmus by a second operator, using a sterile syringe with hypodermic needle to flush embryos out for collection. The pressurised fluid flowed

through the tube along with embryos, which were then collected in the dish. The procedure was then repeated for the second oviduct.

Uterus flushing:

First, a small hole was made at the anterior end of the uterus, into which one end of the sterile plastic tube was inserted. The other end of the tube was placed in the sterile glass dish. Next, 10 ml of pre-warmed manipulation medium was injected into the posterior end of the uterine horn by a second operator. Consequently, the direction of uterine flushing was from the cervix to the isthmus. The procedure was repeated for the second uterine horn.

7.3.1 Embryo culture

Rabbit embryos were cultured for 48h and 72h in 20-40 μ l drops of the appropriate culture medium (RDH+BSA or additional additives, depending on the group/experiment variant) in a sterile 35 mm plastic Petri dish (Corning). Drops were then covered with embryo-tested mineral oil (Sigma Aldrich) to prevent the medium from evaporating. Embryos were washed successively in three drops of clean culture medium before being placed in collective culture (7-20 embryos per drop).

7.3.2 Embryo culture with a time-lapse system

To visualise morphodynamic changes in embryos during *in vitro* development, embryos at the zygote stage were placed in the culture medium and incubated for 74 h under Primo Vision EVO+ (Vitrolife) camera. A drop of 40 μ l culture medium was placed in the sterile culture dish containing 9-16 microwells (dedicated for Primo Vision system) and was covered by mineral oil. Freshly collected zygotes were transferred to a previously prepared culture dish. The culture dish with microwells allowed for individual monitoring of up to 16 embryos at a time, while maintain them in a group co-culture.

7.3.3 Treatment with ROCK kinase inhibitor

The inhibitor of ROCK kinases function (ROCKi, Y-27632, batch 4720, Tocris) was dissolved in water recommended for media (Water for analysis, Millipore, Emsure) and stored in aliquots at -80°C. Once thawed, aliquot was used on the same day. Embryos collected at 1.0 dpc were cultured for 48h (up to the equivalent to 3.0 dpc), or 72h (equivalent to 4.0 dpc) in culture medium containing 20 µM ROCK inhibitor. A control group of embryos was simultaneously set up in a separate dish in the same incubator. Embryos in each culture dish were washed through several drops of medium. After 48h or 72h of culture, embryo quality was assessed under a stereomicroscope.

7.4 Embryo fixation

Fixation aims to preserve all proteins and cell structures in the embryo at a given stage of development. Embryos were fixed following *in vitro* culture or directly after collection/retrieval from donor females. To prevent embryos from sticking to the bottom of the dish, 4-well or 24-well plates were coated with agar solution (1% agar and 0.9% NaCl). Like in the case for embryo culture, every washing or incubation step implied transferring embryos into a different well within the plate. Thus, embryos were first washed in phosphate-buffered saline (PBS), and then briefly transferred into 4% PFA (Sigma-Aldrich) in PBS + 0.1% Tween-20 (Sigma-Aldrich) and 0.01% Triton X-100 (Sigma-Aldrich) as a fixative. Embryo fixation was then performed for 20 minutes at room temperature in a second well containing the aforementioned PFA solution. Finally, embryos were washed out the PFA in PBS. After fixation, embryos were either immediately subjected to immunostaining or stored in PBS at 4°C for not longer than one week.

7.5 Removal of embryonic coats

Both the mucin coat and *zona pellucida* overlying rabbit embryos make it difficult to perform immunofluorescence assays. However, it is crucial to remove coats after

fixation, because chemical removal of embryonic coats from live embryos may disrupt the embryo structure and even the localisation of specific proteins. Thus, fixed rabbit embryos were individually transferred into drops of 0.03% PVP (Polyvinylpyrrolidone, Sigma-Aldrich) in PBS (3 mg/ml) in a 60-mm plastic dish. The PVP prevented the sticking of embryos without coats to the bottom of the dish and to manipulating needles. Coats were mechanically removed from embryos by using 0.33 x 12 mm 29G x ½ Luer Lock injection needles (KD-Medical) under a stereomicroscope.

7.6 Immunofluorescent detection of proteins

Indirect immunofluorescent staining was performed to determine the presence and localisation of factors related to polarity and the Hippo pathway. In this method, primary antibodies bind specifically to the antigen of the protein of interest. Then secondary antibodies conjugated with a fluorescent dye were used to detect the antigen-bound primary antibody. The list of the primary and secondary antibodies used to detect these proteins in rabbit embryos is presented in **Tables 2** and **3**. The immunostaining procedure was performed on a 96-well plate dish coated with agar as described previously.

To allow the antibodies to penetrate cells and access proteins, cell membrane permeabilisation was performed for 20 minutes in a 0.55% Triton X-100 solution in PBS. In the next step, embryos were washed three times for 5 minutes in wells filled with PBX (0.1% Triton 100-X in PBS). To block the formaldehyde groups formed during the fixation, embryos were incubated in ammonium chloride solution (NH₄Cl, 2.6mg/ml in PBS) for 10 minutes at room temperature. Then, embryos were washed three times for 5 minutes (3 x 5 min) in wells filled with PBX. To block epitopes and prevent nonspecific binding of antibodies, embryos were incubated in blocking buffer (10% Donkey serum solution in PBS) for 40 minutes at room temperature. After blocking, embryos were placed into a solution of the primary antibody diluted in blocking buffer and were incubated overnight at 4°C to form an antibody-antigen complex (**Table 1**).

1° Antibody	Host	Ig	Clonality	Dilution	Source
Active YAP	Rabbit	IgG	Polyclonal	1:100	Abcam, ab97959
aPKC	Mouse	IgG	Monoclonal	1:100	Santa Cruz, sc-17781
Phospho-ERM	Rabbit	IgG	Polyclonal	1:100	Cell Signaling, #3141
β-catenin	Rabbit	IgG	Polyclonal	1:100	Abcam, ab2365
GATA3	Goat	IgG	Polyclonal	1:100	R&D System, AF2605

Table 1. Primary antibodies used for immunofluorescent staining of embryos

After primary antibodies incubation, embryos were washed three times for 5 minutes (3x 5 min) in PBX. Then, embryos were incubated in blocking buffer for 40 minutes at room temperature, followed by incubation in a solution of secondary antibodies diluted in blocking buffer. Finally, embryos were incubated in the dark for 75 minutes at 4°C in the solution of secondary antibodies in the blocking buffer (**Table 2**). After blocking, embryos were washed three times for 5 minutes (3x 5 min) in wells filled with PBX.

2° Antibody	antigen	Conjugated-dye	Clonality	Dilution	Company/Cat. number
Donkey IgG	rabbit	AlexaFluor 647	Polyclonal	1:500	ThermoFisher (A31573)
Donkey IgG	goat	AlexaFluor 568	Polyclonal	1:500	ThermoFisher (A11057)
Donkey IgG	mouse	AlexaFluor 488	Polyclonal	1:500	ThermoFisher (A21202)
Donkey IgG	mouse	AlexaFluor 647	Polyclonal	1:500	ThermoFisher (A21202)

Table 2. Secondary antibodies conjugated with fluorochromes used for immunofluorescent staining of embryos

7.7 Phalloidin staining

Phalloidin staining was performed to determine the distribution of F-actin (a component of cytoskeleton structure) in rabbit embryos. After the indirect Immunofluorescent staining procedure was completed, the embryos were transferred into a solution of Phalloidin TRITC (200 units/mL in PBS; Sigma Aldrich) and incubated for 45 minutes at room temperature.

7.8 Nuclear staining

Counterstaining of chromatin after Immunofluorescent staining procedure was performed by incubating embryos for 30 minutes in bisBenzimide Hoechst 33342 solution (5 µg/ml, Molecular Probes).

7.9 Embryo imaging by confocal microscope

Image acquisition was performed under an inverted confocal microscope (Nikon A1R, Japan), equipped with NIS-Elements Confocal software (Nikon, Japan), Nomarski and Hoffman contrast; lasers 405 nm, 488 nm, 561 nm, 640 nm; hybrid scanner and resonance scanner. To obtain 3D images, embryos were placed in a drop of PBS under mineral oil in a 35-mm Nunc Glass Bottom Dish (Thermo Scientific, 0.16–0.19 mm borosilicate cover glass). Optical sections were taken through the whole embryo every 2 µm under the 20× lens, which later allowed for the generation of a 3D image and the viewing of embryos in cross-sections at any depth.

7.10 Confocal image analysis

Images from the confocal microscope were analysed using the IMARIS graphics software 9.8.2 (Copyright © 1993-2021 Bitplane AG/Oxfords Instruments). The cell nuclei were identified using the "spot" option, setting the detection diameter around 7

μm in the Hoechst channel. The number of nuclei detected by the software was verified manually. The protein signal was similarly analysed in the appropriate channel to determine the number of YAP and GATA3 positive cells. In the experiment with a ROCK inhibitor, control and experimental embryos were imaged during one session using the same confocal settings configuration (voltage values, scan speed, excitation, laser motion, detector sensitivity, aperture diameter, etc.). To quantify aPKC intensity signal in the apical domain of the outside cells, the ImageJ software (National Institutes of Health, USA) was used. The Plot Profile Tool (blue plot) examined pixel intensities along a straight $15\ \mu\text{m}$ line drawn across the apical domain and cytoplasm of the outside cells. Plots were normalised using Isqcurvefit function in MATLAB2020a (Gaussian fit, orange plot). The method of measurement (marked by violet lines) is presented below (**Figure 6**):

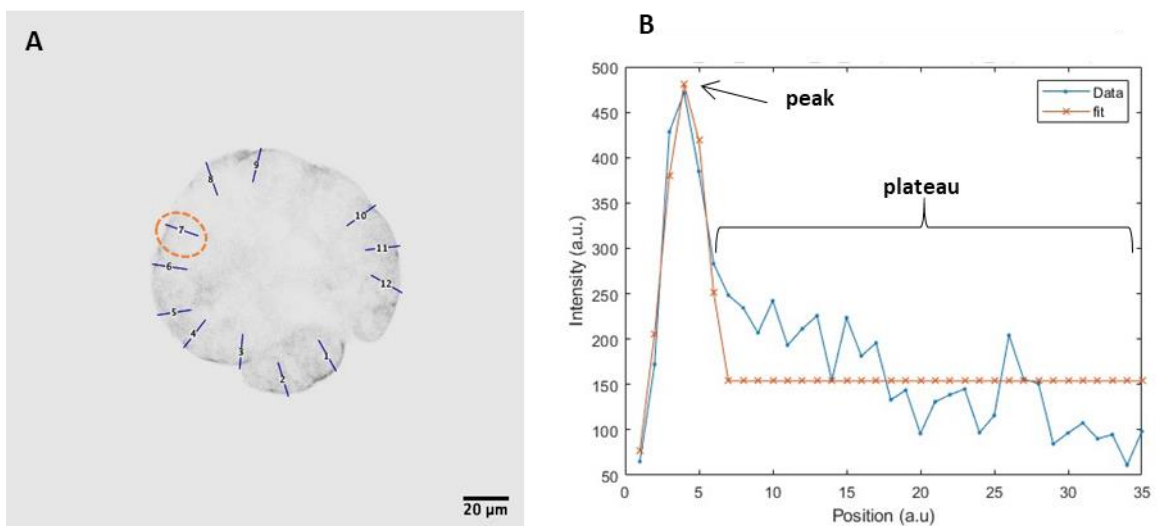


Figure 6. A scheme of aPKC pixel intensity measurements in outside cells of the embryo (violet lines) (A). Representative line profile of signal intensity (blue plot) fitted by Gaussian normalisation (orange plot) in the outer cell (B).

7.11 Molecular biology methods

7.11.1 Sample collection for gene expression analysis

For RNA isolation, 5 embryos per developmental stage were collected. Stages included embryos at 1.5 dpc (pre-compaction embryos), 2.5 dpc (post-compaction embryos), 3.25 dpc (2 x VI stage blastocysts and 3 x VII stage blastocysts) and blastocysts at 4.0 dpc with TE and ICM treated as separate groups. Embryos at 1.5-3.25 dpc were frozen with embryonic coats, while embryos at 4.0 dpc were frozen without coats and split into TEs and ICMs (detailed below). 1.5 ml tubes containing samples for freezing in 10 µl of RNase- and DNase-free PBS with 0.03% PVP (3mg/ml) were immersed in liquid nitrogen and stored at -80 °C.

To separately collect TE and ICM from 4.0 dpc blastocyst, embryos were dissected approximately in half, across the embryonic-abembryonic axis, using a glass needle on a dish coated with agar solution. As a result, the part corresponding to the abembryonic portion exclusively consisted of TE cells. The embryonic part, containing both ICM and some TE cells, was subsequently subjected to immunosurgery procedure in order to isolate the ICM (Solter and Knowles, 1975). Prior to dissection, embryo mucin coats were pre-digested by incubation in 0.5% pronase (Sigma Aldrich) for 45 sec at 38°C (heating stage), followed by thorough washing in manipulation medium. Embryos were then incubated for 30-45 min on a heating stage in the fresh manipulation medium under mineral oil, and the zona pellucida and remaining mucin coat were mechanically removed with sharp needles (0.3mm). ICMs with attached remaining TE cells were incubated for 40 min in 20% anti-rabbit serum (Sigma) (diluted in manipulation medium) on a heating stage. After serum incubation, embryos were transferred into drops of 20% guinea pig complement (Merk Millipore) in manipulation medium covered by mineral oil, and incubated for 15-20 min at 38.5°C. This procedure allowed for lysis of the remaining TE cells, which were then removed from ICMs by pipetting.

7.11.2 RNA extraction

Isolation of total RNA from embryos was performed using the High Pure miRNA Isolation Kit (Roche Applied Science, Germany), according to the manufacturer's protocol.

To effectively lyse embryo cells and embryonic coats, 312 μ l binding buffer was added to each thawed sample and vortexed. Then, samples were frozen in liquid nitrogen and were quickly thawed and vortexed briefly for 2 min. In the next step, samples were mixed several times using a sterile injection needle, and the samples were vortexed and shortly centrifuged. 200 μ l binding enhancer was added to each sample. The solution was transferred into a column placed inside the filter tube combined with the collection tube, and the sample was centrifuged (30s, 13000 x g). The supernatant was removed, and 500 μ l of a wash buffer was placed on the column and centrifuged (30 sec, 13000 x g). The supernatant was removed again, and washing was repeated with 300 μ l of wash buffer followed by centrifugation (30 sec, 13000 x g). The supernatant was removed, and the sample was centrifugation (60 sec, 13000 x g) to dry the filter column completely. Then, the column was placed into a sterile Eppendorf tube (1.5 ml). For RNA elution, 30 μ l elution buffer was added to the RNA binding column and then incubated for 60 sec at room temperature, followed by centrifugation (13000 x g). The elution step was repeated once more in the same way. Eluted RNA was stored at -80°C until further analysis.

7.11.3 RNA precipitation

RNA precipitation was performed using the Pellet Paint NF Co-Precipitant kit (Merck Millipore, USA). 2 μ l of Pellet Paint NF Co-Precipitant and 0.1 volume (μ l) of the sample of 3M sodium acetate at pH 5.2 were added to the sample containing RNA. Then 150ul of isopropanol was added, vortexed and incubated for 2 min at room temperature. The sample was centrifuged at the 13000 x g for 10 min. Dark blue pellets were visible after centrifugation. The supernatant was removed, taking care not to damage the pellets. The pellets were then washed with 70% ethanol, shaken and centrifuged. The supernatant was removed, and pellets were washed with 100% ethanol, vortexed and

centrifuged. After removing the supernatant, the pellets were air-dried at room temperature. The pellets were suspended in 20 μl of DNase- and RNase-free water. Precipitated RNA templates were frozen at $-20\text{ }^{\circ}\text{C}$, and on the next day, the concentration and purity of the RNA were assessed using the NanoDrop spectrophotometer (Spectrophotometer ND-1000; NanoDrop Technologies).

7.11.4 Reverse transcription PCR

The reverse transcription polymerase chain reaction (RT-PCR) for each sample was performed from 200 ng of total RNA using the Transcriptor First Strand cDNA Synthesis Kit (Roche Applied Science). The reaction mix was prepared according to the manufacturer's protocol. See the table below (Table 3.1)

Reagent	Volume (per 1 reaction)
Total RNA	x μl (200 ng) (calculated)
Random hexamer primer	2 μl
Anchored-oligo (dt) primer	1 μl
Water, PCR Grade	x μl (calculated)
Total	13 μl

Table 3.1 Reaction components for cDNA synthesis

RNA was appropriately topped up to 10 μl with water, and a solution of two types of primers (2 μl random hexamer primer + 1 μl anchored-oligo (dt) primer) was added. To denature primers and secondary RNA structure, well mixed and centrifuged samples were incubated for 10 min at 65°C . Then, the tubes were immediately cooled down on ice. In the meantime, the master mix was prepared and later added to samples (see **Table 3.2** below for details).

Reagents	Volume (per 1 reaction)
Transcriptor High Fidelity Reaction Buffer 5x conc.	4 μ l
Protector RNase Inhibitor	0.5 μ l
Deoxynucleotide Mix (dNTP Mix)	2 μ l
Transcriptor Reverse, Transcriptase	0.5 μ l
Total	20 μ l

Table 3.2 Master mix components per 1 reaction

Then, tubes were gently mixed and centrifuged, then incubated for 10 min at 25°C, followed by 60 min incubation at 50°C. To inactivate Transcriptor Reverse Transcriptase, samples were incubated at 85°C for 5 min, then immediately cooled down on ice or placed at 4°C. To increase the volume of the cDNA samples, 10 μ l of PCR-grade water was added to each sample. The obtained cDNA was either immediately subjected for real-time PCR assay or stored at -20°C.

7.11.5 Primer design

The primer pairs were designed using Primer-BLAST I (NCBI), Primer3 (version 4.1.0) and the RefSeq IV.80 database for rabbit transcripts. Additionally, primers were checked with the OligoAnalyzerTM tool. Detailed information about primers and the conditions and qualitative indices of the PCR analyses are presented in **Table 3.3**.

Gene	Sequence (5' -> 3') Forward primer	Sequence (3' -> 5') Reverse primer	Product length (bp)	Annealing temp. (°C)
TEAD1	CCTACCCCATCCAGCCAGC	GGGTCTCGCTGCTGTTCGA	157	62
TEAD2	GGCCAGAAGGAAGTCAAGAGA	AACTGGAAAAGCTCCGAGGTC	180	62
TEAD3	TCCTTTGGCAAGCAGGTGGT	GTGAAGTTCTCCAGCACGCT	176	62
TEAD4	TCGTACACATCGGCCAGTCA	TCCCCGTTCAAAGAGCTCCT	125	62
LATS1	AACCCAGTCATCCCCAAGCA	AGGAGCTGGTGTAATCGCAGT	160	62
LATS2	TCAAAACCTGGGCATCGGT	CTGTTCCGGTTCAGCACAT	116	62
YAP	ATGAACCCCAAGACGGCCAA	GCTCGAACATGCTGTGGTGT	158	62
HPRT1	CAGGACTGAAAGGCTTGCTC	AATCCAGCAGGTCAGCAAAG	110	62
H2AFZ	GCCATCCTGGAGTACCTCAC	AGCAAGTTGCAAATGACGAG	102	62
YWHAZ	GGTCTGGCCCTTAACTTCTCTG TGTTCTA	GCGTGCTGTCTTTGTATGATTCT	142	62

Table 3.3 Primers used for real-time PCR

7.11.6 Quantitative PCR

To compare the levels of expression of specific genes between 5 rabbit embryo samples (1.5, 2.5, 3.25, TE from 4.0 dpc, ICM from 4.0 dpc), RT-qPCR analyses were performed. Experiments were carried out using the LightCycler FastStart DNA Master SYBR Green I kit (Roche Applied Science) in a 96-well optical plate on a LightCycler 96 thermocycler (Roche Applied Science). Three biological replicates were analysed for each stage, each sample containing 5 embryos. All samples were analysed in 2-3 technical repetitions under the following reaction conditions:

Reagents	Volume (per 1 reaction)
LightCycler® 480 SYBR Green I Master	0.8 µl
Forward primer, 130nM	0.2 µl
Reverse primer, 130nM	0.2 µl
MgCl ₂ , 1,8mM	0.7 µl
cDNA	1 µl
Water, PCR Grade	7.1 µl
Total	10 µl

Table 3.4 Proportion composition of RT-qPCR mix per 1 sample

The qPCR protocol included a preincubation step and 45 cycles of 3-step amplification. After qPCR, a melting curve analysis was performed with continuous recording of fluorescent emission intensity changes (see **Table 3.5**). For PCR efficiency adjustment (data normalisation), a $\Delta\Delta C_t$ method was used, using the geometric average of *H2AFZ*, *HPRT1* and *YWHAZ* as housekeeping normalisation factors (Mamo et al. 2007; Piliszek, Madeja, and Plusa 2017).

Steps	Temperature	Time	Cycles
Preincubation	95°C	10 min	1
3-step amplification	Denaturation	95°C	10 sec
	Primer annealing	62°C	10 sec
	Elongation	72°C	10 sec
Melting Curve	95°C	10 sec	1
	67°C	60 sec	1
	97°C	60 sec	1
Cooling	37°C	∞	1

Table 3.5 Real-time PCR program

7.11.7 Agarose gel electrophoresis

The PCR products were visualised via 2% agarose gel electrophoresis to confirm the specificity of the primers. Agarose gel was prepared by dissolving 2g of agarose powder (Sigma-Aldrich) in 100ml of 1x TBE buffer (EURx Molecular Biology Products) + 5µl/100ml SimplySafe™ (EURx Molecular Biology Products). The PCR products were mixed with DNA loading buffer (6x conc., EURx Molecular Biology Products) and directly loaded on the gel, along with a 50-500bp ladder marker (EURx Molecular Biology Products). Electrophoresis was performed for 30min at 100V in TBE. The resulting bands were imaged on a UV light illuminator (BIO-RAD Laboratories, Inc.) to assess the size of the amplicons.

7.12 Reagents and kits used in the study

Components	Catalogue number	Supplier	Concentration
5xTBE	210920	EURx Molecular Biology Products	1x conc.
6x Loading buffer	E0260-01	EURx Molecular Biology Products	1x conc.
Agar	A1296	Sigma Aldrich	1%
Agarose	A9539-500G	Sigma Aldrich	1.5-2%
Ammonium chloride (NH ₄ Cl)	A9434-500G	Sigma Aldrich	2.6mg/ml
Anti-Rabbit Serum antibody produced in goat, whole	R5131-2ML	Sigma Aldrich	20%

antiserum			
Bovine Serum Albumin, fraction V	A3311-100G	Sigma Aldrich	0.30%
Guinea pig complement	234395	Merk Millipore	20%
DMEM	11966025	Thermofisher	30%
Donkey serum	D9663-10ML	Sigma Aldrich	10%
FBS (Fetal Bovine Serum)	11573397	Gibco	10%
Ham's F10	41550-021	Thermofisher	30%
Hoechst 33342	H3570	Molecular Probes	5 µl/ml
Ketamine	VetaKetam	Vet-Agro	30-40mg per kg body weight
Paraformaldehyde (PFA)	158127-500G	Sigma Aldrich	4%
Perfect Plus DNA Ladder	E3145-02	EURx Molecular Biology Products	7 µl per 1 reaction
Phalloidin TRITC	P1951	Sigma Aldrich	200 units/mL
Polyvinylpyrrolidone (PVP)	PVP40-50G	Sigma Aldrich	3mg/ml
PRONASE® Protease, type XIV	P-5147	Sigma Aldrich	0.50%
RPMI1640	11879-020	Thermofisher	30%
SimplySafe™	E4600-01	EURx Molecular Biology Products	5µl/100ml

Sodium Chloride Pure P.A. (NaCl)	794121116	POCH SA	0.9%
TCM-199	M2520	Sigma Aldrich	
Triton X-100	X100-100ML	Sigma Aldrich	0.01%
Tween 20	P9416-50ML	Sigma Aldrich	0.1%
Water for analysis	HC99826454	Merk Millipore, Emsure	
Water PCR Grade	E0211	EURx Molecular Biology Products	
Xylazine	Xylapan	Vetoquinol	3-5mg per kg body weight
Y-27632 (ROCKi)	batch4720	Tocris	20µM

Table 4.1 Chemical reagents used in this study

Kit	Catalogue number	Supplier
High Pure miRNA Isolation Kit	5080576001	Roche Applied Science
LightCycler FastStart DNA Master SYBR Green I qPCR Kit	12239264001	Roche Applied Science
Pellet Paint NF Co-Precipitant kit	70748-3	Merk Millipore
Transcriptor First Strand cDNA Synthesis Kit	4896866001	Roche Applied Science

Table 4.2 Kits used in this study

7.13 Statistical analysis

Statistical analysis was performed using the GraphPad Prism 8.0.1 software. The normal distribution normality of the data was assessed with Shapiro-Wilk test. Comparison between two groups was performed by unpaired two-tailed t-Student and Mann-Whitney test, for normally and not normally distributed data, respectively. Comparisons of more than two groups were done by one-way ANOVA (for normally distributed data) or Kruskal-Wallis test (for not normally distributed data), where either YAP localisation or cell category were considered as independent factors. In case of statistical significance indicated by ANOVA or Kruskal-Wallis test, further post-hoc analysis with the use of Tukey's test or Dunn's test was incorporated. For correlation assessment, Pearson's correlation coefficient was calculated. To determine if there is a significant relationship between two categorical variables for control and ROCK inhibited embryos group Chi-Square test was used. All results were considered as statistically significant for $p < 0.05$. Data on graphs are presented as mean \pm SEM (where applies).

8 Results

8.1 Timeline of *in vitro* rabbit embryo development from zygote to blastocyst stage

During mammalian preimplantation development, embryonic cells differentiate into trophectoderm (TE) and inner cell mass (ICM). To follow these crucial events during *in vitro* development, time-lapse live-imaging was employed, with photographs taken every 20 minutes using a Primovision EVO+ system (**Figure 7**). For this study, rabbit zygotes (one-cell stage), collected approximately 22-24 hpc (hours *post coitum*), were collected from donor females and placed in a culture dish for 74h. (**Figure 7. a1**). After fertilisation, the embryo undergoes series of cell divisions leading to cell number increase. At 8-cell stage, the surface of contact between blastomeres increases, which is indicative of compaction initiation. The compaction process in rabbits is initiated at 1.5 dpc, and a fully compact morula can be observed around 3.0 dpc (stage III – V) (**Figure 7. d3-h**). Later on, at 3.25 dpc (stage VI) a U-shaped cavity is formed (**Figure 7. i1**), which subsequently increases its volume. These morphodynamic changes, known as the cavitation process, lead to blastocyst formation (**Figure 7. i1-i2**). In the **Figure 7** there are presented developmental stages I-VIII of rabbit embryo correlated with changes in its morphology and time after fertilisation.

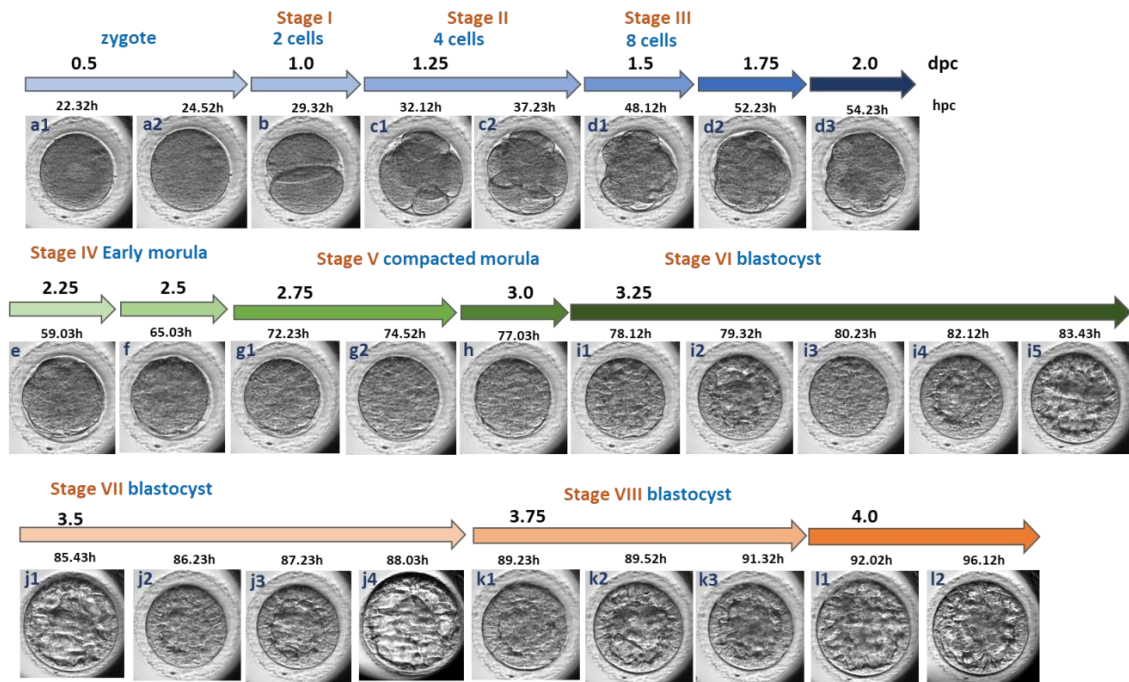


Figure 7. Consecutive stages of *in vitro* development of rabbit embryo from zygote to mid-blastocyst stage. Time-lapse images were acquired every 20 min.

My research combines analyses of both *in vivo* and *in vitro* developing embryos. Thus, it is important to understand that embryonic development under both conditions is not fully equivalent, which is widely described in (C. E. Adams 1970; Sanyal and Naftolin 1983; Hegele-Hartung, Fischer, and Beier 1988). Rabbit blastocyst stage embryo comprises anywhere between 60 and 5000 cells, and encompasses several distinct stages, thus representing much broader diversity than the canonical mouse blastocyst. Therefore, to analyse embryos at more comparable stages, Piliszek and colleagues have introduced the staging classification system for preimplantation rabbit embryo development, which is based on the total embryo cell number and correlates with the number of cell division rounds (**Table 5**) (Piliszek, Madeja, and Plusa 2017). Such staging system can be also applied to the analysis of rabbit embryos after *in vitro* culture.

Stage	Cell number	Time after fertilisation	Morphology
I	2	16-22 hpc	2-cell stage
II	4	21-30 hpc	4-cell stage
III	8	1.0-1.5 dpc	8-cell stage
IV	16-31	1.5-2.5 dpc	Early morula
V	32-63	2.5-3.25 dpc	Morula
VI	64-127	3.0-3.5 dpc	Compact morula/cavitating blastocyst
VII	128-255	3.0-3.75 dpc	Blastocyst
VIII	256-511	3.25-3.75 dpc	Blastocyst
IX	512-1023	3.5-4.25 dpc	Blastocyst

Table 5. Time frames of preimplantation rabbit embryo development (in vivo). Modified from Piliszek et al. 2017.

8.2 Analysis of relative expression levels of genes involved in the Hippo pathway cascade in rabbit embryos at consecutive stages: 1.5, 2.5, 3.25, 4.0 dpc.

To reveal which main factors of the Hippo pathway could play a role in rabbit embryo development/TE differentiation, I analysed gene expression levels of *TEAD1*, *TEAD2*, *TEAD3*, *TEAD4*, *LATS1*, *LATS2*, and *YAP* at developmental stages 1.5, 2.5, 3.25, 4.0 (TE), and 4.0 (ICM) dpc (**Figure 8. A-F**). Validation of several primer pairs for gene *TEAD2* was unsuccessful, and so results for this gene are not presented. The statistical analysis of data for genes *TEAD1*, *TEAD3*, *TEAD4*, *LATS1*, and *LATS2* was performed by ordinary one-way ANOVA, whereas Kruskal-Wallis test was used for *YAP* gene expression analysis (data did not exhibit a normal distribution).

The analysis of the relative gene expression levels revealed that there were no *LATS1* and *TEAD1* transcripts observed at 1.5 dpc (indicated by the black asterisk) followed by upregulation at 2.5 dpc (**Figure 8A, 8D**). For all other genes at the analysed stages no

significant differences were observed. No differences were found at 4.0 dpc between TE and ICM for all analysed genes.

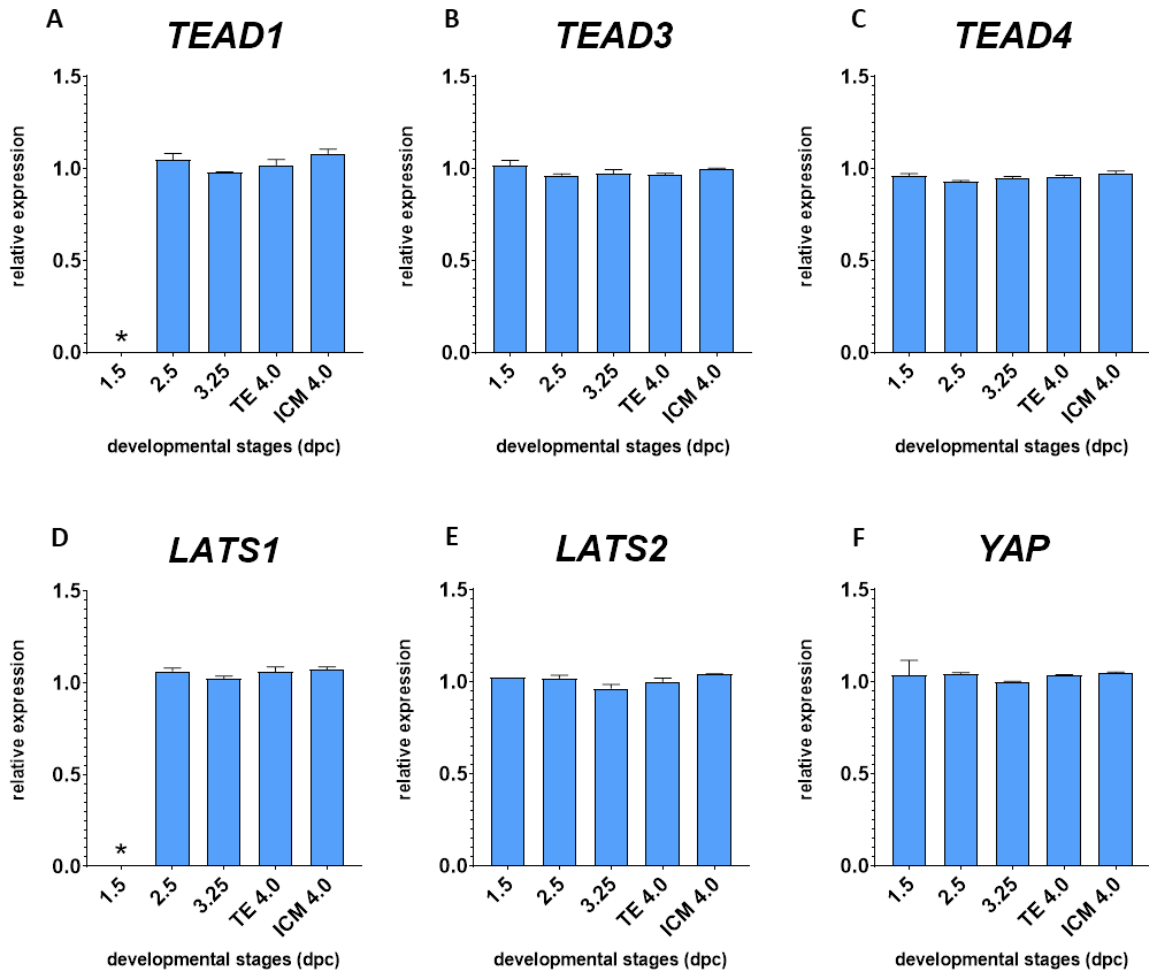
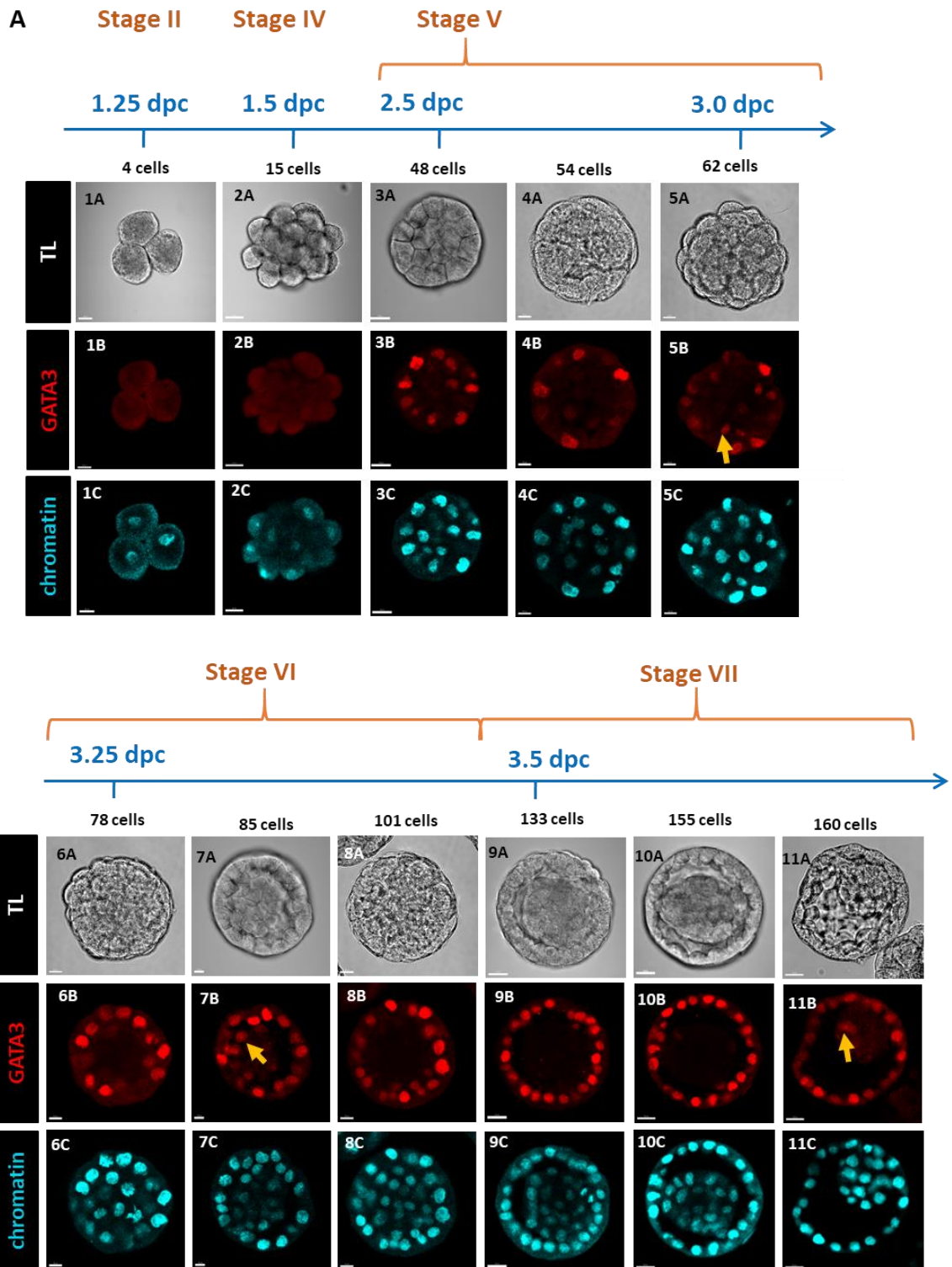


Figure 8. Expression level of specific genes involved in the Hippo pathway regulation at consecutive stages. No significant differences between developmental stages for all genes of interest; comparison between stages for TEAD1, TEAD3, TEAD4, LATS1, and LATS2 present $p > 0.05$ (ordinary one-way ANOVA test, Kruskal-Wallis test $p > 0.05$).

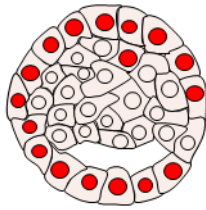
These results imply that in most of the cases there are no differences in the mRNA level between specific stages. Therefore, these results suggest that the Hippo pathway is regulated by additional agents other than transcripts levels of these genes in the rabbit embryo.

8.3 Localisation of the early TE marker GATA3 in the preimplantation rabbit embryo

To validate GATA3 as a TE marker in rabbits, embryos at consecutive stages were immunostained for GATA3. Representative images of embryos from 4-cell stage to mid-blastocyst stage are presented below (**Figure 9**). In 4-8-cell stage embryos (stages II-III), I did not detect any GATA3 positive cells (number of embryos analysed n=26) (**Figure 9, panel 1**). In embryos at 16-cell stage (stage IV), I detected three cells with GATA3 nuclear distribution in only one embryo (n=5) (**Figure 9, panel 2**). GATA3 is detected at 2.5 dpc in 66% of the total cells (stage V, n=6). From this point onwards, the percentage of GATA3-positive nuclei successively increases in outer cells and decreases in inside cells (which will form ICM after cavitation) (**Figure 9, panels 3-5**). From 3.25 dpc (stage VI) onwards, GATA3 is mainly restricted to TE cells (approx. 67% of TE cells are GATA3 positive). However, at stage VI, I detected GATA3 in 10% of ICM cells (n=16) (**Figure 9, panels 6-8**). At stage VII, GATA3 signal is still detected in 4% of ICM cells (**Figure 9, panels 9-11**, yellow arrow). As the number of cells in the embryo increases, the percentage of GATA3-positive nuclei gradually increases up to 74% of TE cells at stage VII (n=6).



B Schematic representation



3.25 dpc

Figure 9. Distribution of GATA3 in preimplantation rabbit embryos in vivo.

A Representative single z-section confocal images of embryos at stages II-VII immunofluorescently labelled for GATA3 (red), chromatin (blue) and representative cross-section transmitted light (TL) image. The TE marker GATA3 starts to be detected in rabbit embryos not earlier than 2.5 dpc (stage V). Before that time, the nuclear distribution of GATA3 is usually not detected (**panels 1 and 2**). From stage V on, it is visible in most nuclei of early morula (**panels 3 and 4**). Later on, at 3.0 dpc (shortly before cavitation), GATA3 is observed in both the inside cells (yellow arrow) and outside cells (**panel 5**). Since cavitation starts around 3.25 dpc, GATA3 signal is progressively restricted to TE cells. However, GATA3 signal is also found in nuclei of single ICM cells (yellow arrow) (**panels 6-8**). At stage VII, the number of TE cells with GATA3-positive nuclei increases (**panels 9-11**). **B** Schematic representation of GATA3 localisation (red) at 3.25 dpc. Scale bars: 20µm.

Based on the observations presented, I conclude that GATA3 localisation becomes mostly restricted to TE cells as early as 3.25 dpc, and it remains so during TE development. Therefore, GATA3 can be described as an early and specific marker for TE-lineage in the rabbit embryo.

8.4 Localisation of cell polarity-related factors in the preimplantation rabbit embryo

Multiple studies have reported that acquisition of cell polarity is an essential process that affects further events such as TE and ICM differentiation (Ducibella and Anderson 1979; 'Induction of Polarity in Mouse 8-Cell Blastomeres: Specificity, Geometry, and Stability' 1981; Assémat et al. 2008). Research on mouse embryos have revealed multiple factors associated with cell polarity and the Hippo pathway regulation, including apicobasal proteins Pard6, Pard3, aPKC, Par1 (EMK1), Scribble, as well as

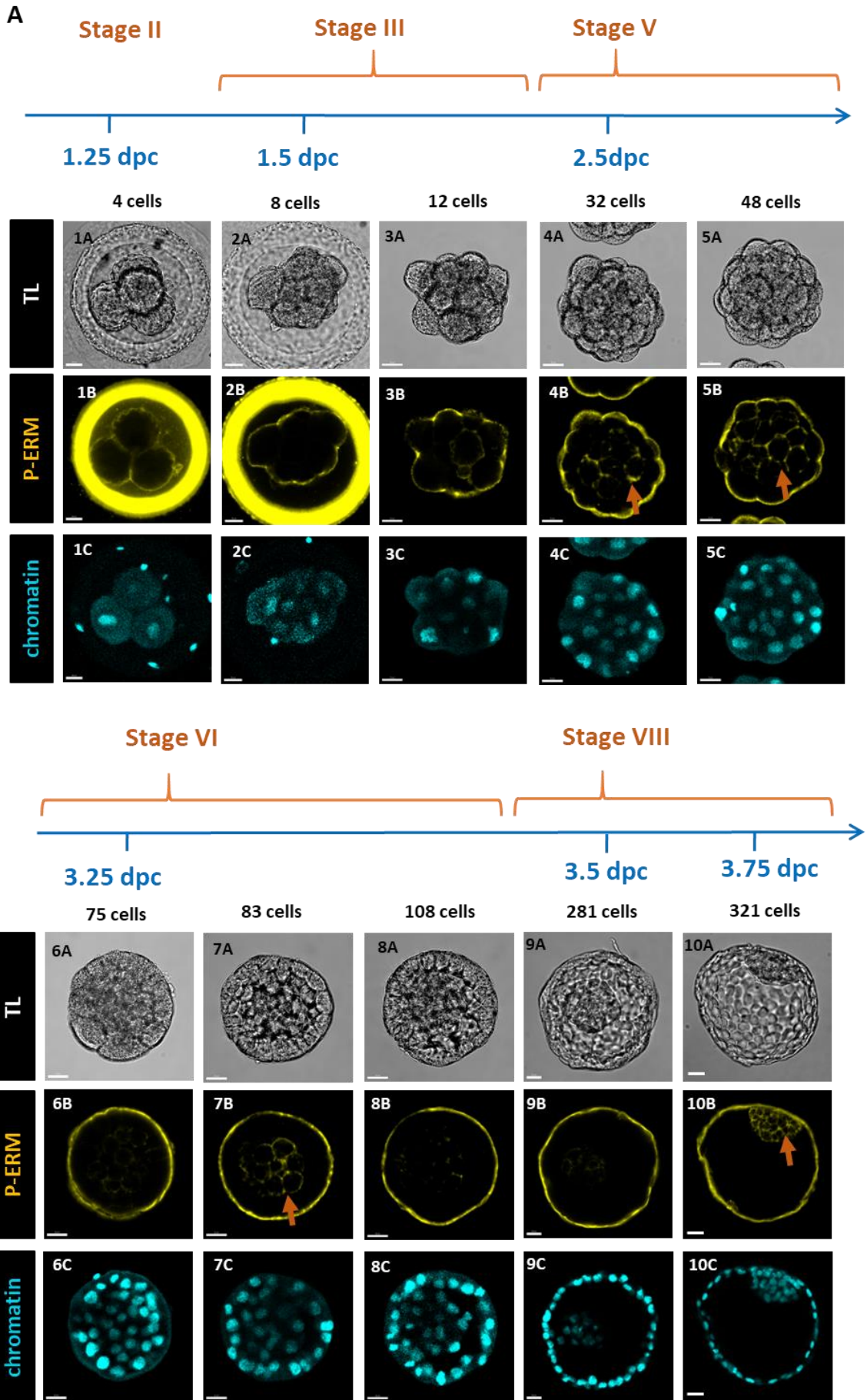
proteins related to the cytoskeleton and cell adhesion such as Ezrin, filamentous actin (F-actin), E-cadherin or β -catenin.

To investigate the presence and localisation of cell polarity-associated factors in the rabbit embryo, immunostaining for phospho-Ezrin, aPKC, F-actin and β -catenin from 4-cell stage to the mid-blastocyst was performed (presented below). However, antibodies against proteins PARD6, SCRIBBLE or E-CADHERIN from rabbit were not available.

8.4.1 P-Ezrin (P-ERM)

Ezrin is a membrane protein that belongs to the protein family ERM (Ezrin, Radixin, Moesin), described to be cross-linkers between the cytoskeleton and plasma membrane involved in mouse embryo compaction (Takeuchi et al. 1994; J. Chen, Cohn, and Mandel 1995; Kondo et al. 1997). However, only the phosphorylated form of Ezrin (phosphorylation of T567) can interact with F-actin.

To investigate how phosphorylated Ezrin (p-Ezrin) is distributed in the preimplantation rabbit embryo I analysed the localisation of p-Ezrin in consecutive development stages, using antibody against p-ERM. My analysis reveals that p-Ezrin is localised in the cell cortex as early as 4-cell stage, but not in a polarised manner (n=19) (**Figure 10. panel 1**). At 8-cell stage, p-Ezrin starts to be restricted to the apical surface of the outer cells, and it remains so during further stages (n=38) (**Figure 10. panels 2-3**). However, p-Ezrin is detected in non-polarised manner in inside cells in the majority of morulae at stage V (89%, n=27, red arrows) (**Figure 10, panels 4 and 5**) and in 87% of blastocysts at stages VI-VIII (n=45) (**Figure 10, panels 7 and 10**).



B Schematic representation



Figure 10. Localisation of p-Ezrin at specific developmental stages in rabbit embryos.

A Representative single z-section confocal pictures of embryos at stages II-VII immunofluorescently labelled for p-Ezrin (yellow), nuclei (blue) and representative cross-section transmitted light (TL) image. The protein p-Ezrin is detected evenly in the plasma membrane of cells from the embryo as early as 4-cell stage (stage II) (**panel 1**). At 8-cell stage it starts to be localised in the apical membranes and it remains so during later stages (**panel 2-10**). p-Ezrin localisation can be also detected in inside cells of compacting morulae (**panel 4 and 5**), as well as in cavitating embryos (**panel 7**) and in mid-blastocysts (**panel 10**) (indicated by red arrows). **B** Schematic representation of p-Ezrin localisation (yellow) at 1.5 dpc. Scale bars: 20µm.

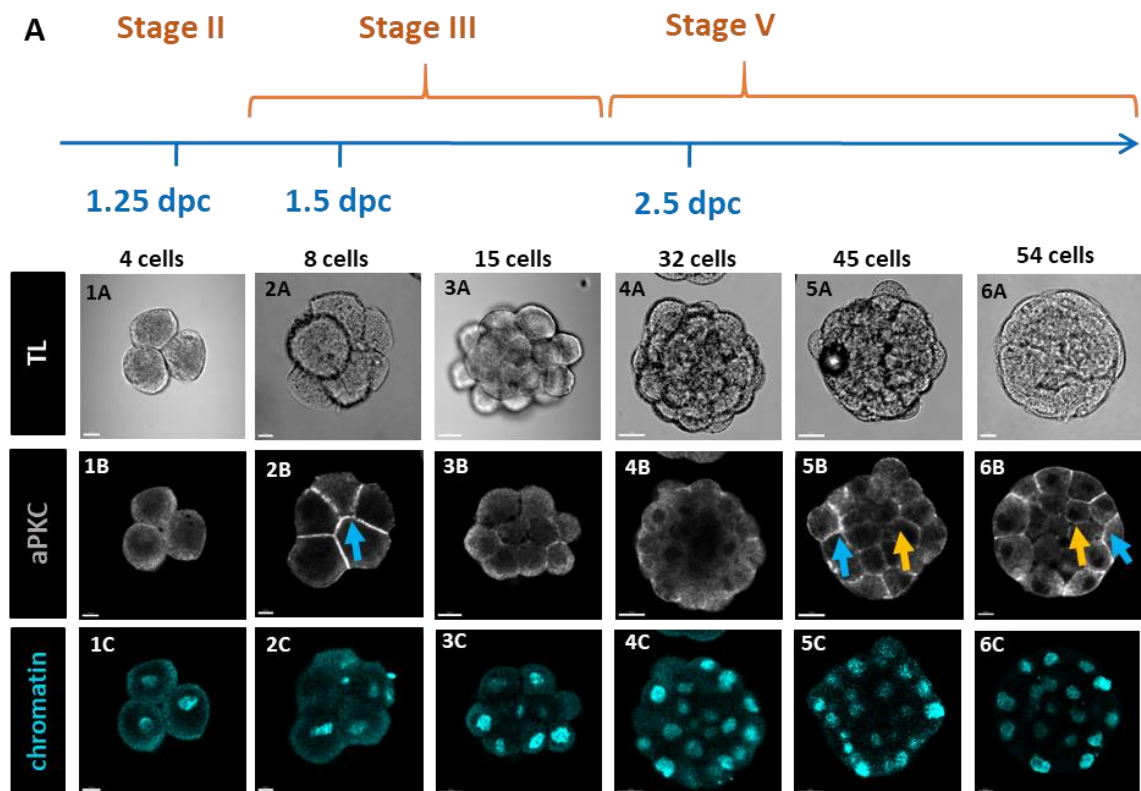
To conclude, concomitant with the initiation of compaction, p-Ezrin starts to localise in the apical domains of the outside cells. Therefore, the analysis suggests that as early as 8-cell stage, blastomeres become polarised. Consequently, p-Ezrin is an early marker of polarisation in the rabbit embryo.

8.4.2 Atypical protein kinase C (aPKC)

Atypical protein kinase C (aPKC) is a member of the Par-aPKC apical complex and is involved in apical-basal cell polarity establishment in mice and other species. It plays a crucial role in the polarisation of outside cells of the mouse embryo, which leads to the acquisition of TE fate ('Induction of Polarity in Mouse 8-Cell Blastomeres: Specificity, Geometry, and Stability' 1981; Plusa et al. 2005; Ralston and Rossant 2008; Gerri et al. 2020).

To investigate aPKC localisation during the rabbit embryo preimplantation development, I immunostained embryos against aPKC protein. I detected aPKC localisation in the basolateral domains of blastomeres as early as 8-cell stage (n=10) (**Figure 11. panel 2**, blue arrows). However, I detected aPKC in the cytoplasm at stage II

(n=24) (**Figure 11. panel 1**). Later on, the aPKC localisation seems to be more concentrated in outside cells in the basolateral domain (blue arrows) (**Figure 11. panel 3**). Shortly before cavitation (stage V, n=19 and stage VI, n=24), aPKC is still detected in the basolateral domain of outer cells (blue arrows) (**Figure 11. panel 4-6**). The distribution of aPKC from 3.25 dpc (stage VI, n=24) progressively changes in outside cells from the basolateral to the apical domain (magenta arrows). However, aPKC is also present in the cell cortex of ICM cells (yellow arrows) at the blastocyst stage (**Figure 11. panel 7-8**). In developing blastocyst at stages VII (n=5) and VIII (n=4), the apical distribution of aPKC in TE cells is more distinct, whereas in ICM cells it remains uniformly distributed in the cell cortex (**Figure 11. panel 10-13**).



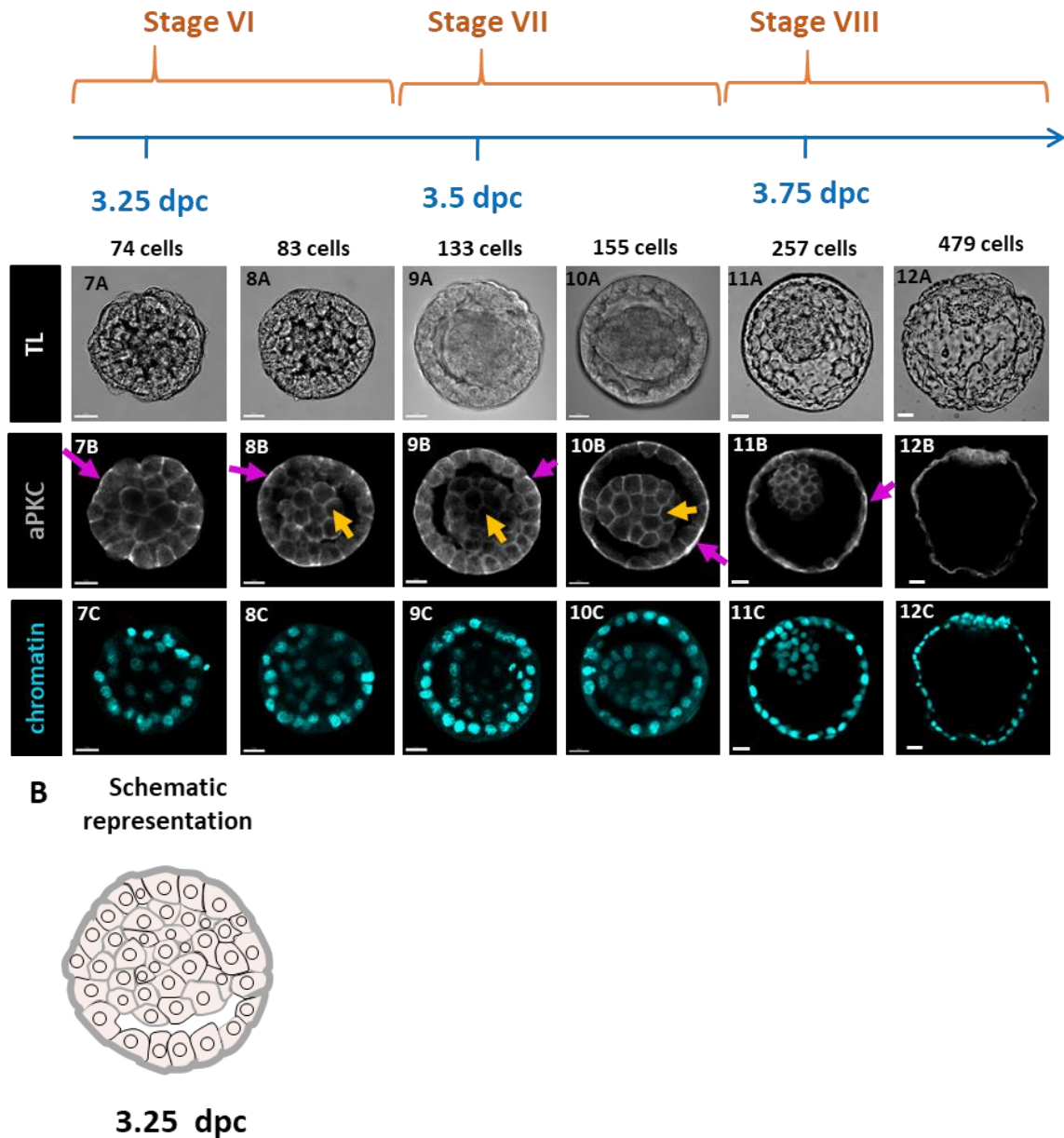


Figure 11. Localisation of aPKC during preimplantation development of the rabbit embryo.

A Confocal images of representative single z-sections of embryos at stages II-VII immunofluorescently labelled for aPKC (white), nuclei (blue) and representative cross-section transmitted light (TL) image. Polarity marker aPKC is detected from 8-cell stage in the basolateral domain of cells (blue arrow) (**panels 2-3**). In compacting morulae, before cavitation (stage V) aPKC is observed in basolateral domains of outer cells (blue arrows) and it is localised in apolar manner in the inner cells (yellow arrows) (**panel 4 and 6**). Later on, simultaneously with cavitation initiation its basolateral distribution in TE starts to be replaced with the localisation in the apical domain (magenta arrows), approximately at stage 3.0-3.25 dpc. aPKC remains evenly distributed within the whole cell cortex in ICM cells during blastocyst development (**panels 7-12**).

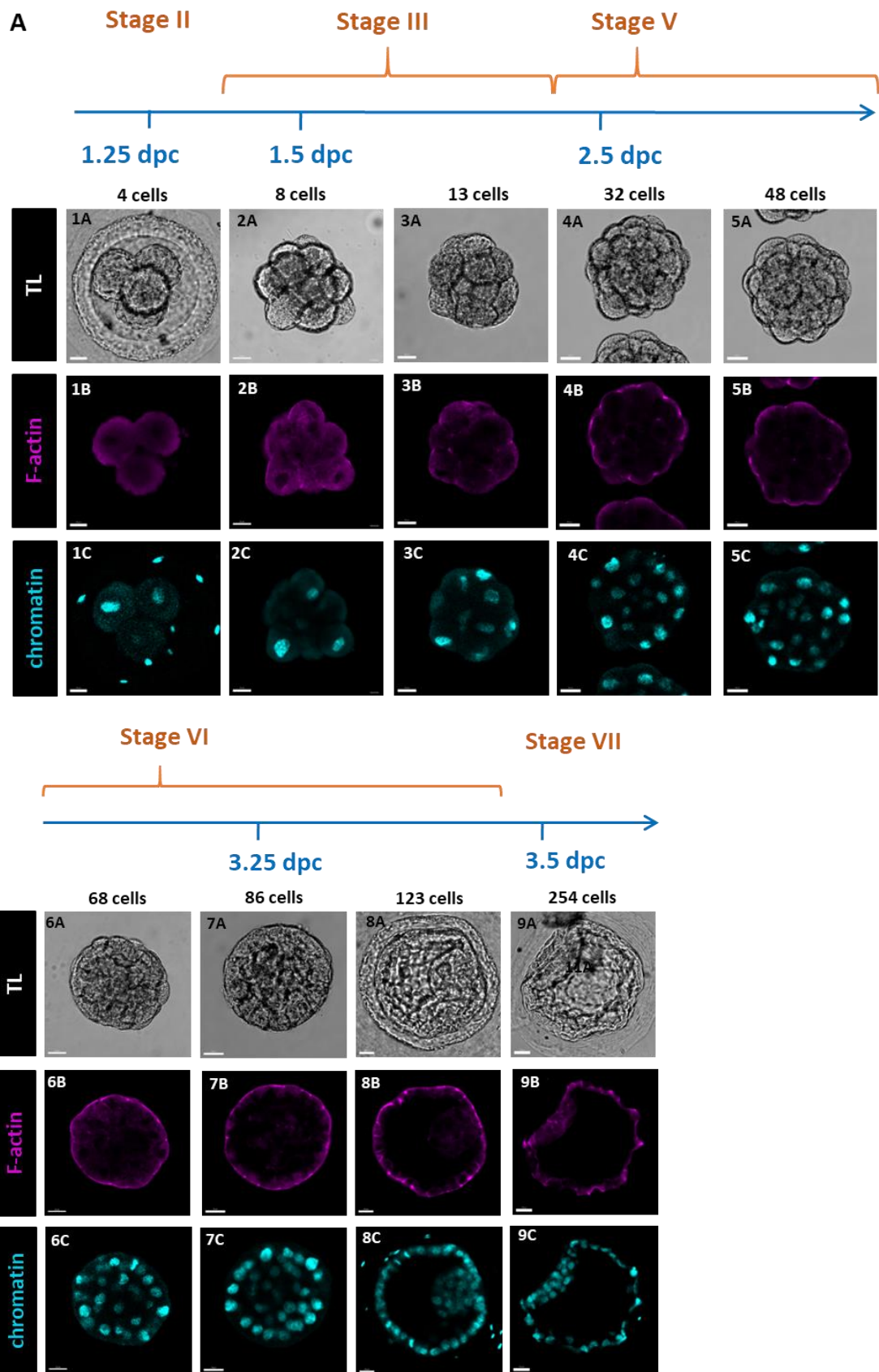
B Schematic representation of aPKC localisation (white) at 3.25 dpc. Scale bars: 20µm, (30 µm for 479-cells embryo).

My data provide evidence that in the rabbit embryo, changes in aPKC distribution are linked to the process of polarization of the outer cells. This may suggest that, similarly to what has been reported in mice, cattle or humans (Plusa et al. 2005; A. Suzuki and Ohno 2006; Gerri et al. 2020), aPKC is visibly related to apicobasal polarity and TE differentiation in rabbit embryos. However, unlike in mice, aPKC localises in the basolateral domain of the outside cells for an extended period of time before cavitation.

8.4.3 F-actin

Filamentous actin (F-actin) is a member of cytoskeletal structure, associated with polarisation during compaction and blastocyst formation (McLaren and Smith 1977; Ducibella et al. 1975; Tan et al. 2015; Okuno et al. 2020). It was postulated that F-actin is involved in downregulating the Hippo pathway by sequestering AMOT to the apical surface (Sun and Irvine 2016; Hirate et al. 2013; 2015).

I analysed F-actin localisation in the rabbit embryo from 1.5 dpc stage onwards. The protein is detected at 1.5 stage it mostly diffused in the cytoplasm (stages III-IV n=42 and n=24) (**Figure 12. panels 2 and 3**). As early as 2.5 dpc, F-actin becomes more specifically localised at the apical domain of outside cells, while it still remains visible in the cytoplasm (**Figure 12. panel 4**). F-actin signal becomes progressively restricted to the apical domain as development progresses. In compacting morulae, the protein is not detected in the cytoplasm of inner cells, while in outer cells it continues to be localised in the apical domains (stage V, n=41) (**Figure 12. panel 4-6**). During cavity formation, F-actin is more visibly accumulated in the apical domains of TE cells (stage VI, n=41) (**Figure 12. panel 7-8**). By contrast, the signal keep decreasing in the inside cells. At mid-blastocyst stage, F-actin remains exclusively restricted to the apical domains of TE cells, while in ICM cells it is detected in the surface between adherent outer cells AJs regions (stage VII, n= 19) (**Figure 12. panel 9**).



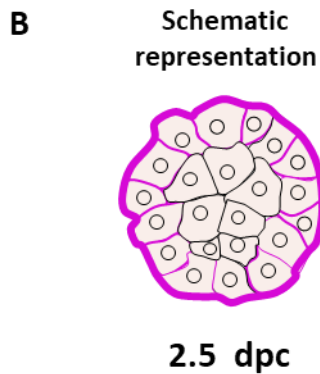


Figure 12. Distribution of F-actin at specific stages of rabbit embryo development in vivo.

A Representative single z-section confocal images of embryos at stages II-VII immunofluorescently stained for F-actin (magenta), nuclei (blue) and representative cross-section transmitted light (TL) image. F-actin is one of cytoskeleton components, that begins to accumulate in the apical cortex at 8-cell stage (**panel 2**). Later on, from 2.5 dpc (stage V), it starts to be restricted to outside cells (**panel 4**). When the compaction starts, F-actin signal decreases from cell-cell contacts in inside cells, however it is more concentrated in outside cells (**panel 4-6**). During cavitation, F-actin is highly accumulated in the apical surface of TE cells (**panel 7-8**), instead at the mid-blastocyst F-actin localisation is also detected in ICM cells (**panel 9**). **B** Schematic representation of F-actin localisation (magenta) at 1.5 dpc. Scale bars: 20 μ m (30 μ m for 254-cells embryo).

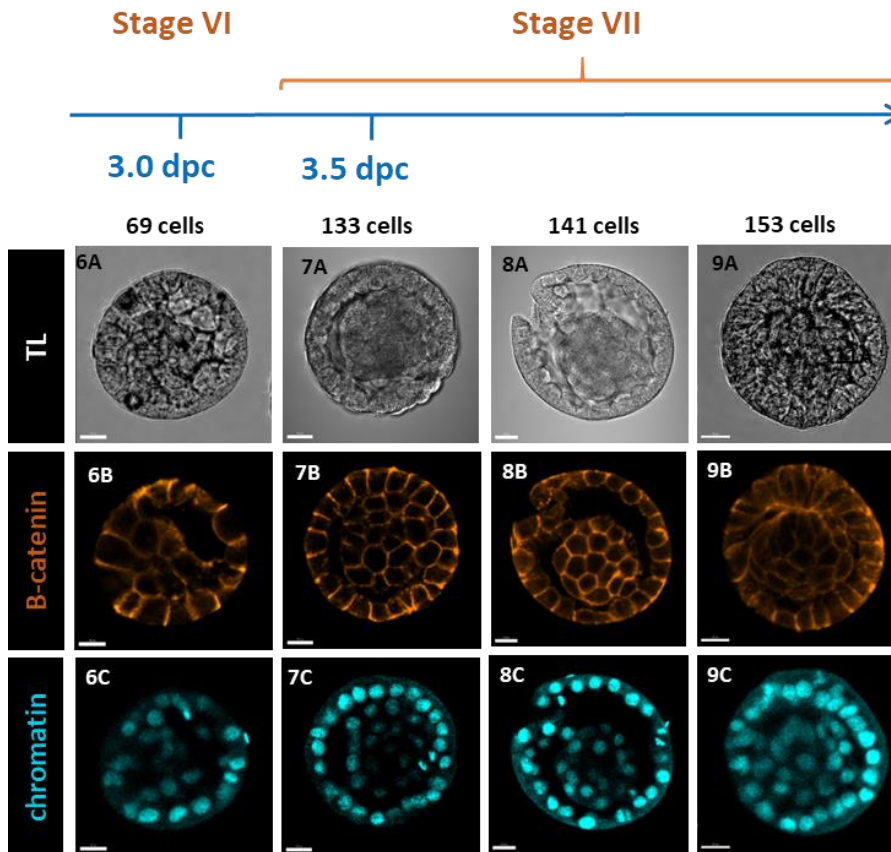
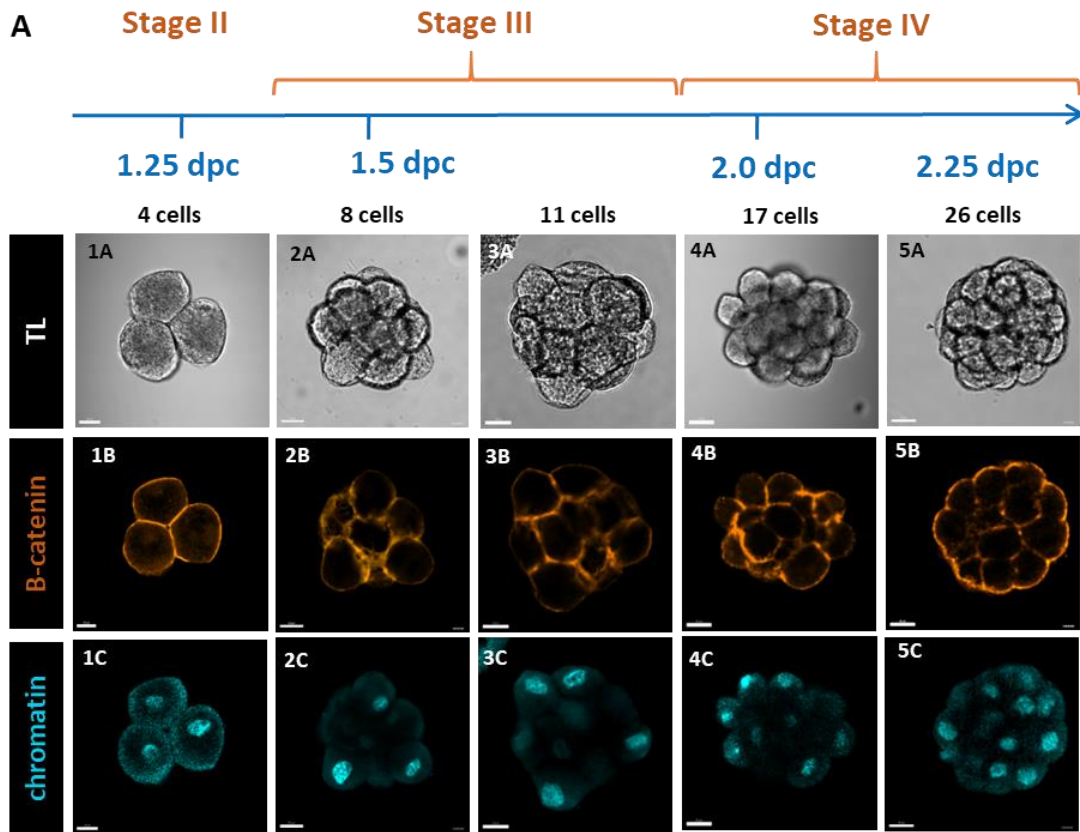
The change in F-actin distribution from early morula to blastocyst stage coinciding with the development of the apical domain in the outside cells. That may suggest that F-actin is involved in the TE/ICM differentiation, as a main factor responsible for cell polarisation in the rabbit embryo.

8.4.4 β -catenin

In mammals, β -catenin is an adaptor protein binding to E-cadherin. It plays a leading role in the Wnt/ β -catenin pathway cascade, which is involved in the early stages of the mouse embryo development (Lindström et al. 2015).

In rabbits, the protein is visible in the cell cortex from 4-cell stage (Stage II, n=24) (**Figure 13. panel 1**). As early as 8-cell stage (Stage III, n=10), whereas inside cells exhibit evenly distributed β -catenin all over the plasma membrane, outside cells display the signal localized only to the basolateral domain (**Figure 13. panels 2-3**). During the initiation of compaction, β -catenin appears to be detected on the

basolateral and apical surfaces of outer cells (stage IV, n=8) (**Figure 13. panels 4-5**). Later, at 3.0 dpc (stage VI, n=6), when GATA3 is already present in the outside cells, β -catenin is strongly concentrated in the basolateral domains of TE cells, unlike in the ICM cells, where the protein is localised in the cell cortex, but in a non-polarised manner (**Figure 13. panels 6-7**). The distribution pattern of this protein in the TE and ICM cells is maintained until the mid-blastocyst stage (stage VII, n=4) (**Figure 13. panels 8-9**).



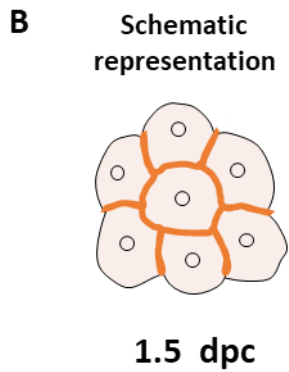


Figure 13. Distribution of β -catenin at consecutive stages of rabbit embryo development in vivo.

A Representative single z-section confocal images of embryos at stages II-VII immunofluorescently stained for β -catenin (orange), nuclei (blue) and representative cross-section transmitted light (TL) image. The polarity-associated protein β -catenin can be detected in the rabbit embryo from 4-cell stage (**panel 1**). Not later than 8-cell stage (1.5 dpc), it is restricted to the basolateral domain in the outside cells, however the distribution is not polarised in inside cells (**panels 2-3**). In developing morulae β -catenin signal can be also detected in both the apical and basolateral domains of the outside cells (**panels 4-5**). In the blastocyst, β -catenin is restricted to TE cells, however distribution of the signal shows no polarisation in the ICM (**panels 6-7**). This distribution pattern is maintained until mid-blastocyst (Stage VII) (**panels 8-9**). **B** Schematic representation of β -catenin localisation (orange) at 1.5 dpc. Scale bars: 20 μ m.

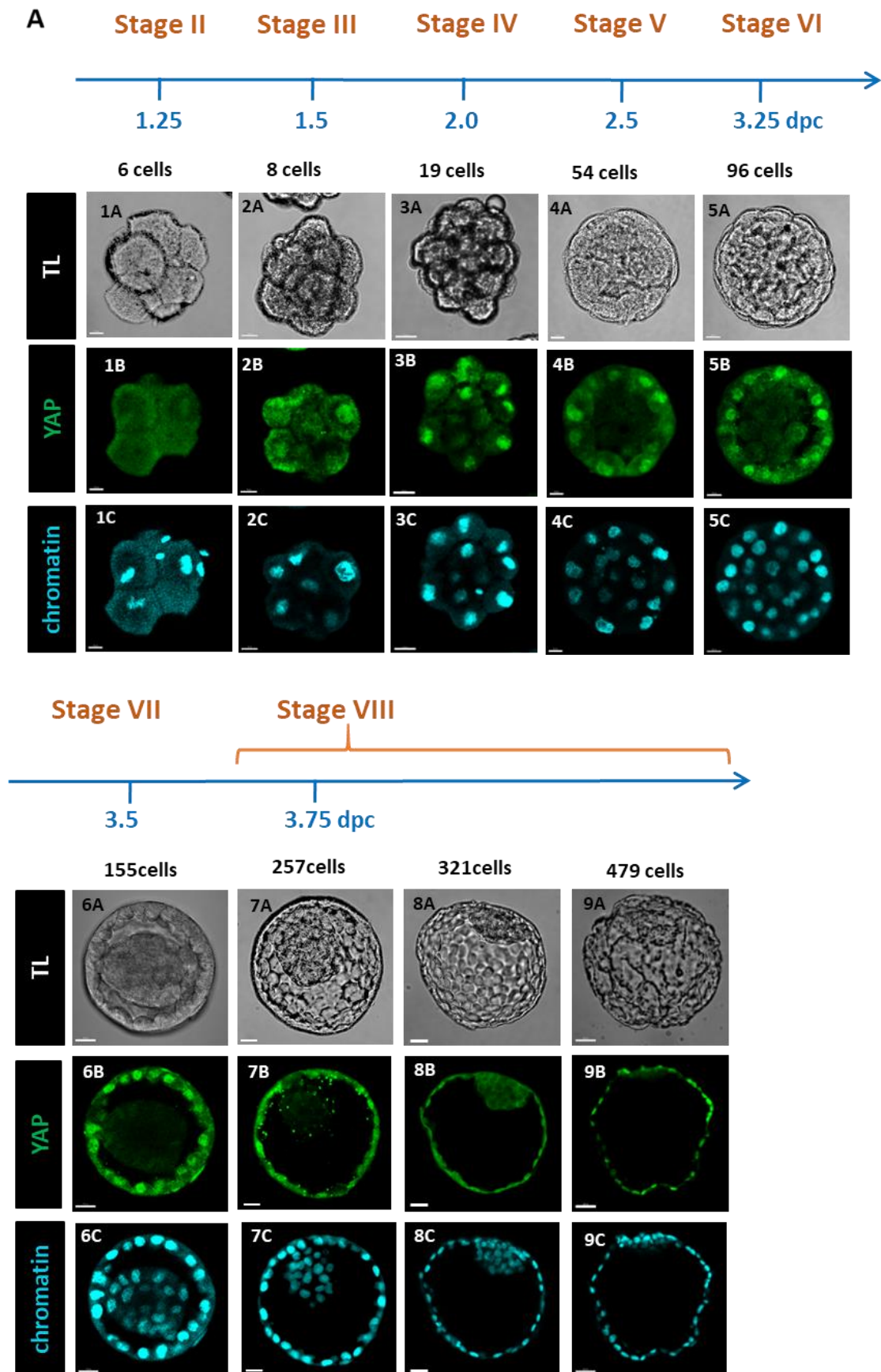
My analysis indicates that polarity-associated β -catenin localisation is restricted to the basolateral domain of the outside cells as early as 3.0 dpc (stage VI) during cavity formation. Therefore, it is reasonable to conclude that β -catenin is also involved in establishing apicobasal polarity in the rabbit embryo.

8.5 YAP localisation in the rabbit embryo from 8-cell stage to the blastocyst stage

YAP protein, also called YAP1 (Yes-associated protein 1), plays a crucial role in mammalian embryo development. YAP, known as a co-activator of transcription factor family TEAD4, acts downstream of the Hippo pathway. Nuclear localisation of YAP is required for the activation of TE-specific genes. In the mouse embryo, as early as 16-cell stage YAP starts to be visible in nuclei of the outside cells, while in inside cells, it is localised in the cytoplasm (Nishioka et al. 2009; Chan et al. 2011). Later on, at the blastocyst stage, YAP is detected in the nuclei of the majority of TE cells, whereas in

ICM cells, it remains in the cytoplasm (Nishioka et al. 2008; 2009; Hirate et al. 2015; Gu et al. 2022)

To investigate the role of YAP during the rabbit embryo preimplantation development, I analysed the subcellular YAP localisation in embryos at consecutive stages (**Figure 14**). Cytoplasmic and weak nuclear signal of YAP are observed in rabbit embryos even before 8-cell stage (**Figure 14. panel 1**). From 8-cell stage, YAP is observed in the nuclei of the majority of cells (**Figure 14. panel 2-3**). At 2.5 dpc (stage IV), in the outside cells YAP starts to be restricted to the nuclei (**Figure 14. panel 4**). In cavitating embryos, at 3.25 dpc (stage VI), nuclear and cytoplasmic YAP continues to be restricted to TE cells (**Figure 14. panel 5**). The number of YAP-positive nuclei in TE gradually increases concomitantly with blastocyst development. At the same time, in ICM cells, YAP is predominantly localised in the cytoplasm (**Figure 14. panels 6-9**). A detailed quantitative analysis of YAP localisation in rabbit embryos is presented in the following paragraphs.



B Schematic representation

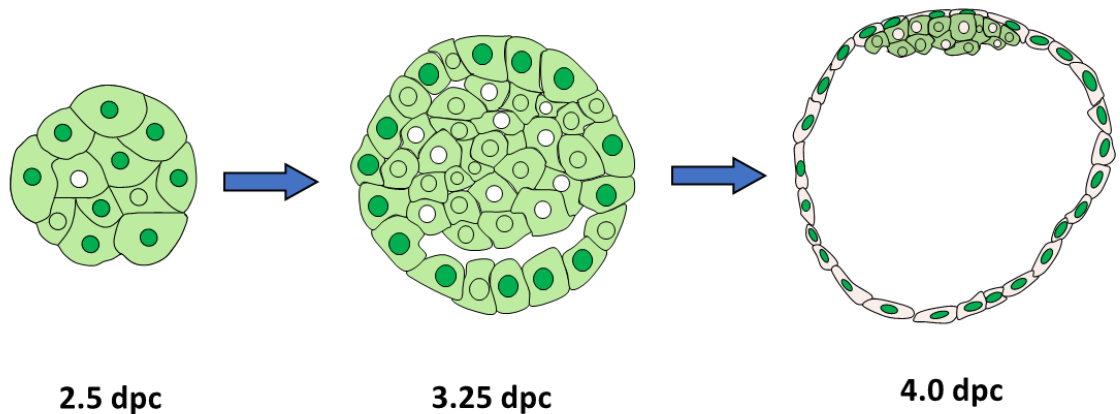


Figure 14. YAP localisation at consecutive stages of rabbit embryo development in vivo.

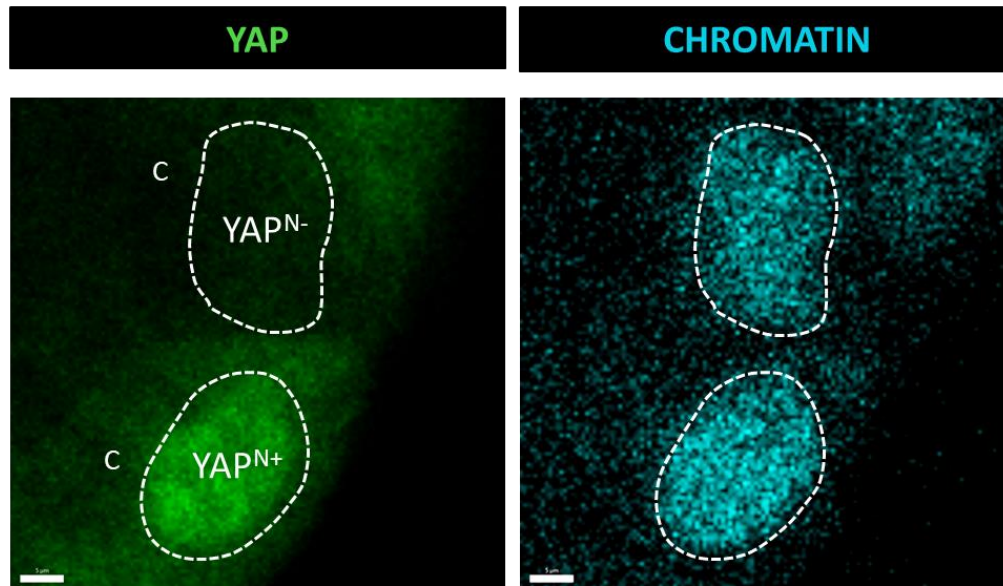
A Representative single z-section confocal images of embryos at stages II-VIII immunofluorescently stained for YAP (green), and nuclei (blue) and representative cross-section transmitted light (TL) image. A weak nuclear YAP signal is visible at 6-cell stage (**panel 1**). At 8-cell stage, the nuclear localisation of YAP is detected in most cells (**panels 2-3**). At 2.5 dpc the nuclear distribution of YAP starts to be reduced in inner cells and becomes progressively restricted to outside cells (**panel 4**). From 3.25 dpc onwards, when the TE and ICM lineages become morphologically distinguished, the YAP signal starts to concentrate in the nuclei of TE cells, while in ICM cells, it remains mostly cytoplasmic (**panels 5-8**). At later stages, TE cells maintain exclusively the nuclear distribution of YAP (**panel 8**). **B** Schematic representation of YAP localisation (green) at 2.5, 3.25 and 4.0 dpc. Scale bars: 20 μ m (30 μ m for 257-cells embryo).

My analysis shows that the temporal pattern of YAP nuclear localisation seems to accompany the initiation of TE differentiation. Similar to mice, YAP starts to be detected in nuclei as early as 8-cell stage. Later, its nuclear distribution becomes more restricted to outer cells. In contrast, cytoplasmic localisation of YAP in ICM cells is maintained until late blastocyst stage.

8.5.1 Nuclear localisation of YAP at stages II-IX

Nuclear localisation of YAP (active YAP) indicates in which cells of the embryo the Hippo pathway is inactive, and in which ones the TE program is initiated in the mouse embryo (Nishioka et al. 2008). To scrutinise the dynamics of YAP distribution during early rabbit development, I analysed the percentage of cells with YAP-positive nuclei

(YAP^{N+}) at stages II-IX. All cells without YAP nuclear signal (YAP^{N-}) were categorised as YAP-negative nuclei (**Figure 15**).



YAP^{N-} a cell with YAP-negative nucleus

YAP^{N+} a cell with YAP-positive nucleus

Figure 15. Nuclear and non-nuclear localisation of YAP in two adjacent TE cells at 3.25 dpc embryo. The embryo was stained for YAP (green) and chromatin (Hoechst, blue). The image depicts a cell with no YAP signal in the nucleus (YAP^{N-}, top) and a cell presenting the nuclear localisation of YAP (YAP^{N+}, bottom). Cell nucleus area is outlined in white. "C"= cytoplasm. Scale bars = 5µm

For embryos at stages II, III and IV, I calculated the percentage of YAP^{N+} cells from the total number of cells. The average contribution of YAP^{N+} and YAP^{N-} cells to the total cell count of the embryo is presented below (**Figure 16. A-C**). For embryos at stages V-IX, when the embryo is morphologically composed of inside/ICM cells and outside/TE, I counted the contribution of YAP^{N+} and YAP^{N-} cell categories separately for the inside and outside compartments (the inside and outside cells). The average contribution of YAP^{N+} and YAP^{N-} cells at stages V-IX is presented below (**Figure 16. D-H**).

In embryos at stage II (21-31 hpc; n=10), the percentage of YAP^{N+} cells (78%) was higher than the percentage of YAP^{N-} cells (22%) (**Figure 16. A**). In embryos at stage III (1.0-1.5 dpc; n=18), average percentage of YAP^{N+} cells was 49% and for YAP^{N-} cells 51%

(Figure 16. B). At stage IV (1.5-2.5 dpc; n=8), the average contribution of YAP^{N+} cells (71%) was higher than YAP^{N-} cells (29%) **(Figure 16. C).**

In the inside cells of embryos at stage V (2.5-3.25 dpc; n=4) the average percentage of YAP^{N+} cells (21%) was lower than the average percentage of YAP^{N-} cells (79%). In the outside cells of embryos at stage V, the average contribution of YAP^{N+} cells (74%) was higher than the percentage of YAP^{N-} cells (26%) **(Figure 16. D).** For stage VI (3.0-3.5 dpc; n=9), the ICM percentage contribution of YAP^{N+} cells was lower (16%) than the contribution of YAP^{N-} cells (84%). However, the percentage of YAP^{N+} cells in TE was 78%, constituting a clear majority over the participation of YAP^{N-} cells (22%) **(Figure 16. E).** In embryos at stage VII (3.0-3.75 dpc; n=14) the ICM contribution of YAP^{N+} cells was lower (1%) than the contribution of cells with YAP^{N-} cells (99%). In TE cells the percentage of YAP^{N+} cells reached 59%, while the percentage of YAP^{N-} cells was 41% **(Figure 16. F).** At stage VIII (3.25-3.75 dpc; n=17), I verified that in the ICM, the percentage of YAP^{N+} cells was 41%, while the percentage of YAP^{N-} cells was 59%. In contrast, in TE cells, the percentage of YAP^{N+} cells was higher (74%) than the average contribution of YAP^{N-} cells (26%) **(Figure 16. G).** In embryos at stage IX (3.5-4.25 dpc) (n=11), the ICM contribution of YAP^{N+} cells was 49%, while the percentage of YAP^{N-} cells reached 50%. In TE cells, I determined that the contribution of YAP^{N+} cells (96%) was significantly higher than the average percentage of YAP^{N-} cells (4%) **(Figure 16. H).**

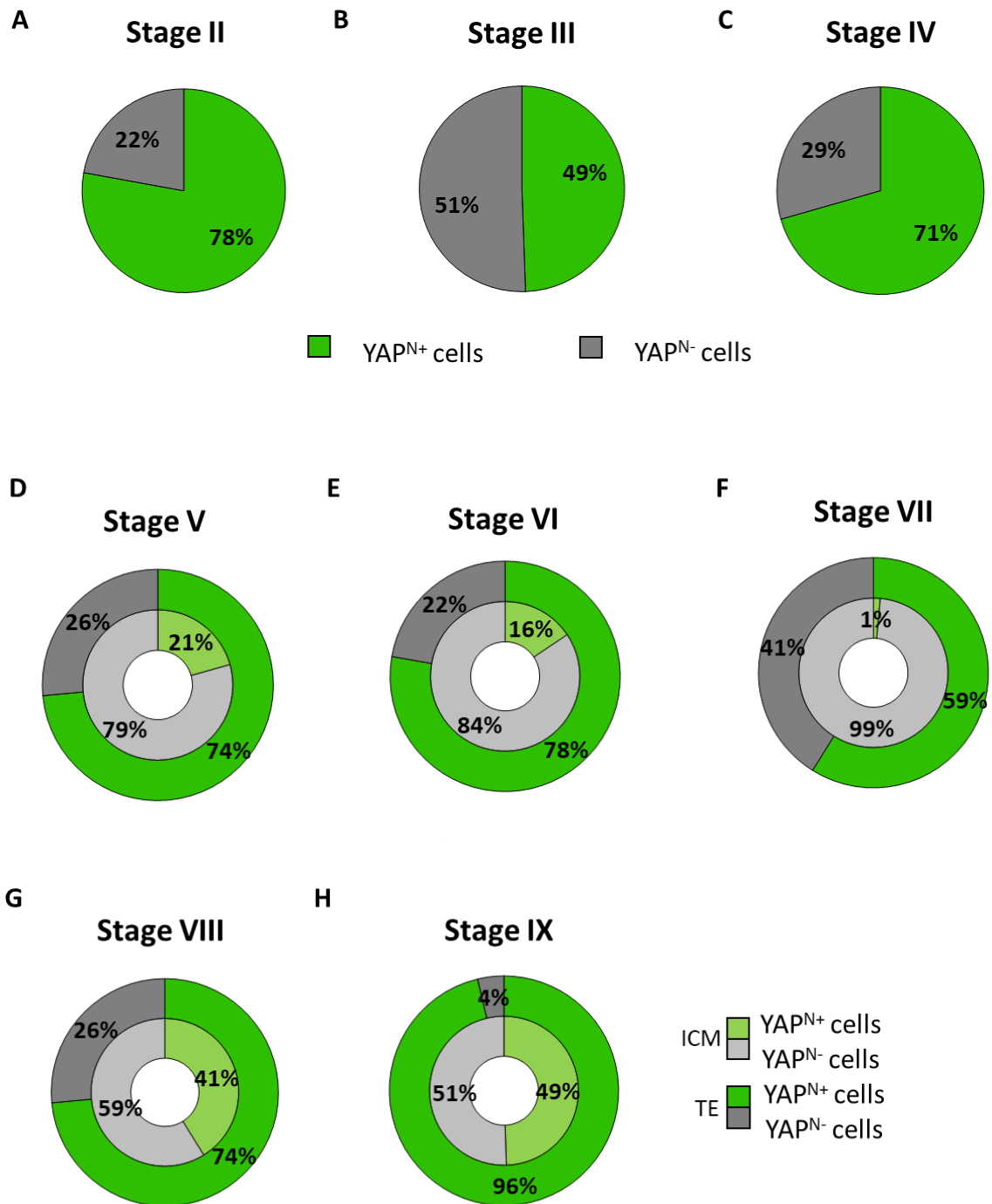
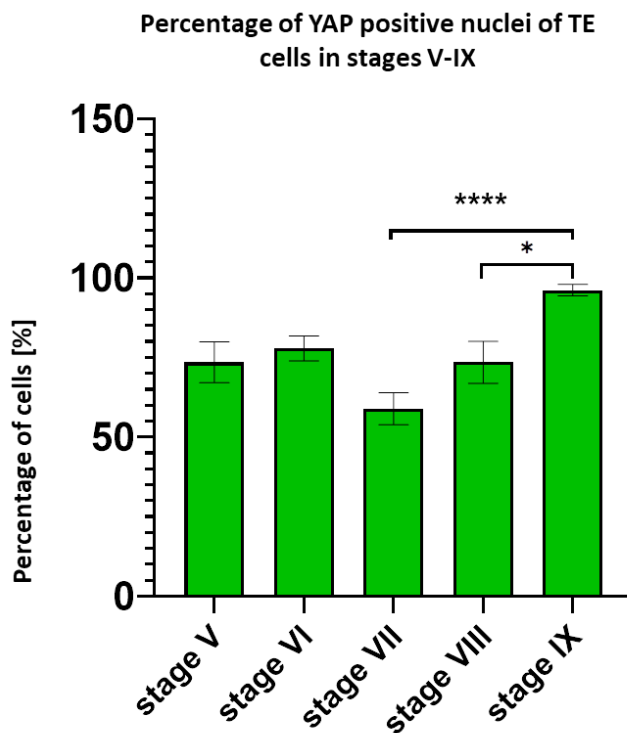


Figure 16. The contribution of nuclei positive and negative for YAP at stages II-IX of the rabbit embryo. **A-C** Percentage contribution of YAP^{N+} cells compared to the percentage contribution of YAP^{N-} cells at stages II-IV. **D-H** ICM and TE contribution of YAP^{N+} cells and YAP^{N-} cells at stages V-IX. Graphs V-IX are composed of double rings, where the inner ring corresponds to ICM cells, and the outer ring corresponds to TE cells.

To investigate differences in the relative contribution of YAP^{N+} cells between stages V-IX in outside/TE compartment, I used Kruskal-Wallis test analysis (considering the developmental stage as an independent factor) (**Figure 17**). The percentages of nuclear distribution of YAP for stages V and VI do not differ significantly and reach 74% and 78%, respectively. In embryos at stage VII, the percentage of YAP^{N+} cells decreases to 59%. Then, at stage VIII, it progressively increases to 74%, and at stage IX it reaches up to 96%. The average percentage of YAP^{N+} cells in TE was significantly different among stages, as indicated by Kruskal-Wallis test (p-value<0.001). Statistically significant differences were found using Dunn's multiple comparison test, between stages VII and IX (p-value<0.0001) and between stages VIII and IX (p-value<0.05) (**Figure 17**).



*Figure 17. Comparison of the YAP^{N+} cells contribution in the outside compartment between stages V-IX. Percentage of outside/TE cells with YAP nuclear localisation. Post-hoc comparisons are denoted by symbol * (*p<0.05; ****p<0.0001; Dunn's multiple comparison test).*

In embryos at stage II, YAP^{N+} cells already represent more than a half of the total cell number. Shortly before cavitation, at the morula stage V, the percentage increases up to 74% in outside cells. At stage VII, the proportion of YAP^{N+} cells decreases to less than 60% in TE. At stages VIII and IX, the percentage of YAP^{N+} cells in TE increases to

74% and 96%, respectively. The analyses of subcellular YAP localisation presented here suggest that the nuclear localisation of YAP coincides with the differentiation of the TE lineage in rabbit embryos.

8.5.2 Analysis of subcellular YAP localisation at stages III-VII

In the previous section (7.5.1) I analysed YAP nuclear distribution at consecutive rabbit developmental stages and noticed that YAP is present in the nucleus as well as in the cytoplasm. Therefore, I decided to further assess subcellular YAP localisation. In the mouse, different subcellular localisations of YAP imply distinct functions of this protein in the cell, and three categories of YAP cytoplasmic-nuclear localisation can be distinguished (Mihajlović and Bruce 2016). To assess the subcellular YAP localisation dynamics in early rabbit development, I analysed embryos stained for YAP at consecutive developmental stages (III-VII). Based on knowledge from mice, the first category represents the cells where the nuclear YAP signal is visibly stronger than YAP cytoplasmic signal (**N>C**). The second category comprises the cells where the nuclear and cytoplasmic signals appear equal (**N=C**), and the third category - the cells where the nuclear YAP signal is visibly weaker than the cytoplasmic signal (**N<C**). The following figure depicts nuclei with all three different categories described above (Figure 18).

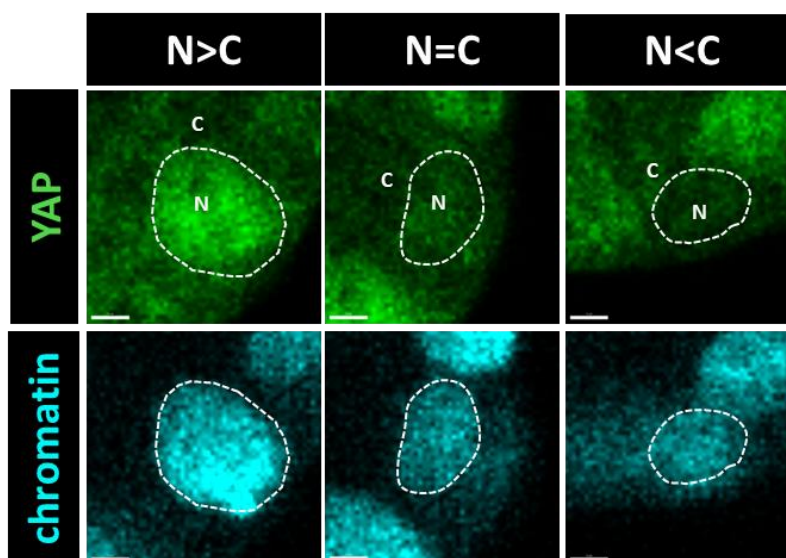


Figure 18. Confocal images representing three categories of subcellular YAP localisation in TE cells at 3.25 dpc. Nuclear YAP signal appears to be stronger than its cytoplasm signal (N>C). Nuclear and cytoplasmic signals are approximately equal (N=C). The nuclear YAP signal appears to be weaker than the cytoplasmic signal (N<C). The embryo labelled for YAP (green) and chromatin (Hoechst, blue). The area of the cell nucleus is outlined in white. “C”= cytoplasm. Scale bars = 5µm.

To quantify the subcellular YAP localisation dynamics in the early rabbit development (stages III-IV, i.e., between 8 and 16 cells), I counted cells with three categories of YAP localisation (N>C, N=C, N<C). Data are presented as the average percentage contribution of particular YAP localisation categories. The percentages of the three YAP distribution types were calculated relative to the total cell number. For the early stages III-IV, the percentage of cells with N>C YAP localisation reached 12.6%, the N=C localisation was approx. 39.8%, and N<C was equal to 47.6% of the total cell number (Figure 19).

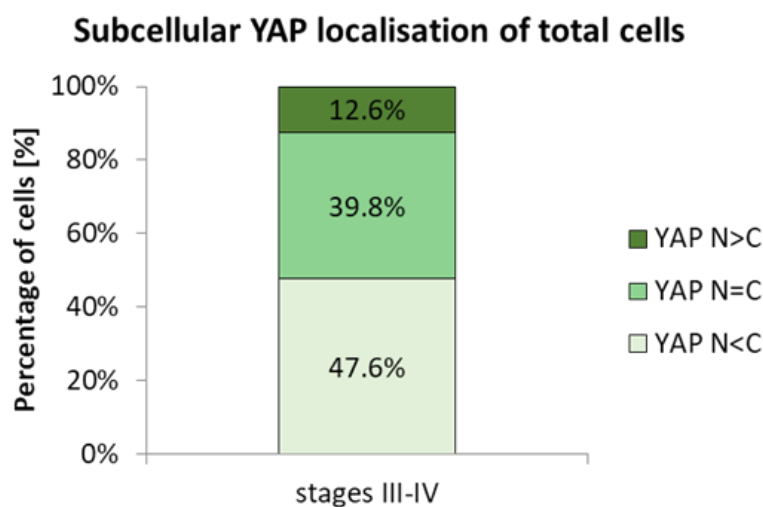
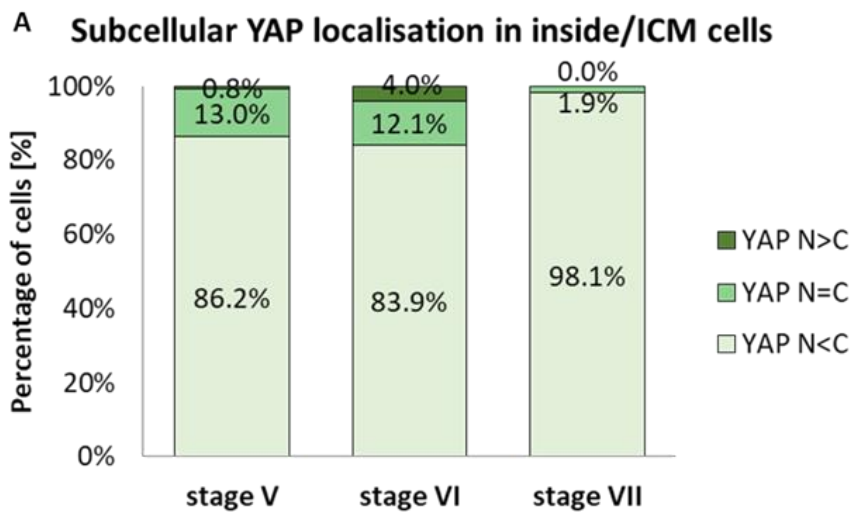


Figure 19. Contribution of cells with different patterns of subcellular YAP localisation in rabbit embryos at stages III-IV. Average contributions of cells exhibiting: the nuclear YAP signal stronger than the cytoplasmic signal (N>C), approximately equal signal intensity (N=C), and the nuclear distribution of YAP with weaker signal than in the cytoplasm (N<C), in embryos at stages III-IV.

Quantification of cells with different patterns of YAP localisation (N>C, N=C, N<C YAP) was also performed for embryos at stages V, VI and VII, where the inside/ICM cells and outside/TE cells were analysed separately (hereon referred to as the inside

compartment and outside compartment, respectively). For comparisons of the three categories of cells across the three developmental stages (V, VI, and VII) in the inside and outside compartments, an ordinary one-way ANOVA test was used, or the Kruskal-Wallis test (when analysed data did not exhibit normal distribution), for which the embryo developmental stage was considered the independent factor.

In the inside compartment, the average contribution of cell category N>C YAP reached equal, small values in all analysed stages (0.8% at stage V, 4% at stage VI, and 0% at stage VII) ($p>0.05$, Kruskal-Wallis test) (**Figure 20. B**). The average contribution of cells with N=C YAP in the inside compartment (13% at stage V, 12.1% at stage VI, 1.9% at stage VII) was not significantly different between stages ($p>0.05$, Kruskal-Wallis test) (**Figure 20. C**). The contribution of cells with N<C YAP was equal to 86.2% at stage V, 83.9% at stage VI, and 98.1% at stage VII, Kruskal-Wallis test revealed that mean values were statistically different between stages ($p<0.05$). Post-hoc analysis confirmed a significant difference between stages VI and VII (Dunn's multiple comparison test, $p<0.05$) (**Figure 20. D**).



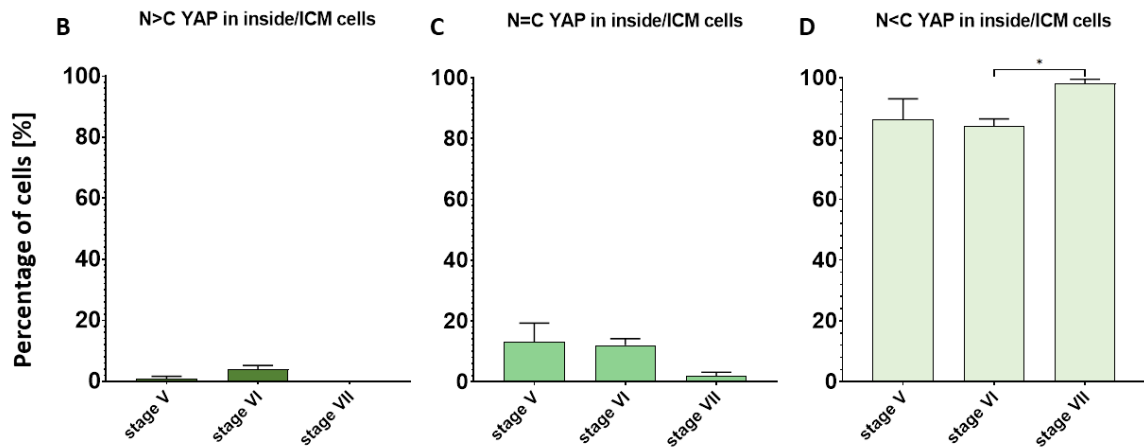


Figure 20. Percentages of subcellular YAP localisation in the inside compartment at stages V-VII.

A Proportion of averaged percentages of inside cells exhibiting more intense nuclear YAP signal than in the cytoplasm ($N>C$), approximately equally intense signals ($N=C$), and nuclear YAP signal weaker than cytoplasmic signal ($N<C$) (stages V, VI and VII). **B** Comparison between stages V, VI and VII of cells with YAP $N>C$ signal, **C** of cells with YAP $N=C$ signal, **D** of the percentages of cells with YAP $N<C$ signal in the inside compartment. Post-hoc comparisons are denoted by * (* p -value <0.05 ; Dunn's multiple comparison test).

In the next step, I analysed the patterns of subcellular YAP localisation in the **outside compartment** at the same developmental stages. I confirmed that the mean percentage of cells with $N>C$ YAP in the outside compartment was statistically different among stages (p -value <0.01 , Kruskal-Wallis test). Using post-hoc comparisons I found that the percentage of cells with $N>C$ YAP at stage V (49.4%) and VI (48.8%) were significantly higher than in embryos at stages VII (8.7%) (stage V vs. VII p -value <0.05 ; stage VI vs. VII p -value <0.01 ; Dunn's multiple comparison test) (**Figure 21. B**). The participation of cells with $N=C$ YAP in the outside compartment (28% at stage V, 24% in embryos at stage VI and 58% at stage VII) was significantly different among stages (p -value <0.05 , Kruskal-Wallis test). Using post-hoc test I indicated a significant difference in the percentage of $N=C$ YAP between stages VI and VII (Dunn's multiple comparison test, p -value <0.05) (**Figure 21. C**). The average percentage of cells with $N<C$ YAP in the outside compartment did not significantly differ between stages (23% at stage V, 27.2% at stage VI, 33.6% at stage VII) (p -value >0.05 , one-way ANOVA test) (**Figure 21. D**).

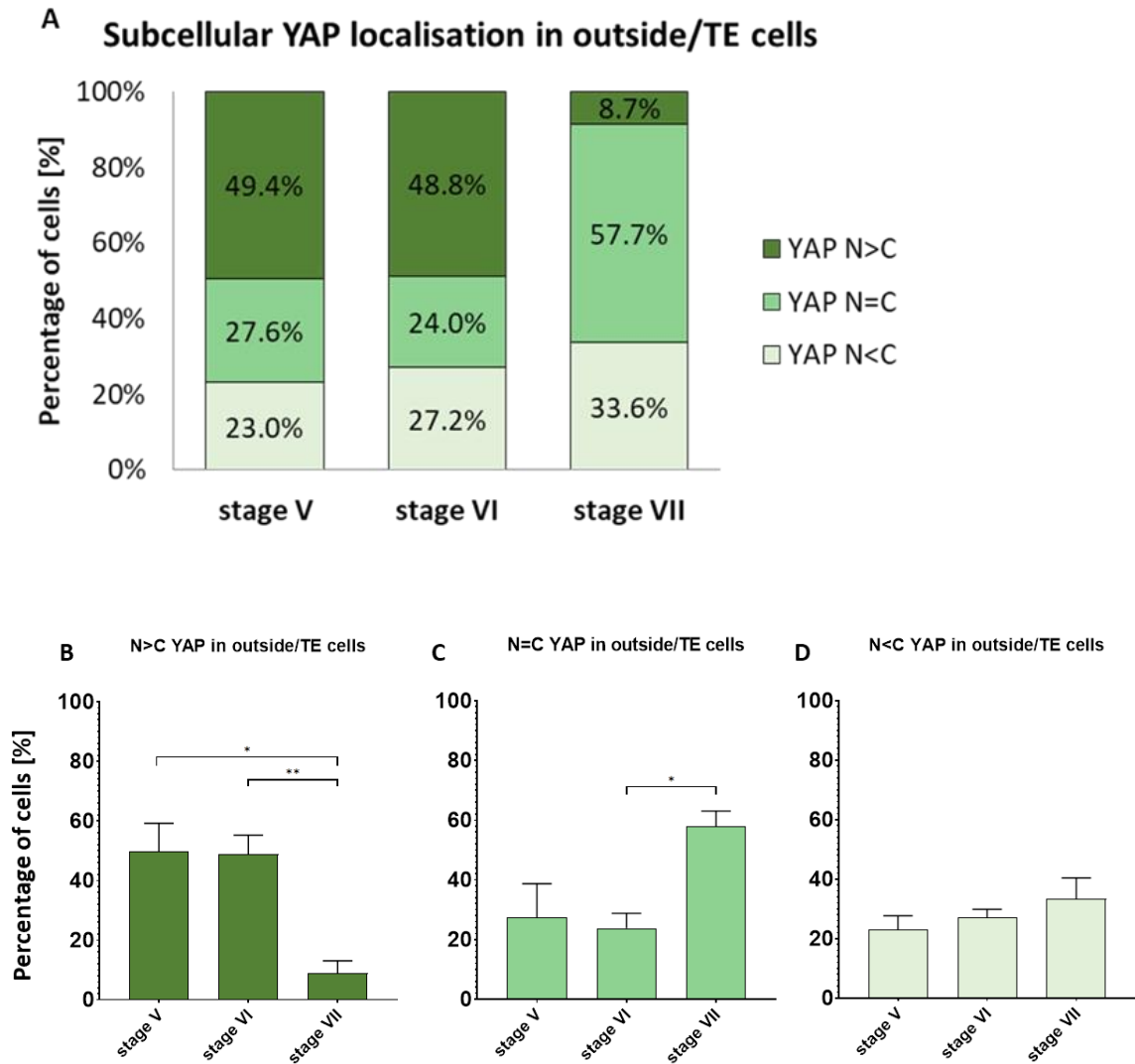


Figure 21. Contribution of cells with different subcellular YAP localisation patterns in outside/TE cells at stages V-VII.

A Proportion of average percentages in outside cells exhibiting nuclear YAP signal greater than cytoplasmic signal (N>C) approximately equal signals (N=C) or nuclear YAP signal weaker than cytoplasmic signal (N<C), of embryos at stage V, VI and VII. **B** Comparison between stages V, VI and VII of the percentages of outside/TE cells with YAP N>C signal. **C** Comparison between stages V, VI and VII of the percentages of outside/TE cells with YAP N=C signal. **D** Comparison between stages V, VI and VII of the percentages of outside/TE cells with YAP N<C signal. Post-hoc comparisons are denoted by * (*p-value <0.05; **p-value <0.01; Dunn's multiple comparison test).

To summarise, YAP is predominantly excluded from the nuclei of the inside/ICM cells from late morula (stage V) to the mid-blastocyst (stage VII) indicating that Hippo pathway remains active in the inside cells. Instead, in the outside/TE cells YAP is

maintained in majority of nuclei strongly suggesting differential activity between these compartments.

8.6 Colocalisation of YAP and GATA3

To investigate whether the nuclear localisation of YAP, which is related to the Hippo pathway activity, coincides with GATA3 in the inside and outside cells of the rabbit embryo, I analysed colocalisation of YAP and GATA3 in the nuclei at consecutive stages of rabbit development. (**Figure 22**). Before compaction (stage III-IV), YAP is already detected in some nuclei, even if they are devoid of GATA3 signal (**Figure 22. panel A3 and A4**). In compacting morulae, shortly before cavitation (stage V), most outer cells exhibit nuclear GATA3 signal (**Figure 22. panel B**). After cavitation (stages VI and VII), GATA3 and YAP are both present in the nuclei of most of the TE cells (**Figure 22. panels C-D**). Detailed quantification of the data is presented below.

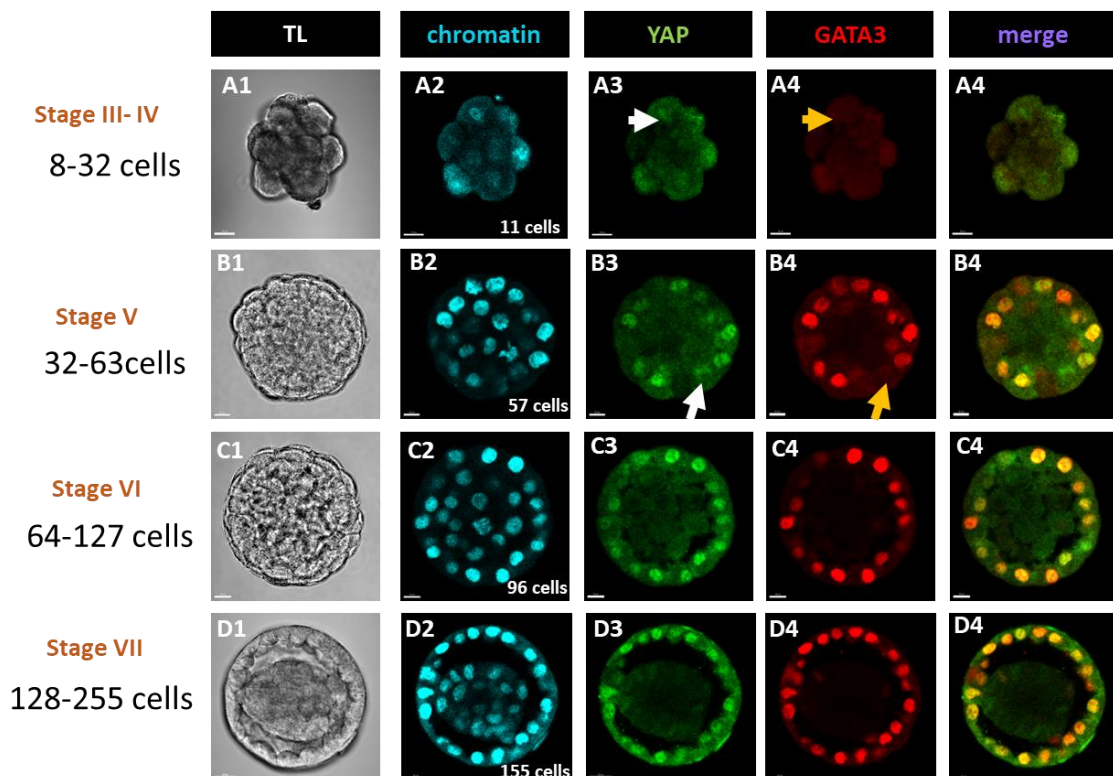


Figure 22. Colocalisation of YAP and TE marker GATA3. Representative single z-section confocal images of embryos at stages: III-IV, V, VI and VII stained for YAP (green), GATA3 (red), and chromatin (Hoechst, blue), and transmitted light (TL) single z-section images (A1-D1). Nuclei positive for YAP are marked by white arrows. In embryos at stages III-IV, YAP distribution in

nuclei starts to be detected in both outer and inner cells. However, no GATA3-positive cells are observed yet (**panel A4**). As early as stage V and shortly before cavitation, many YAP and GATA3-positive nuclei are detected, however certain cells show YAP-positive nuclei but with no GATA3 signal (**panel B3, B4**). In both stages: VI and VII, GATA3 and YAP nuclear colocalisation is observed in most TE cells (**panels C5 and D5**). Nuclei negative for GATA3 are marked by yellow arrows. Scale bars = 20 μ m.

To quantify the colocalisation of YAP and GATA3 in nuclei (data presented in the section **7.6**), I considered the contribution of cells in rabbit embryos at consecutive developmental stages in four categories:

- cells with nuclei positive for YAP and negative for GATA3 (**YAP+/GATA3-**)
- cells with nuclei double positive for YAP and GATA3 (**YAP+/GATA3+**)
- cells with nuclei positive for GATA3 and negative for YAP (**YAP-/GATA3+**)
- cells with nuclei double negative for YAP and GATA3 (**YAP-/GATA3-**)

Simultaneously, I subdivided the analysis of YAP and GATA3 colocalisation into abovementioned four categories: stages III-IV (8-31 cells, n = 5), stage V (32-63 cells, n = 5), stage VI (64-127 cells, n = 16) and stage VII (128-255 cells, n = 6).

8.6.1 YAP and GATA3 colocalisation in morula stage embryos (stages III-IV)

In embryos at stages III-IV (**Figure 23**), I calculated the average percentage of cells with double positive nuclei (YAP+/GATA3+) per embryo to be 3.8% of the total number of cells. The percentage of cells with nuclei positive for YAP (YAP+/GATA3-) in the embryo reached 48.6%. Similarly, the average percentage of cells with nuclei double negative for YAP and GATA3 (YAP-/GATA3-) was equal to 47.6% per embryo. At this developmental stage, I did not detect cells positive for GATA3 only (YAP-/GATA3+) (0%). In embryos at stages III-IV, I detected no YAP-/GATA3+ cells, whereas in the same embryos I observed cells with nuclear signal of both YAP and GATA3. A graphical representation of the data from the individual embryos and a detailed statistical analysis of embryos at stages III-IV can be found in the supplementary data (**Figure S1**).

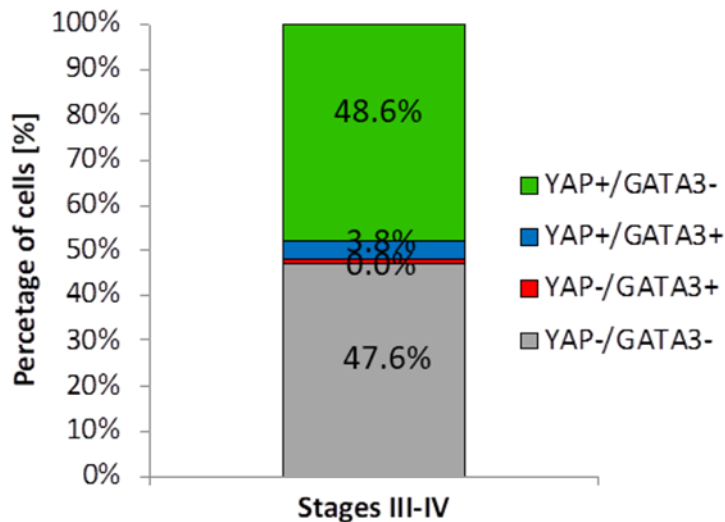


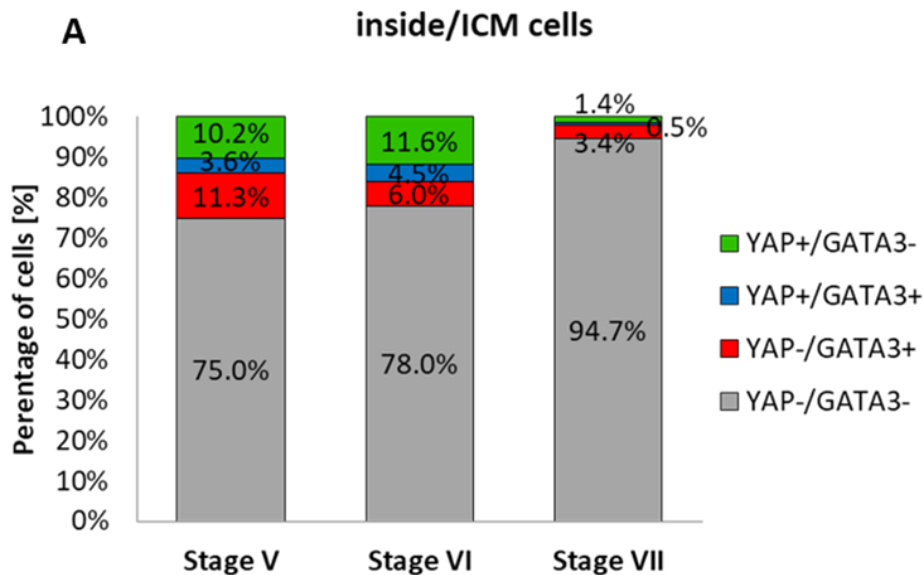
Figure 23. Quantification of YAP+ and GATA3+ cells in embryos at stages III-IV. Contribution of total cells with YAP-positive and GATA3-negative nuclei (YAP+/GATA3- cells), GATA3-positive nuclei only (YAP-/GATA3+ cells), double positive nuclei (YAP+/GATA3+ cells), and double negative nuclei for YAP and GATA3 (YAP-/GATA3- cells) in rabbit embryos at stages III-IV.

Taken together, these data show that in embryos at stages III-IV, YAP is localised in the nuclei in almost half of the cells, however only a very low percentage of cells exhibit colocalisation of both proteins (merely 4% of the total cell number). Interestingly, YAP-/GATA3+ cells were not observed, which suggests that GATA3 is likely not required for YAP nuclear localisation at stages III-IV of rabbit development. Rather, translocation of YAP into the nucleus might be required for GATA3 initiation in the nucleus of cells at the morula stage.

8.6.2 YAP and GATA3 colocalisation in the inside cells at stages V, VI and VII

The graphical representation of the quantification of YAP and GATA3 colocalisation in inside/ICM cells among stages V, VI and VII is presented in **Figure 24**. To compare the relative contributions of the four cell categories (YAP+/GATA3-, YAP+/GATA3+, YAP-/GATA3+, YAP-/GATA3- cells), the ordinary one-way ANOVA test was used (or Kruskal-Wallis test, when the analysed data did not exhibit a normal distribution), with the

developmental stage as an independent factor. The contribution of YAP+/GATA3- cells in the inside compartment (10.2% at stage V, 11.6% at stage VI and 1.4% at stage VII) was statistically different among stages (p-value<0.05, Kruskal-Wallis test). Using multiple post-hoc tests I determined that the contribution of YAP+/GATA3- cells was significantly higher at stage VI than at stage VII (p-value<0.05, Dunn's multiple comparisons test). The participation of YAP+/GATA3+ cells (3.6% at stage V, 4.5% at stage VI and 0.5% at stage VII) was not statistically different between these stages (p-value>0.05, Kruskal-Wallis test). The participation of YAP-/GATA3+ cells in the inside compartment (11.3% at stage V, 6.0% at stage VI and 3.4% at stage VII) also did not differ between stages (p-value>0.05, Kruskal-Wallis test). Above data did not exhibit normal distribution, probably because of small number of cells in these categories. The percentage of YAP-/GATA3- cells in the inside compartment (75.0% in stage V, 78.0% at stage VI, and 94.7% at stage VII) was statistically different among stages, (p-value<0.01, ordinary one-way ANOVA test). As indicated by post-hoc tests, the contribution of YAP-/GATA3- cells at stage V was significantly lower than at stage VI and stage VII (p-value<0.05, Tukey's multiple comparisons test).



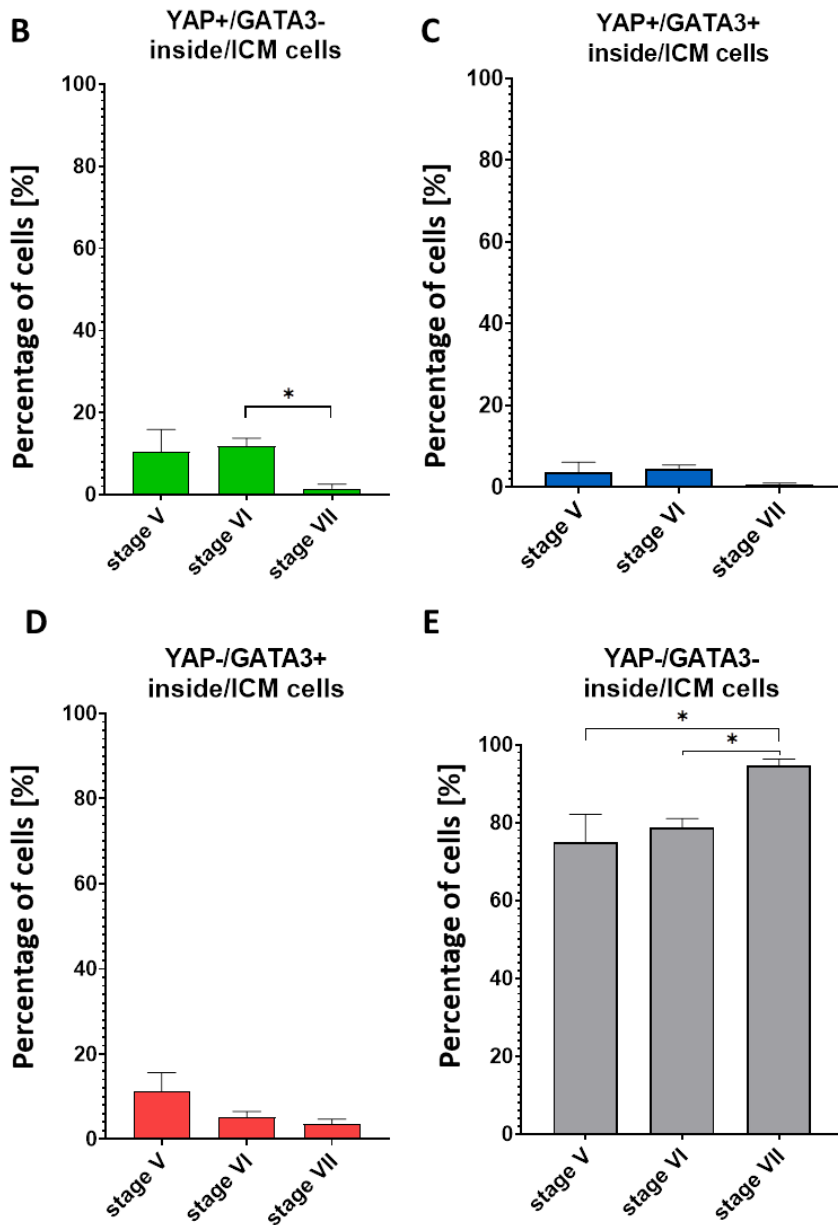


Figure 24. Relative contributions of cells positive and negative for YAP and GATA3 in embryos at stages V, VI and VII in the inside compartment. **A** Proportions of four different categories of cells in the inside compartment of embryos at stages V, VI and VII. **B** Contribution of cells with nuclei positive for YAP only (YAP+/GATA3- cells), **C** nuclei double positive for YAP and GATA3 (YAP+/GATA3+ cells), **D** nuclei positive for GATA3 only (YAP-/GATA3+ cells), **E** nuclei double negative for YAP and GATA3 (YAP-/GATA3- cells) in the outside compartment from embryos at stage V, VI and VII. Post-hoc comparisons are denoted by * (* p-value < 0.05, Tukey's multiple comparison test and Dunn's multiple comparison test).

Cells categorised as YAP+/GATA3-, YAP+/GATA3+ and YAP-/GATA3+ contributed only in small percentage to the inside compartment (up to 11.6%). In the inside cells, YAP-/GATA3- category displays the highest value at all three stages V, VI and VII.

Therefore, my observations indicate that YAP is excluded from the nuclei in the majority of the inside cells from stage V (late morula) to stage VII (mid blastocyst). Also, GATA3 is observed in a minority of inside cells at stages V-VII, however YAP does not colocalise in every GATA3 positive cell.

8.6.3 YAP and GATA3 colocalisation in the outside cells at stages V, VI and VII

The analysis of YAP and GATA3 colocalisation in outside/TE cells along stages V, VI and VII is presented in **Figure 25**. Similarly to the results previously presented for inside cells, in the outside cells statistical analyses included ordinary one-way ANOVA or Kruskal-Wallis test, when appropriate (a developmental stage was an independent factor). In this case, the mean percentage of YAP+/GATA3- cells in the outside compartment (27.1% at stage V, 18.1% at stage VI and 14.1% at stage VII) did not significantly differ among stages (p -value >0.05 , Kruskal-Wallis test). Data did not exhibit normal distribution, probably because of small number of cells in this category. For the YAP+/GATA3+ cells, the mean percentages (49.9% at stage V, 54.7% at stage VI and 52.4% at stage VII) did not represent significant differences (p -value >0.05 , ordinary one-way ANOVA test). The percentage of YAP-/GATA3+ cells (6.2% at stages V, 12.4% at stage VI, and 13.3% at stage VII) also did not differ significantly between stages (p -value >0.05 , ordinary one-way ANOVA test). Also, no differences between stages were detected for the mean percentage of YAP-/GATA3- cells in the outside compartment (p -value >0.05 , ordinary one-way ANOVA test). A graphical representation of the individual embryos (inside/ICM and outside/TE cells) at particular stages V-VII can be found in the supplementary data (**Figures S2-S4**).

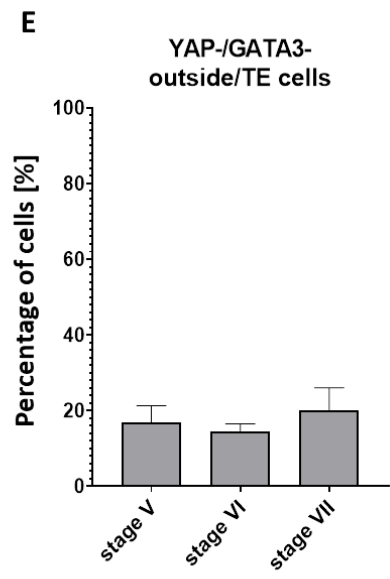
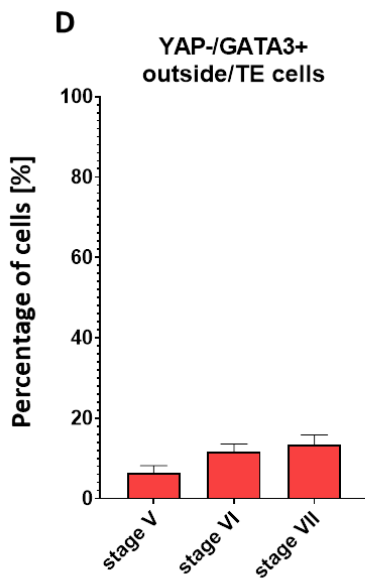
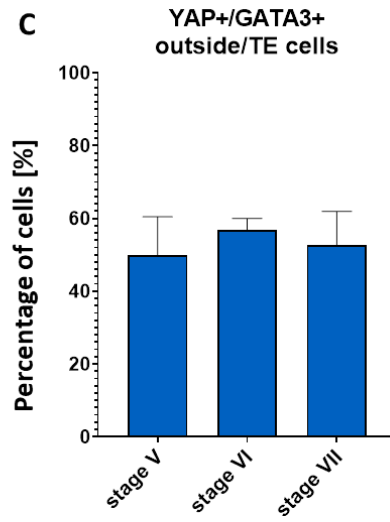
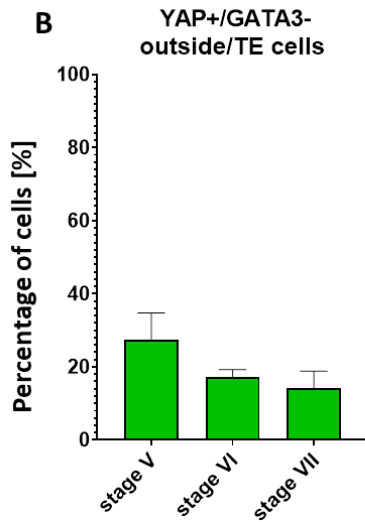
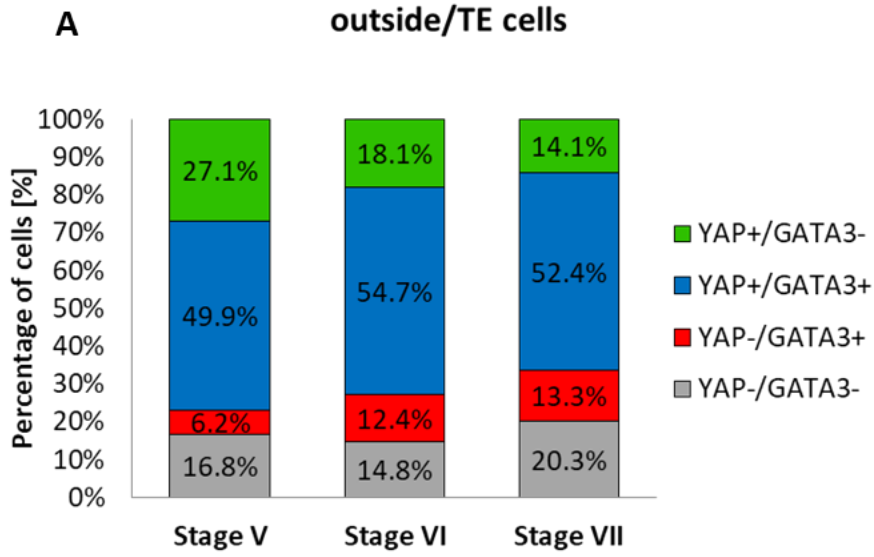


Figure 25. Contribution of YAP+ and GATA3+ cells in embryos at stages V, VI and VII in the outside compartment. A Contribution of four different categories of cells in the outside compartment of embryos at stages: V, VI and VII. B Contribution of cells with nuclei positive for YAP only (YAP+/GATA3- cells), C nuclei double positive for YAP and GATA3 (YAP+/GATA3+ cells), D nuclei positive for GATA3 only (YAP-/GATA3+ cells), and E nuclei double negative for YAP and GATA3 (YAP-/GATA3- cells) from embryos at stage V, VI and VII in the outside compartment (ordinary one-way ANOVA test, Kruskal-Wallis test; p-value>0.05)

In the outside compartment, the decrease in the contribution of YAP+/GATA3- cells from stage V to stage VII (from 27% to 14%) does not pose a statistically significant difference. As regards YAP+/GATA3+ cells, values seem to be maintained at similar levels (below 55%) at all three stages V, VI and VII. The contribution of TE YAP-/GATA3+ cells does not significantly increase from stage V to VII (6% to 13%). The percentages of YAP-/GATA3- cells in the outside compartment are similar at all stages V-VII, not higher than 21%.

To summarise, YAP is localised in nuclei in the majority of the outside cells from stage V (late morula) to stage VII (mid-blastocyst). Noteworthy, in all analysed stages cells double positive for YAP and GATA3 represented the largest category. However, cells negative for YAP and GATA3 signals are also detected in the outside compartment.

8.7 Analysis of the role of the Hippo pathway and polarity in the rabbit embryo via inhibition of the ROCK kinase function

To verify whether TE differentiation by means of the Hippo pathway/establishment of cell polarity is mediated by RHO-associated protein kinase activity, I analysed the effect of ROCK inhibition on rabbit embryo *in vitro* development.

8.7.1 Inhibition of ROCK kinase

Two different hallmarks were considered for the effect of ROCK kinase inhibition on embryo development: the establishment of cell polarity at the morula stage and the formation of the blastocyst. Consequently, I cultured 2-cell stage embryos in 20 μ M of the ROCK kinase inhibitor ("ROCKi", Y-27632) for two different time regimes that would allow to analyse each of these events separately: 48h culture to analyse cell polarity, and 72h to assess blastocyst formation. Simultaneously, control groups (without inhibitor) were set up in parallel for each time frame (**Figure 26**).

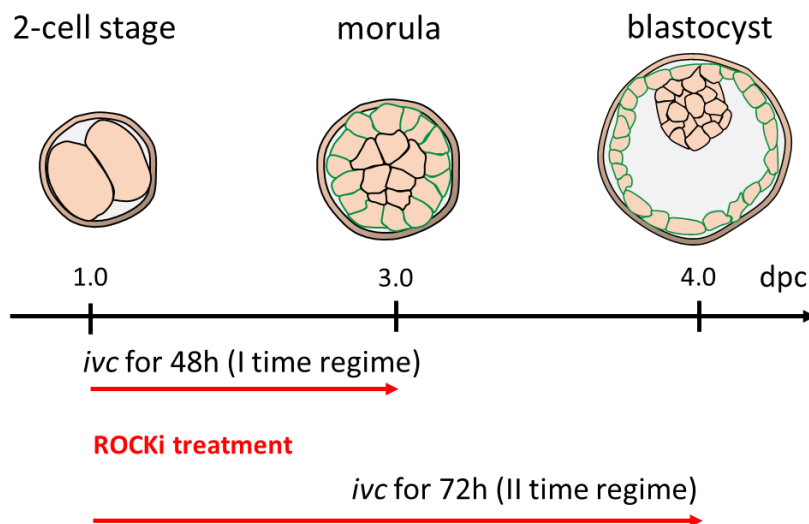


Figure 26. Representative scheme of the experimental strategy to assess *in vitro* development of rabbit embryos in 20 μ M of ROCK-inhibitor Y-27632 (+ control cultured in RDH+BSA (the culture medium) with no ROCK inhibitor).

After the short time regime (48h of culture) of ROCK inhibition treatment, embryos exhibited altered morphology compared to the control group (**Figure 27. A, B**). ROCK-inhibited embryos were less compacted, and individual cells were easily distinguishable (**Figure 27. B'**), which was not possible in control embryos (**Figure 27. B'**).

Secondly, I analysed the cavitation efficiency between the treated and control embryos. After the extended time regime (72h of culture), ROCK-inhibited embryos displayed impaired cavitation (36% cavitation, n=33) when compared to the control group (88% cavitation, n=25) (**Figure 28. A, A1 and B, B1**). Difference of percentage of cavitated embryos between the control and experimental group was statistically significant, as indicated by Chi-square (Fisher's exact) test (p -value<0.0001) (**Figure 28. C**).

ivc for 48h

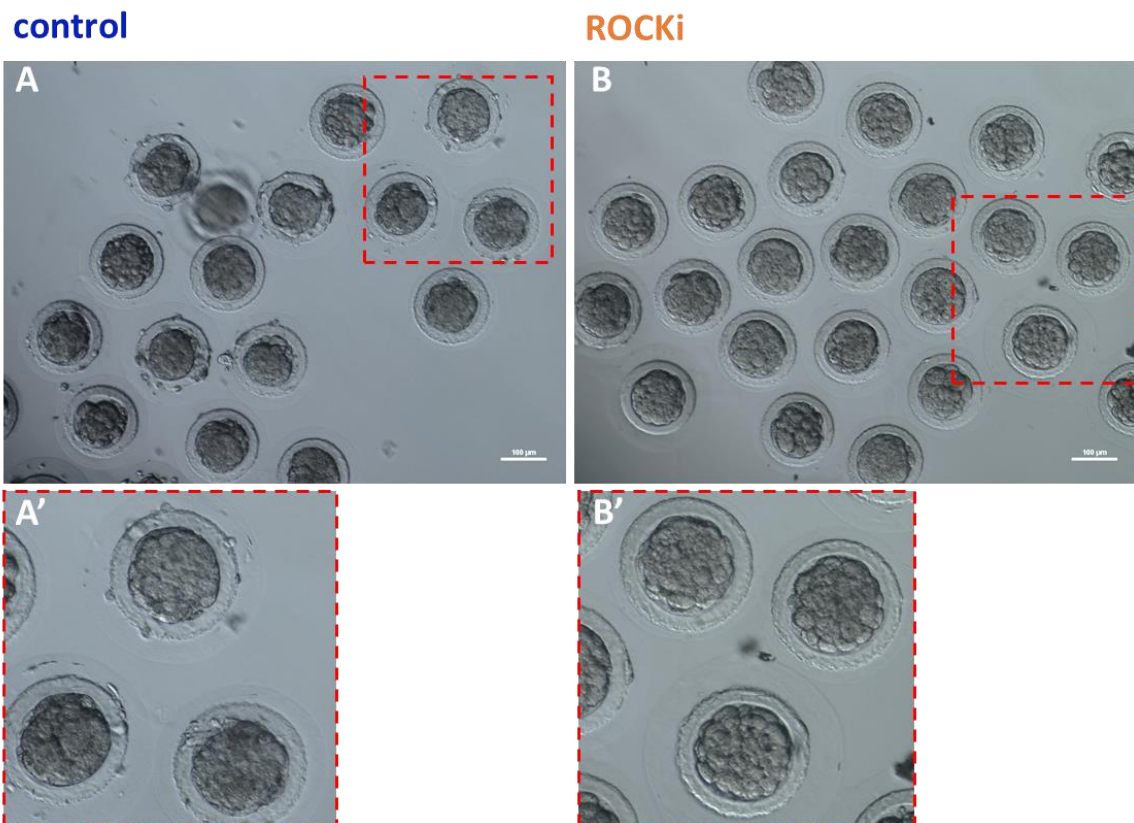


Figure 27. Effect of ROCK inhibition treatment in rabbit embryos after 48h of in vitro culture. **A** Control group (n=46). **B** ROCKi embryos (n=51). Inserts show enlarged details of embryos for each group (**A'** and **B'**). Individual cells can be discerned from each other in embryos from the treated group. Scale bar = 100 μ m

ivc for 72h

control

cavitation=88%

n = 25 (22/25)

ROCKi

cavitation=36%

n = 33 (12/33)

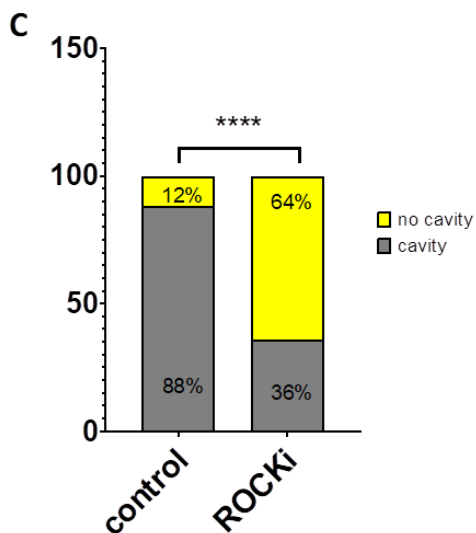
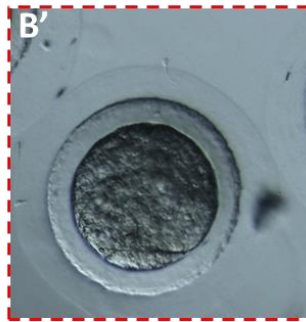
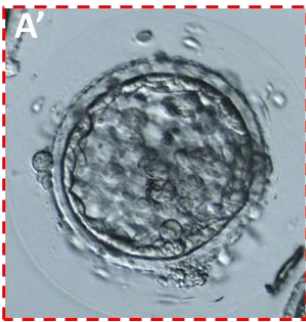
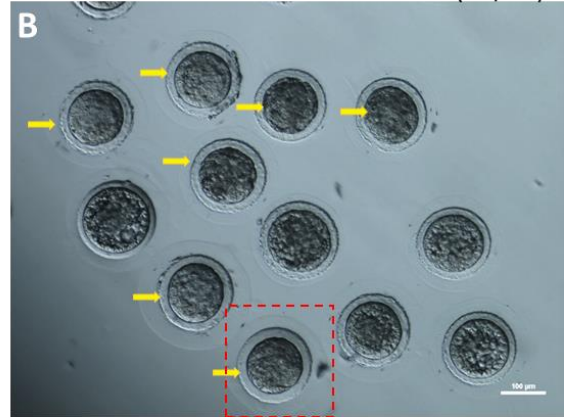
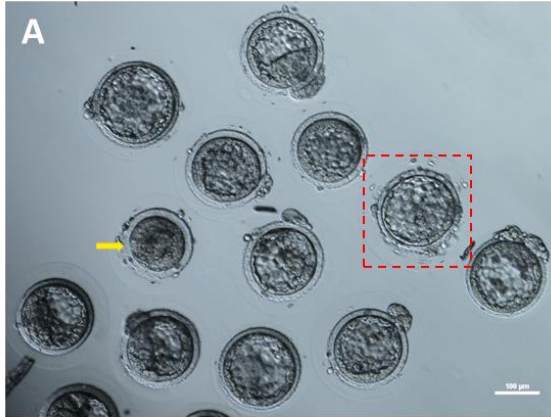


Figure 28. Embryos after 72h of in vitro culture.

A Representative images of control embryos, **B** and ROCKi embryos after 72h of culture. Embryos that failed to cavitate are marked by yellow arrows. **A'** and **B'** Inserts show enlarged details of one embryo for each group, embryo with a cavity in the control (**A'**) and embryo with no cavity in the treated group (**B'**). **C** Averaged percentages of blastocysts (cavity) and morulae (no cavity) in

control and experimental groups presented in the graph, Chi-square test, **** p -value <0.0001 . Scale bar = $100\mu\text{m}$.

Above data imply that inhibition of the ROCK kinase activity in the embryo severely affects compaction and cavitation during rabbit preimplantation development.

8.7.2 Embryo growth after ROCK inhibition

To further assess the role of ROCK in embryonic development I studied the size of embryos. In particular, I measured the diameter of embryos after 48h and 72h of culture. To assess possible differences in average diameter values between the control and experimental (ROCKi) groups, I applied unpaired t-test or Mann-Whitney test (when data did not exhibit a normal distribution). Average diameter values for embryos deriving from the short time regime did not show significant differences between the control ($113.4\mu\text{m}$) and experimental groups ($114.6\mu\text{m}$) (Mann-Whitney test, p -value >0.05) (**Figure 29. A and C**). In contrast, the average diameter of ROCKi embryos from the short time regime was significantly smaller than in the control group ($124.1\mu\text{m}$ vs $139.5\mu\text{m}$, respectively) (unpaired t-test, $p<0.001$) (**Figure 29. B and D**).

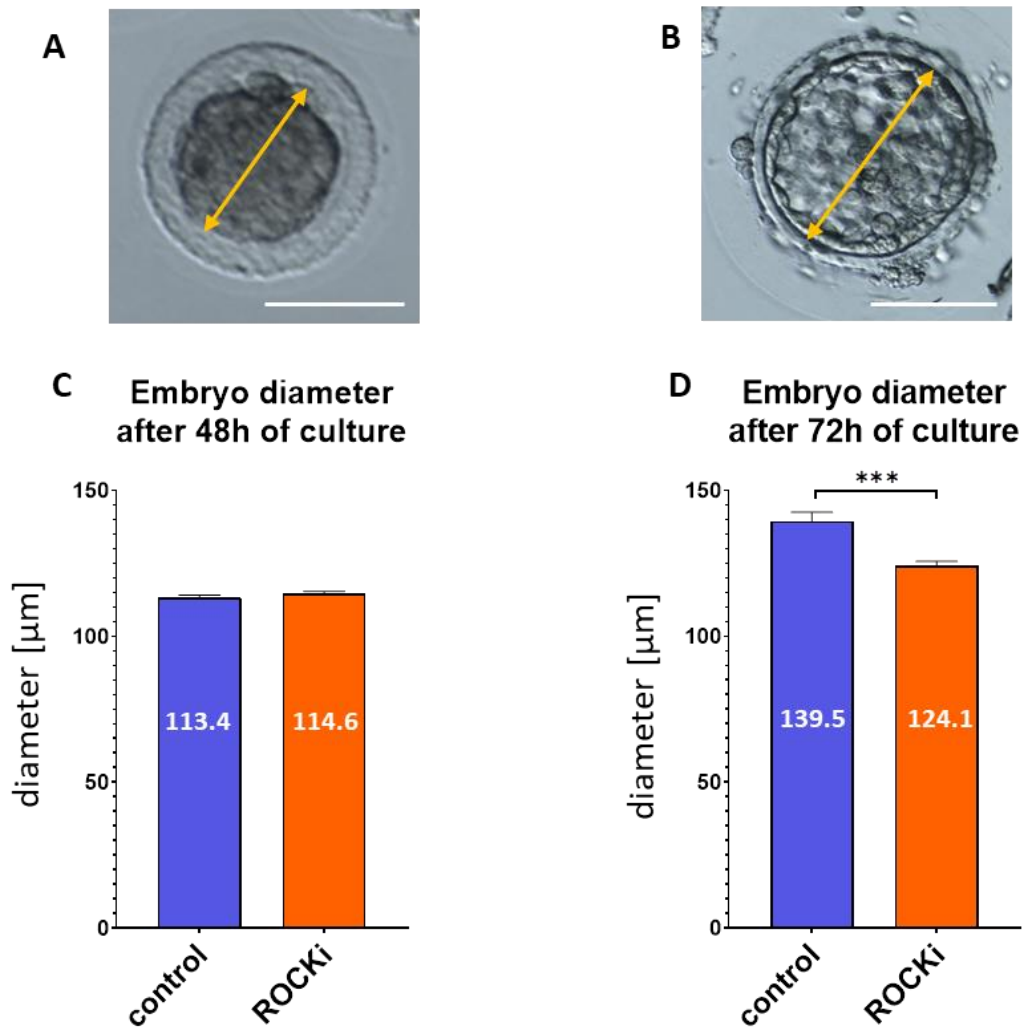


*Figure 29. Average diameter values of the control and ROCK-inhibited (ROCKi) embryos after 48h and 72h of in vitro culture. A Image representing the morula diameter after 48h of culture; B Image representing the morula/blastocyst diameter after 72h of culture. C Comparison of the size (diameter) of embryos between control and experimental groups after 48h of culture. D Comparison of the size (diameter) of embryos between control and experimental groups after 72h of culture. (***) $p < 0.005$; unpaired t-test; Mann-Whitney test. Scale bar =100 μm.*

Rabbit embryos after 48h of culture with ROCK inhibitor had similar mean diameter compared to control embryos. In contrast, the mean diameter of ROCKi embryos after 72h culture was significantly smaller compared to control embryos. Therefore, both the ratio of cavitated embryos and embryo size were affected after ROCK inhibition treatment, which suggests that ROCK activity might regulate crucial aspects of embryo development manifested in the ability to form the blastocyst cavity and to achieve proper embryo growth.

To investigate whether ROCK inhibition during *in vitro* culture affects cell proliferation, I calculated the total cell number and the TE and ICM contribution of the control and experimental embryos after 48h and 72h of culture (**Figure 30**). Due to the fact that ROCK-inhibited embryos did not develop a cavity, when control embryos were already cavitated, for consistency TE and ICM were subsequently categorized as the inside and outside cells. I compared the total cell number between the control and experimental groups using unpaired t-test and Mann Whitney test (data did not exhibit normal distribution). After 48h of culture, embryos from the control group had a significantly higher average total cell number (59 cells) compared to embryos from the experimental group (49 cells) (p -value <0.01 , Mann Whitney test). After 72h of culture, control embryos also exhibited a higher average total cell number (127 cells) compared to experimental embryos (94 cells) (p -value <0.01 , unpaired t-test).

Total number of cells in rabbit embryos cultured *in vitro*

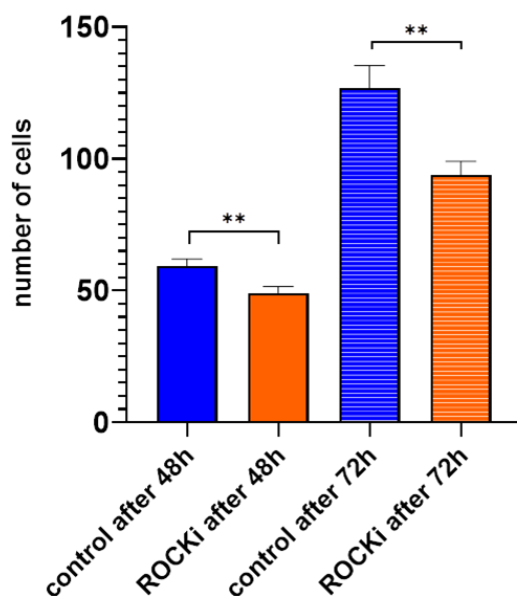


Figure 30. Total cell count of rabbit embryos after two different time intervals (48h and 72h) in *in vitro* culture. Quantification of total cell number in rabbit embryos after 48h and 72h of culture with ROCK inhibitor. (** p <0.01 ; unpaired t-test)

To assess cell proliferation after the culture with ROCK inhibition, I analysed the contribution of inside and outside cells in the embryo after 48h and 72h of culture (**Figure 31**). For both time regimes, the relative contributions of inside and outside cells were similar (p -value >0.05 , unpaired t-test). For both the control and ROCKi groups after 48h of culture, inside cells represented 23% of the total count, whereas the remaining 77% corresponded to the outside cells. In case of embryos cultured for 72h, the inside compartment represented 18% of the total cells in control embryos and 19% in the ROCKi group. As for the outside cells, their contribution was 82% in control embryos and 81% in the treated ones.

Percentage of inside and outside cells after 48h and 72h of culture

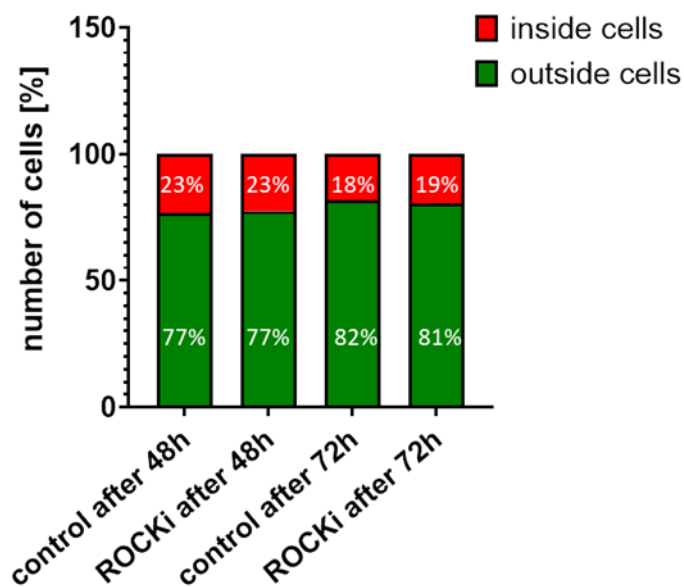


Figure 31. Representation of the relative contributions of inside and outside cells in embryos cultured for different time intervals in the presence and absence of the ROCK inhibitor (ROCKi). Values represent averaged percentages of the outside (green) and inside cells (red) for every group of embryos considered (after 48h and 72h of culture, control group and treated with ROCK inhibitor) (unpaired t-test).

In conclusion, ROCK inhibition leads to a decreased cell number in the rabbit embryo. However, neither the 48h nor the 72h group showed differences in the proportions of inside and outside cells between the control and ROCK-inhibited.

8.8 Influence of ROCK inhibition on the Hippo pathway and the distribution of polarity markers

To investigate if the inhibition of ROCK kinase affects the process of TE differentiation and the establishment of polarity regulated by the Hippo pathway in the rabbit model, localisation of a series of proteins was conducted by immunostaining after 48h of *in vitro* culture of treated embryos. First, cultured embryos (control and ROCKi groups) were immunostained against the TE marker GATA3 (**Figure 32**), as well as the Hippo pathway and polarity-related factors YAP, aPKC, β -catenin, and F-actin (**Figure 33**). Signals of the antibodies revealed that, after ROCK inhibition treatment, YAP and GATA3 are localised both in inside and outside cells of control (**Figure 32. 1C, 1C', 1D, 1D'**) and ROCK-inhibited embryos (**Figure 32. 2C, 2C', 2D, 2D'**) (details and quantitative data included in **section 4.9.1** below).

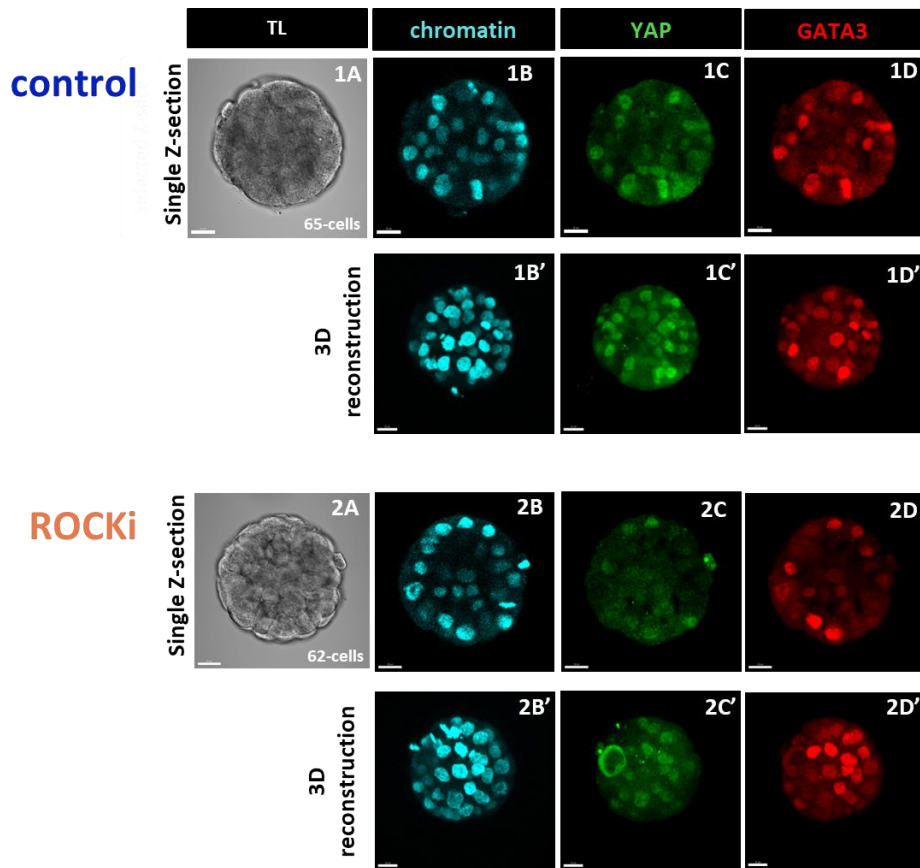


Figure 32. Localisation of YAP, GATA3 and aPKC in rabbit embryos after 48h of in vitro culture. Staining performed for chromatin (Hoechst, blue); YAP (green), GATA3 (red) and aPKC (gray). (1) Control embryos (2) Embryos treated for ROCK inhibition (ROCKi). Representative confocal images: single transmitted light (TL) image (1A, 2A), a single section (panels 1B-E, and 2B-E) and 3D projections (1B'-E', and 2B'-E'). In both control and ROCKi embryos, GATA3 and YAP signals are visible in the inside and outside cells (1C, 1C', 1D, 1D', 2C, 2C', 2D, 2D'). Scale bars = 20 μ m

First, I analysed polarisation of cortex proteins in TE cells within embryos treated with the ROCK inhibitor. I observed that, whereas in control embryos aPKC is accumulated in the apical domain only in a low proportion of cells (details in **chapter 7.8.1** below), and yet barely detected (**Figure 33. 1C, 1C'**), in 65% of ROCKi embryos this protein becomes highly accumulated in the apical domains adopting a cap-like shape (**Figure 33. 2C, 2C'**, yellow arrow). Moreover, I detected that the distribution of β -catenin and F-actin is altered in embryos after ROCK inhibition treatment. In control embryos, β -catenin is distinctly detected at the basolateral cellular domains, colocalising with junctions between adjacent cells (**Figure 33. 1D, 1D'**). In comparison, in ROCK-inhibited embryos, not only is this protein visibly accumulated in the basolateral domains, but also in the apical domains of the outside cells (**Figure 33. 2D, 2D'**). F-actin localisation

in apical surfaces and TJs regions of the outside cells is visibly reduced in the experimental group (**Figure 33. 2E, 2E'**, yellow arrows) compared to the control group, where it is restricted to apical domains of the outside cells (**Figure 33. 1E, 1E'**).

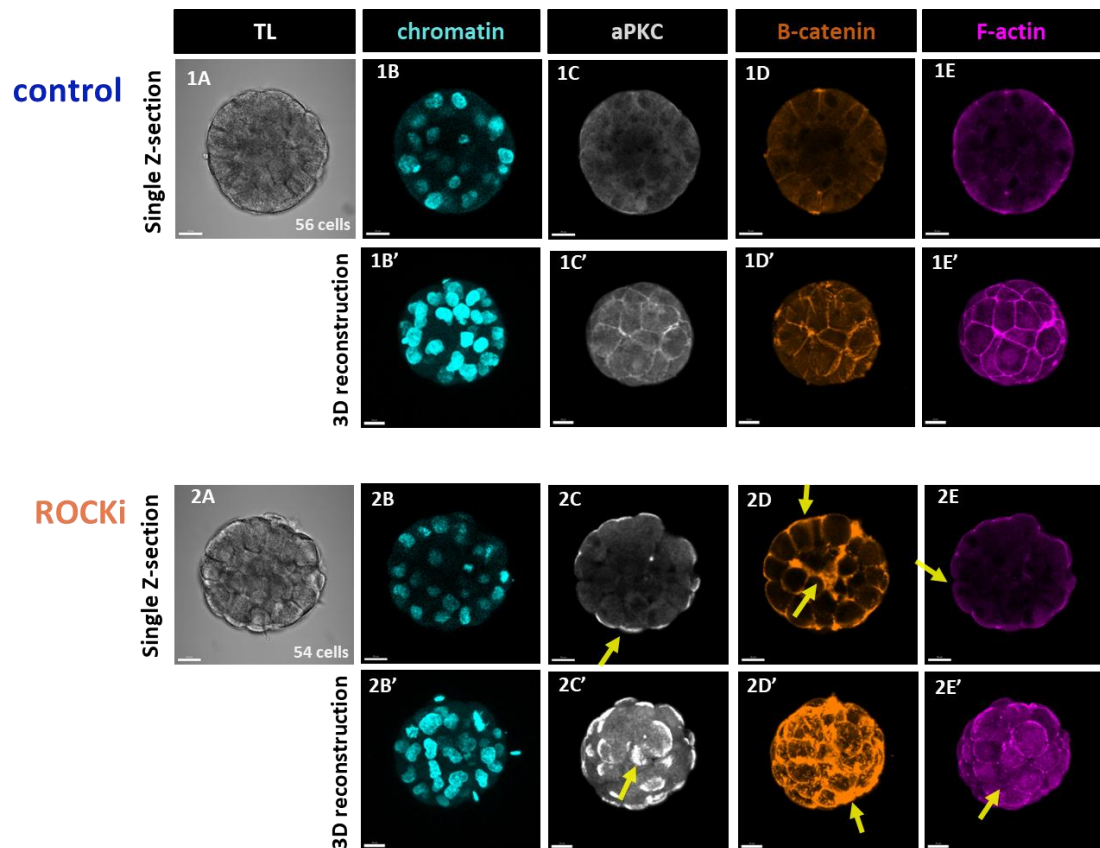


Figure 33. Localisation of β -catenin, F-actin and aPKC after ROCK inhibition treatment. Representative confocal images: cross-section transmitted light (TL) image (**panels 1A, 2A**), single optical section (**panels 1B-E and 2B-E**) and 3D projections (**panels 1B'-E' and 2B'-E'**). The confocal images of embryos after 48h of culture with or without ROCK inhibitor, immunostained for chromatin (Hoechst, blue); aPKC (white), β -catenin (orange) and F-actin (magenta). Unlike in control embryos, in ROCKi embryos aPKC is localised to the apical surfaces in larger proportion of the outside cells. In some experimental embryos, aPKC is highly aggregated in the apical domains resembling the 'cap' shape (**panels 2C, 2C'**), unlike it is observed in the control embryos (**panels 1C, 1C'**). β -catenin in ROCK-treated embryos is more accumulated in basolateral domains and is also detected at the apical domains of the outside cells (**panels 2D, 2D'**), whereas in the control embryos it is localised only in the basolateral domains of the outer cells (**panels 1D, 1D'**). F-actin signal in experimental embryos appears reduced in apical domains of the outside cells (**panels 2E, 2E'**) compared to its localisation in control embryos (**panels 1E, 1E'**). Yellow arrows show altered protein distribution. Scale bars = 20 μ m

Based on these results, it is reasonable to state that ROCK inhibition treatment does not affect YAP and GATA3 localisation in nuclei after 48h of culture. However, the inhibition of ROCK kinase changes the localisation of aPKC, β -catenin and F-actin, which might suggest that ROCK regulates acquisition of polarity in the rabbit embryo.

8.8.1 Colocalisation of YAP and GATA3 after ROCK inhibition treatment

To assess the colocalisation between subcellular YAP and GATA3, I calculated contribution of YAP+/GATA3- cells, YAP-/GATA3+ cells, YAP+/GATA3+ cells and YAP-/GATA3- cells in the inside and outside compartments. To compare the contribution of these four cell categories between control and experimental groups I used unpaired t-test or Mann-Whitney test (when the analysed data did not exhibit a normal distribution).

In the inside compartment, ROCKi embryos exhibited a similar proportion of the different cell types than the observed for the control group (**Figure 34**). Specifically, the average percentage of YAP+/GATA3- cells was 25% and 24.2% in control and experimental group, respectively (p -value>0.05, Mann-Whitney test). Mean percentage of YAP+/GATA3+ cells was 19.2% in control embryos and 22.3% in experimental embryos (p -value>0.05, Mann-Whitney test). The contribution of YAP-/GATA3+ cells was 7.8% for control embryos, and 10.1% in experimental embryos (p -value>0.05, Mann-Whitney test). Data did not exhibit normal distribution, probably because of small number of cells in these categories. Mean percentage of YAP-/GATA3- cells was 47.9% and 43.4% for control and experimental group respectively (p -value>0.05, unpaired t-test).

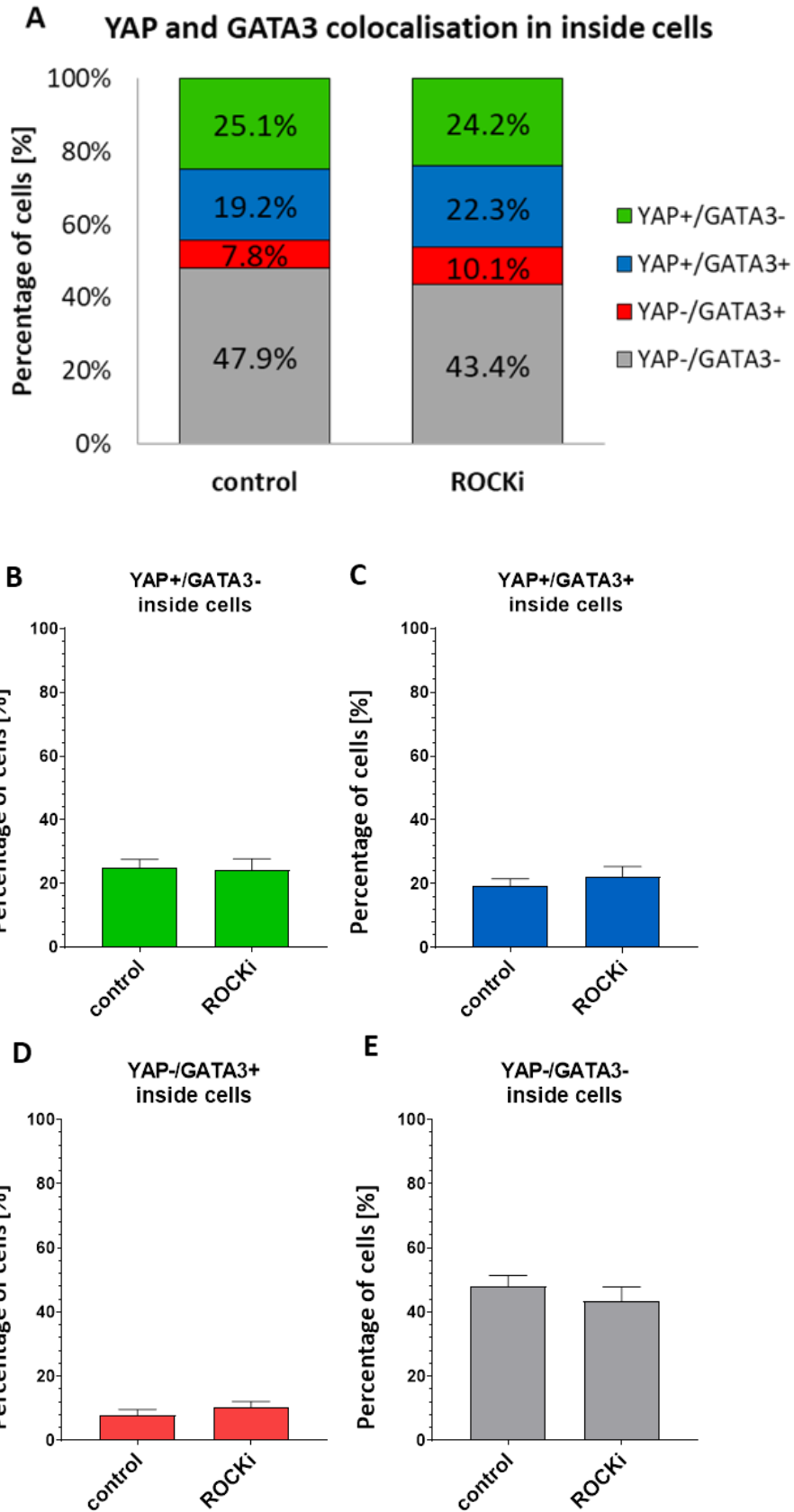


Figure 34. Colocalisation of YAP and GATA3 in inside cells of control and ROCK-inhibited embryos. A Compared percentages of YAP+/GATA3- cells, YAP+/GATA3+ cells, YAP-/GATA3+ cells, and YAP-/GATA3- cells from control embryos (n=36) and ROCK-inhibited embryos (n=34) in the inside

compartment. **B** The percentage of YAP+/GATA3- cells of control and ROCK-inhibited embryos. **C** The percentage of YAP+/GATA3+ cells of control and ROCK-inhibited embryos. **D** The percentage of YAP-/GATA3+ cells of control and ROCK-inhibited embryos. **E** The percentage of YAP-/GATA3- cells of control and experimental embryos in the inside compartment (unpaired t-test, Mann-Whitney test, 3 independent experiments).

Next aim was to link YAP nuclear localisation with TE differentiation (defined by the presence of GATA3) **in the outside cells** of embryos with inhibited ROCK kinase activity. Similarly to what has been described above, no significant differences between groups were found regarding the relative contributions of all four cell categories to the outside compartment (**Figure 35**). The percentage of YAP+/GATA3- cells in control embryos was 31.7%, whereas in experimental embryos was 30.2% (p-value>0.05, Mann-Whitney test). The average percentage of YAP-/GATA3+ cells for control embryos was 7%, and 8.1% in the experimental embryos (p-value>0.05, Mann-Whitney test). The percentage of YAP+/GATA3+ cells in control was 40.2%, whereas in the experimental embryos was 37.2% (p-value>0.05, unpaired t-test). Eventually, the contribution of YAP-/GATA3- cells in control embryos was 21%, and in the experimental embryos was 24.5% (p-value>0.05, Mann-Whitney test). Data of mean contribution of YAP+/GATA3-, YAP-/GATA3+ and YAP-/GATA3- cells did not exhibit normal distribution, probably because of small number of cells in these categories. A graphical representation of the data from the individual embryos of the control and the experimental group can be found in the supplementary data (**Figures S5 and S6**).

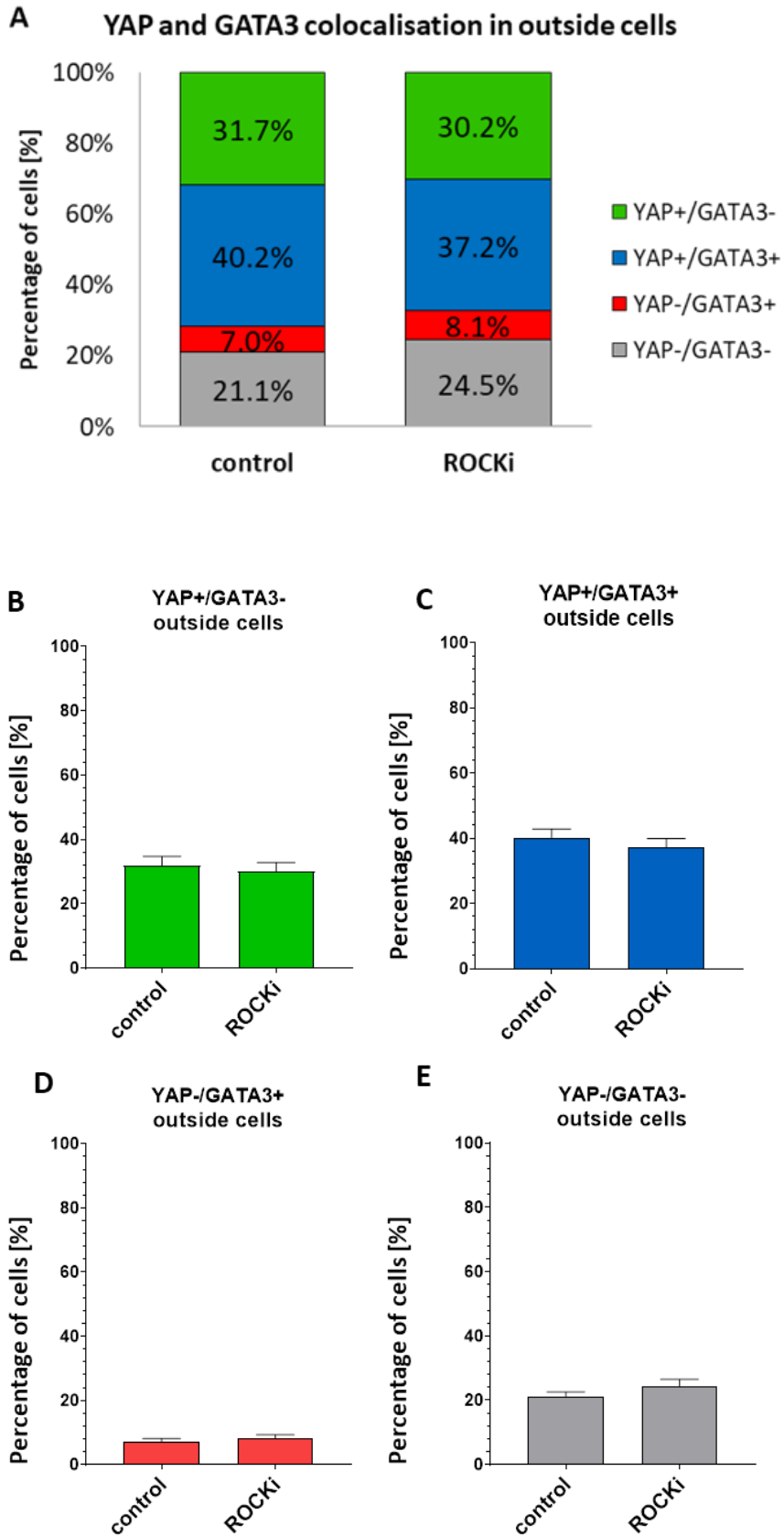


Figure 35. Colocalisation of YAP and GATA3 in outside cells of control and ROCK-inhibited embryos. A Proportion of averaged percentages of YAP+/GATA3- cells, YAP+/GATA3+ cells, YAP-/GATA3+ cells, and YAP-/GATA3- cells from ROCK-inhibited embryos (n=34) and control embryos (n=36) in

the outside compartment. B The percentage of YAP+/GATA3- cells of control and ROCK-inhibited embryos. C The percentage of YAP+/GATA3+ cells of control and ROCK-inhibited embryos. D The percentage of YAP-/GATA3+ cells of control and ROCK-inhibited embryos. E The percentage of YAP-/GATA3- cells of control and ROCK-inhibited embryos (unpaired t-test, Mann-Whitney test, 3 independent experiments).

My analysis indicates that after ROCK inhibitor treatment, contributions of YAP+/GATA3-, YAP+/GATA3+, YAP-/GATA3+, and YAP-/GATA3- cells do not statistically differ neither in the outside nor the inside compartment. Therefore, it seems likely that ROCK kinase is not involved in the process of TE differentiation in the early rabbit embryos.

8.8.2 Subcellular YAP localisation in embryos cultured for 48h with ROCK kinase inhibitor

The treatment with the ROCK kinase inhibitor did not seem to affect the pattern of GATA3 and YAP nuclear localisation, meaning TE differentiation. However, differences found in polarisation prompted me to investigate specific pattern of subcellular distribution of YAP in ROCK inhibited embryos as a possible link between polarisation and the Hippo pathway. For this purpose, I compared the relative contributions of inside and outside cells with YAP N>C (nuclear signal more intense than cytoplasmic signal), YAP N=C (nuclear signal equal to cytoplasmic signal) and YAP N<C localisation (nuclear signal weaker than cytoplasmic signal). Similarly to the analyses described above, unpaired t-test or Mann-Whitney test were employed. **(Figure 36).**

In the inside compartment, no significant differences in percentage contributions of all three categories of YAP localisation between the control and experimental group were observed, and the specific results were as follows. In the control group, the percentage of cells with N>C YAP localisation in the inside compartment was 19.8%, whereas in experimental embryos it was 21.9% (p-value>0.05, unpaired t-test). The contribution of cells with N=C YAP localisation in the inside compartment was 26.7% in the control embryos and in experimental embryos was 24.5% (p-value>0.05, Mann-Whitney test). The data did not exhibit normal distribution, probably because of small number of cells

in this category. The contribution of cells with N<C YAP localisation in the inside compartment was 53.5% in the control group, and in the ROCKi embryos was 53.6% (p-value>0.05, unpaired t-test).

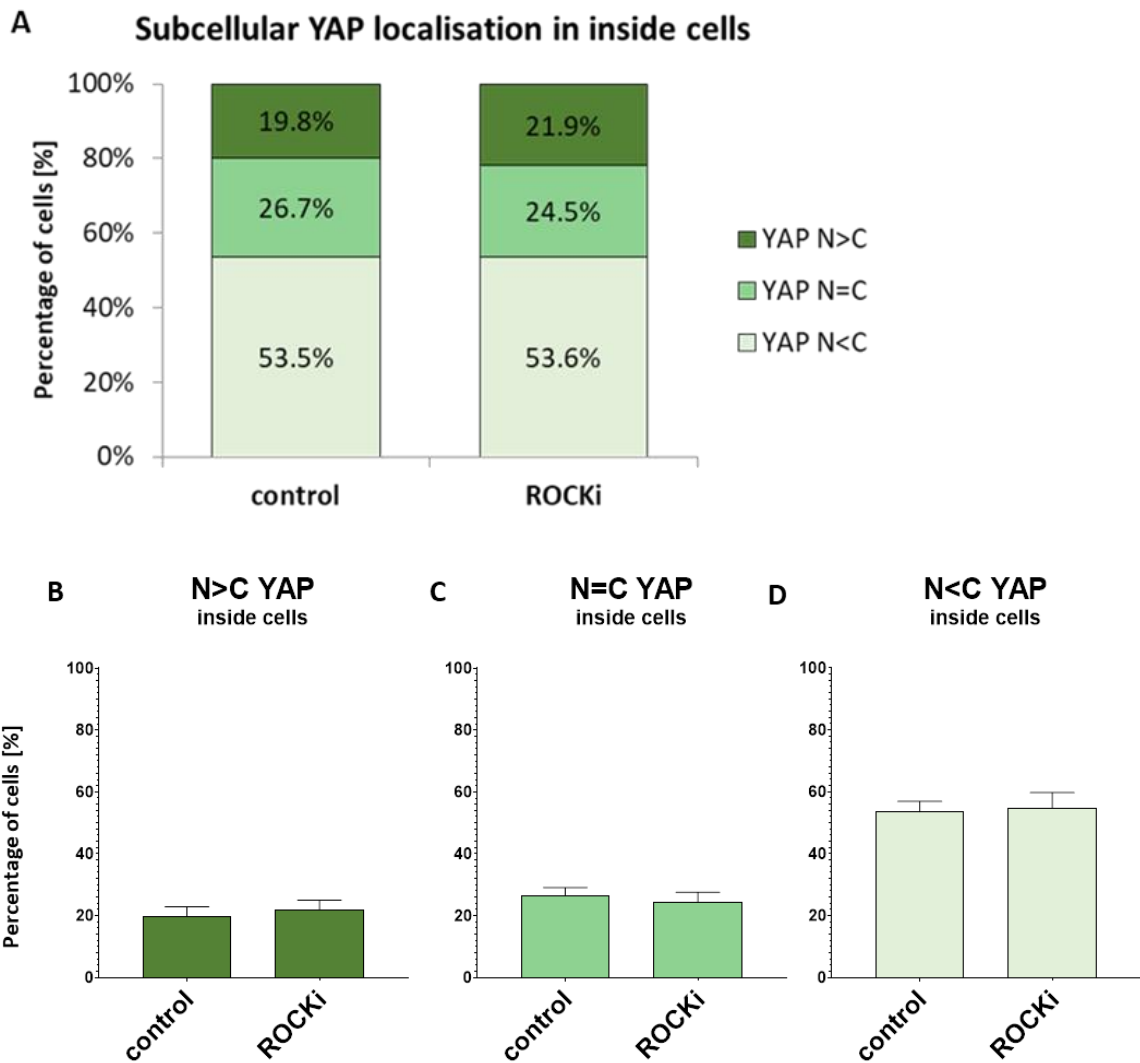


Figure 36. Proportional contributions of inside cells with different patterns of subcellular YAP localisation in control and ROCK-treated embryos. A Comparison between control (n=34) and ROCKi (n=36) embryos of the proportion of averaged percentages of inner cells exhibiting (B) N>C YAP, (C) N=C YAP and (D) N<C YAP signal (unpaired t-test, Mann-Whitney test, 3 independent experiments).

The analysis of subcellular YAP localisation (N>C, N=C and N<C YAP) in ROCK-inhibited and control embryos was also performed in **the outside cells** through an identical approach. Just like described for the inside compartment, no differences were found in

treated embryos when compared to the control group (**Figure 37**). Specifically: for cells with N>C YAP localisation, the calculated average values were 46.5% and 44.7% for the control and the experimental groups, respectively (p-value>0.05, unpaired t test); cells with N=C YAP signals represented 26.5% in the control group and 22.7% in the treated group (p-value>0.05, unpaired t test); and for N<C YAP type cells the average values were 27% in control embryos and 32.6% in ROCKi embryos (p-value>0.05, unpaired t test).

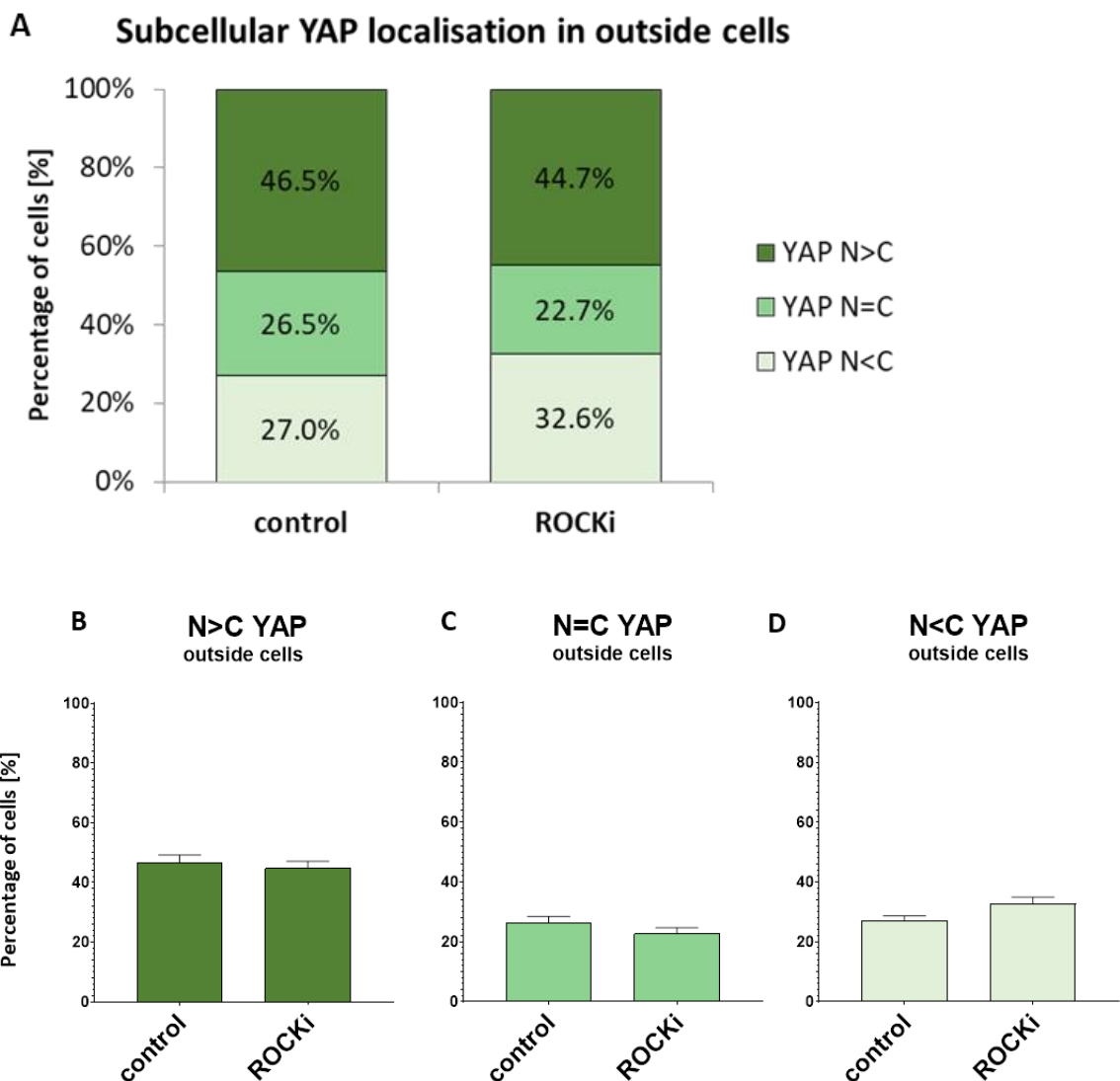


Figure 37. Percentage contribution of subcellular YAP localisation in outside cells of control and ROCK-treated embryos.

A The proportion of average percentages of outer cells exhibiting N<C YAP signal, N>C YAP or N=C YAP localisation in the control (n = 34) or ROCK-inhibited (n = 36) embryos. **B** The percentage of YAP N>C in outside cells of control and ROCK-inhibited embryos. **C** The percentage

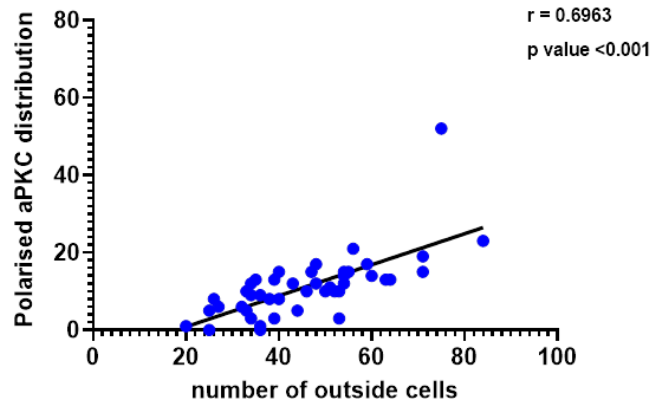
of YAP N=C in the outside cells of control and ROCK-inhibited embryos. **D** The percentage of YAP N<C in the outside cells of control and ROCK-inhibited embryos (unpaired test, 3 independent experiments)

This analysis shows that the proportions of cells with YAP N<C, N=C and N>C are not significantly different after ROCK inhibition treatment for both inside and outside compartments. It may suggest that ROCK does not modulate subcellular YAP localisation in the inside and outside cells of rabbit embryos.

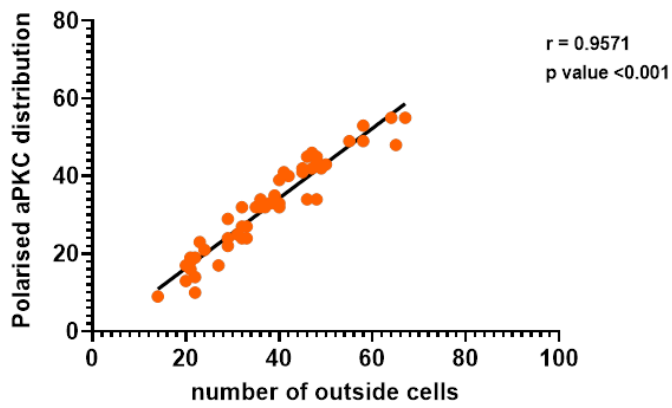
8.8.3 Localisation of aPKC in the outside cells after 48h of culture with ROCK kinase inhibition

To quantify the difference that I already described in the section **7.8**, I decided to perform more detailed analysis of aPKC distribution in cortex of outside/TE cells in embryos after ROCK inhibition treatment. Although ROCK function inhibition seems to have no effect on YAP nuclear localisation in TE cells, it does lead to excessive aPKC accumulation in the apical domain of TE cells. To this end, I investigated the correlation between the number of cells in the outside compartment and polarised localisation of aPKC in those same cells. In the experimental group, correlation was stronger ($r=0.9571$; $p\text{-value}<0.001$) than in the control group ($r=0.6963$; $p\text{-value}<0.001$) (**Figure 38. A and B**). To compare the averaged percentages of the outside cells with polarised distribution of aPKC between the control ($n=46$) and ROCK-treated embryos ($n=51$), I used Mann-Whitney test. The contribution of outside cells with apically localised aPKC in experimental embryos (84%, $n=51$) is significantly higher compared to the control embryos (23%, $n=46$) (**Figure 38. C**).

A Number of outside cells with polarised aPKC in control group



B Number of outside cells with polarised aPKC in ROCKi group



C The percentage of the outside cells with polarised aPKC

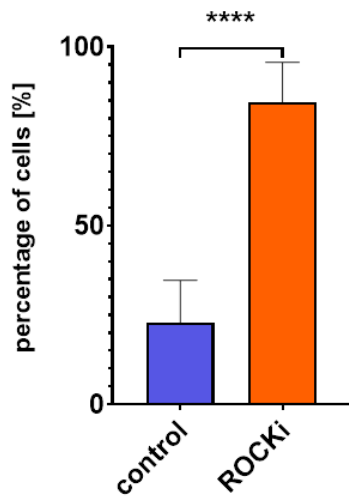


Figure 38. The contribution of aPKC localising in a polarised manner in outside cells in control and ROCK-inhibited embryos.

A. Correlation between the total number of outside cells and the number of outside cells with aPKC localisation in apical domains for the control embryos ($r=0.6963$; $p<0.001$; $n=46$). **B.** Correlation between the total number of outside cells and the number of outside cells with aPKC localisation in apical domains for the control embryos and for the ROCK-inhibited embryos ($r=0.9571$; $p<0.001$; $n=51$). **C.** In control and ROCK-inhibited embryos, the percentage of outer cells with aPKC distribution in apical domains (relative to all outer cells). (** $p<0.001$, Pearson correlation coefficients; **** $p<0.0001$, Mann-Whitney test, 3 independent experiments)

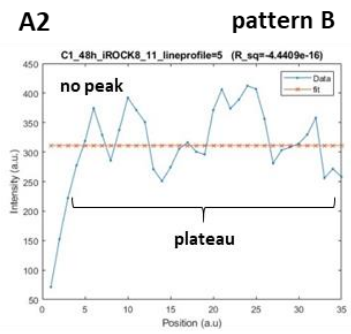
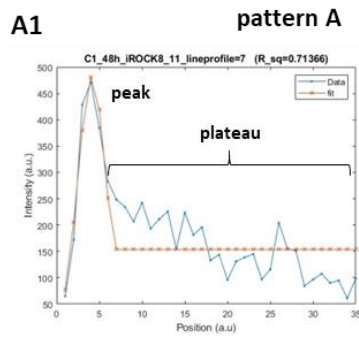
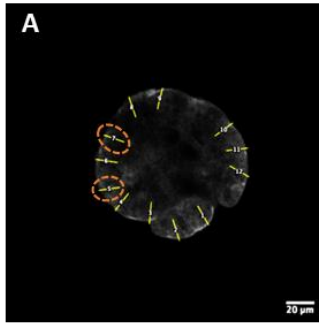
The presented analysis shows that, after ROCK kinase inhibition treatment, embryos exhibit a higher proportion of cells with aPKC distributed in a polarised manner compared to control embryos at the morula stage. Therefore, it suggests that ROCK influences cell polarisation in rabbit embryos through aPKC regulation.

8.8.4 Signal intensity profiles of aPKC in the apical domain of outside cells after ROCK inhibition

Inhibition of ROCK kinase leads to the modified distribution of aPKC in embryos as I had shown above. In order to provide a detailed measurement of such changes, I quantified the intensity of the aPKC signal distributed in outside cells, and compared the results obtained for both control and ROCK-inhibited groups of embryos in the level of protein signal intensity. Using ImageJ, I measured intensity profiles across the cortex and apical membrane for TE cells (approximately 10 measurements per embryo) (**Figures 39. A and B**). I analysed 30 embryos ($n_{\text{control}}=15$, $n_{\text{ROCKi}}=15$) derived from 3 independent experiments. The plots of signal intensity were created along the appointed lines. Two different patterns of intensity profile were revealed in the outside cells of embryos by this approach. Pattern A - the profile is composed of one peak (which corresponds to the aPKC signal in the apical domain) and a plateau phase. This pattern represents the profile observed in both the control and the experimental groups (**Figure 39. A1, B1**). Pattern B - the plot does not display an initial peak, only the plateau (**Figure 39. A2**). Because the comparison of mean fluorescence intensity between different samples is not completely reliable according to the limitations of the

immunostaining technique, I analysed differences in the ratios between peak and plateau values. To statistically compare ratios from control and ROCK inhibited embryos I used Mann-Whitney test, since the data did not exhibit normal distribution. As expected, the ratio of the amplitudes in the outside cells was higher for the experimental group than for the control group (**Figure 39. C**). Therefore, this quantification confirms that ROCK inhibition leads to increased differences between cortical and cytoplasmic localisation of aPKC the outside cells.

control



ROCKi

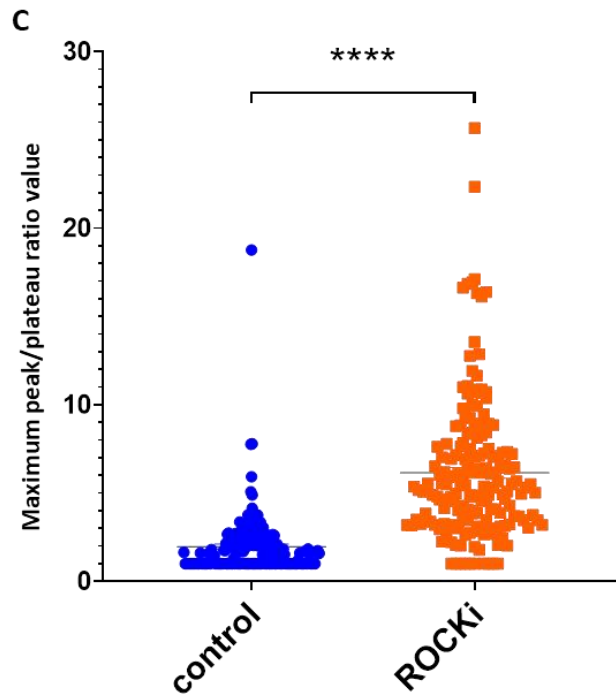
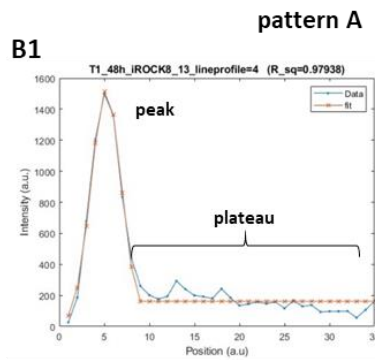
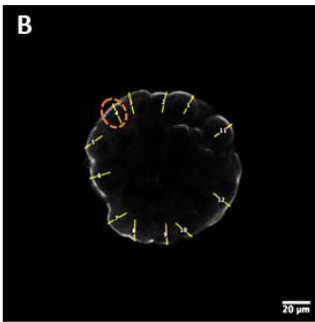


Figure 39. Changes in aPKC distribution after ROCK inhibition treatment in the rabbit embryo.

A The representative confocal z-section of the control embryo, **B** and the ROCK-inhibited embryo after 48h of in vitro culture. **A-B** In order to quantify differences in aPKC distribution in the apical domain after treatment, the intensity profile of the aPKC signal was obtained at ~10 similar arbitrary locations within each embryo from both groups (yellow lines). **A1, A2, B1** Representative intensity profiles (blue line). A plot (the intensity profile) generally shows one peak of intensity corresponding to the apical domains and a plateau region observed with much

lower signal intensity. A Gaussian curve (orange line) was fitted to all profiles obtained from every embryo ($n=30$) to acquire precise values for each peak and plateau. **C** Graph of Individual values presenting ratio of maximum peak and plateau in the outside cells of control and ROCK-inhibited embryos (10 lines per embryo, $n=15$ per group). ($***p<0.0001$, Mann–Whitney test; $n=30$ embryos, 3 independent experiments).

According to the results described above, I concluded that ROCK kinase inhibition by Y-27632 leads to enrichment of the apical domain in aPKC within individual outside cells in rabbit embryos. Additionally, the number of outer cells with aPKC localised in a polarised manner per embryo is significantly increased after ROCK inhibition. Altogether, these observations point to a direct involvement of ROCK kinase in controlling cell polarisation in the early embryo in rabbit.

9 Discussion

During preimplantation development, totipotent blastomeres undergo the first cell-fate decision to differentiate into the inner cell mass (ICM, which will further give rise to the embryo proper and yolk sac) or the trophectoderm (TE), the extra-embryonic lineage (Hoos and Hoffman 1980; Papaioannou and Ebert 1988; Muyan and Boime 1997; Hoffman, Breinan, and Blaeuer 1999; Yoshinaga 2013; Pedersen et al. 2017). The TE will further give rise to the embryonic part of the placenta, and it is directly involved in the process of implantation. Therefore, correct development of the trophectoderm is crucial for fetal gestation and a successful pregnancy to term (Cross 2005).

Most studies concerning early lineage differentiation have been conducted on mice, which is the main model of embryo development in mammals. Even though preimplantation development has been also investigated in mammalian species other than mice, embryo development under *in vitro* conditions in those species caused artefacts related to lower quality of embryos compared to *in vivo* development. In order to avoid these issues, I chose the rabbit as an experimental model. The rabbit is also a more representative model of mammalian embryo development because it is evolutionarily closer to other non-rodent mammals, including humans. Furthermore and, similarly to mouse, the rabbit model allows for the analysis of *in vivo* developed embryos (Graur et al., 1996; Fan and Watanabe, 2003; Honda et al., 2008; Bosze and Houdebine, 2010; Okamoto et al., 2011; Fischer et al., 2012; Piliszek et al., 2017). However, despite being considered a pioneer model in mammalian embryology, the rabbit is currently not widely used in research of embryonic development, including the differentiation of first cell lineages.

The Hippo pathway was found to be involved in regulating a variety of biological processes, including cell growth and proliferation, tissue regeneration and repair, and cancer development (Zhao et al. 2007; F.-X. Yu and Guan 2013). Importantly, the Hippo pathway was also found as one of the major players during TE/ICM differentiation in several mammalian species, including mice, cattle, pigs, and humans (Nishioka et al. 2009; Hirate et al. 2013; Sharma and Madan 2020; Gerri et al. 2020).

Although the Hippo signalling mechanism has been widely studied in mice, and its key components and regulators have been confirmed in other species, the involvement of the Hippo pathway in the rabbit embryo has yet to be uncovered. Since the rabbit is such a convenient model which allows us to study embryos obtained *in vivo*, we can learn a lot about mammalian development by studying how the Hippo pathway is regulated in the rabbit embryo. Therefore, the primary goal of this research was to investigate the role of the Hippo pathway in TE differentiation in rabbit embryos.

9.1 Expression of genes involved in the Hippo pathway

To investigate the role of the Hippo pathway in the differentiation of TE, first, I analysed the expression level of its selected components. To the best of my knowledge, this work is the first to examine the relative expression levels of genes involved in the Hippo pathway regulation (*TEAD1*, *TEAD3*, *TEAD4*, *LATS1*, *LATS2*, and *YAP*) among early rabbit developmental stages, including 1.5, 2.5, 3.25 and 4.0 dpc.

9.1.1 *TEAD1-4*

TEAD family members (TEAD1-4) are transcription factors within the Hippo pathway, which are activated by YAP/TAZ (Vassilev et al. 2001). Therefore, their activity during the first cell-fate decision is expected to be crucial.

In the present research, I found that during the initiation of compaction in rabbit embryos (1.5 dpc), *TEAD1* expression level was below the detection threshold. Starting at compacting morula stage (2.5 dpc), I detected expression of *TEAD1* at similar levels until the blastocyst (4.0 dpc). The analysis of *TEAD2* relative expression level was not possible due to technical issues. The expression levels of *TEAD3* and *TEAD4* also did not differ between consecutive developmental stages.

My results on *TEAD1* transcripts levels in rabbit embryos resemble those previously reported in mice and humans between the 8-cell stage and the compact morula, where transcripts were observed at low levels (Boroviak et al. 2018). However, in marmosets and swine, a high expression level of *TEAD1* was detected already at the

zygote stage, and it gradually increased up to the compact morula stage (Boroviak et al. 2018; Kong et al. 2020). Unlike I demonstrated in rabbits, in early human blastocyst (5 dpi), the expression level of *TEAD1* gene was 2-time higher in ICM than in TE cells (Petropoulos et al. 2016). In the early porcine blastocyst, the *TEAD1* expression level was 19-times higher in TE cells than in ICM cells (Kong et al. 2020).

Similar to rabbit embryos, *TEAD2* and *TEAD3* were expressed at visibly low levels up to the compact morula and no differences in expression levels were observed between different stages in mice, marmosets and humans (Boroviak et al. 2018). In human blastocysts, *TEAD2* was expressed at higher levels in TE than in ICM cells, while the expression level of *TEAD3* was higher in ICM than in TE cells (Petropoulos et al. 2016). Different results were obtained from porcine embryos, where an increased expression level of *TEAD3* was detected at the compact morula stage compared to earlier stages. Similarly to rabbits, in porcine blastocysts the gene expression of *TEAD2* and *TEAD3* was barely detected in both ICM and TE (Kong et al. 2020).

The present results on rabbits differ from those obtained in mice, cattle, humans and swine. In human and swine embryos, *TEAD4* transcript levels gradually increase up to the morula stage (Boroviak et al. 2018; Emura et al. 2019; Kong et al. 2020; Sakurai et al. 2017). In contrast to rabbit blastocysts, a decreased *Tead4* expression is observed in mice (Nishioka et al. 2009). Unlike in the species described above, in marmosets, the expression of *TEAD4* is slightly decreased at 8-cell stage and the compact morula stage compared to earlier stages (Boroviak et al. 2018). In human blastocysts, the *TEAD4* expression level is higher in TE than in ICM cells (Petropoulos et al. 2016). Observations in rabbits are similar to bovine and porcine blastocysts, where *TEAD4* is expressed at similar levels in TE and ICM cells (Negrón-Pérez et al. 2018; Emura et al. 2019; Kong et al. 2020).

Comparing my findings for rabbit embryos with transcriptomic data from other species, I noticed both important similarities and discrepancies. *TEAD4* mRNA is observed at a high level in mice and humans (Petropoulos et al. 2016; Boroviak et al. 2018; Kong et al. 2020). In marmosets and pigs, *TEAD1* and *TEAD4* expression was observed at high levels from the zygote to the compact morula (Boroviak et al. 2018; Kong et al. 2020), unlike in mice, humans and rabbits. Furthermore, in both rabbits and cattle, no differences in expression levels of *TEAD4* and *YAP* were observed between

TE and ICM. Low *TEAD1* transcripts levels are observed from 8-cell stage to the compact morula in rabbits, mice, and humans, while at the blastocyst stage, the dynamics of *TEAD1* expression is different in rabbits, humans and cattle. Expression of *TEAD2* is detected at low levels during preimplantation development of mice, humans and pigs (Boroviak et al. 2018; Petropoulos et al. 2016; Kong et al. 2020). *TEAD3* transcripts are detected on very low levels and do not differ between stages up to compact morula in rabbits, which is similarly observed in mice, marmosets and humans. Although my results confirmed the presence of transcripts of all TEAD members in rabbit embryos, this analysis of relative gene expression levels did not allow to determine which of them is essential.

9.1.2 *LATS1/2*

LATS1/2 kinases belong to the Hippo pathway cascade. When the Hippo pathway is active in the inside cells at the morula stage, *LATS1/2* kinases prevent YAP/TAZ localisation in nuclei (Nishioka et al. 2009).

According to my results, *LATS1* expression level was below the detection threshold in rabbit embryos at 1.5 dpc. From compacting morula (2.5 dpc) to the blastocyst stage (4.0 dpc), *LATS1* expression level did not differ between stages, even between ICM and TE of blastocysts at 4.0 dpc. Similarly, *LATS2* was expressed at equal levels in embryos at 1.5, 2.5, and 3.25 dpc and in TE and ICM of embryos at 4.0 dpc.

My results are contradictory to the transcriptomic data analysis performed on mice, marmosets and humans, where *LATS1* expression levels are detected starting from the zygote stage, and then a decrease is observed from 8-cell stage to the compact morula (Boroviak et al. 2018). In human and bovine blastocysts, unlike in rabbits, a higher expression level of *LATS1* is observed in TE compared to ICM (Petropoulos et al. 2016; Negrón-Pérez and Hansen 2018). Observation in rabbits was consistent with results in porcine embryos, where *LATS1* was expressed at a low level and did not differ between 8-cell stage and the blastocyst stage; moreover, there was also no visible difference between TE and ICM cells (Kong et al. 2020).

Similarly to rabbit, in mouse and human embryos, *LATS2* transcript levels do not differ between 8-cell stage and compact morula (Boroviak et al. 2018). However, in human blastocysts (5, 6 and 7 dpi) a higher expression level of *LATS2* was observed in ICM than in TE cells (Petropoulos et al. 2016), unlike in bovine blastocysts, where a subset of TE cells exhibited the highest *LATS2* expression compared to Epi or PrE cell populations (Negrón-Pérez and Hansen 2018). Different observations were reported in marmosets, where *LATS2* expression level visibly decreased from 8-cell stage to compact morula (Boroviak et al. 2018). Similar to marmosets, and unlike in rabbits, the expression level of *LATS2* in pigs is the highest in the oocytes and then it gradually decreases towards the blastocyst stage (Emura et al. 2020).

In conclusion, rabbits and pigs share similar *LATS1* expression dynamics from 8-cell stage to the blastocyst stage, while different observations were obtained in mice, marmosets and humans. Similar *LATS2* transcript levels were observed between 8-cell stage and the compact morula stage in rabbits, mice and humans, suggesting *LATS2* expression dynamics is conserved in these species. A distinct pattern of *LATS2* expression level is present in marmosets. In human blastocysts, *LATS2* transcript levels were higher in ICM than in TE, differently than in rabbits, where there were no differences, and in cattle, where *LATS2* expression level was higher in TE than in ICM. The presence of *LATS1/2* mRNA transcripts in rabbit embryos suggests that those proteins may be involved in the Hippo pathway during the first cell-fate decision. However, the fact that there is no difference between the subsequent stages of development implies there might be another regulatory mechanism involved.

9.1.3 YAP

YAP is the primary mouse downstream regulator of the Hippo pathway, required for the activation of the transcription factor TEAD4, which drives the expression of genes essential for TE specification, such as *Cdx2* and *Gata3* (Yagi et al. 2007; Nishioka et al. 2008; 2009; Rayon et al. 2014; Yagi et al. 2007).

In the present study, I found no significant differences in the expression levels of *YAP* between rabbit embryos at 1.5 dpc, compacting morulae at 2.5 dpc or blastocysts at

3.25 and 4.0 dpc, unlike in murine (Boroviak et al. 2018) and porcine embryos (Kong et al. 2020). Additionally, no significant difference in *YAP* expression level was found between TE and ICM cells of rabbit blastocyst, similarly to bovine embryos (Fujii et al. 2010; Ozawa et al. 2012). The present data from rabbits are different from results obtained from several species, including mice, swine and humans, where high gene expression of *YAP* is detected starting from the zygote stage, and once embryos achieve 8-cell stage *YAP* transcript levels subsequently decrease until the blastocyst stage (C. Yu et al. 2016; Kong et al. 2020; Emura et al. 2020; Boroviak et al. 2018). In contrast to rabbits, mice, humans and pigs, during preimplantation development of marmoset embryos, *YAP* expression level was below the detection threshold, suggesting that some other mechanisms are responsible for TE differentiation in this species.

Comparing *YAP* transcript levels during cavitation in human (at 5 and 7 dpi) and porcine blastocysts, a higher expression level of *YAP* is observed in ICM than in TE cells (Petropoulos et al. 2016; Kong et al. 2020). However, in rabbit and bovine embryos, no significant difference in *YAP* expression level between TE and ICM is observed (Fujii et al. 2010; Ozawa et al. 2012). The presence of *YAP* transcripts in rabbit embryos suggests that the resulting protein might be involved in the Hippo pathway regulation during TE/ICM differentiation. However, the fact that there is no difference between the subsequent stages and even between ICM and TE of the mid-blastocyst stage implies that another, *YAP*-independent regulatory mechanism might be involved.

Altogether, in mice, marmosets and humans, *TEAD3* transcript is barely detectable up to the compact morula stage and does not differ between subsequent stages. In rabbits, expression levels of *TEAD4* and *YAP* are equal between ICM and TE, similar to cattle (Negrón-Pérez et al., 2018). In humans and mice, similarly to rabbits, *LATS2* expression levels do not change from 8-cell stage to compact morula. In porcine embryos, *LATS1* transcript was observed at a similarly low level from 8-cell stage to the blastocyst.

Furthermore, my findings have been confirmed recently by our lab in collaboration with dr hab. Piotr Pawlak (University of Life Sciences in Poznan) through transcriptomic analysis of rabbit embryos. According to the analysis of whole rabbit embryos

(unpublished data), *TEAD1*, *TEAD2*, *TEAD3*, *LATS1* were expressed at very low levels in rabbits at 2.0 dpc and 3.0 dpc, while *YAP*, *TEAD4* and *LATS2* transcripts were detected, but their expression levels did not differ between 2.0 dpc and 3.0 dpc. Therefore, *TEAD4* is the most probable candidate from the TEAD family, which is involved in the Hippo pathway in rabbit embryos, similarly to mouse and human models.

In conclusion, I discovered in most cases no differences in the expression levels of analysed genes between consecutive developmental stages in the rabbit embryo, in contrast to data from other mammalian species. Therefore, the activity of Hippo pathway components in rabbits is more likely to be modulated by the post-translation modifications or by changes in protein activity, including the protein subcellular localisation, phosphorylation or interactions with other proteins, than through the gene transcription. Thus, I propose that all analysed genes of the Hippo pathway and their downstream effectors are maintained in preimplantation rabbit embryos at constant expression levels throughout preimplantation development as it is commonly observed in different cellular signalling pathways (reviewed in El-Brolosy and Stainier 2017).

9.2 TE-specific transcription factors in the rabbit embryo

Studies on mice uncovered that TE lineage differentiation is controlled by several transcription factors, including *CDX2*, *GATA3*, *Eomes* and *TFAP2C*. *CDX2* and *GATA3* act downstream of the Hippo pathway (Russ et al. 2000; Niwa et al. 2005; Strumpf et al. 2005; Dietrich and Hiragi 2007; Yagi et al. 2007; Nishioka et al. 2008; Home et al. 2009; Ralston et al. 2010; Choi et al. 2012; Cao et al. 2015), and *TFAP2C* acts upstream of the Hippo pathway in mice (Choi et al. 2012; Cao et al. 2015).

The transcriptional activity of *Cdx2*, the gene associated with TE fate, is activated by *TEAD4*. However, unlike *TEAD4*, *CDX2* is restricted to TE lineage during early mouse development (Strumpf et al. 2005; Yagi et al. 2007; Nishioka et al. 2008; Home et al. 2012). In *Cdx2*-deficient mice, embryos did not exhibit cavitation failure, whereas at further developmental stages, a failure of TE maintenance and epithelial integrity was reported. Additionally, those embryos exhibited ectopic expression of *Oct4* and *Nanog*

(Strumpf et al. 2005; Wu, Duggan, and Chalfie 2001). In porcine and bovine embryos, depletion of *CDX2* also did not disrupt cavity formation. However, *CDX2* was confirmed to be a crucial player during the process of blastocyst hatching (Bou et al. 2017) and the development of post-hatching embryos (Berg et al. 2011). In mouse embryos, *Cdx2* expression is detected as early as the morula stage, while in the blastocyst, it is restricted to TE cells (Strumpf et al. 2005). Unlike in mice, the nuclear *CDX2* localisation was not confirmed before the blastocyst stage in several other mammals, including cattle, pigs, sheep and humans (Kuijk, Geijsen, and Cuppen 2015; Berg et al. 2011; Madeja et al. 2013; Moradi et al. 2015; Sakurai et al. 2016; Bou et al. 2017). According to unpublished data from our lab, *CDX2* localisation in the rabbit embryo is not detected before the mid blastocyst stage, therefore, is not suitable as an early TE marker. Furthermore, it was recently discovered by our lab that *GATA3* is potentially an earlier TE-marker in rabbit embryos (Filimonow et al., manuscript in preparation). For this reason, I decided to assess whether *GATA3* is a determining factor of TE differentiation by the analysis of the protein localisation at the consecutive stages of rabbit preimplantation development. Based on the mouse model, *GATA3* is another transcription factor involved in TE lineage differentiation, also acting downstream of *TEAD4* (Home et al. 2009; Ralston et al. 2010). In the present research, I demonstrated that *GATA3* protein distribution in rabbit embryos is detected in most cells of the compacting morula at 2.5 dpc (stage V), and it is restricted to TE cells once the cavitation begins. The emergence of *GATA3* protein in the rabbit embryo is slightly delayed compared to mice, where *GATA3* protein localisation is detectable within nuclei around 16-cell stage and is predominantly localised in the outer cells shortly before cavitation, and then it is upregulated in TE cells at the blastocyst stage (Ralston et al. 2010). *GATA3* was found in mice to be colocalised with *CDX2* in TE cells. Even though *GATA3* is also activated by *TEAD4*-*YAP/TAZ*, it is thought to be induced independently of *CDX2* (Ralston et al. 2010). Noteworthy, *Gata3*-downregulated mouse embryos exhibited failure in blastocyst formation (Home et al. 2009). Furthermore, in both equine and bovine embryos, the gene expression of *GATA3* was detected at a higher level in TE compared to ICM (Smith et al. 2010; Ozawa et al. 2012; Iqbal et al. 2014).

Taken together, in rabbit embryos, GATA3 starts to be restricted to TE cells concomitant with cavitation, which may suggest the possible GATA3 involvement in the specification of outer cells into TE lineage. Therefore, it likely plays a crucial role during TE differentiation, as observed in mouse embryos. Consequently, by this research, I have shown that, unlike the previously mentioned CDX2, GATA3 remains a good candidate as an initiation factor of TE lineage in rabbit embryos. My findings have been recently confirmed by a similar observation by Bouchereau and colleagues, who reported high expression levels of *GATA3* in rabbit morulae at 2.7 dpc (Bouchereau et al. 2022).

9.3 Polarity-associated factors

Compaction and polarisation are two major events during early mammalian development that induce the establishment of cell junctions and distributions of the appropriate set of proteins required for the first cell-fate decision in the embryo. As a result of asymmetric divisions, the mammalian late morula/cavitating embryo is composed of two types of cells. Polarised outside cells are thought to give rise to the epithelial layer of the blastocyst (TE), whereas ICM will develop from centrally located apolar cells (Rossant and Vijn 1980; Tom P. Fleming 1987).

In the present study, I have discovered that polarisation is initiated in rabbit embryos at the 8-cell stage, while a whole set of cell polarity markers (p-Ezrin, aPKC, F-actin or β -catenin) is visible at the apical surface of the outside cells when cavitation begins. In contrast to my results, Koyama and colleagues reported that polarisation is not observed earlier than 32-cell stage in the rabbit embryo, however, at 64-cell stage nearly 100% of outer cells of the embryo were polarised (Koyama et al. 1994). Koyama and colleagues analysed cell polarisation in rabbit and bovine embryos using scanning electron microscopic (SEM) analysis of microvilli surfaces. In their method of analysing, polarised blastomeres exhibited the apical domain covered by microvilli, while apolar blastomeres were covered by microvilli uniformly on the plasma membrane surface. Their findings in cattle indicated that polarisation in bovine embryos is initiated even

earlier, at 9-15-cell stage, and after 16-cell stage the majority of the outside cells were polarised (Koyama et al. 1994).

By analysing time-lapse movies, I verified that in rabbits the compaction process is initiated around 8-cell stage, whereas the completion of compaction is observed at 64-cell stage, shortly before cavitation (**Figure 7**). Therefore, it suggests that polarisation and compaction are simultaneously induced in rabbits. However, different observations were reported from two other studies. In particular, the first study reported compaction at 8-16-cell stage by observation of the *in vitro* developed rabbit embryos (Sultana et al. 2009), while the other study, using SEM analysis of the microvilli distribution, claimed that it was visible not earlier than 32-64-cell stage (Ziomek, Chatot, and Manes 1990). The discrepancies between my observations and the earlier studies might result from differences in methods of assessment of polarisation and compaction. While earlier studies relied on morphological cues, currently available methods of polarity factors detection allow for more precise observation of the moment of cell polarisation and compaction. On the other hand, in the later study, Sultana and colleagues (2009) assessed the moment of compaction in rabbits by analysing embryos that developed under *in vitro* conditions. Due to the fact that timeline of *in vitro* embryo development slightly differs from the development *in vivo*, it is difficult to compare these results to those obtained by Ziomek and colleagues (Ziomek, Chatot, and Manes 1990). However, the findings of Sultana and colleagues (2009) are more similar to my results.

Observations in rabbits revealed similarities with those features already known in mice, where, concomitant with compaction, the cell polarity is initiated as early as the 8-cell stage (Reeve and Ziomek 1981; Pratt et al. 1982). However, compaction in mouse embryos is completed at 8-cell stage, while in rabbits, it is initiated at 8-cell stage and completed at 3.0 dpc.

In order to investigate whether cell polarisation controls the first cell fate decision in rabbits, I investigated the distribution of the four factors associated with apicobasal polarity, such as p-Ezrin, aPKC, F-actin and β -catenin in rabbit embryos at consecutive preimplantation stages.

9.3.1 P-Ezrin

Based on the mouse model, phospho-Ezrin (p-Ezrin) is one of the first apical markers localised in a polarised manner in the outside cells (Reeve and Ziomek 1981; Louvet et al. 1996; Louvet-Vallée et al. 2001). My observations of p-Ezrin immunolocalisation in rabbits are similar to findings in mice, where it is localised to the apical surface of outer cells as early as the 8-cell stage, and it remains so until the blastocyst stage (Louvet et al. 1996; Liu et al. 2013). Noteworthy, apart from the strong p-Ezrin signal in apical domains of the outside cells of the rabbit morula, I detected a weak p-Ezrin signal in the cell-cell contacts of inner cells. This non-polar localisation of p-Ezrin in the inside cells is maintained until the blastocyst stage (**Figure 40**). Therefore, it is possible to hypothesise that Ezrin is the earliest factor involved in 8-cell blastomere polarisation in rabbits. The fact that p-Ezrin is localised evenly in the cell cortex of the inside cells suggests that it can also play a potential role in ICM lineage specification. Moreover its expression was also confirmed in Epi lineage in vitro model – ES cells (Liu et al. 2013).

9.3.2 aPKC

aPKC is highly evolutionary conserved in mammals, and it is known to regulate the apicobasal polarity of outer cells at the morula stage (Gerri et al. 2020). Additionally, aPKC is thought to control cytoskeleton proteins, which are responsible for apical domains and tight junction formation required for blastocyst development (Johnson and Ziomek 1981a; Eckert et al. 2004; Ralston and Rossant 2008; Gerri et al. 2020).

Although the distribution and role of aPKC in mice during the first cell lineage differentiation have been studied (Plusa et al. 2005; Dard et al. 2009; Saiz and Plusa 2013), it has been unknown in the rabbit embryo until the present study. In the rabbit embryo, I observed no aPKC distribution up to the 8-cell stage. From there onwards, the protein is localised in the cell contacts and basolateral surfaces, whereas unlike in mice, no nuclear localisation was detected until the expanded blastocyst. During rabbit compaction, the basolateral pattern of aPKC in outer cells seems to be maintained until shortly before cavity formation. On the contrary, in the mouse morula, aPKC is localised in the apical domains of outer cells already before 32-cell stage, but it is also

distributed in nuclei and cell contacts (Plusa et al. 2005; Dehghani and Hahnel 2005; Ralston and Rossant 2008; Saiz and Plusa 2013). In this research, I have shown that aPKC during compaction is visible in the cell contacts and basolateral surfaces of the outer cells of the rabbit embryo. Interestingly, it can be also visible evenly in the cell cortex of the inside cells up to the mid-blastocyst stage. Concomitant with the initiation of the blastocyst formation - from 3.25 dpc - aPKC localisation changes from basolateral to apical domains in TE cells, which may suggest that, similarly to mice, cattle or even humans (Plusa et al. 2005; Gerri et al. 2020), aPKC plays a functional role in the apicobasal polarity and during the first cell-fate specification of the rabbit embryo (**Figure 40**).

9.3.3 F-actin

It was revealed that mechanical forces are involved in the control of the first cell-fate decision through a cell contractility-mediated mechanism (Samarage et al. 2015; Maître et al. 2015; 2016). In this mechanism, the apical domain is formed during polarisation, leading to decreased cell contractility. Thus, the polar cells are maintained on the outer surface of the embryo. The apolar cell with no apical domain or inheriting only a small amount of the apical domain indicates an increased ability to contract and may internalise to the inner cell compartment (Maître et al. 2016). F-actin is also considered to be a contractile component that is excluded from the apical domains of the outer cells of the morula to the surrounding surface and forms actin rings, as described in recent studies on mouse embryos (Zhu et al. 2017; Okuno et al. 2020). The function of F-actin in the preimplantation embryo of mammals other than mice has been poorly investigated, therefore, I decided to analyse the localisation of the protein in rabbit embryos. I have shown that F-actin in rabbit embryos is predominantly localised in the apical domains and cell contacts (tight junction regions - TJ regions) of outer cells at 2.5 dpc before the fully compact morula. Before that time, it localises in the cytoplasm as well in cell-cell junctions, unlike in mice (Liu et al. 2013; Zenker et al. 2017; 2018), where F-actin is localised in a polarised manner earlier, from 16-cell stage. The F-actin apical distribution in the outside/TE cells is maintained prior

to the mid-blastocyst stage, in both rabbits and mice. Therefore, similarly to mice (Zenker et al. 2017; 2018), the distribution of F-actin in the rabbit embryo from early morula to blastocyst becomes oriented on the apical surfaces of outside cells, concomitant with the initiation of TE specification. Thus, the presented dynamics of F-actin localisation at consecutive stages suggest that the protein might be involved in the first-cell fate decision in rabbit embryos (**Figure 40**).

9.3.4 β -catenin

β -catenin, encoded by *CTNNB1* gene, is a major component of cell adhesion that promotes embryonic development and adult stem cells proliferation through the Wnt/ β -catenin pathway (H. Xie et al. 2008). In mouse embryos it was reported that during the first cell-fate decision, β -catenin and α -catenin build a protein complex with E-cadherin, NF2 and AMOT (Hirate et al. 2013). During mouse preimplantation development, β -catenin is detected in the cell membrane from the zygote stage. In contrast, from the 8-cell stage, it becomes restricted to basolateral surfaces of outer cells and remains so until the blastocyst stage (H. Xie et al. 2008; Pieters et al. 2016). While mouse zygotes deficient in β -catenin undergo normal preimplantation development (Pieters et al. 2016), some studies suggest that β -catenin is essential later, during implantation (H. Xie et al. 2008; Messerschmidt et al. 2016). The cortical localisation of β -catenin was also confirmed in bovine embryos (Modina et al. 2007; Tribulo et al. 2017; Gerri et al. 2020). Furthermore, β -catenin is a marker of basolateral domains in human embryos at the 8-cell stage and late compacted morula (Gerri et al. 2020).

In pre-compacted rabbit embryos (stage II), I have noticed that similarly to mice (Pieters et al. 2016), β -catenin is localised evenly in the cortex and cell contacts. However, as soon as compaction is initiated (stage III), the protein signal gradually decreases in the apical surfaces to become more restricted to basolateral domains. In the rabbit embryo, similarly to mice and cattle (Barcroft et al. 1998; Messerschmidt et al. 2016), I observed that the strong basolateral distribution in the outer cells is maintained up to the blastocyst stage. Nonetheless, β -catenin can also be detected in

the inner cells of the morula, and TE cells of the blastocyst. However, it is localised in a non-polarised manner. Similar β -catenin distributions in ICM have also been reported in mouse and bovine embryos (Modina et al. 2007; Pieters et al. 2016; Tribulo et al. 2017). Therefore, these data suggest the possibility that Wnt/ β -catenin signalling is evolutionarily conserved during the differentiation of the first cell lineages in mice, cattle and rabbits. Upon the 8-cell stage (stage III), β -catenin is strongly accumulated in cell contacts and basolateral surfaces, which strongly suggests that the protein is involved in the initiation of the compaction process, cell adhesion and cell polarity. Even though β -catenin is localised in the inside/ICM cells, but not in a polarised manner, the protein can be considered as a basolateral marker in mice, cattle, humans and rabbits. This hypothesis could be further confirmed by functional experiments using the gene knockout of *CTNNB1* in preimplantation rabbit embryos.

It has been shown in epithelial cells that β -catenin induces AJs formation by forming a complex with E-cadherin (Gumbiner 2005). The fact that β -catenin is localized in a polarised manner in the outer cells of the embryo at the transition from the morula to the blastocyst stage suggests that cadherins are present in rabbits similarly to mice (Ohsugi et al. 1997; Stephenson, Yamanaka, and Rossant 2010). Although currently available antibodies did not allow me to analyse E-cadherin localisation in rabbit embryos, according to transcriptomic data (unpublished data in collaboration with dr hab. Piotr Pawlak, University of Life Sciences in Poznan), *CDH1* transcripts are detected at low levels in rabbit embryos. The comparison of protein localisation, associated with cell polarity, was summarised in **Figure 40**.

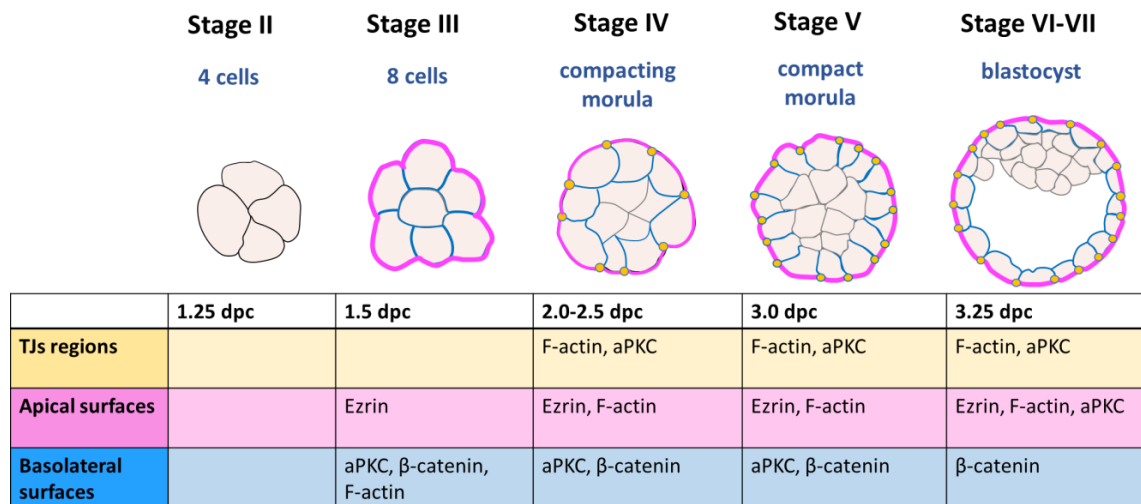


Figure 40. Cell polarity-associated factors distribution in outer/TE cells across rabbit developmental stages II-VII. Tight-junctions (TJs) regions are marked in yellow, and both F-actin with aPKC start to be visible in these regions since the compaction begins (stage IV) in the rabbit embryo. The apical domain (magenta) and the earlier apical marker P-Ezrin is observed in the apical surfaces before compaction (8-cell stage). aPKC is initially localised in the basolateral domains since 8-cell stage, then at 3.25 dpc, its distribution is predominant in the apical domains. F-actin is localised in a polarised manner from 2.5 dpc, whereas β -catenin is detected in basolateral surfaces from 8-cell stage.

9.4 Dynamic patterns of YAP localisation during early rabbit development

YAP is one of the major downstream effectors of the Hippo pathway. The protein, together with its paralog, TAZ, is a transcriptional coactivator that, when phosphorylated, remains deactivated in the cytoplasm (Zhao et al. 2007). Inhibition of the Hippo pathway core cascade results in YAP/TAZ dephosphorylation, which contributes to YAP/TAZ translocation into nuclei, where it binds to TEAD4 (L. Chen et al. 2010). The TEAD4-YAP/TAZ association promotes the activation of proliferation-related genes, and in the mouse morula, it induces the expression of genes associated with TE fate (Strumpf et al. 2005; Nishioka et al. 2009; Ralston et al. 2010).

In this research, I have shown that cytoplasmic and nuclear YAP localisation is detected in rabbit embryos as early as 4-cell stage (stage II). Then, up to the fully compacted embryo, it is localised in both the cytoplasm and nuclei. However, YAP localisation in the nuclei is predominant in the outer cells. These observations are consistent with

findings reported in mice (Strumpf et al. 2005; Hirate et al. 2015). According to my results, YAP mRNA levels in rabbit blastocysts at 4.0 dpc did not differ between ICM and TE. However, the protein immunolocalisation findings suggest that the Hippo pathway activity is regulated by subcellular YAP localisation (nuclei/cytoplasm). Similar to what was observed in mice (Strumpf et al. 2005; Hirate et al. 2015), in rabbits during the transition from the morula to the blastocyst, the majority of outside cells exhibit YAP localisation in the nuclei, while in the inside cells, YAP is predominantly localised in the cytoplasm. Also, in porcine (Emura et al. 2020) and bovine embryos (Negrón-Pérez, Zhang, and Hansen 2017), YAP is localised in the cytoplasm and the nuclei until the morula stage. Then, from the morula to the blastocyst stage, it was mainly detected in the nuclei of TE cells. Interestingly, in cattle, before compaction, the localisation of p-YAP can be visible in both the nuclei and cytoplasm, while in compact embryos it can be detected only in the nuclei (Sharma and Madan 2020) (**Figure 42**).

Investigating YAP subcellular localisation in rabbit embryos, I noticed that in the outside compartment, concomitant with the embryo growth, YAP protein is displaced from the cytoplasm to the nuclei, and the number of cells with YAP nuclear localisation (YAP N>C and N=C) is gradually increasing from the morula at stage V to the blastocyst at stage VII. In the inside compartment, the percentage contribution of nuclear YAP localisation is below 16% from stage V to VII (**Figure 41**). Within these stages, cells with N>C category constituted the smallest subset in the inside compartment. The presence of the YAP signal in the nuclei of the ICM cells was also observed during the mouse blastocyst development by Hashimoto and Sasaki (Hashimoto and Sasaki 2019). They have reported that the number of YAP-positive cells increases with development and YAP colocalises with the epiblast marker SOX2. They postulated that TEAD-YAP activity is crucial during epiblast formation (inducing expression of pluripotency factors) in mouse blastocysts (Hashimoto and Sasaki 2019). Additionally, similar observations were confirmed in humans (Qin et al. 2016), which suggests that this process is evolutionarily conserved.

To summarise, the results of YAP distribution dynamics analysis during the preimplantation rabbit embryo development indicate that YAP is localised in nuclei before cavitation and compaction. However, its nuclear localisation becomes restricted to outer cells when compaction begins, suggesting the involvement of YAP in TE

differentiation. Moreover, the presence of YAP protein might be regulated in the embryo through mechanisms controlling the protein localisation in the nucleus or the cytoplasm rather than on the gene activity level. It is likely that the Hippo pathway regulates YAP in rabbits in a similar way to mice, pigs or humans (Hirate et al. 2015; Gu et al. 2022; Gerri et al. 2020).

9.5 Colocalisation of GATA3 and YAP in preimplantation embryo

It was confirmed that the transcription factor GATA3 induces TE specification in the outer cells of mouse morula downstream of the Hippo pathway transcription factor TEAD4 (Ralston et al. 2010). *Gata3* is expressed in mouse embryos as early as 4-cells stage, while during blastocyst development, the protein was found to be selectively localised in the TE cells, in contrast to ICM cells (Home et al. 2009). Ralston and colleagues have confirmed that *Gata3* is co-expressed with *Cdx2* during blastocyst development. Although both CDX2 and GATA3 are induced by TEAD4-YAP/TAZ association, GATA3 activity is not dependent on CDX2. Therefore, it may suggest that CDX2 and GATA3 act independently in parallel cascades downstream of *Tead4* to promote the gene expression of other TE-related transcription factors (Ralston et al. 2010). Similar to mouse, cow and human embryos (Gerri et al. 2020), I observed that the evolutionarily conserved protein GATA3 colocalises with the coactivator YAP in rabbit embryos from morula to the blastocyst stage.

In this study I have shown that in rabbit early morulae (stages III-IV), only a small subset of cells (~4%) with YAP+/GATA3+ nuclei is observed, and at the same time, there are already YAP+/GATA3- cells present in the embryo, which suggests that at this stage, GATA3 is not present without nuclear YAP. Therefore, YAP is likely required for GATA3 activation at the early morula stage, however, for the rabbit model this hypothesis requires confirmation. The relative contribution of cells positive only for YAP (YAP+/GATA3-) is almost 50% at stages III-IV. Notably, the presence of GATA3+/YAP- cells in the inside and outside compartments between stages V-VII may suggest that during further development, GATA3 maintenance does not require YAP. In the outer cells, proportions of YAP+/GATA3+ cells remain at similar levels between all

stages from V to VII (around 50%). Noteworthy, similarly to the recent research concerning rabbit embryos (Bouchereau et al. 2022), I have confirmed by GATA3 immunostaining that induction of the TE/ICM specification in rabbit blastomeres starts at the early morula stage. It is possible that YAP nuclear localisation in the polarising outer cells is needed initially in the embryo to activate the TE program by inducing transcriptional factors such as GATA3 (**Figure 41**).

To summarise, no GATA3+/YAP- cells were observed in rabbit embryos at stages III-IV, indicating that before cavitation, YAP may be obligatory for GATA3 activation. Since the moment when cavitation is initiated, GATA3+/YAP- cells are present in the outside cells at stages V-VII, suggesting that YAP might not be required for the maintenance of GATA3 in the cavitating embryos. Therefore, I conclude that YAP in rabbits is crucial for the induction of GATA3 in the compacting embryo, whereas during cavitation, some different mechanisms, not dependent on YAP, may control the maintenance of GATA3 in nuclei, or it might remain through positive feedback of GATA3. The representative scheme of YAP and GATA3 localisation is presented in **Figure 41**.

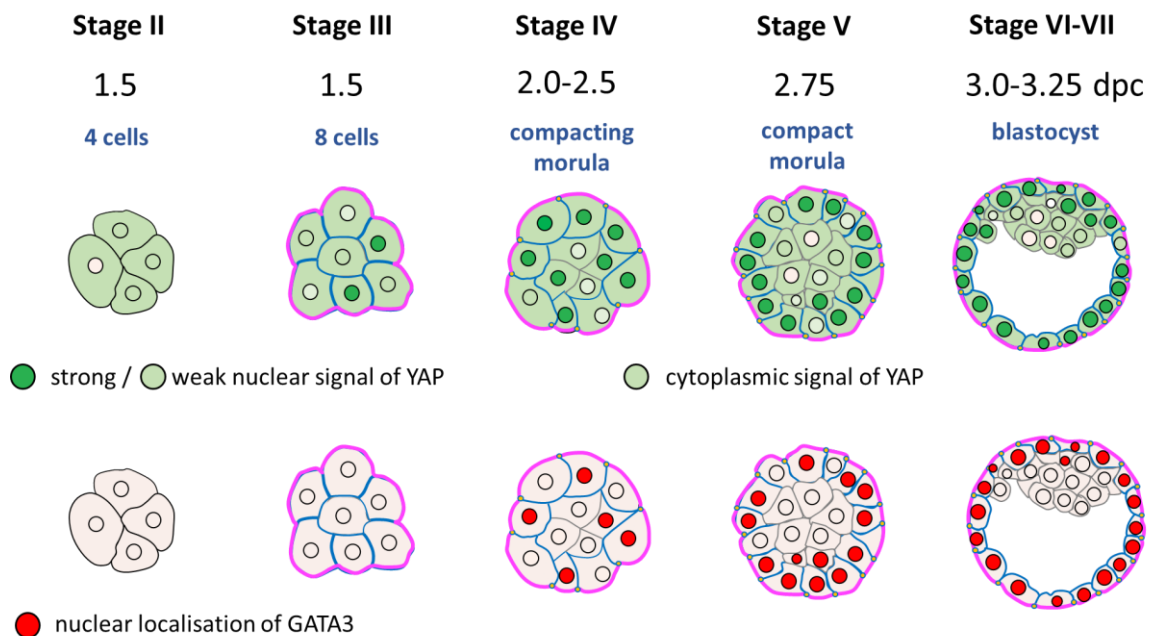


Figure 41. Representative scheme of YAP and GATA3 colocalisation in the rabbit embryo across rabbit developmental stages II-VII. YAP cytoplasmic and nuclear distribution (green), and GATA3 localisation (red). During the compaction process, at stage IV (2.0-2.5 dpc) YAP and GATA3 nuclear colocalisation is observed in the rabbit embryo.

9.6 The influence of the RHO-ROCK signalling on the Hippo pathway and TE differentiation

Studying the process of Hippo pathway regulation in the outside and inside cells during the transition from the morula to the blastocyst stage is essential for understanding the mechanism of the first cell-fate specification. It has been reported in mice that the Hippo pathway inactivation is required for nuclear YAP localisation and TEAD-mediated gene expression, which leads to the formation of the first polarised epithelium (TE) (Nishioka et al. 2009; Hirate et al. 2013).

Active RHO small GTPases have been reported as a downstream regulator of cell polarisation and the Hippo pathway in the outer cells of mouse morula by acting upstream of Amot and Nf2 (Clayton, Hall, and Johnson 1999; Shi et al. 2017; Alarcon and Marikawa 2018). Notably, the chemical inhibition of RHO-ROCK signalling leads to disruptions of the apicobasal polarity, tight junction biogenesis and activation of the Hippo pathway in the outer cells (Kono, Tamashiro, and Alarcon 2014; Mihajlović and Bruce 2016). The fact that RHO-ROCK signalling controls the capacity to form a blastocyst cavity was confirmed in mice (Kono, Tamashiro, and Alarcon 2014; Mihajlović and Bruce 2016), swine (J. Y. Zhang et al. 2014; Kwon, Kim, and Choi 2016), cattle (Kohri et al. 2020) and in humans (Huang et al. 2016).

In this study, using the specific small molecule Y-27632 inhibitor (ROCKi), I assessed the effect of ROCK activity inhibition from the 2-cell (1.0 dpc) to the morula (3.0 dpc) or to the blastocyst stage (4.0 dpc) on rabbit embryo development. Similarly to previous studies on mice (Kono, Tamashiro, and Alarcon 2014; Mihajlović and Bruce 2016), swine (J. Y. Zhang et al. 2014; Kwon, Kim, and Choi 2016), cattle (Kohri et al. 2020) and humans (Huang et al. 2016), I demonstrated that rabbit embryos after 72h of culture with ROCKi (extended time regime) exhibited impaired blastocyst formation. Notably, embryos after shorter, 48h culture with ROCKi (short time regime), already seemed to exhibit morphological alterations. In particular, blastomeres at the late morula stage were less compacted compared to the control group. This observation was similar to findings in porcine embryos (Kwon, Kim, and Choi 2016), while no such phenomenon was observed in mice, cattle or humans (Alarcon and Marikawa 2018; Kono, Tamashiro, and Alarcon 2014; Negrón-Pérez et al. 2018; Pillai et al. 2022; Huang et al.

2016). Furthermore, the total number of cells in embryos after ROCK inhibition was lower compared to the control group (both after 48h and 72h of culture). However, when I compared the ratio of inner and outer cells, I noticed no differences between ROCK-treated and control embryos (in both time regimes). Similar results were obtained in porcine morulae cultured with 20 μ M ROCKi for 24h, which exhibit significantly lower number of cells compared to the control embryos (Kwon, Kim, and Choi 2016). Noteworthy, the average cell number of murine embryos after ROCK inhibition treatment was not altered by culturing 2-cell embryos until 8-, 16- or 32-cell stage (Mihajlović and Bruce 2016). Therefore, my findings indicate that ROCK inhibition impairs the developmental progression and cell proliferation of the rabbit embryo. Even though in my research on rabbits there was no difference in average embryo diameter after 48h of culture with ROCK inhibitor supplementation, after 72h of culture, ROCK-treated embryos had significantly smaller diameters than control embryos. On the contrary, bovine blastocysts cultured with ROCKi (Y-27632) from 8 to 10 dpi (days post insemination) showed a significant increase in embryo size and proportion of CDX2-positive cells (Pillai et al. 2022). Thus, ROCK activity is essential for the quality and embryo size in rabbits and pigs from the onset of the TE formation, while in cattle it appears to be dispensable. In contrast, during the embryo cleavage and compaction processes, ROCK inhibition treatment did not affect the diameter and cell number of the rabbit embryo. Using immunofluorescent staining of proteins of interest, including the coactivator YAP, TE transcription factor GATA3, the apical domain markers aPKC and F-actin, and basolateral domain marker β -catenin, I addressed the effect of ROCK inhibition treatment (48h) on Hippo pathway activity, cell polarisation and TE differentiation. After ROCK inhibition treatment, rabbit morulae (3.0 dpc) exhibited no changes in the average numbers of YAP+/GATA3- cells, YAP+/GATA3+ cells, GATA3+/YAP- cells and YAP-/GATA3- cells in the inside and outside compartments compared to the control groups. This is in contrast to previous observations in mice (Mihajlović and Bruce 2016) and cattle, where in 5.0 dpc embryos cultured for additional 12h with RHOA inhibitor C3, the total percentages of CDX2+ and YAP+ cells were visibly lower than in the control embryos (Kohri et al. 2020). According to my findings, the ROCK inhibition in rabbit embryos does not seem to affect the subcellular YAP localisation after 48h of culture. In contrast to rabbits, ROCK-

inhibited mouse embryos cultured from 2-cell stage for 48h exhibited a decreased ratio of N>C YAP cells compared to the control group (Mihajlović and Bruce 2016). Therefore, it seems reasonable to conclude that ROCK does not suppress the Hippo pathway through subcellular localisation of YAP in the outer cells of the rabbit compact morula. In case of this species, regulation of the Hippo pathway might be carried out by some additional factors other than ROCK during embryo cleavage.

Although ROCK inhibition did not disrupt YAP and GATA3 distribution in the rabbit embryo, localisation of aPKC, F-actin and β -catenin after the ROCK treatment was visibly altered. Similarly to those findings reported in mice (Mihajlović and Bruce 2016), after ROCK treatment of rabbit embryos, I detected large accumulations of aPKC on the apical surfaces of the outer cells, whereas its distribution was neither observed in the basolateral domains of the outer cells nor in the inner cells. Furthermore, the F-actin signal in rabbit embryos seemed to be reduced after ROCK inhibition, and signal mislocalisations in the apical surfaces were detected similarly to mouse embryos (Mihajlović and Bruce 2016).

As regards β -catenin, my results demonstrated an excessive accumulation of the protein in the cell-cell contacts, as well as ectopic localisation in the apical domains of outer cells after treating rabbit embryos with the ROCK kinase inhibitor. These observations resemble results reported in mice (Mihajlović and Bruce 2016), where researchers also observed the apical distribution of the protein in the outer cells of murine embryos after ROCK activity inhibition. It seems that in both rabbits and mice alike, differentiation of both apical and basolateral domains is impaired by ROCK kinase inhibition, suggesting ROCK-mediated regulation of apicobasal polarity is conserved between these groups of animals.

My detailed analysis of aPKC distribution demonstrated that after ROCK inhibition in the rabbit embryo, the average number of the outside cells with aPKC localised on the apical surface is higher when compared to control embryos. Moreover, the analysis of the intensity profiles of the aPKC signal in the apical surfaces of the outer cells indicated a significant difference between ROCK inhibitor-treated and control embryos. The difference between the amplitudes of the maximum peak (which corresponds to the apical signal of aPKC) and the plateau (which corresponds to the cytoplasmic signal of aPKC) was higher for the ROCK-inhibited embryos than for the

control group. Such result means that the inhibition of the ROCK kinase participation in the Hippo pathway in the rabbit embryo causes apical accumulation of aPKC in the blastomeres.

To conclude the above-discussed results, the disruption of apicobasal polarisation observed in rabbit embryos after ROCK inhibition treatment does not lead to activation of the Hippo pathway in the outer cells of the morula. In consequence, YAP and GATA3 remain in the nuclei. Therefore, even though ROCK controls cell polarisation, it is likely not regulating the Hippo pathway in rabbits. Furthermore, these findings suggest that cell polarity is not essential in regulating the nuclear/cytoplasmic YAP localisation in the outer cells of the rabbit morula at 3.0 dpc, which is contradictory to the mouse model.

9.7 Differences in the regulation of the Hippo signalling between rabbits and other mammalian species

One of my research aims was to compare the rabbit model with the mouse in the context of the role of Hippo pathway and cell polarisation in first cell fate decision. This topic has been widely investigated in the mouse model compared to other species (Nishioka et al. 2009; Cockburn et al. 2013; Kono, Tamashiro, and Alarcon 2014; Hirate et al. 2012; 2013; 2015; Sasaki 2017). Thus, the mouse was the major point of reference. However, the preimplantation development in other mammals is recently more commonly investigated, which allows for broader comparisons (reviewed in Piliszek and Madeja 2018; Ptusa and Piliszek 2020; Filimonow et al. 2022). Therefore, I decided to compare TE differentiation of the rabbit embryo with different mammals (**Figure 42**).

In the rabbit embryo, ROCK kinases positively regulate F-actin and aPKC function in the polarised cell, similar to mice (Mihajlović and Bruce 2016). In humans and cattle, such observations were not conducted yet, however, in these species, both F-actin and aPKC are localised in the apical domain of the outer cells both in morulae and blastocysts (Gerri et al. 2020).

In rabbit embryos, aPKC is localised in the basolateral domains of outer cells before cavitation, unlike what has been reported in mice, humans and cattle, where the protein is restricted to apical domains (Plusa et al. 2005; Hirate et al. 2015; Gerri et al. 2020). During the transition from the morula to the blastocyst stage, P-Ezrin is accumulated in the apical surfaces of outer/TE cells in rabbits and mice (Louvet et al. 1996). Even though in mice cell polarity was reported to modulate the Hippo pathway through the regulation of YAP subcellular localisation, there is no evidence of a similar mechanism neither in rabbit nor in bovine embryos.

According to my data, I concluded that in rabbit embryos ROCK does not promote YAP/TAZ localisation in nuclei of TE. Therefore, ROCK kinases might not be involved in the Hippo pathway suppression, unlike it was reported in mice (Mihajlović and Bruce 2016).

Inactive Hippo pathway in the outer/TE cell allows for YAP/TAZ translocation to the nucleus in rabbits, mice and humans (Hirate et al. 2015; Gerri et al. 2020). On the contrary, in cattle, phosphorylated YAP/TAZ is observed in both TE and ICM cells, and the function of LATS1/2 kinases is not well understood (Sharma and Madan 2020). Two additional studies reported that the active form of YAP is also localised in the cell nuclei at the morula stage (Gerri et al. 2020), and the nuclear signal of YAP is restricted to TE cells in blastocysts (Negrón-Pérez and Hansen 2018).

In rabbits, the active form of YAP is present in the outside and TE cells of the morula and blastocyst stage, unlike it was reported in mice, humans and cattle (Gerri et al. 2020; Negrón-Pérez, Zhang, and Hansen 2017; Negrón-Pérez and Hansen 2018). In the nucleus of outer cells, YAP association with TEAD4 promotes expression of *GATA3* and *CDX2* in rabbits, similarly as observed in mice, humans and cattle, to induce TE differentiation (Strumpf et al. 2005; Ralston and Rossant 2008; Gerri et al. 2020). Then again, just like in mice and humans, in the majority of inside cells of the rabbit embryo YAP is not localised in the nuclei, and TE-related specific genes are not activated, thus contributing to specification into ICM (Strumpf et al. 2005; Ralston and Rossant 2008; Gerri et al. 2020).

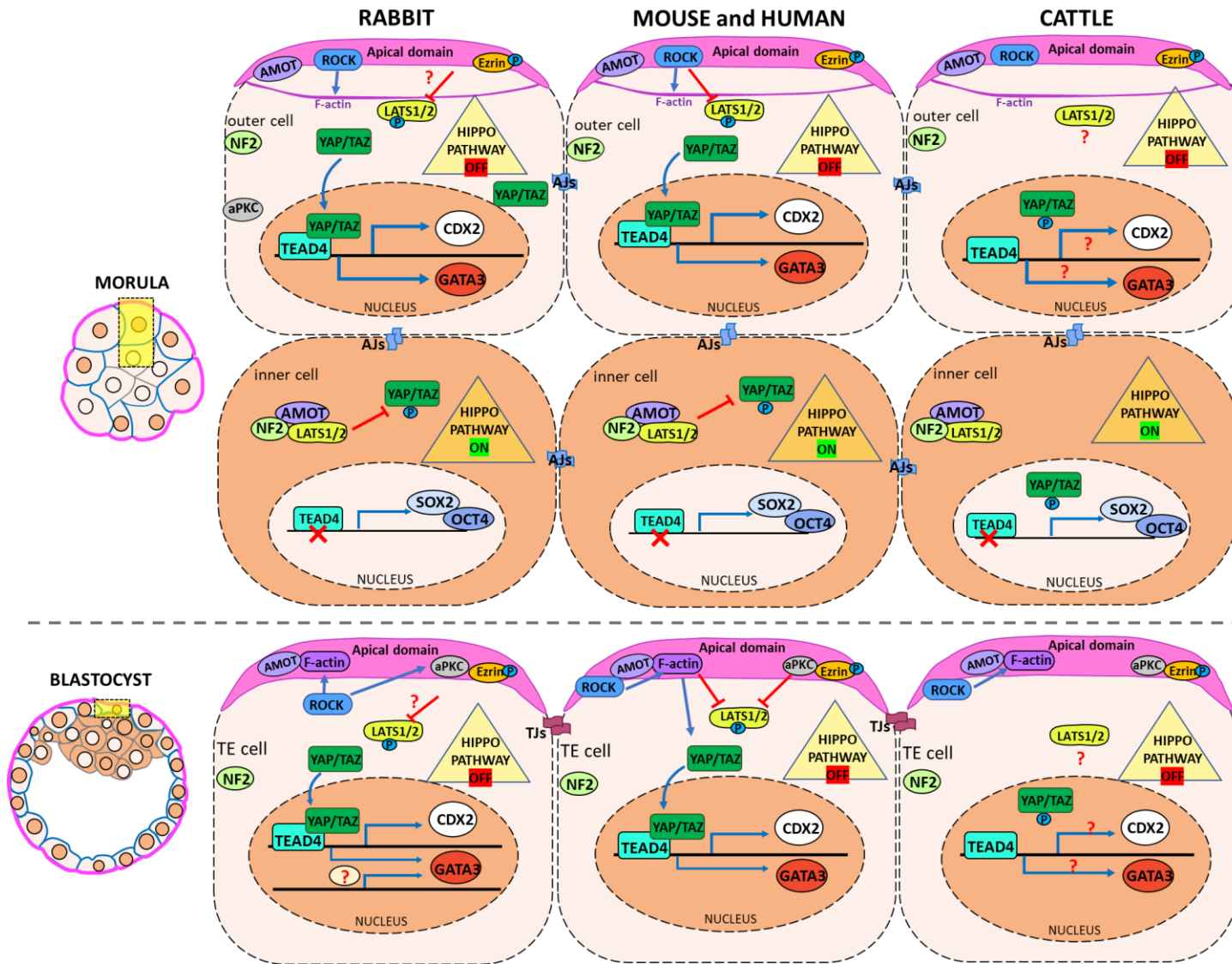


Figure 42. Proposed model of the Hippo pathway regulation in rabbit morula and blastocyst, compared to mice, humans and cattle. Similarities and differences in regulation of cell polarisation and YAP/TAZ localisation within cytoplasm/nuclei in the situation of active and inactive Hippo pathway across different mammalian species.

9.8 Conclusions

Summarising my research of the role of the Hippo pathway in trophectoderm differentiation in rabbit embryos, I conclude that:

- TEAD4 is the most probable candidate from the TEAD family, which is involved in the Hippo pathway in rabbit embryos, similarly to mouse and human models
- Levels of transcript of analysed Hippo pathway genes are similar between stages and ICM/TE compartment, which suggests additional mechanism of the Hippo pathway activity regulation
- GATA3 is the early marker of TE lineage in the rabbit embryo
- Cell polarity, concomitantly with compaction, is initiated upon 8-cell stage in the rabbit embryo, and both are continuous processes until 64-cell stage
- YAP localisation starts to be restricted to nuclei of TE cells at 3.0-3.25 dpc
- YAP might be required for initiation of *GATA3* expression in TE cells, but the maintenance of *GATA3* likely involves a YAP-independent mechanism
- ROCK controls the cell polarisation in TE cells of the embryo
- Cell polarity is not essential for the regulation of subcellular YAP localisation in the outer cells of the rabbit compact morula, meaning cell polarity is not involved in the Hippo pathway regulation during TE specification

9.9 The limitation of the study and further directions

The Hippo pathway in the mouse embryos is considered as the one of the major regulators of the first-cell fate decision, along with cell polarity and cell adhesion. This research sheds light on early events of cell differentiation in the rabbit embryo and the potential function of the Hippo pathway during trophectoderm development. In addition, it will be a helpful resource for further studies on trophectoderm development in non-rodent mammals.

In order to acquire a better understanding of the Hippo pathway regulation in rabbit embryos, immunolocalisation of AMOT and LATS1/2 across the preimplantation stages up to blastocyst formation would be needed. However, at the time of this study, suitable antibodies were not available. In addition, functional experiments in which AMOT and LATS1/2 functions are inhibited or downregulated would also be worth considering. It would be interesting to investigate the role of LATS1/2 by means of an inhibitor- a promising candidate is a lysophosphatidic acid (LPA), reported to lead to upregulation of YAP (F.-X. Yu et al. 2012).

Additionally, scrutiny of TEAD4 exact binding sites using ATAC seq would be an approach worth considering. The generation of *TEAD4*, *YAP* or *TAZ* knockout mouse lines could also help to understand the TEAD4-YAP/TAZ complex activity and, thereby, how the Hippo pathway is regulated in the rabbit embryo and what are the players downstream of this pathway.

It has been shown that contractility of blastomeres is involved during the first lineage decision in the mouse model (Samarage et al. 2015; Maître et al. 2015; 2016). To validate whether the contractility function is involved in first cell lineage differentiation in the rabbit embryo, the role of F-actin and myosin II, which are known to play important role in cell contractility, will need to be researched more widely.

To investigate the function of RHO-ROCK cascade in the Hippo pathway regulation in rabbit embryos other methods of target protein or gene inactivation might be applied. For instance, ROCK1/2-downregulation by RNA silencing in 4-8-cell stage embryo or creation of ROCK1/2 knockout (KO) rabbits. Such approach would allow for conducting *in vivo* experiments, allowing to overcome limitations of embryo culture *in vitro*.

My investigation has underlined the importance of species-specific preimplantation development studies and has shown that there are still many unresolved questions related to mammalian embryo development. This study is following the trend of comparative research, which allows not only to discover interspecies differences, but also to identify common aspects of preimplantation development within mammalian class.

10 References

- Aberle, H., H. Schwartz, and R. Kemler. 1996. 'Cadherin-Catenin Complex: Protein Interactions and Their Implications for Cadherin Function'. *Journal of Cellular Biochemistry* 61 (4): 514–23. [https://doi.org/10.1002/\(SICI\)1097-4644\(19960616\)61:4%3C514::AID-JCB4%3E3.0.CO;2-R](https://doi.org/10.1002/(SICI)1097-4644(19960616)61:4%3C514::AID-JCB4%3E3.0.CO;2-R).
- Adams, C. E. 1970. 'The Development of Rabbit Eggs after Culture in Vitro for 1-4 Days'. *Journal of Embryology and Experimental Morphology* 23 (1): 21–34.
- Adams, Cynthia L., Yih-Tai Chen, Stephen J Smith, and W. James Nelson. 1998. 'Mechanisms of Epithelial Cell–Cell Adhesion and Cell Compaction Revealed by High-Resolution Tracking of E-Cadherin–Green Fluorescent Protein'. *The Journal of Cell Biology* 142 (4): 1105–19.
- Alarcon, Vernadeth B. 2010. 'Cell Polarity Regulator PARD6B Is Essential for Trophectoderm Formation in the Preimplantation Mouse Embryo¹'. *Biology of Reproduction* 83 (3): 347–58. <https://doi.org/10.1095/biolreprod.110.084400>.
- Alarcon, Vernadeth B., and Yusuke Marikawa. 2018. 'ROCK and RHO Playlist for Preimplantation Development: Streaming to HIPPO Pathway and Apicobasal Polarity in the First Cell Differentiation'. *Advances in Anatomy, Embryology, and Cell Biology* 229: 47–68. https://doi.org/10.1007/978-3-319-63187-5_5.
- Amano, Mutsuki, Masanori Nakayama, and Kozo Kaibuchi. 2010. 'Rho-Kinase/ROCK: A Key Regulator of the Cytoskeleton and Cell Polarity'. *Cytoskeleton (Hoboken, N.J.)* 67 (9): 545–54. <https://doi.org/10.1002/cm.20472>.
- Amin, Ehsan, Badri Nath Dubey, Si-Cai Zhang, Lothar Gremer, Radovan Dvorsky, Jens M. Moll, Mohamed S. Taha, et al. 2013. 'Rho-Kinase: Regulation, (Dys)Function, and Inhibition'. *Biological Chemistry* 394 (11): 1399–1410. <https://doi.org/10.1515/hsz-2013-0181>.
- Anani, Shihadeh, Shivani Bhat, Nobuko Honma-Yamanaka, Dayana Krawchuk, and Yojiro Yamanaka. 2014. 'Initiation of Hippo Signaling Is Linked to Polarity Rather than to Cell Position in the Pre-Implantation Mouse Embryo'. *Development (Cambridge, England)* 141 (14): 2813–24. <https://doi.org/10.1242/dev.107276>.
- Aragona, Mariaceleste, Tito Panciera, Andrea Manfrin, Stefano Giullitti, Federica Michielin, Nicola Elvassore, Sirio Dupont, and Stefano Piccolo. 2013. 'A Mechanical Checkpoint Controls Multicellular Growth through YAP/TAZ Regulation by Actin-Processing Factors'. *Cell* 154 (5): 1047–59. <https://doi.org/10.1016/j.cell.2013.07.042>.
- Ardern, Hazel A., G. Martin Benson, Keith E. Suckling, Muriel J. Caslake, James Shepherd, and Chris J. Packard. 1999. 'Apolipoprotein B Overproduction by the Perfused Liver of the St. Thomas' Mixed Hyperlipidemic (SMHL) Rabbit'. *Journal of Lipid Research* 40 (12): 2234–43. [https://doi.org/10.1016/S0022-2275\(20\)32098-8](https://doi.org/10.1016/S0022-2275(20)32098-8).
- Assémat, Emeline, Elsa Bazellières, Emilie Pallesi-Pocachard, André Le Bivic, and Dominique Massey-Harroche. 2008. 'Polarity Complex Proteins'. *Biochimica et Biophysica Acta (BBA) - Biomembranes, Apical Junctional Complexes Part I*, 1778 (3): 614–30. <https://doi.org/10.1016/j.bbamem.2007.08.029>.

- Bakker, Julie, and Michael J. Baum. 2000. 'Neuroendocrine Regulation of GnRH Release in Induced Ovulators'. *Frontiers in Neuroendocrinology* 21 (3): 220–62. <https://doi.org/10.1006/frne.2000.0198>.
- Barcroft, L. C., A. Hay-Schmidt, A. Caveney, E. Gilfoyle, E. W. Overstrom, P. Hyttel, and A. J. Watson. 1998. 'Trophectoderm Differentiation in the Bovine Embryo: Characterization of a Polarized Epithelium'. *Reproduction* 114 (2): 327–39. <https://doi.org/10.1530/jrf.0.1140327>.
- Berg, Debra K., Craig S. Smith, David J. Pearton, David N. Wells, Ric Broadhurst, Martyn Donnison, and Peter L. Pfeffer. 2011. 'Trophectoderm Lineage Determination in Cattle'. *Developmental Cell* 20 (2): 244–55. <https://doi.org/10.1016/j.devcel.2011.01.003>.
- Betteridge, K. J., and J. -E. Fléchon. 1988. 'The Anatomy and Physiology of Pre-Attachment Bovine Embryos'. *Theriogenology*, Annual Conference of the International Embryo Transfer Society, 29 (1): 155–87. [https://doi.org/10.1016/0093-691X\(88\)90038-6](https://doi.org/10.1016/0093-691X(88)90038-6).
- Bissell, M. J., and J. Aggeler. 1987. 'Dynamic Reciprocity: How Do Extracellular Matrix and Hormones Direct Gene Expression?' *Progress in Clinical and Biological Research* 249: 251–62.
- Boroviak, Thorsten, Giuliano G. Stirparo, Sabine Dietmann, Irene Hernando-Herraez, Hisham Mohammed, Wolf Reik, Austin Smith, Erika Sasaki, Jennifer Nichols, and Paul Bertone. 2018. 'Single Cell Transcriptome Analysis of Human, Marmoset and Mouse Embryos Reveals Common and Divergent Features of Preimplantation Development'. *Development (Cambridge, England)* 145 (21): dev167833. <https://doi.org/10.1242/dev.167833>.
- Bou, Gerelchimeg, Shichao Liu, Mingju Sun, Jiang Zhu, Binghua Xue, Jia Guo, Yueming Zhao, et al. 2017. 'CDX2 Is Essential for Cell Proliferation and Polarity in Porcine Blastocysts'. *Development (Cambridge, England)* 144 (7): 1296–1306. <https://doi.org/10.1242/dev.141085>.
- Bouchereau, Wilhelm, Luc Jouneau, Catherine Archilla, Irène Aksoy, Anais Moulin, Nathalie Daniel, Nathalie Peynot, et al. 2022. 'Major Transcriptomic, Epigenetic and Metabolic Changes Underlie the Pluripotency Continuum in Rabbit Preimplantation Embryos'. *Development* 149 (17): dev200538. <https://doi.org/10.1242/dev.200538>.
- Bretscher. 1983. 'Purification of an 80,000-Dalton Protein That Is a Component of the Isolated Microvillus Cytoskeleton, and Its Localization in Nonmuscle Cells'. *The Journal of Cell Biology* 97 (2): 425–32.
- Brunner, Michael, Xuwen Peng, Gong Xin Liu, Xiao-Qin Ren, Ohad Ziv, Bum-Rak Choi, Rajesh Mathur, et al. 2008. 'Mechanisms of Cardiac Arrhythmias and Sudden Death in Transgenic Rabbits with Long QT Syndrome'. *The Journal of Clinical Investigation* 118 (6): 2246–59. <https://doi.org/10.1172/JCI33578>.
- Cao, Zubing, Timothy S. Carey, Avishek Ganguly, Catherine A. Wilson, Soumen Paul, and Jason G. Knott. 2015. 'Transcription Factor AP-2 γ Induces Early Cdx2 Expression and Represses HIPPO Signaling to Specify the Trophectoderm Lineage'. *Development (Cambridge, England)* 142 (9): 1606–15. <https://doi.org/10.1242/dev.120238>.
- Chan, Siew Wee, Chun Jye Lim, Yaan Fun Chong, Ajaybabu V. Pobbati, Caixia Huang, and Wanjin Hong. 2011. 'Hippo Pathway-Independent Restriction of TAZ and

- YAP by Angiomotin'. *The Journal of Biological Chemistry* 286 (9): 7018–26. <https://doi.org/10.1074/jbc.C110.212621>.
- Chavatte-Palmer, Laigre, Simonoff E, Chesné P, Challah-Jacques M, and Renard Jp. 2008. 'In Utero Characterisation of Fetal Growth by Ultrasound Scanning in the Rabbit'. *Theriogenology*. *Theriogenology*. 15 April 2008. <https://doi.org/10.1016/j.theriogenology.2007.12.013>.
- Chen, J., J. A. Cohn, and L. J. Mandel. 1995. 'Dephosphorylation of Ezrin as an Early Event in Renal Microvillar Breakdown and Anoxic Injury'. *Proceedings of the National Academy of Sciences of the United States of America* 92 (16): 7495–99. <https://doi.org/10.1073/pnas.92.16.7495>.
- Chen, Lingyi, Dekun Wang, Zhaoting Wu, Liping Ma, and George Q. Daley. 2010. 'Molecular Basis of the First Cell Fate Determination in Mouse Embryogenesis'. *Cell Research* 20 (9): 982–93. <https://doi.org/10.1038/cr.2010.106>.
- Choi, Inchul, Timothy S. Carey, Catherine A. Wilson, and Jason G. Knott. 2012. 'Transcription Factor AP-2 γ Is a Core Regulator of Tight Junction Biogenesis and Cavity Formation during Mouse Early Embryogenesis'. *Development (Cambridge, England)* 139 (24): 4623–32. <https://doi.org/10.1242/dev.086645>.
- Clayton, L., Alan Hall, and M. H. Johnson. 1999. 'A Role for Rho-like GTPases in the Polarisation of Mouse Eight-Cell Blastomeres'. *Developmental Biology* 205 (2): 322–31. <https://doi.org/10.1006/dbio.1998.9117>.
- Cockburn, Katie, Steffen Biechele, Jodi Garner, and Janet Rossant. 2013. 'The Hippo Pathway Member Nf2 Is Required for Inner Cell Mass Specification'. *Current Biology: CB* 23 (13): 1195–1201. <https://doi.org/10.1016/j.cub.2013.05.044>.
- Cockburn, Katie, and Janet Rossant. 2010. 'Making the Blastocyst: Lessons from the Mouse'. *The Journal of Clinical Investigation* 120 (4): 995–1003. <https://doi.org/10.1172/JCI41229>.
- Codelia, Veronica A., Gongping Sun, and Kenneth D. Irvine. 2014. 'Regulation of YAP by Mechanical Strain through Jnk and Hippo Signaling'. *Current Biology: CB* 24 (17): 2012–17. <https://doi.org/10.1016/j.cub.2014.07.034>.
- Crosby, I. M., F. Gandolfi, and R. M. Moor. 1988. 'Control of Protein Synthesis during Early Cleavage of Sheep Embryos'. *Reproduction* 82 (2): 769–75. <https://doi.org/10.1530/jrf.0.0820769>.
- Cross, J. C. 2005. 'How to Make a Placenta: Mechanisms of Trophoblast Cell Differentiation in Mice--a Review'. *Placenta* 26 Suppl A (April): S3-9. <https://doi.org/10.1016/j.placenta.2005.01.015>.
- Dard, Nicolas, Tran Le, Bernard Maro, and Sophie Louvet-Vallée. 2009. 'Inactivation of APK λ Reveals a Context Dependent Allocation of Cell Lineages in Preimplantation Mouse Embryos'. Edited by Neil Hotchin. *PLoS ONE* 4 (9): e7117. <https://doi.org/10.1371/journal.pone.0007117>.
- Dard, Nicolas, Sophie Louvet-Vallée, Angélica Santa-Maria, and Bernard Maro. 2004. 'Phosphorylation of Ezrin on Threonine T567 Plays a Crucial Role during Compaction in the Mouse Early Embryo'. *Developmental Biology* 271 (1): 87–97. <https://doi.org/10.1016/j.ydbio.2004.03.024>.
- Davies, S P, H Reddy, M Caivano, and P Cohen. 2000. 'Specificity and Mechanism of Action of Some Commonly Used Protein Kinase Inhibitors.' *Biochemical Journal* 351 (Pt 1): 95–105.

- De Paepe, Caroline, Greet Cauffman, An Verloes, Johan Sterckx, Paul Devroey, Herman Tournaye, Inge Liebaers, and Hilde Van de Velde. 2013. 'Human Trophoblast Cells Are Not yet Committed'. *Human Reproduction* 28 (3): 740–49. <https://doi.org/10.1093/humrep/des432>.
- Dehghani, Hesam, and Ann C. Hahnel. 2005. 'Expression Profile of Protein Kinase C Isozymes in Preimplantation Mouse Development'. *Reproduction* 130 (4): 441–51. <https://doi.org/10.1530/rep.1.00571>.
- DeRan, Michael, Jiayi Yang, Che-Hung Shen, Eric C. Peters, Julien Fitamant, Puiyee Chan, Mindy Hsieh, et al. 2014. 'Energy Stress Regulates Hippo-YAP Signaling Involving AMPK-Mediated Regulation of Angiomin-like 1 Protein'. *Cell Reports* 9 (2): 495–503. <https://doi.org/10.1016/j.celrep.2014.09.036>.
- Dietrich, J.-E., and T. Hiragi. 2007. 'Stochastic Patterning in the Mouse Pre-Implantation Embryo'. *Development* 134 (23): 4219–31. <https://doi.org/10.1242/dev.003798>.
- Dong, Jixin, Georg Feldmann, Jianbin Huang, Shian Wu, Nailong Zhang, Sarah A. Comerford, Mariana F. Gayyed, Robert A. Anders, Anirban Maitra, and Duoqia Pan. 2007. 'Elucidation of a Universal Size-Control Mechanism in Drosophila and Mammals'. *Cell* 130 (6): 1120–33. <https://doi.org/10.1016/j.cell.2007.07.019>.
- Du, Xingrong, Yongli Dong, Hao Shi, Jiang Li, Shanshan Kong, Donghua Shi, Ling V. Sun, Tian Xu, Kejing Deng, and Wufan Tao. 2014. 'Mst1 and Mst2 Are Essential Regulators of Trophoblast Differentiation and Placenta Morphogenesis'. *PLOS ONE* 9 (3): e90701. <https://doi.org/10.1371/journal.pone.0090701>.
- Duby, R. T., M. B. Cunniff, J. M. Belak, J. J. Balise, and J. M. Robl. 1993. 'Effect of Milking Frequency on Collection of Milk from Nursing New Zealand White Rabbits'. *Animal Biotechnology* 4 (1): 31–42. <https://doi.org/10.1080/10495399309525783>.
- Duc Dodon, Madeleine, Julien Villaudy, Louis Gazzolo, Robyn Haines, and Michael Lairmore. 2012. 'What We Are Learning on HTLV-1 Pathogenesis from Animal Models'. *Frontiers in Microbiology* 3. <https://www.frontiersin.org/articles/10.3389/fmicb.2012.00320>.
- Ducibella, T., D. F. Albertini, E. Anderson, and J. D. Biggers. 1975. 'The Preimplantation Mammalian Embryo: Characterization of Intercellular Junctions and Their Appearance during Development'. *Developmental Biology* 45 (2): 231–50. [https://doi.org/10.1016/0012-1606\(75\)90063-9](https://doi.org/10.1016/0012-1606(75)90063-9).
- Ducibella, T., and E. Anderson. 1979. 'The Effects of Calcium Deficiency on the Formation of the Zonula Occludens and Blastocoel in the Mouse Embryo'. *Developmental Biology* 73 (1): 46–58. [https://doi.org/10.1016/0012-1606\(79\)90136-2](https://doi.org/10.1016/0012-1606(79)90136-2).
- Ducibella, T., T. Ukena, M. Karnovsky, and E. Anderson. 1977. 'Changes in Cell Surface and Cortical Cytoplasmic Organization during Early Embryogenesis in the Preimplantation Mouse Embryo'. *Journal of Cell Biology* 74 (1): 153–67. <https://doi.org/10.1083/jcb.74.1.153>.
- Dunn, C. S., M. Mehtali, L. M. Houdebine, J. P. Gut, A. Kirn, and A. M. Aubertin. 1995. 'Human Immunodeficiency Virus Type 1 Infection of Human CD4-Transgenic Rabbits'. *The Journal of General Virology* 76 (Pt 6) (June): 1327–36. <https://doi.org/10.1099/0022-1317-76-6-1327>.

- Dupont, Sirio, Leonardo Morsut, Mariaceleste Aragona, Elena Enzo, Stefano Giulitti, Michelangelo Cordenonsi, Francesca Zanconato, et al. 2011. 'Role of YAP/TAZ in Mechanotransduction'. *Nature* 474 (7350): 179–83. <https://doi.org/10.1038/nature10137>.
- Eckert, Judith J., Amanda McCallum, Andrew Mears, Martin G. Rumsby, Iain T. Cameron, and Tom P. Fleming. 2004. 'PKC Signalling Regulates Tight Junction Membrane Assembly in the Pre-Implantation Mouse Embryo'. *Reproduction (Cambridge, England)* 127 (6): 653–67. <https://doi.org/10.1530/rep.1.00150>.
- El-Brolosy, Mohamed A., and Didier Y. R. Stainier. 2017. 'Genetic Compensation: A Phenomenon in Search of Mechanisms'. *PLoS Genetics* 13 (7): e1006780. <https://doi.org/10.1371/journal.pgen.1006780>.
- Emura, Natsuko, Yuriko Saito, Ruri Miura, and Ken Sawai. 2020. 'Effect of Downregulating the Hippo Pathway Members YAP1 and LATS2 Transcripts on Early Development and Gene Expression Involved in Differentiation in Porcine Embryos'. *Cellular Reprogramming* 22 (2): 62–70. <https://doi.org/10.1089/cell.2019.0082>.
- Emura, Natsuko, Nobuyuki Sakurai, Kazuki Takahashi, Tsutomu Hashizume, and Ken Sawai. 2016. 'OCT-4 Expression Is Essential for the Segregation of Trophectoderm Lineages in Porcine Preimplantation Embryos'. *The Journal of Reproduction and Development* 62 (4): 401–8. <https://doi.org/10.1262/jrd.2016-040>.
- Emura, Natsuko, Kazuki Takahashi, Yuriko Saito, and Ken Sawai. 2019. 'The Necessity of TEAD4 for Early Development and Gene Expression Involved in Differentiation in Porcine Embryos'. *The Journal of Reproduction and Development* 65 (4): 361–68. <https://doi.org/10.1262/jrd.2018-120>.
- Enders, null, and null Blankenship. 1999. 'Comparative Placental Structure'. *Advanced Drug Delivery Reviews* 38 (1): 3–15. [https://doi.org/10.1016/s0169-409x\(99\)00003-4](https://doi.org/10.1016/s0169-409x(99)00003-4).
- Fan, Jianglin, and Teruo Watanabe. 2003. 'Transgenic Rabbits as Therapeutic Protein Bioreactors and Human Disease Models'. *Pharmacology and Therapeutics* 3 (99): 261–82. [https://doi.org/10.1016/S0163-7258\(03\)00069-X](https://doi.org/10.1016/S0163-7258(03)00069-X).
- Filimonow, Katarzyna, Anna Chołoniowska, Katarzyna Michniak, and Anna Piliszek. 2022. 'Różnicowanie pierwszych linii komórkowych w zarodkach ssaków - różnice i podobieństwa międzygatunkowe'. *Postępy Biochemii*, January. https://doi.org/10.18388/pb.2021_417.
- Fleming, T. P., L. Butler, X. Lei, J. Collins, Q. Javed, B. Sheth, N. Stoddart, A. Wild, and M. Hay. 1994. 'Molecular Maturation of Cell Adhesion Systems during Mouse Early Development'. *Histochemistry* 101 (1): 1–7. <https://doi.org/10.1007/BF00315824>.
- Fleming, Tom P. 1987. 'A Quantitative Analysis of Cell Allocation to Trophectoderm and Inner Cell Mass in the Mouse Blastocyst'. *Developmental Biology* 119 (2): 520–31. [https://doi.org/10.1016/0012-1606\(87\)90055-8](https://doi.org/10.1016/0012-1606(87)90055-8).
- Fletcher, Georgina C., Maria-Del-Carmen Diaz-de-la-Loza, Nerea Borreguero-Muñoz, Maxine Holder, Mario Aguilar-Aragon, and Barry J. Thompson. 2018. 'Mechanical Strain Regulates the Hippo Pathway in Drosophila'. *Development (Cambridge, England)* 145 (5): dev159467. <https://doi.org/10.1242/dev.159467>.

- Foote, R. H., and E. W. Carney. 2000. 'The Rabbit as a Model for Reproductive and Developmental Toxicity Studies'. *Reproductive Toxicology (Elmsford, N.Y.)* 14 (6): 477–93. [https://doi.org/10.1016/s0890-6238\(00\)00101-5](https://doi.org/10.1016/s0890-6238(00)00101-5).
- Fujii, Takashi, Satoru Moriyasu, Hiroki Hirayama, Tsutomu Hashizume, and Ken Sawai. 2010. 'Aberrant Expression Patterns of Genes Involved in Segregation of Inner Cell Mass and Trophectoderm Lineages in Bovine Embryos Derived from Somatic Cell Nuclear Transfer'. *Cellular Reprogramming* 12 (5): 617–25. <https://doi.org/10.1089/cell.2010.0017>.
- Gailite, Ieva, Birgit L. Aerne, and Nicolas Tapon. 2015. 'Differential Control of Yorkie Activity by LKB1/AMPK and the Hippo/Warts Cascade in the Central Nervous System'. *Proceedings of the National Academy of Sciences* 112 (37). <https://doi.org/10.1073/pnas.1505512112>.
- Genevet, Alice, and Nicolas Tapon. 2011. 'The Hippo Pathway and Apico–Basal Cell Polarity'. *Biochemical Journal* 436 (2): 213–24. <https://doi.org/10.1042/BJ20110217>.
- Gerri, Claudia, Afshan McCarthy, Gregorio Alanis-Lobato, Andrej Demtschenko, Alexandre Bruneau, Sophie Loubersac, Norah M. E. Fogarty, et al. 2020. 'Initiation of a Conserved Trophectoderm Program in Human, Cow and Mouse Embryos'. *Nature* 587 (7834): 443–47. <https://doi.org/10.1038/s41586-020-2759-x>.
- Goissis, Marcelo D., and Jose B. Cibelli. 2014. 'Functional Characterization of CDX2 during Bovine Preimplantation Development in Vitro'. *Molecular Reproduction and Development* 81 (10): 962–70. <https://doi.org/10.1002/mrd.22415>.
- Gu, Bin, Brian Bradshaw, Min Zhu, Yu Sun, Sevan Hopyan, and Janet Rossant. 2022. 'Live Imaging YAP Signalling in Mouse Embryo Development'. *Open Biology* 12 (1): 210335. <https://doi.org/10.1098/rsob.210335>.
- Gumbiner, Barry M. 2005. 'Regulation of Cadherin-Mediated Adhesion in Morphogenesis'. *Nature Reviews Molecular Cell Biology* 6 (8): 622–34. <https://doi.org/10.1038/nrm1699>.
- Gumbiner, Barry M., and Nam-Gyun Kim. 2014. 'The Hippo-YAP Signaling Pathway and Contact Inhibition of Growth'. *Journal of Cell Science* 127 (4): 709–17. <https://doi.org/10.1242/jcs.140103>.
- Hamatani, Toshio, Mark G. Carter, Alexei A. Sharov, and Minoru S. H. Ko. 2004. 'Dynamics of Global Gene Expression Changes during Mouse Preimplantation Development'. *Developmental Cell* 6 (1): 117–31. [https://doi.org/10.1016/s1534-5807\(03\)00373-3](https://doi.org/10.1016/s1534-5807(03)00373-3).
- Hanzel, D., H. Reggio, A. Bretscher, J. G. Forte, and P. Mangeat. 1991. 'The Secretion-Stimulated 80K Phosphoprotein of Parietal Cells Is Ezrin, and Has Properties of a Membrane Cytoskeletal Linker in the Induced Apical Microvilli'. *The EMBO Journal* 10 (9): 2363–73. <https://doi.org/10.1002/j.1460-2075.1991.tb07775.x>.
- Harper. 1961. 'The Time of Ovulation in the Rabbit Following the Injection of Luteinizing Hormone'. *The Journal of Endocrinology*. *J Endocrinol.* April 1961. <https://doi.org/10.1677/joe.0.0220147>.
- Haruta, Y., L. J. Maguire, D. S. Rootman, and J. M. Hill. 1987. 'Recurrent Herpes Simplex Virus Type 1 Corneal Epithelial Lesions after Radial Keratotomy in the Rabbit'. *Archives of Ophthalmology (Chicago, Ill.: 1960)* 105 (5): 692–94. <https://doi.org/10.1001/archophth.1987.01060050110048>.

- Harvey, Kieran F., Xiaomeng Zhang, and David M. Thomas. 2013. 'The Hippo Pathway and Human Cancer'. *Nature Reviews Cancer* 13 (4): 246–57. <https://doi.org/10.1038/nrc3458>.
- Hashimoto, Masakazu, and Hiroshi Sasaki. 2019. 'Epiblast Formation by TEAD-YAP-Dependent Expression of Pluripotency Factors and Competitive Elimination of Unspecified Cells'. *Developmental Cell* 50 (2): 139-154.e5. <https://doi.org/10.1016/j.devcel.2019.05.024>.
- Heape, Walter, and Adam Sedgwick. 1997. 'Ovulation and Degeneration of Ova in the Rabbit'. *Proceedings of the Royal Society of London. Series B, Containing Papers of a Biological Character* 76 (509): 260–68. <https://doi.org/10.1098/rspb.1905.0019>.
- Hegele-Hartung, Christa, Bernd Fischer, and Henning M. Beier. 1988. 'Development of Preimplantation Rabbit Embryos after In-Vitro Culture and Embryo Transfer: An Electron Microscopic Study'. *The Anatomical Record* 220 (1): 31–42. <https://doi.org/10.1002/ar.1092200105>.
- Hirate, Yoshikazu, Katie Cockburn, Janet Rossant, and Hiroshi Sasaki. 2012. 'Tead4 Is Constitutively Nuclear, While Nuclear vs. Cytoplasmic Yap Distribution Is Regulated in Preimplantation Mouse Embryos'. *Proceedings of the National Academy of Sciences of the United States of America* 109 (50): E3389–90. <https://doi.org/10.1073/pnas.1211810109>.
- Hirate, Yoshikazu, Shino Hirahara, Ken-ichi Inoue, Hiroshi Kiyonari, Hiroshi Niwa, and Hiroshi Sasaki. 2015. 'Par-APKC-Dependent and -Independent Mechanisms Cooperatively Control Cell Polarity, Hippo Signaling, and Cell Positioning in 16-Cell Stage Mouse Embryos'. *Development, Growth & Differentiation* 57 (8): 544–56. <https://doi.org/10.1111/dgd.12235>.
- Hirate, Yoshikazu, Shino Hirahara, Ken-ichi Inoue, Atsushi Suzuki, Vernadeth B. Alarcon, Kazunori Akimoto, Takaaki Hirai, et al. 2013. 'Polarity-Dependent Distribution of Angiomotin Localizes Hippo Signaling in Preimplantation Embryos'. *Current Biology* 23 (13): 1181–94. <https://doi.org/10.1016/j.cub.2013.05.014>.
- Hirate, Yoshikazu, and Hiroshi Sasaki. 2014. 'The Role of Angiomotin Phosphorylation in the Hippo Pathway during Preimplantation Mouse Development'. *Tissue Barriers* 2 (February): e28127. <https://doi.org/10.4161/tisb.28127>.
- Hodge, Richard G., and Anne J. Ridley. 2016. 'Regulating Rho GTPases and Their Regulators'. *Nature Reviews Molecular Cell Biology* 17 (8): 496–510. <https://doi.org/10.1038/nrm.2016.67>.
- Hoffman, Loren H., D. Rachel Breinan, and Gareth L. Blaeuer. 1999. 'The Rabbit as a Model for Implantation: In Vivo and In Vitro Studies'. In *Embryo Implantation: Molecular, Cellular and Clinical Aspects*, edited by Daniel D. Carson, 151–60. Proceedings in the Serono Symposia USA Series. New York, NY: Springer. https://doi.org/10.1007/978-1-4612-1548-6_13.
- Home, Pratik, Soma Ray, Debasree Dutta, Illya Bronshteyn, Melissa Larson, and Soumen Paul. 2009. 'GATA3 Is Selectively Expressed in the Trophectoderm of Peri-Implantation Embryo and Directly Regulates Cdx2 Gene Expression'. *The Journal of Biological Chemistry* 284 (42): 28729–37. <https://doi.org/10.1074/jbc.M109.016840>.
- Home, Pratik, Biswarup Saha, Soma Ray, Debasree Dutta, Sumedha Gunewardena, Byunggil Yoo, Arindam Pal, et al. 2012. 'Altered Subcellular Localization of

- Transcription Factor TEAD4 Regulates First Mammalian Cell Lineage Commitment'. *Proceedings of the National Academy of Sciences of the United States of America* 109 (19): 7362–67. <https://doi.org/10.1073/pnas.1201595109>.
- Hong, Audrey W., Zhipeng Meng, Hai-Xin Yuan, Steven W. Plouffe, Sungho Moon, Wantae Kim, Eek-Hoon Jho, and Kun-Liang Guan. 2017. 'Osmotic Stress-Induced Phosphorylation by NLK at Ser128 Activates YAP'. *EMBO Reports* 18 (1): 72–86. <https://doi.org/10.15252/embr.201642681>.
- Hoos, P. C., and L. H. Hoffman. 1980. 'Temporal Aspects of Rabbit Uterine Vascular and Decidual Responses to Blastocyst Stimulation'. *Biology of Reproduction* 23 (2): 453–59. <https://doi.org/10.1095/biolreprod23.2.453>.
- Houliston, E., S. J. Pickering, and B. Maro. 1987. 'Redistribution of Microtubules and Pericentriolar Material during the Development of Polarity in Mouse Blastomeres'. *The Journal of Cell Biology* 104 (5): 1299–1308. <https://doi.org/10.1083/jcb.104.5.1299>.
- Hu, Jiafen, Xuwen Peng, Lynn R. Budgeon, Nancy M. Cladel, Karla K. Balogh, and Neil D. Christensen. 2007. 'Establishment of a Cottontail Rabbit Papillomavirus/HLA-A2.1 Transgenic Rabbit Model'. *Journal of Virology* 81 (13): 7171–77. <https://doi.org/10.1128/JVI.00200-07>.
- Huang, Sunxing, Chenhui Ding, Qingyun Mai, Yanwen Xu, and Canquan Zhou. 2016. 'Inhibition of Rho-associated Protein Kinase Increases the Ratio of Formation of Blastocysts from Single Human Blastomeres'. *Molecular Medicine Reports* 13 (3): 2046–52. <https://doi.org/10.3892/mmr.2016.4766>.
- 'Induction of Polarity in Mouse 8-Cell Blastomeres: Specificity, Geometry, and Stability'. 1981. *The Journal of Cell Biology* 91 (1): 303–8. <https://doi.org/10.1083/jcb.91.1.303>.
- Iqbal, Khursheed, James L. Chitwood, Geraldine A. Meyers-Brown, Janet F. Roser, and Pablo J. Ross. 2014. 'RNA-Seq Transcriptome Profiling of Equine Inner Cell Mass and Trophectoderm'. *Biology of Reproduction* 90 (3): 61. <https://doi.org/10.1095/biolreprod.113.113928>.
- Jedrusik, Agnieszka, Alexander W. Bruce, Meng H. Tan, Denise E. Leong, Maria Skamagki, Mylene Yao, and Magdalena Zernicka-Goetz. 2010. 'Maternally and Zygotically Provided Cdx2 Have Novel and Critical Roles for Early Development of the Mouse Embryo'. *Developmental Biology* 344 (1–2): 66–78. <https://doi.org/10.1016/j.ydbio.2010.04.017>.
- Johnson, M. H., and B. Maro. 1984. 'The Distribution of Cytoplasmic Actin in Mouse 8-Cell Blastomeres'. *Journal of Embryology and Experimental Morphology* 82 (August): 97–117.
- Johnson, M. H., and C. A. Ziomek. 1981. 'The Foundation of Two Distinct Cell Lineages within the Mouse Morula'. *Cell* 24 (1): 71–80. [https://doi.org/10.1016/0092-8674\(81\)90502-x](https://doi.org/10.1016/0092-8674(81)90502-x).
- Johnston, Daniel St, and Julie Ahringer. 2010. 'Cell Polarity in Eggs and Epithelia: Parallels and Diversity'. *Cell* 141 (5): 757–74. <https://doi.org/10.1016/j.cell.2010.05.011>.
- Kawagishi, Rikako, Masahiro Tahara, Kenjiro Sawada, Yoshihide Ikebuchi, Kenichiro Morishige, Masahiro Sakata, Keiichi Tasaka, and Yuji Murata. 2004. 'Rho-Kinase Is Involved in Mouse Blastocyst Cavity Formation'. *Biochemical and Biophysical*

- Research Communications* 319 (2): 643–48.
<https://doi.org/10.1016/j.bbrc.2004.05.040>.
- Kidder, G. M., and J. R. McLachlin. 1985. 'Timing of Transcription and Protein Synthesis Underlying Morphogenesis in Preimplantation Mouse Embryos'. *Developmental Biology* 112 (2): 265–75. [https://doi.org/10.1016/0012-1606\(85\)90397-5](https://doi.org/10.1016/0012-1606(85)90397-5).
- Kim et al. 2011. 'E-Cadherin Mediates Contact Inhibition of Proliferation through Hippo Signaling-Pathway Components'. 2011. <https://doi.org/10.1073/pnas.1103345108>.
- Kohri, Nanami, Hiroki Akizawa, Sakie Iisaka, Hanako Bai, Masashi Takahashi, and Manabu Kawahara. 2020. 'The Role of RHOA Signaling in Trophectoderm Cell-Fate Decision in Cattle'. *Biochemical and Biophysical Research Communications* 528 (4): 713–18. <https://doi.org/10.1016/j.bbrc.2020.05.210>.
- Kondo, Takahisa, Kosei Takeuchi, Yoshinori Doi, Shigenobu Yonemura, Shigekazu Nagata, Shoichiro Tsukita, and Sachiko Tsukita. 1997. 'ERM (Ezrin/Radixin/Moesin)-Based Molecular Mechanism of Microvillar Breakdown at an Early Stage of Apoptosis'. *The Journal of Cell Biology* 139 (3): 749–58.
- Kong, Qingran, Xu Yang, Heng Zhang, Shichao Liu, Jianchao Zhao, Jiaming Zhang, Xiaogang Weng, Junxue Jin, and Zhonghua Liu. 2020. 'Lineage Specification and Pluripotency Revealed by Transcriptome Analysis from Oocyte to Blastocyst in Pig'. *The FASEB Journal* 34 (1): 691–705. <https://doi.org/10.1096/fj.201901818RR>.
- Kono, Kanako, Dana Ann A. Tamashiro, and Vernadeth B. Alarcon. 2014. 'Inhibition of RHO-ROCK Signaling Enhances ICM and Suppresses TE Characteristics through Activation of Hippo Signaling in the Mouse Blastocyst'. *Developmental Biology* 394 (1): 142. <https://doi.org/10.1016/j.ydbio.2014.06.023>.
- Korotkevich, Ekaterina, Ritsuya Niwayama, Aurélien Courtois, Stefanie Friese, Nicolas Berger, Frank Buchholz, and Takashi Hiiragi. 2017. 'The Apical Domain Is Required and Sufficient for the First Lineage Segregation in the Mouse Embryo'. *Developmental Cell* 40 (3): 235–247.e7. <https://doi.org/10.1016/j.devcel.2017.01.006>.
- Koyama, H., H. Suzuki, X. Yang, S. Jiang, and R. H. Foote. 1994. 'Analysis of Polarity of Bovine and Rabbit Embryos by Scanning Electron Microscopy'. *Biology of Reproduction* 50 (1): 163–70. <https://doi.org/10.1095/biolreprod50.1.163>.
- Kuijk, Ewart, Niels Geijsen, and Edwin Cuppen. 2015. 'Pluripotency in the Light of the Developmental Hourglass'. *Biological Reviews* 90 (2): 428–43. <https://doi.org/10.1111/brv.12117>.
- Kwon, Jeongwoo, Nam-Hyung Kim, and Inchul Choi. 2016. 'ROCK Activity Regulates Functional Tight Junction Assembly during Blastocyst Formation in Porcine Parthenogenetic Embryos'. *PeerJ* 4 (April): e1914. <https://doi.org/10.7717/peerj.1914>.
- La Ville, A., P. R. Turner, R. M. Pittilo, S. Martini, C. B. Marenah, P. M. Rowles, G. Morris, G. A. Thomson, N. Woolf, and B. Lewis. 1987. 'Hereditary Hyperlipidemia in the Rabbit Due to Overproduction of Lipoproteins. I. Biochemical Studies'. *Arteriosclerosis (Dallas, Tex.)* 7 (2): 105–12. <https://doi.org/10.1161/01.atv.7.2.105>.
- Laeno, Arlene May A., Dana Ann A. Tamashiro, and Vernadeth B. Alarcon. 2013. 'Rho-Associated Kinase Activity Is Required for Proper Morphogenesis of the Inner

- Cell Mass in the Mouse Blastocyst¹. *Biology of Reproduction* 89 (5): 122, 1–13. <https://doi.org/10.1095/biolreprod.113.109470>.
- Larue, L., M. Ohsugi, J. Hirchenhain, and R. Kemler. 1994. 'E-Cadherin Null Mutant Embryos Fail to Form a Trophectoderm Epithelium'. *Proceedings of the National Academy of Sciences* 91 (17): 8263–67. <https://doi.org/10.1073/pnas.91.17.8263>.
- Léandri, R. D., C. Archilla, L. C. Bui, N. Peynot, Z. Liu, C. Cabau, A. Chastellier, J. P. Renard, and V. Duranthon. 2009. 'Revealing the Dynamics of Gene Expression during Embryonic Genome Activation and First Differentiation in the Rabbit Embryo with a Dedicated Array Screening'. *Physiological Genomics* 36 (2): 98–113. <https://doi.org/10.1152/physiolgenomics.90310.2008>.
- Lee, Hane, Junsu Kang, Soungyub Ahn, and Junho Lee. 2019. 'The Hippo Pathway Is Essential for Maintenance of Apicobasal Polarity in the Growing Intestine of *Caenorhabditis Elegans*'. *Genetics* 213 (2): 501–15. <https://doi.org/10.1534/genetics.119.302477>.
- Lei, Qun-Ying, Heng Zhang, Bin Zhao, Zheng-Yu Zha, Feng Bai, Xin-Hai Pei, Shimin Zhao, Yue Xiong, and Kun-Liang Guan. 2008. 'TAZ Promotes Cell Proliferation and Epithelial-Mesenchymal Transition and Is Inhibited by the Hippo Pathway'. *Molecular and Cellular Biology* 28 (7): 2426–36. <https://doi.org/10.1128/MCB.01874-07>.
- Leung, C. Y., M. Zhu, and M. Zernicka-Goetz. 2016. 'Chapter Six - Polarity in Cell-Fate Acquisition in the Early Mouse Embryo'. In *Current Topics in Developmental Biology*, edited by Melvin L. DePamphilis, 120:203–34. Mammalian Preimplantation Development. Academic Press. <https://doi.org/10.1016/bs.ctdb.2016.04.008>.
- Leung, Chuen Yan, and Magdalena Zernicka-Goetz. 2013. 'Angiomotin Prevents Pluripotent Lineage Differentiation in Mouse Embryos via Hippo Pathway-Dependent and -Independent Mechanisms'. *Nature Communications* 4: 2251. <https://doi.org/10.1038/ncomms3251>.
- Levy, J. B., M. H. Johnson, H. Goodall, and B. Maro. 1986. 'The Timing of Compaction: Control of a Major Developmental Transition in Mouse Early Embryogenesis'. *Journal of Embryology and Experimental Morphology* 95 (June): 213–37.
- Lim, Hui Yi Grace, Yanina D. Alvarez, Maxime Gasnier, Yiming Wang, Piotr Tetlak, Stephanie Bissiere, Hongmei Wang, Maté Biro, and Nicolas Plachta. 2020. 'Keratins Are Asymmetrically Inherited Fate Determinants in the Mammalian Embryo'. *Nature* 585 (7825): 404–9. <https://doi.org/10.1038/s41586-020-2647-4>.
- Lindström, Nils O, Melanie L Lawrence, Sally F Burn, Jeanette A Johansson, Elvira RM Bakker, Rachel A Ridgway, C-Hong Chang, et al. 2015. 'Integrated β -Catenin, BMP, PTEN, and Notch Signalling Patterns the Nephron'. Edited by Elaine Fuchs. *ELife* 4 (February): e04000. <https://doi.org/10.7554/eLife.04000>.
- Liu, Hongjie, Zhaoting Wu, Xianle Shi, Wenzhi Li, Chang Liu, Dekun Wang, Xiaoying Ye, et al. 2013. 'Atypical PKC, Regulated by Rho GTPases and Mek/Erk, Phosphorylates Ezrin during Eight-Cell Embryocompaction'. *Developmental Biology* 375 (1): 13–22. <https://doi.org/10.1016/j.ydbio.2013.01.002>.
- Lorthongpanich, Chanchao, Daniel M. Messerschmidt, Siew Wee Chan, Wanjin Hong, Barbara B. Knowles, and Davor Solter. 2013. 'Temporal Reduction of LATS

- Kinases in the Early Preimplantation Embryo Prevents ICM Lineage Differentiation'. *Genes & Development* 27 (13): 1441–46. <https://doi.org/10.1101/gad.219618.113>.
- Louvet, S., J. Aghion, A. Santa-Maria, P. Mangeat, and B. Maro. 1996. 'Ezrin Becomes Restricted to Outer Cells Following Asymmetrical Division in the Preimplantation Mouse Embryo'. *Developmental Biology* 177 (2): 568–79. <https://doi.org/10.1006/dbio.1996.0186>.
- Louvet-Vallée, S., N. Dard, A. Santa-Maria, J. Aghion, and B. Maro. 2001. 'A Major Posttranslational Modification of Ezrin Takes Place during Epithelial Differentiation in the Early Mouse Embryo'. *Developmental Biology* 231 (1): 190–200. <https://doi.org/10.1006/dbio.2000.0147>.
- Ma, Shenghong, Zhipeng Meng, Rui Chen, and Kun-Liang Guan. 2019. 'The Hippo Pathway: Biology and Pathophysiology'. *Annual Review of Biochemistry* 88 (1): 577–604. <https://doi.org/10.1146/annurev-biochem-013118-111829>.
- Madeja, Zofia E., Jaroslaw Sosnowski, Kamila Hryniewicz, Ewelina Warzych, Piotr Pawlak, Natalia Rozwadowska, Berenika Plusa, and Dorota Lechniak. 2013. 'Changes in Sub-Cellular Localisation of Trophoblast and Inner Cell Mass Specific Transcription Factors during Bovine Preimplantation Development'. *BMC Developmental Biology* 13 (1): 32. <https://doi.org/10.1186/1471-213X-13-32>.
- Maître, Jean-Léon, Ritsuya Niwayama, Hervé Turlier, François Nédélec, and Takashi Hiiragi. 2015. 'Pulsatile Cell-Autonomous Contractility Drives Compaction in the Mouse Embryo'. *Nature Cell Biology* 17 (7): 849–55. <https://doi.org/10.1038/ncb3185>.
- Maître, Jean-Léon, Hervé Turlier, Rukshala Illukkumbura, Björn Eismann, Ritsuya Niwayama, François Nédélec, and Takashi Hiiragi. 2016. 'Asymmetric Division of Contractile Domains Couples Cell Positioning and Fate Specification'. *Nature* 536 (7616): 344–48. <https://doi.org/10.1038/nature18958>.
- Mamo, Solomon, Arpad Baji Gal, Szilard Bodo, and Andras Dinnyes. 2007. 'Quantitative Evaluation and Selection of Reference Genes in Mouse Oocytes and Embryos Cultured in Vivo and in Vitro'. *BMC Developmental Biology* 7 (1): 14. <https://doi.org/10.1186/1471-213X-7-14>.
- Maro, B., M. H. Johnson, S. J. Pickering, and G. Flach. 1984. 'Changes in Actin Distribution during Fertilization of the Mouse Egg'. *Journal of Embryology and Experimental Morphology* 81 (June): 211–37.
- Matsunari, H, Watanabe M, Hasegawa K, Uchikura A, Nakano K, Umeyama K, Masaki H, et al. 2020. 'Compensation of Disabled Organogeneses in Genetically Modified Pig Fetuses by Blastocyst Complementation'. *Stem Cell Reports* 14 (1). <https://doi.org/10.1016/j.stemcr.2019.11.008>.
- McBride, Alison A. 2017. 'Oncogenic Human Papillomaviruses'. *Philosophical Transactions of the Royal Society B: Biological Sciences* 372 (1732): 20160273. <https://doi.org/10.1098/rstb.2016.0273>.
- McConnell, Josie, Linda Petrie, Fiona Stennard, Kenneth Ryan, and Jennifer Nichols. 2005. 'Eomesodermin Is Expressed in Mouse Oocytes and Pre-Implantation Embryos'. *Molecular Reproduction and Development* 71 (4): 399–404. <https://doi.org/10.1002/mrd.20318>.

- McLaren, A., and R. Smith. 1977. 'Functional Test of Tight Junctions in the Mouse Blastocyst'. *Nature* 267 (5609): 351–53. <https://doi.org/10.1038/267351a0>.
- Meirelles, F. V., A. R. Caetano, Y. F. Watanabe, P. Ripamonte, S. F. Carambula, G. K. Merighe, and S. M. Garcia. 2004. 'Genome Activation and Developmental Block in Bovine Embryos'. *Animal Reproduction Science, Research and Practice* III. 15th International Congress on Animal Reproduction, 82–83 (July): 13–20. <https://doi.org/10.1016/j.anireprosci.2004.05.012>.
- Mendez, Susana, Christine L. Hatem, Anup K. Kesavan, Javier Lopez-Molina, M. Louise M. Pitt, Arthur M. Dannenberg, and Yukari C. Manabe. 2008. 'Susceptibility to Tuberculosis: Composition of Tuberculous Granulomas in Thorbecke and Outbred New Zealand White Rabbits'. *Veterinary Immunology and Immunopathology* 122 (1–2): 167–74. <https://doi.org/10.1016/j.vetimm.2007.11.006>.
- Meng, Zhipeng, Toshiro Moroishi, and Kun-Liang Guan. 2016. 'Mechanisms of Hippo Pathway Regulation'. *Genes & Development* 30 (1): 1–17. <https://doi.org/10.1101/gad.274027.115>.
- Messerschmidt, Daniel, Wilhelmine N. de Vries, Chanchao Lorthongpanich, Sathish Balu, Davor Solter, and Barbara B. Knowles. 2016. 'β-Catenin-Mediated Adhesion Is Required for Successful Preimplantation Mouse Embryo Development'. *Development (Cambridge, England)* 143 (11): 1993–99. <https://doi.org/10.1242/dev.133439>.
- Mihajlović, Aleksandar I., and Alexander W. Bruce. 2016. 'Rho-Associated Protein Kinase Regulates Subcellular Localisation of Angiomotin and Hippo-Signalling during Preimplantation Mouse Embryo Development'. *Reproductive Biomedicine Online* 33 (3): 381–90. <https://doi.org/10.1016/j.rbmo.2016.06.028>.
- Mihajlović, Aleksandar I., and Alexander W. Bruce. 2017. 'The First Cell-Fate Decision of Mouse Preimplantation Embryo Development: Integrating Cell Position and Polarity'. *Open Biology* 7 (11): 170210. <https://doi.org/10.1098/rsob.170210>.
- Miyoshi, I., S. Yoshimoto, M. Fujishita, I. Kubonishi, H. Taguchi, and Y. Ohtsuki. 1984. 'Infectious Transmission of Human T-Cell Leukemia Virus to Animals'. *Princess Takamatsu Symposia* 15: 121–27.
- Modina, Silvia, Francesco Abbate, Germana P. Germanà, Antonio Lauria, and Alberto M. Luciano. 2007. 'β-Catenin Localization and Timing of Early Development of Bovine Embryos Obtained from Oocytes Matured in the Presence of Follicle Stimulating Hormone'. *Animal Reproduction Science* 100 (3–4): 264–79. <https://doi.org/10.1016/j.anireprosci.2006.07.008>.
- Moon et al. 2017. 'Phosphorylation by NLK Inhibits YAP-14-3-3-Interactions and Induces Its Nuclear Localization'. *EMBO Reports* 18 (1): 61–71. <https://doi.org/10.15252/embr.201642683>.
- Moradi, Mehdi, Ahmad Riasi, Somayyeh Ostadhosseini, Mehdi Hajian, Morteza Hosseini, Pouria Hosseinnia, and Mohammad Hossein Nasr-Esfahani. 2015. 'Expression Profile of FGF Receptors in Preimplantation Ovine Embryos and the Effect of FGF2 and PD173074'. *Growth Factors (Chur, Switzerland)* 33 (5–6): 393–400. <https://doi.org/10.3109/08977194.2015.1102138>.
- Moriwaki, Kazumasa, Shoichiro Tsukita, and Mikio Furuse. 2007. 'Tight Junctions Containing Claudin 4 and 6 Are Essential for Blastocyst Formation in

- Preimplantation Mouse Embryos'. *Developmental Biology* 312 (2): 509–22. <https://doi.org/10.1016/j.ydbio.2007.09.049>.
- Müller, Patrick, Katherine W. Rogers, Ben M. Jordan, Joon S. Lee, Drew Robson, Sharad Ramanathan, and Alexander F. Schier. 2012. 'Differential Diffusivity of Nodal and Lefty Underlies a Reaction-Diffusion Patterning System'. *Science (New York, N.Y.)* 336 (6082): 721–24. <https://doi.org/10.1126/science.1221920>.
- Muyan, M., and I. Boime. 1997. 'Secretion of Chorionic Gonadotropin from Human Trophoblasts'. *Placenta* 18 (4): 237–41. [https://doi.org/10.1016/s0143-4004\(97\)80056-2](https://doi.org/10.1016/s0143-4004(97)80056-2).
- Naito, Julie, Kevin R. Mott, Nelson Osorio, Ling Jin, and Guey-Chuen Perng. 2005. 'Herpes Simplex Virus Type 1 Immediate-Early Protein ICP0 Diffuses out of Infected Rabbit Corneas'. *The Journal of General Virology* 86 (Pt 11): 2979–88. <https://doi.org/10.1099/vir.0.81246-0>.
- Nakamura, Tetsuya, Naoki Mine, Etsushi Nakaguchi, Atsushi Mochizuki, Masamichi Yamamoto, Kenta Yashiro, Chikara Meno, and Hiroshi Hamada. 2006. 'Generation of Robust Left-Right Asymmetry in the Mouse Embryo Requires a Self-Enhancement and Lateral-Inhibition System'. *Developmental Cell* 11 (4): 495–504. <https://doi.org/10.1016/j.devcel.2006.08.002>.
- Negrón-Pérez, Verónica M., and Peter J. Hansen. 2018. 'Role of Yes-Associated Protein 1, Angiomotin, and Mitogen-Activated Kinase Kinase 1/2 in Development of the Bovine Blastocyst'. *Biology of Reproduction* 98 (2): 170–83. <https://doi.org/10.1093/biolre/iox172>.
- Negrón-Pérez, Verónica M., Luana T. Rodrigues, Gisele Z. Mingoti, and Peter J. Hansen. 2018. 'Role of ROCK Signaling in Formation of the Trophectoderm of the Bovine Preimplantation Embryo'. *Molecular Reproduction and Development* 85 (5): 374–75. <https://doi.org/10.1002/mrd.22976>.
- Negrón-Pérez, Verónica M., Yanping Zhang, and Peter J. Hansen. 2017. 'Single-Cell Gene Expression of the Bovine Blastocyst'. *Reproduction (Cambridge, England)* 154 (5): 627–44. <https://doi.org/10.1530/REP-17-0345>.
- Nesburn, A. B., M. L. Cook, and J. G. Stevens. 1972. 'Latent Herpes Simplex Virus. Isolation from Rabbit Trigeminal Ganglia between Episodes of Recurrent Ocular Infection'. *Archives of Ophthalmology (Chicago, Ill.: 1960)* 88 (4): 412–17. <https://doi.org/10.1001/archophth.1972.01000030414012>.
- Nesburn, Anthony B., Ilham Bettahi, Gargi Dasgupta, Alami Aziz Chentoufi, Xiuli Zhang, Sylvaine You, Naoyuki Morishige, et al. 2007. 'Functional Foxp3+ CD4+ CD25(Bright+) "Natural" Regulatory T Cells Are Abundant in Rabbit Conjunctiva and Suppress Virus-Specific CD4+ and CD8+ Effector T Cells during Ocular Herpes Infection'. *Journal of Virology* 81 (14): 7647–61. <https://doi.org/10.1128/JVI.00294-07>.
- Neto-Silva, Ricardo M., Simon de Beco, and Laura A. Johnston. 2010. 'Evidence for a Growth-Stabilizing Regulatory Feedback Mechanism between Myc and Yorkie, the Drosophila Homolog of Yap'. *Developmental Cell* 19 (4): 507–20. <https://doi.org/10.1016/j.devcel.2010.09.009>.
- Niakan, Kathy K., and Kevin Egan. 2013. 'Analysis of Human Embryos from Zygote to Blastocyst Reveals Distinct Gene Expression Patterns Relative to the Mouse'. *Developmental Biology* 375 (1): 54–64. <https://doi.org/10.1016/j.ydbio.2012.12.008>.

- Niessen, Carien M., and Cara J. Gottardi. 2008. 'Molecular Components of the Adherens Junction'. *Biochimica et Biophysica Acta* 1778 (3): 562–71. <https://doi.org/10.1016/j.bbamem.2007.12.015>.
- Nikas, G., A. Ao, R. M. Winston, and A. H. Handyside. 1996. 'Compaction and Surface Polarity in the Human Embryo in Vitro'. *Biology of Reproduction* 55 (1): 32–37. <https://doi.org/10.1095/biolreprod55.1.32>.
- Nishioka, Noriyuki, Ken-ichi Inoue, Kenjiro Adachi, Hiroshi Kiyonari, Mitsunori Ota, Amy Ralston, Norikazu Yabuta, et al. 2009. 'The Hippo Signaling Pathway Components Lats and Yap Pattern Tead4 Activity to Distinguish Mouse Trophectoderm from Inner Cell Mass'. *Developmental Cell* 16 (3): 398–410. <https://doi.org/10.1016/j.devcel.2009.02.003>.
- Nishioka, Noriyuki, Shinji Yamamoto, Hiroshi Kiyonari, Hiroko Sato, Atsushi Sawada, Mitsunori Ota, Kazuki Nakao, and Hiroshi Sasaki. 2008. 'Tead4 Is Required for Specification of Trophectoderm in Pre-Implantation Mouse Embryos'. *Mechanisms of Development* 125 (3): 270–83. <https://doi.org/10.1016/j.mod.2007.11.002>.
- Niwa, Hitoshi, Yayoi Toyooka, Daisuke Shimosato, Dan Strumpf, Kadue Takahashi, Rika Yagi, and Janet Rossant. 2005. 'Interaction between Oct3/4 and Cdx2 Determines Trophectoderm Differentiation'. *Cell* 123 (5): 917–29. <https://doi.org/10.1016/j.cell.2005.08.040>.
- Odening, Katja E., Bum-Rak Choi, Gong Xin Liu, Kathryn Hartmann, Ohad Ziv, Leonard Chaves, Lorraine Schofield, et al. 2012. 'Estradiol Promotes Sudden Cardiac Death in Transgenic Long QT Type 2 Rabbits While Progesterone Is Protective'. *Heart Rhythm* 9 (5): 823–32. <https://doi.org/10.1016/j.hrthm.2012.01.009>.
- Oh, Sangphil, Dongjun Lee, Tackhoon Kim, Tae-Shin Kim, Hyun Jung Oh, Chae Young Hwang, Young-Yun Kong, Ki-Sun Kwon, and Dae-Sik Lim. 2009. 'Crucial Role for Mst1 and Mst2 Kinases in Early Embryonic Development of the Mouse'. *Molecular and Cellular Biology* 29 (23): 6309–20. <https://doi.org/10.1128/MCB.00551-09>.
- Ohsugi, M., L. Larue, H. Schwarz, and R. Kemler. 1997. 'Cell-Junctional and Cytoskeletal Organization in Mouse Blastocysts Lacking E-Cadherin'. *Developmental Biology* 185 (2): 261–71. <https://doi.org/10.1006/dbio.1997.8560>.
- Okuno, Tomomi, Wayne Yang Li, Yu Hatano, Atsushi Takasu, Yuko Sakamoto, Mari Yamamoto, Zenki Ikeda, et al. 2020. 'Zygotic Nuclear F-Actin Safeguards Embryonic Development'. *Cell Reports* 31 (13). <https://doi.org/10.1016/j.celrep.2020.107824>.
- Ozawa, Manabu, Miki Sakatani, JiQiang Yao, Savita Shanker, Fahong Yu, Rui Yamashita, Shunichi Wakabayashi, et al. 2012. 'Global Gene Expression of the Inner Cell Mass and Trophectoderm of the Bovine Blastocyst'. *BMC Developmental Biology* 12 (1): 33. <https://doi.org/10.1186/1471-213X-12-33>.
- Pan, DuoJia. 2007. 'Hippo Signaling in Organ Size Control'. *Genes & Development* 21 (8): 886–97. <https://doi.org/10.1101/gad.1536007>.
- Pan, DuoJia. 2010. 'The Hippo Signaling Pathway in Development and Cancer'. *Developmental Cell* 19 (4): 491–505. <https://doi.org/10.1016/j.devcel.2010.09.011>.
- Papaioannou, V. E., and K. M. Ebert. 1988. 'The Preimplantation Pig Embryo: Cell Number and Allocation to Trophectoderm and Inner Cell Mass of the Blastocyst

- in Vivo and in Vitro'. *Development (Cambridge, England)* 102 (4): 793–803. <https://doi.org/10.1242/dev.102.4.793>.
- Pedersen, Hanne Skovsgaard, Gianluca Mazzoni, Lotte Stroebech, Haja N Kadarmideen, Poul Hyttel, and Henrik Callesen. 2017. 'Basic and Practical Aspects of Pregnancy Establishment in Cattle', 8.
- Peng, Xuwen, John A. Knouse, and Krista M. Hernon. 2015. 'Rabbit Models for Studying Human Infectious Diseases'. *Comparative Medicine* 65 (6): 499–507.
- Petropoulos, Sophie, Daniel Edsgård, Björn Reinius, Qiaolin Deng, Sarita Pauliina Panula, Simone Codeluppi, Alvaro Plaza Reyes, Sten Linnarsson, Rickard Sandberg, and Fredrik Lanner. 2016. 'Single-Cell RNA-Seq Reveals Lineage and X Chromosome Dynamics in Human Preimplantation Embryos'. *Cell* 165 (4): 1012–26. <https://doi.org/10.1016/j.cell.2016.03.023>.
- Pieters, Tim, Steven Goossens, Lieven Haenebalcke, Vanessa Andries, Agata Stryjewska, Riet De Rycke, Kelly Lemeire, et al. 2016. 'P120 Catenin-Mediated Stabilization of E-Cadherin Is Essential for Primitive Endoderm Specification'. *PLoS Genetics* 12 (8): e1006243. <https://doi.org/10.1371/journal.pgen.1006243>.
- Piliszek, Anna, and Zofia E. Madeja. 2018. 'Pre-Implantation Development of Domestic Animals'. In *Current Topics in Developmental Biology*, 128:267–94. Elsevier. <https://doi.org/10.1016/bs.ctdb.2017.11.005>.
- Piliszek, Anna, Zofia E. Madeja, and Berenika Plusa. 2017. 'Suppression of ERK Signalling Abolishes Primitive Endoderm Formation but Does Not Promote Pluripotency in Rabbit Embryo'. *Development* 144 (20): 3719–30. <https://doi.org/10.1242/dev.156406>.
- Pillai, Viju Vijayan, Tiffany G. Kei, Shailesh Gurung, Moubani Das, Luiz G. B. Siqueira, Soon Hon Cheong, Peter J. Hansen, and Vimal Selvaraj. 2022. 'RhoA/ROCK Signaling Antagonizes Bovine Trophoblast Stem Cell Self-Renewal and Regulates Preimplantation Embryo Size and Differentiation'. *Development* 149 (7): dev200115. <https://doi.org/10.1242/dev.200115>.
- Plusa, Berenika, Stephen Frankenberg, Andrew Chalmers, Anna-Katerina Hadjantonakis, Catherine A. Moore, Nancy Papalopulu, Virginia E. Papaioannou, David M. Glover, and Magdalena Zernicka-Goetz. 2005. 'Downregulation of Par3 and APKC Function Directs Cells towards the ICM in the Preimplantation Mouse Embryo'. *Journal of Cell Science* 118 (3): 505–15. <https://doi.org/10.1242/jcs.01666>.
- Plusa, Berenika, and Anna Piliszek. 2020. 'Common Principles of Early Mammalian Embryo Self-Organisation'. *Development* 147 (14): dev183079. <https://doi.org/10.1242/dev.183079>.
- Polisca, A., L. Scotti, R. Orlandi, G. Brecchia, and C. Boiti. 2010. 'Doppler Evaluation of Maternal and Fetal Vessels during Normal Gestation in Rabbits'. *Theriogenology* 73 (3): 358–66. <https://doi.org/10.1016/j.theriogenology.2009.09.019>.
- Pratt, H. P. M., C. A. Ziomek, W. J. D. Reeve, and M. H. Johnson. 1982. 'Compaction of the Mouse Embryo: An Analysis of Its Components'. *Development* 70 (1): 113–32.

- Qin, Han, Miroslav Hejna, Yanxia Liu, Michelle Percharde, Mark Wossidlo, Laure Blouin, Jens Durruthy-Durruthy, et al. 2016. 'YAP Induces Human Naive Pluripotency'. *Cell Reports* 14 (10): 2301–12. <https://doi.org/10.1016/j.celrep.2016.02.036>.
- Ralston, Amy, Brian J. Cox, Noriyuki Nishioka, Hiroshi Sasaki, Evelyn Chea, Peter Rugg-Gunn, Guoji Guo, Paul Robson, Jonathan S. Draper, and Janet Rossant. 2010. 'Gata3 Regulates Trophoblast Development Downstream of Tead4 and in Parallel to Cdx2'. *Development* 137 (3): 395–403. <https://doi.org/10.1242/dev.038828>.
- Ralston, Amy, and Janet Rossant. 2008. 'Cdx2 Acts Downstream of Cell Polarization to Cell-Autonomously Promote Trophectoderm Fate in the Early Mouse Embryo'. *Developmental Biology* 313 (2): 614–29. <https://doi.org/10.1016/j.ydbio.2007.10.054>.
- Rayon, Teresa, Sergio Menchero, Andres Nieto, Panagiotis Xenopoulos, Miguel Crespo, Katie Cockburn, Susana Cañon, et al. 2014. 'Notch and Hippo Converge on Cdx2 to Specify the Trophectoderm Lineage in the Mouse Blastocyst'. *Developmental Cell* 30 (4): 410–22. <https://doi.org/10.1016/j.devcel.2014.06.019>.
- Reddy, B. V. V. G., and Kenneth D. Irvine. 2008. 'The Fat and Warts Signaling Pathways: New Insights into Their Regulation, Mechanism and Conservation'. *Development (Cambridge, England)* 135 (17): 2827–38. <https://doi.org/10.1242/dev.020974>.
- Reeve, W. J. 1981. 'Cytoplasmic Polarity Develops at Compaction in Rat and Mouse Embryos'. *Journal of Embryology and Experimental Morphology* 62 (April): 351–67.
- Reeve, W. J., and C. A. Ziomek. 1981. 'Distribution of Microvilli on Dissociated Blastomeres from Mouse Embryos: Evidence for Surface Polarization at Compaction'. *Journal of Embryology and Experimental Morphology* 62 (April): 339–50.
- Reima, I., E. Lehtonen, I. Virtanen, and J. -E. Fléchon. 1993. 'The Cytoskeleton and Associated Proteins during Cleavage, Compaction and Blastocyst Differentiation in the Pig'. *Differentiation* 54 (3): 35–45. <https://doi.org/10.1111/j.1432-0436.1993.tb01586.x>.
- Rock, Jeremy M., Daniel Lim, Lasse Stach, Roksana W. Ogradowicz, Jamie M. Keck, Michele H. Jones, Catherine C. L. Wong, et al. 2013. 'Activation of the Yeast Hippo Pathway by Phosphorylation-Dependent Assembly of Signaling Complexes'. *Science (New York, N.Y.)* 340 (6134): 871–75. <https://doi.org/10.1126/science.1235822>.
- Rodriguez-Boulan, Enrique, and Ian G. Macara. 2014. 'Organization and Execution of the Epithelial Polarity Programme'. *Nature Reviews. Molecular Cell Biology* 15 (4): 225–42. <https://doi.org/10.1038/nrm3775>.
- Rossant, J., and K. M. Vihj. 1980. 'Ability of Outside Cells from Preimplantation Mouse Embryos to Form Inner Cell Mass Derivatives'. *Developmental Biology* 76 (2): 475–82. [https://doi.org/10.1016/0012-1606\(80\)90395-4](https://doi.org/10.1016/0012-1606(80)90395-4).
- Russ, Andreas, Sigrid Wattler, William Colledge, Samuel Aparicio, Mark Carlton, Jonathan Pearce, Sheila Barton, et al. 2000. 'Eomesodermin Is Required for Mouse Trophoblast Development and Mesoderm Formation'. *Nature* 404 (March): 95–99. <https://doi.org/10.1038/35003601>.

- Saiz, Néstor, and Berenika Plusa. 2013. 'Early Cell Fate Decisions in the Mouse Embryo'. *Reproduction* 145 (3): R65–80. <https://doi.org/10.1530/REP-12-0381>.
- Sakurai, Nobuyuki, Kazuki Takahashi, Natsuko Emura, Takashi Fujii, Hiroki Hirayama, Soichi Kageyama, Tsutomu Hashizume, and Ken Sawai. 2016. 'The Necessity of OCT-4 and CDX2 for Early Development and Gene Expression Involved in Differentiation of Inner Cell Mass and Trophectoderm Lineages in Bovine Embryos'. *Cellular Reprogramming* 18 (5): 309–18. <https://doi.org/10.1089/cell.2015.0081>.
- Sakurai, Nobuyuki, Kazuki Takahashi, Natsuko emura, Tsutomu Hashizume, and Ken Sawai. 2017. 'Effects of Downregulating TEAD4 Transcripts by RNA Interference on Early Development of Bovine Embryos'. *The Journal of Reproduction and Development* 63 (2): 135–42. <https://doi.org/10.1262/jrd.2016-130>.
- Samarage, Chaminda R., Melanie D. White, Yanina D. Álvarez, Juan Carlos Fierro-González, Yann Henon, Edwin C. Jesudason, Stephanie Bissiere, Andreas Fouras, and Nicolas Plachta. 2015. 'Cortical Tension Allocates the First Inner Cells of the Mammalian Embryo'. *Developmental Cell* 34 (4): 435–47. <https://doi.org/10.1016/j.devcel.2015.07.004>.
- Sansores-Garcia, Leticia, Wouter Bossuyt, Ken-Ichi Wada, Shigenobu Yonemura, Chunyao Tao, Hiroshi Sasaki, and Georg Halder. 2011. 'Modulating F-Actin Organization Induces Organ Growth by Affecting the Hippo Pathway'. *The EMBO Journal* 30 (12): 2325–35. <https://doi.org/10.1038/emboj.2011.157>.
- Sanyal, M. K., and F. Naftolin. 1983. 'In Vitro Development of the Mammalian Embryo'. *The Journal of Experimental Zoology* 228 (2): 235–51. <https://doi.org/10.1002/jez.1402280209>.
- Sasaki, Hiroshi. 2015. 'Position- and Polarity-Dependent Hippo Signaling Regulates Cell Fates in Preimplantation Mouse Embryos'. *Seminars in Cell & Developmental Biology* 47–48 (December): 80–87. <https://doi.org/10.1016/j.semcd.2015.05.003>.
- Sasaki, Hiroshi. 2017. 'Roles and Regulations of Hippo Signaling during Preimplantation Mouse Development'. *Development, Growth & Differentiation* 59 (1): 12–20. <https://doi.org/10.1111/dgd.12335>.
- Saucedo, Leslie J., and Bruce A. Edgar. 2007. 'Filling out the Hippo Pathway'. *Nature Reviews Molecular Cell Biology* 8 (8): 613–21. <https://doi.org/10.1038/nrm2221>.
- Sawada, Atsushi, Hiroshi Kiyonari, Kanako Ukita, Noriyuki Nishioka, Yu Imuta, and Hiroshi Sasaki. 2008. 'Redundant Roles of Tead1 and Tead2 in Notochord Development and the Regulation of Cell Proliferation and Survival'. *Molecular and Cellular Biology* 28 (10): 3177–89. <https://doi.org/10.1128/MCB.01759-07>.
- Sawada, Atsushi, Yuriko Nishizaki, Hiroko Sato, Yukari Yada, Rika Nakayama, Shinji Yamamoto, Noriyuki Nishioka, Hisato Kondoh, and Hiroshi Sasaki. 2005. 'Tead Proteins Activate the Foxa2 Enhancer in the Node in Cooperation with a Second Factor'. *Development* 132 (21): 4719–29. <https://doi.org/10.1242/dev.02059>.
- Schultz, R. M. 1993. 'Regulation of Zygotic Gene Activation in the Mouse'. *BioEssays: News and Reviews in Molecular, Cellular and Developmental Biology* 15 (8): 531–38. <https://doi.org/10.1002/bies.950150806>.
- Sefton, Mark, Martin H. Johnson, Lesley Clayton, and Josie M.L. McConnell. 1996. 'Experimental Manipulations of Compaction and Their Effects on the

- Phosphorylation of Uvomorulin'. *Molecular Reproduction and Development* 44 (1): 77–87. [https://doi.org/10.1002/\(SICI\)1098-2795\(199605\)44:1<77::AID-MRD9>3.0.CO;2-Q](https://doi.org/10.1002/(SICI)1098-2795(199605)44:1<77::AID-MRD9>3.0.CO;2-Q).
- Seo, Jimyung, and Joon Kim. 2018. 'Regulation of Hippo Signaling by Actin Remodeling'. *BMB Reports* 51 (3): 151–56. <https://doi.org/10.5483/BMBRep.2018.51.3.012>.
- Sharma, Jyoti, and Pavneesh Madan. 2020. 'Characterisation of the Hippo Signalling Pathway during Bovine Preimplantation Embryo Development'. *Reproduction, Fertility, and Development* 32 (4): 392–401. <https://doi.org/10.1071/RD18320>.
- Shi, Xianle, Zixi Yin, Bin Ling, Lingling Wang, Chang Liu, Xianhui Ruan, Weiyu Zhang, and Lingyi Chen. 2017. 'Rho Differentially Regulates the Hippo Pathway by Modulating the Interaction between Amot and Nf2 in the Blastocyst'. *Development* 144 (21): 3957–67. <https://doi.org/10.1242/dev.157917>.
- Shirayoshi, Y., T. S. Okada, and M. Takeichi. 1983. 'The Calcium-Dependent Cell-Cell Adhesion System Regulates Inner Cell Mass Formation and Cell Surface Polarization in Early Mouse Development'. *Cell* 35 (3 Pt 2): 631–38. [https://doi.org/10.1016/0092-8674\(83\)90095-8](https://doi.org/10.1016/0092-8674(83)90095-8).
- Skrzecz, Iwona, and Jolanta Karasiewicz. 1987. 'Decompaction and Recompaction of Mouse Preimplantation Embryos'. *Roux's Archives of Developmental Biology* 196 (6): 397–400. <https://doi.org/10.1007/BF00375780>.
- Smith, Craig S., Debra K. Berg, Martin Berg, and Peter L. Pfeffer. 2010. 'Nuclear Transfer-Specific Defects Are Not Apparent during the Second Week of Embryogenesis in Cattle'. *Cellular Reprogramming* 12 (6): 699–707. <https://doi.org/10.1089/cell.2010.0040>.
- Snyder, B. W., J. Vitale, P. Milos, J. Gosselin, F. Gillespie, K. Ebert, B. F. Hague, T. J. Kindt, S. Wadsworth, and P. Leibowitz. 1995. 'Developmental and Tissue-Specific Expression of Human CD4 in Transgenic Rabbits'. *Molecular Reproduction and Development* 40 (4): 419–28. <https://doi.org/10.1002/mrd.1080400405>.
- Soares, Michael J, Kaela M Varberg, and Khursheed Iqbal. 2018. 'Hemochorial Placentation: Development, Function, and Adaptations+'. *Biology of Reproduction* 99 (1): 196–211. <https://doi.org/10.1093/biolre/iyoy049>.
- Speck, Roberto F., Michael L. Penn, Jörg Wimmer, Ursula Esser, Bishop F. Hague, Thomas J. Kindt, Robert E. Atchison, and Mark A. Goldsmith. 1998. 'Rabbit Cells Expressing Human CD4 and Human CCR5 Are Highly Permissive for Human Immunodeficiency Virus Type 1 Infection'. *Journal of Virology* 72 (7): 5728–34.
- Srinivas, Shankar, and Tristan Argeo Rodriguez. 2017. 'A Tale of Division and Polarization in the Mammalian Embryo'. *Developmental Cell* 40 (3): 215–16. <https://doi.org/10.1016/j.devcel.2017.01.008>.
- Stankova, Viktoria, Nikoloz Tsikolia, and Christoph Viebahn. 2015. 'Rho Kinase Activity Controls Directional Cell Movements during Primitive Streak Formation in the Rabbit Embryo'. *Development* 142 (1): 92–98. <https://doi.org/10.1242/dev.111583>.
- Stephenson, Robert Odell, Yojiro Yamanaka, and Janet Rossant. 2010. 'Disorganized Epithelial Polarity and Excess Trophectoderm Cell Fate in Preimplantation Embryos Lacking E-Cadherin'. *Development (Cambridge, England)* 137 (20): 3383–91. <https://doi.org/10.1242/dev.050195>.

- Strumpf, Dan, Chai-An Mao, Yojiro Yamanaka, Amy Ralston, Kallayanee Chawengsaksophak, Felix Beck, and Janet Rossant. 2005. 'Cdx2 Is Required for Correct Cell Fate Specification and Differentiation of Trophoblast in the Mouse Blastocyst'. *Development* 132 (9): 2093–2102. <https://doi.org/10.1242/dev.01801>.
- Sultana, Fowzia, Masanori Hatori, Nobuhiro Shimosawa, Takashi Ebisawa, and Tadashi Sankai. 2009. 'Continuous Observation of Rabbit Preimplantation Embryos in Vitro by Using a Culture Device Connected to a Microscope'. *Journal of the American Association for Laboratory Animal Science: JAALAS* 48 (1): 52–56.
- Sun, Shuguo, and Kenneth D. Irvine. 2016. 'Cellular Organization and Cytoskeletal Regulation of the Hippo Signaling Network'. *Trends in Cell Biology* 26 (9): 694–704. <https://doi.org/10.1016/j.tcb.2016.05.003>.
- Suzuki, Atsushi, and Shigeo Ohno. 2006. 'The PAR-APKC System: Lessons in Polarity'. *Journal of Cell Science* 119 (6): 979–87. <https://doi.org/10.1242/jcs.02898>.
- Suzuki, H., T. Azuma, H. Koyama, and X. Yang. 1999. 'Development of Cellular Polarity of Hamster Embryos during Compaction'. *Biology of Reproduction* 61 (2): 521–26. <https://doi.org/10.1095/biolreprod61.2.521>.
- Takeuchi, K., N. Sato, H. Kasahara, N. Funayama, A. Nagafuchi, S. Yonemura, S. Tsukita, and S. Tsukita. 1994. 'Perturbation of Cell Adhesion and Microvilli Formation by Antisense Oligonucleotides to ERM Family Members'. *The Journal of Cell Biology* 125 (6): 1371–84. <https://doi.org/10.1083/jcb.125.6.1371>.
- Tan, Kun, Lei An, Shu-Min Wang, Xiao-Dong Wang, Zhen-Ni Zhang, Kai Miao, Lin-Lin Sui, et al. 2015. 'Actin Disorganization Plays a Vital Role in Impaired Embryonic Development of In Vitro-Produced Mouse Preimplantation Embryos'. *PLoS ONE* 10 (6): e0130382. <https://doi.org/10.1371/journal.pone.0130382>.
- Tarkowski, Andrzej K. 1959. 'Experiments on the Development of Isolated Blastomeres of Mouse Eggs'. *Nature* 184 (4695): 1286–87. <https://doi.org/10.1038/1841286a0>.
- Tarkowski, Andrzej K., Aneta Suwińska, Renata Czołowska, and Waław Ożdżeński. 2010. 'Individual Blastomeres of 16- and 32-Cell Mouse Embryos Are Able to Develop into Foetuses and Mice'. *Developmental Biology* 348 (2): 190–98. <https://doi.org/10.1016/j.ydbio.2010.09.022>.
- Tarkowski, Andrzej K., and Joanna Wróblewska. 1967. 'Development of Blastomeres of Mouse Eggs Isolated at the 4- and 8-Cell Stage'. *Development* 18 (1): 155–80. <https://doi.org/10.1242/dev.18.1.155>.
- Taylor, J. M., and J. Fan. 1997. 'Transgenic Rabbit Models for the Study of Atherosclerosis'. *Frontiers in Bioscience: A Journal and Virtual Library* 2 (June): d298-308. <https://doi.org/10.2741/a192>.
- Telford, N. A., A. J. Watson, and G. A. Schultz. 1990. 'Transition from Maternal to Embryonic Control in Early Mammalian Development: A Comparison of Several Species'. *Molecular Reproduction and Development* 26 (1): 90–100. <https://doi.org/10.1002/mrd.1080260113>.
- Thumkeo, Dean, Sadanori Watanabe, and Shuh Narumiya. 2013. 'Physiological Roles of Rho and Rho Effectors in Mammals'. *European Journal of Cell Biology* 92 (10–11): 303–15. <https://doi.org/10.1016/j.ejcb.2013.09.002>.
- Tribulo, Paula, James I. Moss, Manabu Ozawa, Zongliang Jiang, Xiuchun Cindy Tian, and Peter J. Hansen. 2017. 'WNT Regulation of Embryonic Development Likely

- Involves Pathways Independent of Nuclear CTNNB1'. *Reproduction (Cambridge, England)* 153 (4): 405–19. <https://doi.org/10.1530/REP-16-0610>.
- Tsukita, S., Y. Yamazaki, T. Katsuno, A. Tamura, and S. Tsukita. 2008. 'Tight Junction-Based Epithelial Microenvironment and Cell Proliferation'. *Oncogene* 27 (55): 6930–38. <https://doi.org/10.1038/onc.2008.344>.
- Vassilev, Alex, Kotaro J. Kaneko, Hongjun Shu, Yingming Zhao, and Melvin L. DePamphilis. 2001. 'TEAD/TEF Transcription Factors Utilize the Activation Domain of YAP65, a Src/Yes-Associated Protein Localized in the Cytoplasm'. *Genes & Development* 15 (10): 1229–41. <https://doi.org/10.1101/gad.888601>.
- Vestweber, D., A. Gossler, K. Boller, and R. Kemler. 1987. 'Expression and Distribution of Cell Adhesion Molecule Uvomorulin in Mouse Preimplantation Embryos'. *Developmental Biology* 124 (2): 451–56. [https://doi.org/10.1016/0012-1606\(87\)90498-2](https://doi.org/10.1016/0012-1606(87)90498-2).
- Vinot, Stéphanie, Tran Le, Shigeo Ohno, Tony Pawson, Bernard Maro, and Sophie Louvet-Vallée. 2005. 'Asymmetric Distribution of PAR Proteins in the Mouse Embryo Begins at the 8-Cell Stage during Compaction'. *Developmental Biology* 282 (2): 307–19. <https://doi.org/10.1016/j.ydbio.2005.03.001>.
- Vogelsgesang, Martin, Alexander Pautsch, and Klaus Aktories. 2007. 'C3 Exoenzymes, Novel Insights into Structure and Action of Rho-ADP-Ribosylating Toxins'. *Naunyn-Schmiedeberg's Archives of Pharmacology* 374 (5–6): 347–60. <https://doi.org/10.1007/s00210-006-0113-y>.
- Wada, Ken-Ichi, Kazuyoshi Itoga, Teruo Okano, Shigenobu Yonemura, and Hiroshi Sasaki. 2011. 'Hippo Pathway Regulation by Cell Morphology and Stress Fibers'. *Development (Cambridge, England)* 138 (18): 3907–14. <https://doi.org/10.1242/dev.070987>.
- Wang, Kuei-Chun, Yi-Ting Yeh, Phu Nguyen, Elaine Limqueco, Jocelyn Lopez, Satenick Thorossian, Kun-Liang Guan, Yi-Shuan J. Li, and Shu Chien. 2016. 'Flow-Dependent YAP/TAZ Activities Regulate Endothelial Phenotypes and Atherosclerosis'. *Proceedings of the National Academy of Sciences* 113 (41): 11525–30. <https://doi.org/10.1073/pnas.1613121113>.
- Wang, Li, Jiang-Yun Luo, Bochuan Li, Xiao Yu Tian, Li-Jing Chen, Yuhong Huang, Jian Liu, et al. 2016. 'Integrin-YAP/TAZ-JNK Cascade Mediates Atheroprotective Effect of Unidirectional Shear Flow'. *Nature* 540 (7634): 579–82. <https://doi.org/10.1038/nature20602>.
- Wang, Wenqi, Jun Huang, and Junjie Chen. 2011. 'Angiomotin-like Proteins Associate with and Negatively Regulate YAP1'. *The Journal of Biological Chemistry* 286 (6): 4364–70. <https://doi.org/10.1074/jbc.C110.205401>.
- Wang, Wenqi, Zhen-Dong Xiao, Xu Li, Kathryn E. Aziz, Boyi Gan, Randy L. Johnson, and Junjie Chen. 2015. 'AMPK Modulates Hippo Pathway Activity to Regulate Energy Homeostasis'. *Nature Cell Biology* 17 (4): 490–99. <https://doi.org/10.1038/ncb3113>.
- Watanabe, Yoshio. 1980. 'Serial Inbreeding of Rabbits with Hereditary Hyperlipidemia (WHHL-Rabbit): Incidence and Development of Atherosclerosis and Xanthoma'. *Atherosclerosis* 36 (2): 261–68. [https://doi.org/10.1016/0021-9150\(80\)90234-8](https://doi.org/10.1016/0021-9150(80)90234-8).
- Weber, Justus, Haiyong Peng, and Christoph Rader. 2017. 'From Rabbit Antibody Repertoires to Rabbit Monoclonal Antibodies'. *Experimental & Molecular Medicine* 49 (3): e305. <https://doi.org/10.1038/emm.2017.23>.

- Webre, Jody M., James M. Hill, Nicole M. Nolan, Christian Clement, Harris E. McFerrin, Partha S. Bhattacharjee, Victor Hsia, et al. 2012. 'Rabbit and Mouse Models of HSV-1 Latency, Reactivation, and Recurrent Eye Diseases'. *Journal of Biomedicine & Biotechnology* 2012: 612316. <https://doi.org/10.1155/2012/612316>.
- Wennekamp, Sebastian, Sven Mesecke, François Nédélec, and Takashi Hiiragi. 2013. 'A Self-Organization Framework for Symmetry Breaking in the Mammalian Embryo'. *Nature Reviews. Molecular Cell Biology* 14 (7): 452–59. <https://doi.org/10.1038/nrm3602>.
- Wettschureck, Nina, and Stefan Offermanns. 2005. 'Mammalian G Proteins and Their Cell Type Specific Functions'. *Physiological Reviews* 85 (4): 1159–1204. <https://doi.org/10.1152/physrev.00003.2005>.
- Wigle, E. D., H. Rakowski, B. P. Kimball, and W. G. Williams. 1995. 'Hypertrophic Cardiomyopathy. Clinical Spectrum and Treatment'. *Circulation* 92 (7): 1680–92. <https://doi.org/10.1161/01.cir.92.7.1680>.
- Wilde, C., H. Genth, K. Aktories, and I. Just. 2000. 'Recognition of RhoA by Clostridium Botulinum C3 Exoenzyme'. *The Journal of Biological Chemistry* 275 (22): 16478–83. <https://doi.org/10.1074/jbc.M910362199>.
- Wu, Ji, Anne Duggan, and Martin Chalfie. 2001. 'Inhibition of Touch Cell Fate by Egl-44 and Egl-46 in *C. Elegans*'. *Genes & Development* 15 (6): 789–802. <https://doi.org/10.1101/gad.857401>.
- Xie, Dan, Chieh-Chun Chen, Leon M. Ptaszek, Shu Xiao, Xiaoyi Cao, Fang Fang, Huck H. Ng, Harris A. Lewin, Chad Cowan, and Sheng Zhong. 2010. 'Rewirable Gene Regulatory Networks in the Preimplantation Embryonic Development of Three Mammalian Species'. *Genome Research* 20 (6): 804–15. <https://doi.org/10.1101/gr.100594.109>.
- Xie, Huirong, Susanne Tranguch, Xiangxu Jia, Hao Zhang, Sanjoy K. Das, Sudhansu K. Dey, Calvin J. Kuo, and Haibin Wang. 2008. 'Inactivation of Nuclear Wnt- β -Catenin Signaling Limits Blastocyst Competency for Implantation'. *Development* 135 (4): 717–27. <https://doi.org/10.1242/dev.015339>.
- Yagi, Rieko, Matthew J. Kohn, Irina Karavanova, Kotaro J. Kaneko, Detlef Vullhorst, Melvin L. DePamphilis, and Andres Buonanno. 2007. 'Transcription Factor TEAD4 Specifies the Trophectoderm Lineage at the Beginning of Mammalian Development'. *Development* 134 (21): 3827–36. <https://doi.org/10.1242/dev.010223>.
- Yamade, I., T. Ishiguro, and A. Seto. 1991. 'Infection without Antibody Response in Mother-to-Child Transmission of HTLV-I in Rabbits'. *Journal of Medical Virology* 33 (4): 268–72. <https://doi.org/10.1002/jmv.1890330411>.
- Yamaguchi, Hiroto, Miyuki Kasa, Mutsuki Amano, Kozo Kaibuchi, and Toshio Hakoshima. 2006. 'Molecular Mechanism for the Regulation of Rho-Kinase by Dimerization and Its Inhibition by Fasudil'. *Structure* 14 (3): 589–600. <https://doi.org/10.1016/j.str.2005.11.024>.
- Yamanaka, Yojiro, Amy Ralston, Robert O. Stephenson, and Janet Rossant. 2006. 'Cell and Molecular Regulation of the Mouse Blastocyst'. *Developmental Dynamics* 235 (9): 2301–14. <https://doi.org/10.1002/dvdy.20844>.
- Yamashita, Atsushi, Eiji Furukoji, Kousuke Marutsuka, Kinta Hatakeyama, Hiroshi Yamamoto, Shozo Tamura, Yasuo Ikeda, Akinobu Sumiyoshi, and Yujiro Asada.

2004. 'Increased Vascular Wall Thrombogenicity Combined with Reduced Blood Flow Promotes Occlusive Thrombus Formation in Rabbit Femoral Artery'. *Arteriosclerosis, Thrombosis, and Vascular Biology* 24 (12): 2420–24. <https://doi.org/10.1161/01.ATV.0000147767.61336.de>.
- Yan, Li-Ying, Jun-Cheng Huang, Zi-Yu Zhu, Zi-Li Lei, Li-Hong Shi, Chang-Long Nan, Zhen-Jun Zhao, et al. 2006. 'NuMA Distribution and Microtubule Configuration in Rabbit Oocytes and Cloned Embryos'. *Reproduction (Cambridge, England)* 132 (6): 869–76. <https://doi.org/10.1530/rep.1.01224>.
- Yoshinaga, Koji. 2013. 'A Sequence of Events in the Uterus Prior to Implantation in the Mouse'. *Journal of Assisted Reproduction and Genetics* 30 (8): 1017–22. <https://doi.org/10.1007/s10815-013-0093-z>.
- Yu, Chao, Shu-Yan Ji, Yu-Jiao Dang, Qian-Qian Sha, Yi-Feng Yuan, Jian-Jie Zhou, Li-Ying Yan, Jie Qiao, Fuchou Tang, and Heng-Yu Fan. 2016. 'Oocyte-Expressed Yes-Associated Protein Is a Key Activator of the Early Zygotic Genome in Mouse'. *Cell Research* 26 (3): 275–87. <https://doi.org/10.1038/cr.2016.20>.
- Yu, Fa-Xing, and Kun-Liang Guan. 2013. 'The Hippo Pathway: Regulators and Regulations'. *Genes & Development* 27 (4): 355–71. <https://doi.org/10.1101/gad.210773.112>.
- Yu, Fa-Xing, Bin Zhao, Nattapon Panupinthu, Jenna L. Jewell, Ian Lian, Lloyd H. Wang, Jiagang Zhao, et al. 2012. 'Regulation of the Hippo-YAP Pathway by G-Protein-Coupled Receptor Signaling'. *Cell* 150 (4): 780–91. <https://doi.org/10.1016/j.cell.2012.06.037>.
- Zakharova, Elena E., Victoria V. Zaletova, and Alexander S. Krivokharchenko. 2014. 'Biopsy of Human Morula-Stage Embryos: Outcome of 215 IVF/ICSI Cycles with PGS'. *PLoS One* 9 (9): e106433. <https://doi.org/10.1371/journal.pone.0106433>.
- Zeng, Fanyi, Don A Baldwin, and Richard Schultz. 2004. 'Transcript Profiling during Preimplantation Mouse Development'. *Developmental Biology* 272 (2). <https://doi.org/10.1016/j.ydbio.2004.05.018>.
- Zenker, J., M. D. White, R. M. Templin, R. G. Parton, O. Thorn-Seshold, S. Bissiere, and N. Plachta. 2017. 'A Microtubule-Organizing Center Directing Intracellular Transport in the Early Mouse Embryo'. *Science (New York, N.Y.)* 357 (6354): 925–28. <https://doi.org/10.1126/science.aam9335>.
- Zenker, Jennifer, Melanie D. White, Maxime Gasnier, Yanina D. Alvarez, Hui Yi Grace Lim, Stephanie Bissiere, Maté Biro, and Nicolas Plachta. 2018. 'Expanding Actin Rings Zipper the Mouse Embryo for Blastocyst Formation'. *Cell* 173 (3): 776–791.e17. <https://doi.org/10.1016/j.cell.2018.02.035>.
- Zhang, Jin Yu, Huan Sheng Dong, Reza K. Oqani, Tao Lin, Jung Won Kang, and Dong Il Jin. 2014. 'Distinct Roles of ROCK1 and ROCK2 during Development of Porcine Preimplantation Embryos'. *Reproduction* 148 (1): 99–107. <https://doi.org/10.1530/REP-13-0556>.
- Zhang, Kun, Hai-Xia Qi, Zhi-Mei Hu, Ya-Nan Chang, Zhe-Min Shi, Xiao-Hui Han, Ya-Wei Han, et al. 2015. 'YAP and TAZ Take Center Stage in Cancer'. *Biochemistry* 54 (43): 6555–66. <https://doi.org/10.1021/acs.biochem.5b01014>.
- Zhao, Bin, Li Li, Qunying Lei, and Kun-Liang Guan. 2010. 'The Hippo-YAP Pathway in Organ Size Control and Tumorigenesis: An Updated Version'. *Genes & Development* 24 (9): 862–74. <https://doi.org/10.1101/gad.1909210>.

- Zhao, Bin, Li Li, Qing Lu, Lloyd H. Wang, Chen-Ying Liu, Qunying Lei, and Kun-Liang Guan. 2011. 'Angiomotin Is a Novel Hippo Pathway Component That Inhibits YAP Oncoprotein'. *Genes & Development* 25 (1): 51–63. <https://doi.org/10.1101/gad.2000111>.
- Zhao, Bin, Xiaomu Wei, Weiquan Li, Ryan S. Udan, Qian Yang, Joungmok Kim, Joe Xie, et al. 2007. 'Inactivation of YAP Oncoprotein by the Hippo Pathway Is Involved in Cell Contact Inhibition and Tissue Growth Control'. *Genes & Development* 21 (21): 2747–61. <https://doi.org/10.1101/gad.1602907>.
- Zhong, Weiliang, Kang Tian, Xifu Zheng, Linan Li, Weiguo Zhang, Shouyu Wang, and Jianhua Qin. 2013. 'Mesenchymal Stem Cell and Chondrocyte Fates in a Multishear Microdevice Are Regulated by Yes-Associated Protein'. *Stem Cells and Development* 22 (14): 2083–93. <https://doi.org/10.1089/scd.2012.0685>.
- Zhou, Xin, Shuyang Wang, Zhen Wang, Xu Feng, Peng Liu, Xian-Bo Lv, Fulong Li, et al. 2015. 'Estrogen Regulates Hippo Signaling via GPER in Breast Cancer'. *The Journal of Clinical Investigation* 125 (5): 2123–35. <https://doi.org/10.1172/JCI79573>.
- Zhu, Meng, Chuen Yan Leung, Marta N. Shahbazi, and Magdalena Zernicka-Goetz. 2017. 'Actomyosin Polarisation through PLC-PKC Triggers Symmetry Breaking of the Mouse Embryo'. *Nature Communications* 8 (1): 921. <https://doi.org/10.1038/s41467-017-00977-8>.
- Ziomek, C. A., C. L. Chatot, and C. Manes. 1990. 'Polarization of Blastomeres in the Cleaving Rabbit Embryo'. *The Journal of Experimental Zoology* 256 (1): 84–91. <https://doi.org/10.1002/jez.1402560111>.

12 Supplementary data

12.1 Quantification of the contribution of YAP+ and GATA3+ cells in individual embryos at stages III-IV

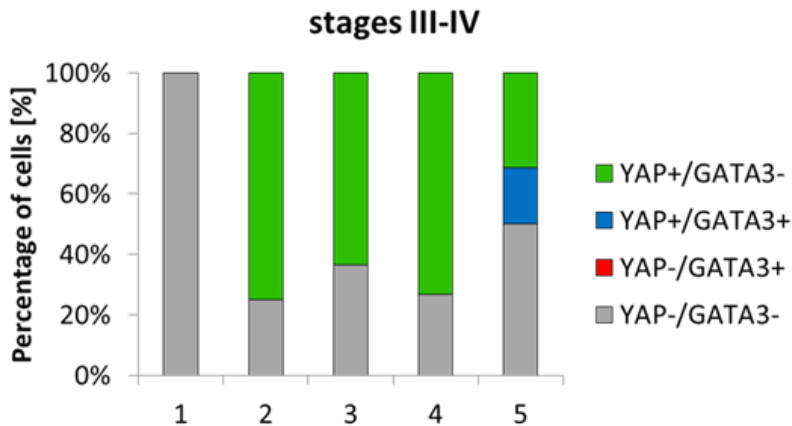


Figure S1. Relative/proportional contribution of YAP+ and GATA3+ cells in individual embryos at stages III-IV. Contribution of YAP+/GATA3- cells, YAP-/GATA3+ cells, YAP+/GATA3+ cells, YAP-/GATA3- cells to the total cell number of embryos at stages III-IV (n=5).

12.2 Quantification of the contribution of YAP+ and GATA3+ cells in inside and outside cells at stage V

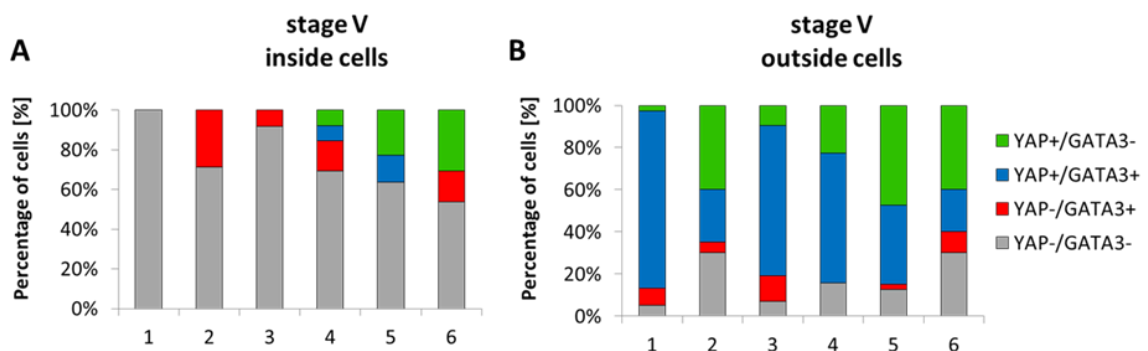


Figure S2. Percentage contribution of YAP+ and GATA3+ cells in individual embryos at stage V. Contribution of YAP+/GATA3- cells, YAP-/GATA3+ cells, YAP+/GATA3+ cells, YAP-/GATA3- cells of the inside (A) and outside compartment (B), in embryos at stage V (n=6).

12.3 Quantification of the contribution of YAP+ and GATA3+ cells in ICM and TE cells at stage VI

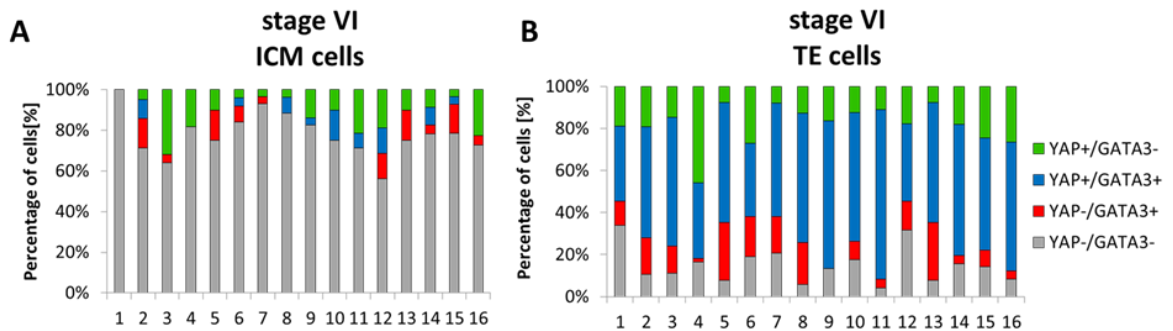


Figure S3. Percentage contribution of YAP+ and GATA3+ cells in individual embryos at stage VI

Contribution of YAP+/GATA3- cells, YAP-/GATA3+ cells, YAP+/GATA3+ cells, YAP-/GATA3- cells of the inside (A) and outside compartment (B), in embryos at stage VI (n=16). Each bar represents one individual embryo.

12.4 Quantification of the contribution of YAP+ and GATA3+ cells in ICM and TE cells at stage VII

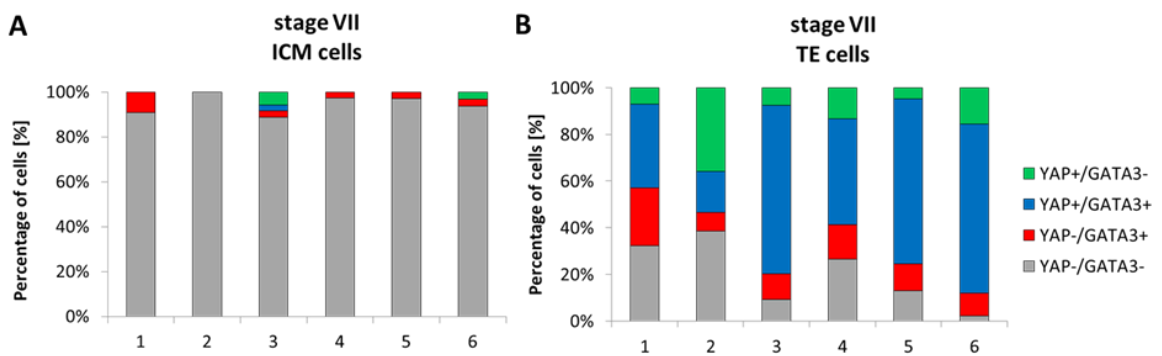


Figure S4. Percentage contribution of YAP+ and GATA3+ cells in individual embryos at stage VII.

Contribution of YAP+/GATA3- cells, YAP-/GATA3+ cells, YAP+/GATA3+ cells, YAP-/GATA3- cells of the inside (A) and outside compartment (B), in embryos at stage VII (n=6). Each bar represents one individual embryo.

12.5 Colocalisation of nuclear YAP and GATA3 in the inside cells of control and ROCK-inhibited embryos

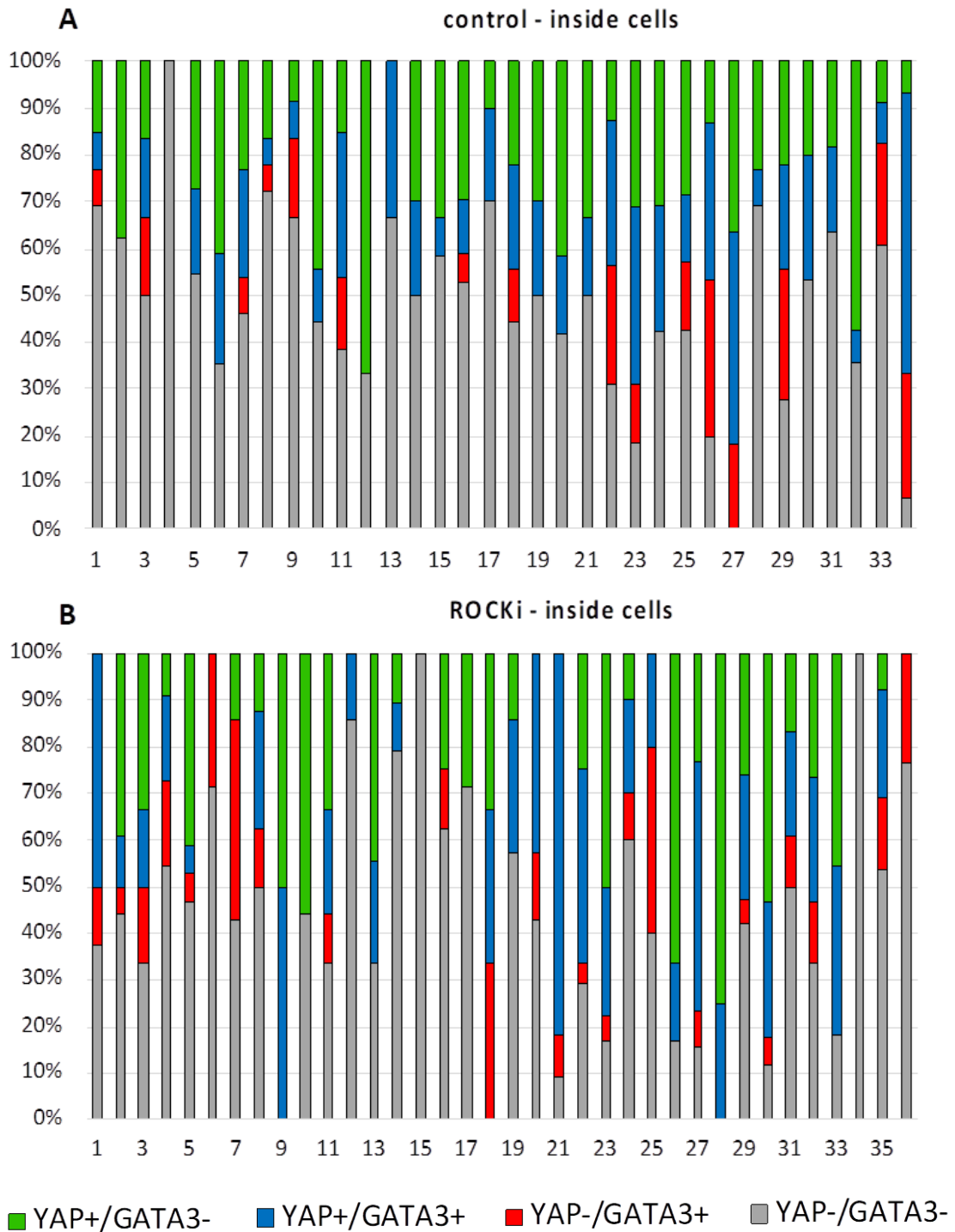
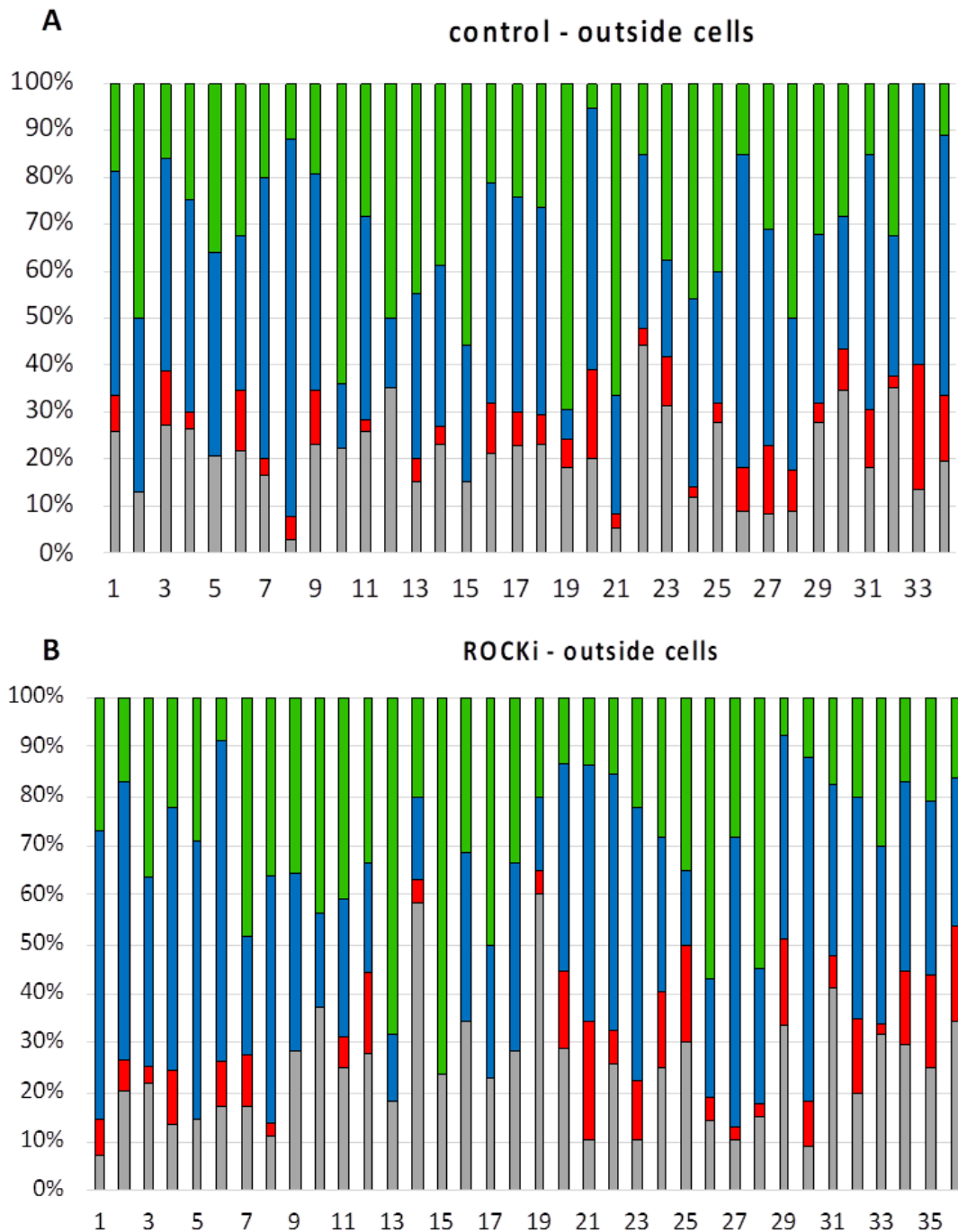


Figure S5. Contribution of YAP+ and GATA3+ cells in the inside compartment of individual control and experimental embryos. Contribution of YAP+/GATA3- cells, YAP-/GATA3+ cells, YAP+/GATA3+

cells, YAP-/GATA3- cells in the inside compartment of control embryos (n=34) (A) and ROCK-inhibited embryos (n=36) (B). Each bar represents one individual embryo.

12.6 Colocalisation of nuclear YAP and GATA3 in the outside cells of control and ROCK-inhibited embryos



■ YAP+/GATA3- ■ YAP+/GATA3+ ■ YAP-/GATA3+ ■ YAP-/GATA3-

Figure S6. Contribution of YAP+ and GATA3+ cells in the outside compartment of individual control and experimental embryos. Contribution of YAP+/GATA3- cells, YAP-/GATA3+ cells, YAP+/GATA3+ cells, YAP-/GATA3- cells in the outside compartment of control embryos (n=34)(A) and ROCK-inhibited embryos (n=36) (B). Each bar represents one individual embryo.